UNIVERSITY OF SOUTHAMPTON

A Palaeolimnological Investigation of Central Patagonian Climate During the Holocene

by

Thomas H. Bishop

A thesis submitted for the
degree of Doctor of Philosophy (PhD)

in the
Faculty of Social and Human Sciences
Geography and Environment

Supervisors:
Peter G. Langdon and Mary E. Edwards

January 2015

ABSTRACT

UNIVERSITY OF SOUTHAMPTON
FACULTY OF SOCIAL AND HUMAN SCIENCES
GEOGRAPHY AND ENVIRONMENT

Doctor of Philosophy (PhD)

A Palaeolimnological Investigation of Central Patagonian Climate During the Holocene

by Thomas H. Bishop

The southern westerly winds are the dominant control on climate in central Patagonia, and there is ample evidence of changes in the position and strength of the winds throughout the Holocene, but the timing, nature and extent of these changes is unclear. This study addresses the lack of palaeoclimatic data for the region east of the North Patagonian Icecap to address the uncertainties surrounding Holocene climate in the central Patagonian region.

By correlating multi-proxy (sediment δ^{13}C & C/N, chironomids and magnetic susceptability) data from two palaeoclimatic reconstructions derived from lake sediment sequences, this study identifies a unique climate history for central Patagonia, where mid-Holocene shifts observed elsewhere in Patagonia are subdued, but late-Holocene aridity between 1,300–2,800 years B.P. and cooler conditions from *c.*1,500 years B.P. onwards are present. Chironomid stratigraphies appear to respond primarily to lake level changes, and recently developed chironomid temperature transfer functions fail to provide reasonable estimates of temperature change over the past *c.*120 years at these study sites.

Modern vegetation δ^{13}C, C/N and modern water δ^{2}H and δ^{18}O data are presented, along with age/depth models for the two study sites derived from ^{14}C, ^{210}Pb, ^{137}Cs and tephrochronological markers. Geochemical data for a number of previously known and unknown tephras are also presented.

Contents

List of Figures

List of Tables

Declaration of Authorship

I,

Thomas Bishop

declare that the thesis entitled

A Palaeolimnological Investigation of Central Patagonian Climate During the Holocene

and the work presented in the thesis are both my own, and have been generated by me as the result of my own original research. I confirm that:

- this work was done wholly or mainly while in candidature for a research degree at this University;
- where any part of this thesis has previously been submitted for a degree or any other qualification at this University or any other institution, this has been clearly stated;
- where I have consulted the published work of others, this is always clearly attributed;
- where I have quoted from the work of others, the source is always given. With the exception of such quotations, this thesis is entirely my own work;
- I have acknowledged all main sources of help;
- where the thesis is based on work done by myself jointly with others, I have made clear exactly what was done by others and what I have contributed myself;

Signed: .....

Date: .....

Acknowledgements

I would like to extend my thanks to the following people:
My supervisory team, Dr. Pete Langdon and Prof. Mary Edwards who have always supported me by way of field support, sharing materials, useful discussion, encouragement and commentary throughout this project. Steve Brooks, based at the Natural History Museum, London, provided support in the field as well as sharing his expertise on chironomid identification and interpretation by way of extensive discussion for which I am particularly grateful. In addition Dr. Julieta Massaferro, Prof. John Dearing, Dr. Ian Croudace, Prof. Melanie Leng, Dr. Charlotte Bryant, Dr. Stuart Jarvis and Dr. Chris Hayward have shared their expertise and insight in Patagonian chironomids, environmental magnetism, radiographic/elemental analysis, stable isotopes, radiocarbon dating, lead isotope age modelling and electron microprobe analysis respectively. Thanks also to my fellow postgraduate students, specifically Robin Wilson and Dr. John Duncan for writing code that enabled the construction of a number of figures in the document, and Dr. Chris Hackney for assisting in typesetting. Dr. Steve Juggins kindly provided a licence for his C2 software. I am grateful to Mr. Olaf and Mrs. Jammie Wündrich for extensive logistical support and their warm hospitality during the 2010 fieldwork phase of this project.

I would like to acknowledge the support of the following organisations:
The Natural Environment Research Council for the provision of a doctoral training grant, radiocarbon (allocations 1465.0410 and 1620.0312), stable isotope (allocation IP-1271-1111) and electron microprobe analytical support (allocation TAU80/1012). The Quaternary Research Organisation funded Itrax analysis through a New Research Workers Award, and the University of Southampton provided a student travel grant to enable completion of stable isotope analysis.

For Jenny

Chapter 1

Introduction

1.1 Palaeoclimatic Reconstructions in the Southern Hemisphere

Palaeoclimate in Patagonia has been a focus of research since the early work of Caldenius (1932), but a recent interest in the importance of the southern westerly winds in modulating global climate has highlighted the lack of palaeoclimatic records from South America, the only continuous landmass along the latitudinal extent of the westerly winds.

Useful records of climate change can, and have been, derived from palaeoecological, palaeolimnological and palaeoenvironmental analysis of terrestrial archives of climate in South America. Continuing trends towards quantitative estimates of past climatic variables offers the possibility of testing model simulations of climate at regional to global scales. Because of the paucity of data it is rarely possible to compare proxy-derived estimates with observational data, leaving methods untested. For well established proxies a consensus can be built through wealth of data, but in poorly studied regions or where the proxy method is relatively new, comparison with instrumental data along with existing proxy data is a useful and appropriate test of its ability. Therefore this work will compare chironomid-inferred palaeoclimatic reconstructions with the best available data for Patagonia as well as producing records of climate change for the Holocene.

1.2 Controversies in Patagonian Palaeoclimate

The Lateglacial and Holocene climate is the focus of a number of controversies that concern the nature, timing and causes of a number of critical palaeoclimatic events and trends, including the Antarctic Cold Reversal, and the Holocene position of the westerlies. The available data for Patagonia are equivocal at best and conflicting at worst, and large gaps in the spatial extent of published records further hamper efforts to

construct a cohesive regional climatic history. On the other hand, post-glacial forest development has been widely studied in the lowlands, but post-glacial lake development, particularly in high altitude environments, has received relatively little attention. Furthermore, chronologies are often poor. For example, there is hemispheric-wide evidence for a mid-Holocene climate change towards modern conditions, but problems in the precision of chronological control in many records precludes establishing an accurate date for this shift. In addition, there are numerous local events that do not conform to any generalised supra-regional palaeoclimatic history; establishing the nature and extent of these events is particularly problematic for understudied areas in central Patagonia, where there are only sparse records.

Meteorological mechanisms for observed palaeoclimatic change are also the subject of conjecture and debate in this region. Nonetheless there is little doubt of the importance of the southern westerly winds, the El Niño Southern Oscillation, Pacific-Decadal Oscillation and Antarctic Oscillation. These are all examples of synoptic patterns that might underpin modes of climate variation in southernmost South America. Given the reliance on one key proxy (pollen) and some poor chronologies (see above), there is need for better comparisons between palaeoclimatic reconstructions.

1.3 The Scope and Focus of This Study

This study aims to provide palaeoclimate reconstructions for central Patagonia for both the recent past (centennial scale) and the Holocene (the past 11,700 years). It utilises a multi-proxy approach involving geochemical proxies for lake and catchment productivity alongside chironomid-based methods, which have recently been used to reconstruct palaeotemperatures, as well as magnetic analysis of bulk sediment. This study explicitly avoids palaeoclimatic proxies already shown to be of less utility in Patagonia (*e.g.* pollen), and makes a critical assessment of the use of chironomid proxies in Patagonia, the use of which is at an early stage in Patagonia. The key aim of the study is to improve the existing record of Holocene climate change for central Patagonia.

1.4 Thesis Structure

The following chapter details the aims and objectives of this study. Chapter 3 introduces the unique characteristics of climate in Patagonia that make it suitable for studying southern hemsiphere climatic processes, followed by an overview of recent and Holocene climate change, demonstrating the current gaps and inadequacies in the literature for Patagonia. Chapter 4 details the study sites and their locale. This is followed in Chapter 5 by an introduction to the methods used as palaeoclimatic and palaeoecological proxies as well as the techniques used to construct age models. The age models for both short and long core sequences are defined fully in Chapter 6. Chapters 7 and 8 present and

discuss respectively the recent climate change observed in the two study sites with a focus of the comparability of chironomid inferred temperatures and the existing literature. Chapters 9 and 10 present the long core data from the two study sites, and Chapter 11 compares these both with another and the published palaeoecological data. Finally, Chapter 12 discusses the implications these data have in understanding climatic processes in the southern hemisphere, followed by a summary of the conclusions of this study.

Chapter 2

Aims and Objectives

2.1 The Need for Further Records of Terrestrial Climate Change in Patagonia

The paucity of palaeoclimatic reconstructions of terrestrial climate change in Patagonia has hampered understanding of changes in hemispheric-scale palaeoclimatic processes such as the southern westerly winds. There is a particular gap in our understanding of regional palaeoclimate in Patagonia between 44–50°S where the westerlies currently dominate year-round. (Palaeo)climate in this region is very strongly coupled with the behaviour of the westerlies. Therfore, this study has the following aims:

- Develop a local palaeoclimatic record for the central Patagonian region.
- Use that record in conjunction with published data to infer regional palaeoclimatic processes and assess the record in relation to global patterns of Holocene climate change.

2.2 Lake Sediments as Climate Archives

The reason for the paucity of climate records is not the lack of appropriate sedimentary archives, but rather poor outcomes of traditional methods of palaeoclimate reconstruction. Lake systems have unique links to their prevailing climate through precipitation-evaporation balance, air temperature and the sensitivity of the ecosystems lakes support. Recent developments in chironomid based studies have allowed quantitative inferences of past temperatures as far back as the last glacial period, and oxygen isotopes have been used to reconstruct changes in lake level, directly related to precipitation-evaporation balance. This project exploits lacustrine proxy records including chironomid and carbon isotope analysis to reconstruct regional temporal

variations in temperature and moisture in southern South America during the Lateglacial and early Holocene.

Lake sediments record information at the catchment scale, and thus deriving regional climate signals from catchment scale palaeoenvironmental records can be complicated by the influence of local catchment processes and lake development. To disentangle catchment scale signals from regional signals multiple, independent palaeoclimate archives can be compared and common elements considered a regional palaeoclimatic signal. Thus this study exploits two lacustrine archives in separate catchments and at different altitudes but within 5km of one another.

In order to achieve aims presented in Section 2.1, this study has the following objectives:

- Identify suitable sites and retrieve lake cores from central Patagonia.
- Analyse those lake cores using modern proxies for palaeoclimate.
- Assess the success and applicability of proxies used (see Section 2.3 below).
- Present modern catchment geochemical data to contextualise and aid interpretation of the proxy data.

2.3 Recent Climate Change

The case for the use of chironomids to infer palaeo-temperatures in South America is not yet fully made as it might be considered to have been for regions in the northern hemisphere, although recent temperature transfer functions have been applied to Holocene and Lateglacial chironomid stratigraphies in Patagonia. A practical test of the performance of chironomid-inferred palaeoclimate over the past century, for which the best constrained data currently exist, will allow an insight into whether published chironomid temperature functions are applicable to lakes in central Patagonia. Short cores that cover the period *c.*AD1850 to present will be used to develop a chironomid inferred palaeoclimate record that can be compared with existing meteorological data and palaeoclimate records. This empirically tests the ability or otherwise of chironomid proxies (both quantitative and qualitative) to act as indicators of palaeoclimate, specifically temperature and precipitation. The same empirical process will be used to test the applicability and utility of carbon isotope and geochemical methods to record palaeolimnological and palaeoclimatic changes. This part of the study has the following objectives:

- Compare palaeoclimatic data to local published records of climate change.
- Assess the sensitivity and accuracy of the palaeoclimatic proxies in the context of published data for recent climate in Patagonia.

2.4 Holocene Climate Change

Once the parameters of the chironomid proxy are established using recent material, the same techniques can be used on long overlapping sequences with greater confidence. Given the known problems with dating lake sediments a combined approach of ^{14}C dating combined with the identification of regionally known tephra layers offers the best possibility of an accurate, precise chronology; careful selection of specific material for radiocarbon dating and verifying its suitability should form part of the project. In this respect, the study aims to:

- In conjunction with the published literature, present a record of Holocene climate change in central Patagonia.
- Address the specific palaeoclimatic controversies, disparities and research gaps detailed in Chapter 3.
- Assess the utility of the proxies used in this study to further contribute to research in Patagonia.

2.5 Chronological Uncertainty in Patagonia

A number of studies in Patagonia are limited by the chronological control applied to sediment sequences, and this hampers cross-correlation between sites. This study can improve the chronological framework for Patagonia, and thus contribute to future developments in palaeoclimatic reconstructions, in several ways:

- Developing geochemical characterisation of major regional tephra layers to allow for their use as isochrons.
- Using radioisotope data (^{137}Cs, ^{210}Pb & ^{14}C) to refine the dates of those tephra layers.
- Where possible, obtain basal dates for sediments in the region to contrain the Lateglacial chronology.

Chapter 3

Literature Review

3.1 Introduction

This literature review is split into three parts: the first contextualises the following two sections with an explanation of the climatic characteristics of southernmost South America. The second section reviews the current literature on palaeoclimate of southern South America during the Holocene and outlines the partly equivocal nature of the literature for this time period. The section concludes by outlining three main climate spaces in Patagonia, a summary of the widespread climate events identified in the literature, and identifying gaps in the current understanding of climate in Patagonia. The final part reviews the available data for recent records (<200 year) for the region, focussing on the differences between northern and southern Patagonia, Tierra del Fuego and the Argentinian steppe, detailing the centennial to decadal-scale processes behind recent changes.

3.2 Characteristics of Climate in Patagonia

3.2.1 The Southern Westerly Winds and Precipitation Gradients

Southernmost South America has key links to hemispheric climate processes, principally the southern westerly winds and the Peru-Chile Humbolt current along the west coast. The southern westerlies are the dominant wind from central Chile, *c.*32–40°S in July, to southernmost South America and the Antarctic *c.*42–62°S; seasonally the westerlies shift up to 10° (Jenny, 2002; Barry and Chorley, 2010; see Figure 3.1). The westerly winds shift in both position and intensity seasonally; in summer the precipitation anomaly driven by the winds spans the latitudes *c.*55–35°S, in winter this span contracts to *c.*53–40°S, and the winds intensify (Garreaud *et al.*, 2009). The westerlies are created by the latitudinal pressure gradient between 40–60°S as a result of the pressure gradient

between the Pacific/Atlantic High Pressure Cell and the Antarctic Trough. Changes in the position of the Antarctic Trough will cause changes in both the strength and position of the westerlies over southern South America. The Antarctic Trough is controlled by the position of the Polar Front, and so expansion of polar ice, for example, would lead to an equatorward shift of the southern limit of the westerlies (Wyrwoll, 2000).

The westerlies are associated with a belt of storm tracks along with orographic rainfall of Pacific maritime air masses over the Patagonian Andes; this causes steep longitudinal precipitation gradients on the western seaboard (Garreaud *et al.*, 2009; see Figure 3.2). It is the high precipitation associated with the westerlies that maintains the Patagonian Icecaps and glaciation in Tierra del Fuego, and some of the highest terrestrial rainfall (>4000mm/year) in the world (ibid). The westerlies also influence the Antarctic Circumpolar Current, which keeps warm waters away from the Antarctic coast and drives the currents along the Peru-Chile margin. Ekman divergence moves deep water equator-ward along this path causing upwelling of deep water along the West coast of Chile (Gnanadesikan and Hallberg, 2000), leading to very high productivity centred around 30–40°S (Anderson *et al.*, 2009). The southern westerly winds have been implicated in controlling CO_2 upwelling (Hodgson and Sime, 2010; Bentley *et al.*, 2009) and in modulating the paired thermo-haline system of North Atlantic Deepwater Water/Antarctic Bottom Water production, both significant regional and global climate modulators (Rahmstorf and England, 1997).

In contrast, the lower latitudes of South America are climatically linked to the Hadley circulation, south-east trade winds and hence the position of the equatorial low. They are also affected by El-Niño Southern Oscillation (ENSO) changes in the Pacific. The ENSO primarily affects precipitation in Patagonia; El Niño conditions cause increased rainfall over parts of Patagonia, although the effect is not as pronounced as in the lower latitudes; the positive temperature anomalies seen below 30°S are not present further south (Garreaud and Aceituno, 2007) — the observed spatial and temporal characteristics of ENSO for the past 200 years are discussed more fully in Section 3.4.

3.2.2 Summary

From a palaeoclimate perspective, the linkage of local climate in southernmost South America to regional/hemispheric processes is the most interesting — the questions usually asked of palaeoclimate data refer to regional/hemispheric climate, but most palaeoclimate archives are local in their response to climate. As such, a strong coupling between regional and local climate needs to be established — for southernmost South America, the controlling influence of the southern westerlies on precipitation, and the sensitivity of these high altitude areas to temperature changes make them ideal locations for palaeoclimate studies.

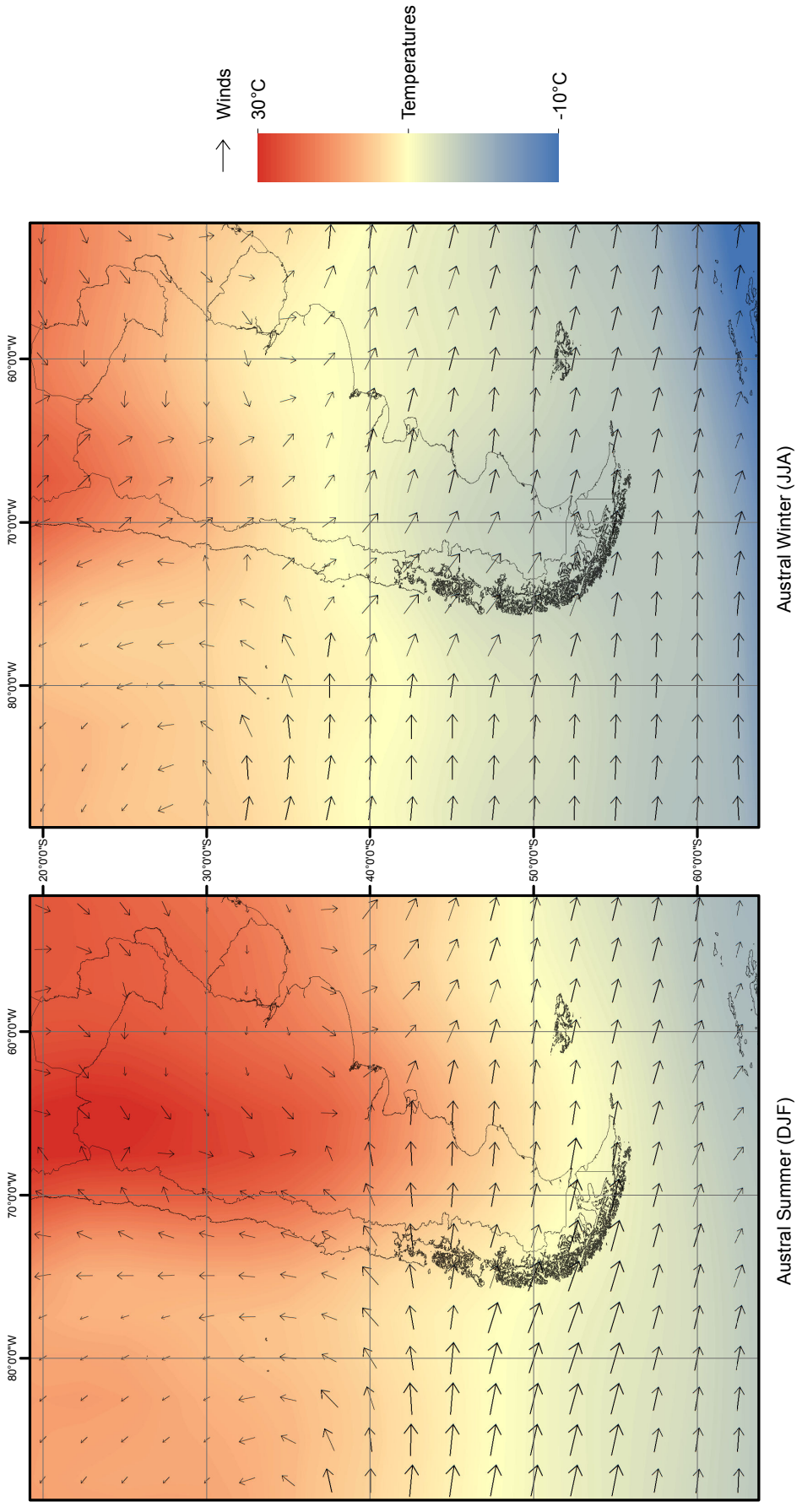

FIGURE 3.1: Average seasonal surface wind speed, direction and temperatures in South America for the period AD1950–2000 from NCAR reanalysis data (Kalnay *et al.*, 1996). Note the stronger summer winds and the latitudinal shift in their extent between summer and winter.

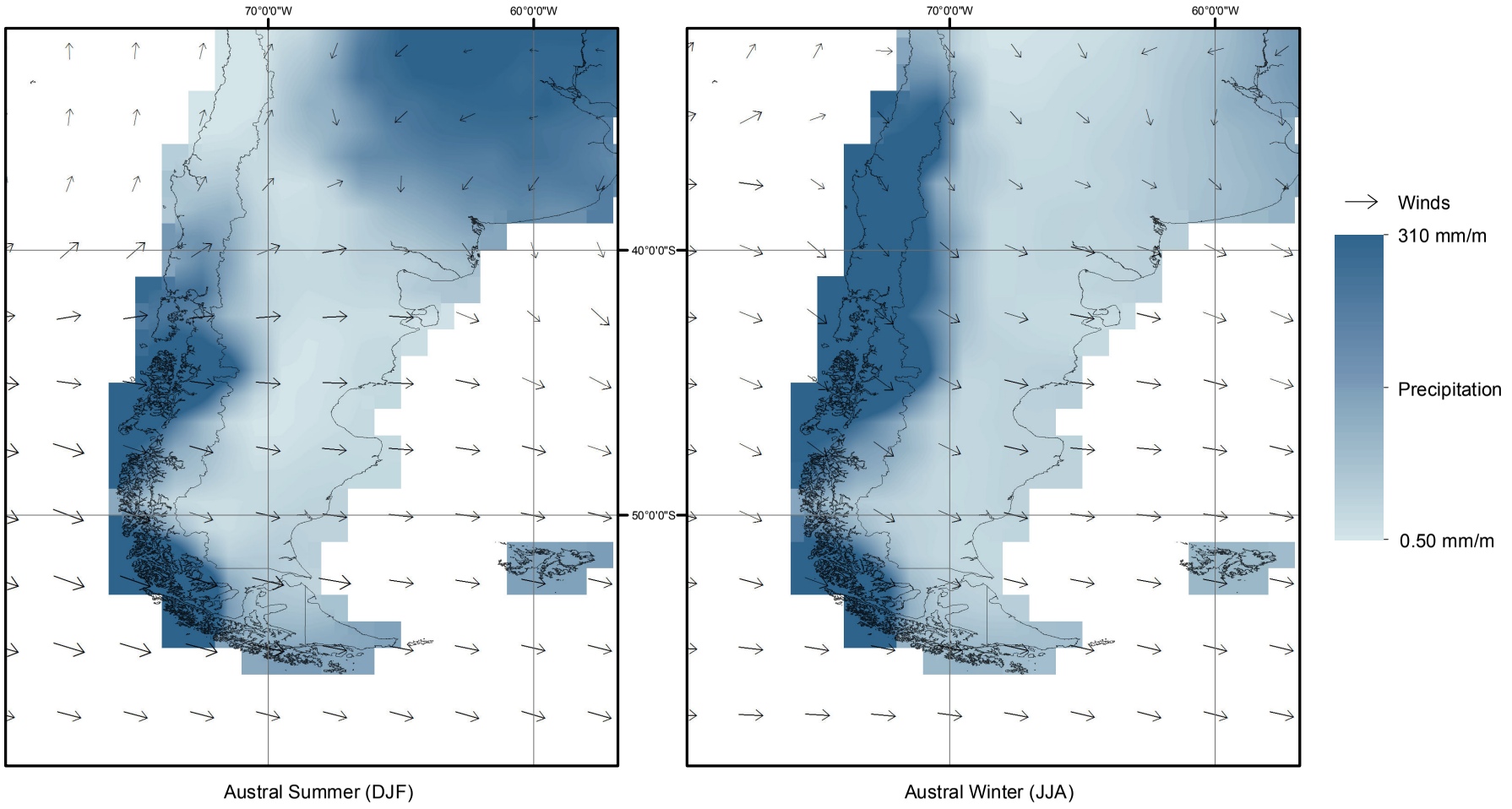

FIGURE 3.2: Average seasonal surface wind speed, direction and precipitation in South America for the period AD1950–2000 from NCAR reanalysis data (Kalnay *et al.*, 1996). Note the stronger summer winds and the latitudinal shift in their extent between summer and winter and the relationship with precipitation.

3.3 Holocene Climate Change in Patagonia

3.3.1 Geographical Distribution of Research and Proxies Commonly Used

Figure 3.3 shows the distribution of sites where Holocene records of palaeoclimate have been produced; Figure 3.4 shows the length of these records. The gaps in the inventory of palaeoclimatic records around 46–48°S lead to problems when attempts are made to synthesise the various records of climate change to discern latitudinal changes in the southern westerlies, particularly the difference between shifts in the position of the westerly winds and changes in the strength of the westerlies. If phenomena that are by definition spatially variable, such as shifts in the westerly winds, are to be understood, a gap in the palaeoclimatic data for the region at the core of the westerly winds is clearly problematic. This study, in part, addresses this geographical gap in the literature.

Although there are numerous archives of long-term change in Patagonia, many studies have focussed on the Lateglacial, answering questions surrounding the Antarctic Cold Reversal in Patagonia. Others focus on recent climate events and address recent climate warming and the "Little Ice Age" in Patagonia. Of those studies that do present data for the Holocene, the vast majority are pollen stratigraphies, the utility of which is discussed in Section 3.3.3. Geochemical indicators of catchment erosion, runoff, or productivity are also used, and isotopes have had limited application as proxies for productivity and hydrological conditions. Chironomid and beetle proxies for palaeoclimate are not numerous but have produced useful and promising results, and peatland archives of palaeoclimate have proved sensitive, not least in Tierra del Feugo.

3.3.2 Termination of the Last Glacial Period

The Antarctic ice-core records have suggested that the last glacial maximum in the southern hemisphere was slightly earlier when compared with the northern hemisphere (shown in Figure 3.5), around 20,000 years B.P. (Blunier and Brook, 2001; Jouzel *et al.*, 2001; Petit *et al.*, 1999; Grootes *et al.*, 2001; Divine *et al.*, 2010), compared to the maximum in Greenland dated at around 18,000 years B.P. (Johnsen *et al.*, 1992). Most Antarctic records of δ^2H and δ^{18}O also suggest a slightly earlier start to deglaciation in Antarctica, with rapid warming around 17,500 years B.P., compared to around 15,000 years in Greenland (ibid), although there is some controversy over some of the chronologies from Antarctica (see Grootes *et al.*, 2001; Stenni *et al.*, 2010).

This asynchronicity has been the subject of considerable debate, as it has been proposed as a feature both of the Quaternary glaciations (Blunier and Brook, 2001; Wolff *et al.*, 2010; Barbante *et al.*, 2006) and Lateglacial climate reversal (Jouzel *et al.*, 1995). The asynchronous timing of the Younger Dryas (12,800–11,000 years B.P.; Johnsen *et al.*

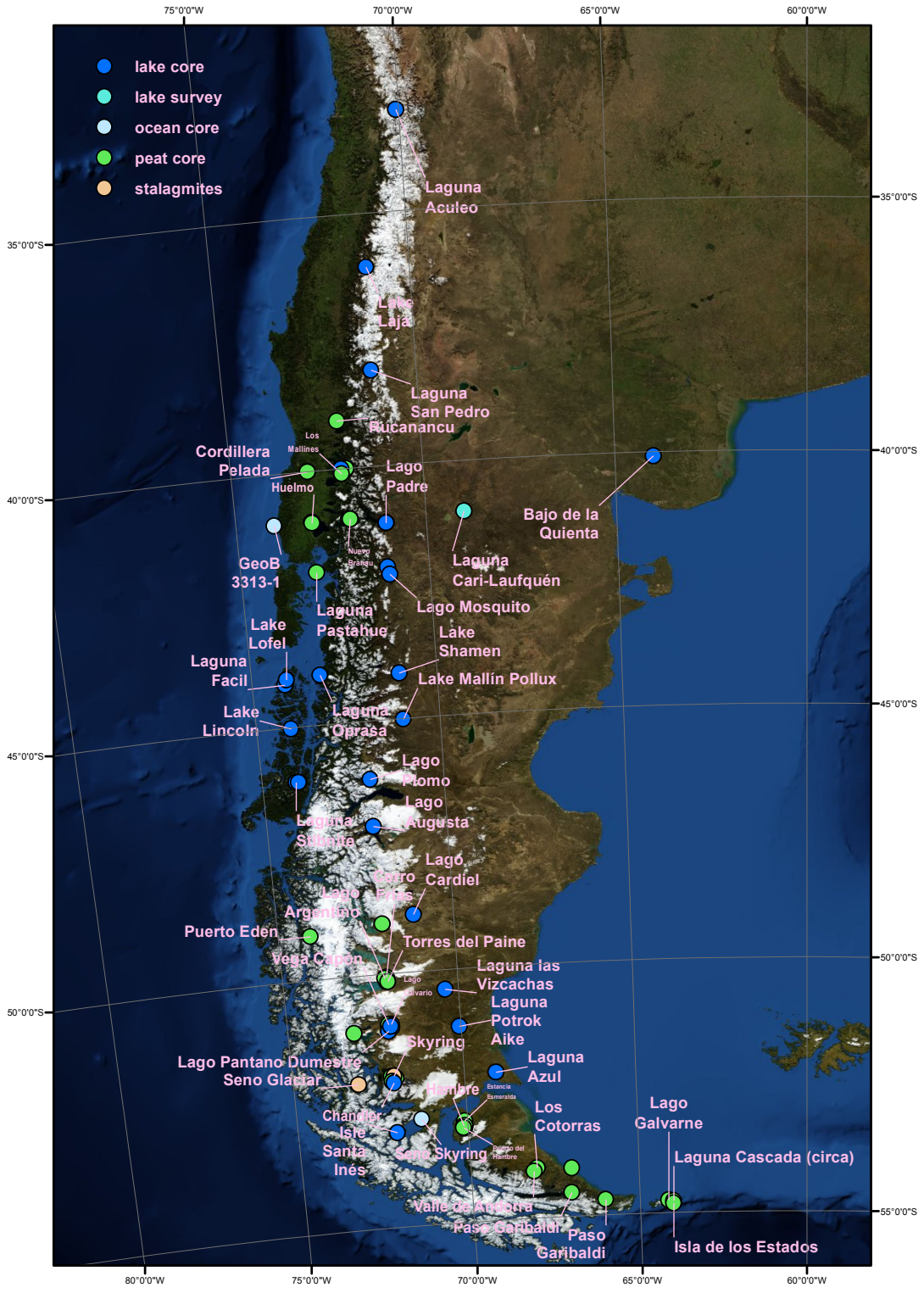

FIGURE 3.3: Selected sites from which available palaeoecological records have been produced for the Holocene and/or Lateglacial in Patagonia. See Appendix B for a list of sources used.

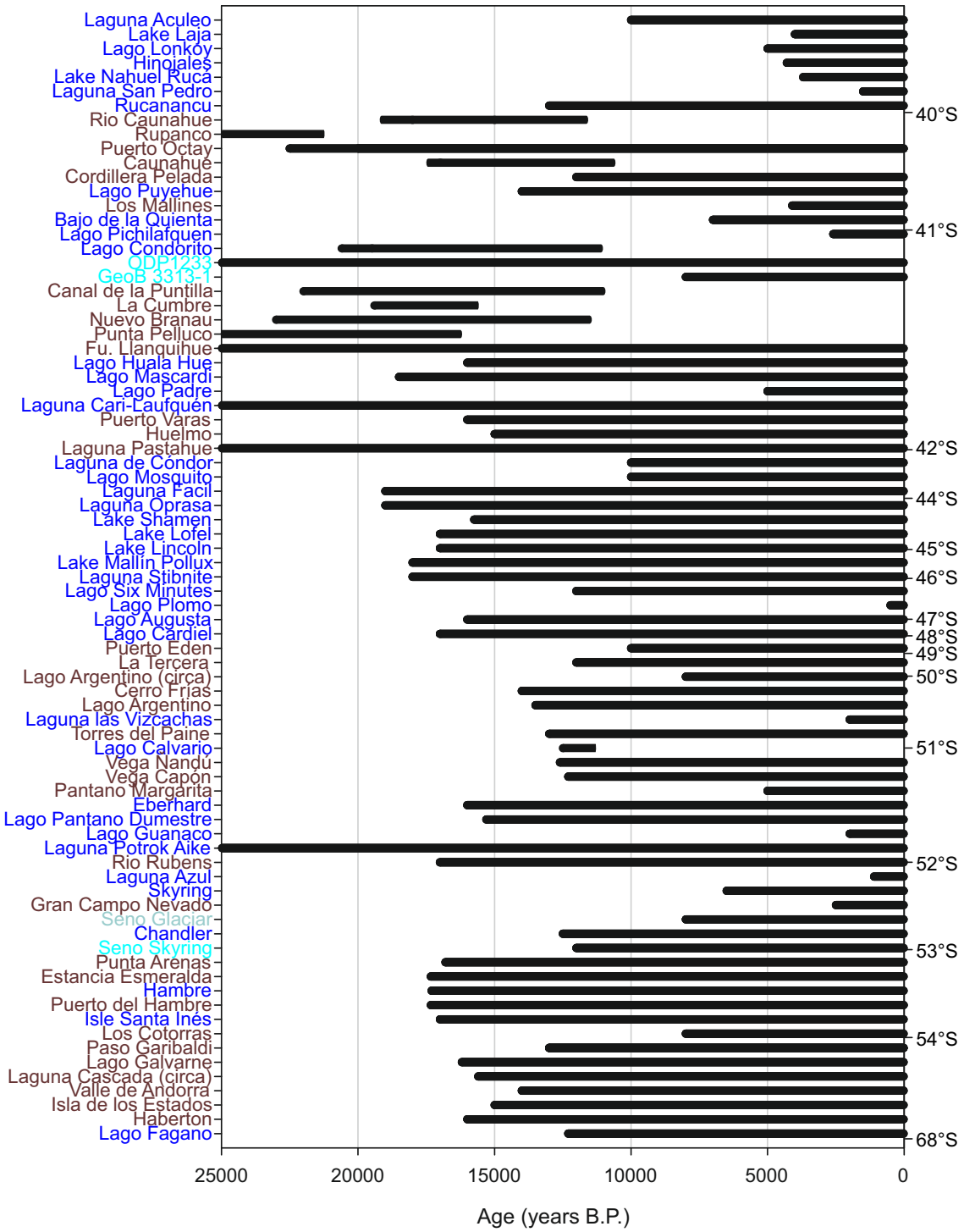

FIGURE 3.4: Time-span of the published data for selected sites from which palaeoecological records have been produced for the Holocene and/or Lateglacial in Patagonia, arranged by latitude (shown on the right). Lake sites are shown in dark blue, bogs or terrestrial sections are shown in brown, ocean cores in light blue and cave sites in grey. See Figure 3.3 for selected locations. See Appendix B for a list of sources used.

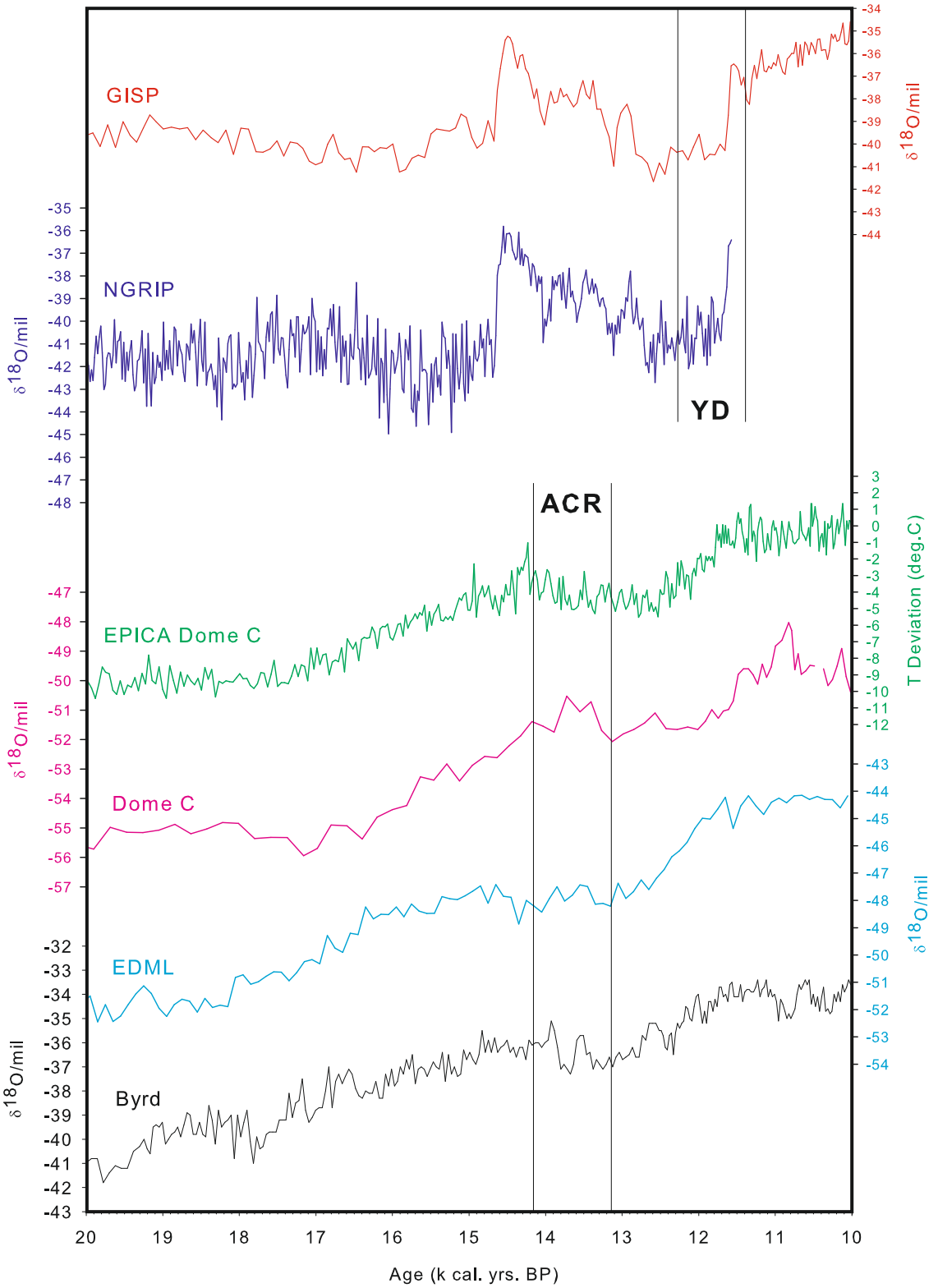

FIGURE 3.5: Summary of Greenland (GISP, NGRIP) and Antarctic (EPICA Dome Condcordia, Dome Concordia, EPICA Dronning Maud Land and Byrd) cores with the accepted ages for both the Younger Dryas (YD) and the Antarctic Cold Reversal (ACR). Note the subtly different timing fir the Antarctic Cold Reversal between the different Antarctic Records. Data from NOAA repositories.

1992) and the Antarctic Cold Reversal (14–12,000 years B.P.; Morgan *et al.* 2002) has been the subject of considerable research interest, particularly in ocean and terrestrial environments, and the expression of a Lateglacial climate reversal in Patagonia is unclear at present. The clear two-step warming in Antarctica during the period 18–11,000 years B.P. is also present in ocean cores from sites across the southern hemisphere (Kaiser *et al.*, 2005; Carter *et al.*, 2008; Barker *et al.*, 2009; Stenni *et al.*, 2001; Andres *et al.*, 2003; Calvo *et al.*, 2007), but in austral regions not directly connected to polar climates the evidence of the presence of the Antarctic Cold Reversal, the Younger Dryas or some event intermediate to the two is equivocal.

Most Patagonian climate records show constant warming throughout the Lateglacial (Bennett *et al.*, 2000; Haberle and Bennett, 2004; McCulloch and Davies, 2001), although this may be a function of the dominance of pollen proxies for climate, where post-glacial forest development may mask any climate signal (Bennett *et al.*, 2000). Other proxies often suggest small oscillations (Wille *et al.*, 2007; Ariztegui *et al.*, 2010; Heusser and Rabassa, 1987; Markgraf, 1991) that are likely to be difficult to detect using pollen proxies. In Tierra del Fuego multi-proxy studies have identified a cool and unstable climate during the Antarctic Cold Reversal (Pendall *et al.*, 2001; Markgraf and Huber, 2010), in keeping with glacial evidence of stand-still or small advances during the Late-glacial across Patagonia (Fogwill and Kubik, 2005; Moreno *et al.*, 2009; Turner *et al.*, 2005).

Cooling has also been inferred from pollen records in the Chilean Lake District during the Lateglacial (Ariztegui *et al.*, 1997; Moreno *et al.*, 1999; Moreno, 1997). There is evidence from the region of a climate deterioration intermediate to the Antarctic Cold Reversal and the Younger Dryas — referred to as the Huelmo-Mascardi Event (Hajdas, 2003), where there is evidence from pollen (Moreno *et al.*, 2001) and chironomids (Massaferro *et al.*, 2009) that suggest a cool, temperate period with two main phases; an initial wet phase between 13,500–12,800 years B.P. followed by a drier phase between 12,800–11,500 years B.P. The nearby Lago Puyehue offers limited support for this hypothesis, identifying an event in the geophysical proxies midway through the Antarctic Cold Reversal and another at the Antarctic Cold Reversal/Younger Dryas boundary (Boës and Fagel, 2007a; Charlet *et al.*, 2007; Bertrand *et al.*, 2008; Boës and Fagel, 2007b; Bertrand *et al.*, 2007), although diatom and pollen proxies do not record any change in the lake during the Lateglacial (Sterken *et al.*, 2007; Vargas-Ramirez *et al.*, 2007), in keeping with other lacustrine sequences in the region (Hoganson and Ashworth, 1992; Massaferro *et al.*, 2005).

There is a similar debate regarding the Lateglacial in New Zealand; pollen and chironomid records suggest cooling of 2–3°C during the Antarctic Cold Reversal (Vandergoes *et al.*, 2008), supported by pollen and speleothem records (Newnham and Lowe, 2000; Hajdas *et al.*, 2006; Williams *et al.*, 2005) although there is some variation in the chronologies. The glacial evidence is controversial but has been invoked as evidence of advance during the Antarctic Cold Reversal (Barrows *et al.*, 2007; Applegate *et al.*,

2008; Santamaria Tovar *et al.*, 2008; Putnam *et al.*, 2010), but there is evidence for a mix of signals spanning the islands (Alloway *et al.*, 2007; Hajdas *et al.*, 2006), indicating the bi-polar see-saw expands into the southern terrestrial mid-latitudes (Newnham *et al.*, 2012).

3.3.3 Vegetation and Fire Variability

The pollen compositions of Patagonian records from the Holocene are dominated by *Nothofagus* (often along with its parasitic mistletoe *Misodendrum*) and Poaceae, with a limited contributions from some shrubs and herbs. Ocean core records of pollen rain from the continent indicate significant changes in the overall composition of pollen rain at the termination of the last glacial in Patagonia (Pisias *et al.*, 2006). There are very low concentrations of forest taxa in records from the Lateglacial, suggesting contracted forests across Patagonia due to ice-cover, cooler conditions and decreased precipitation east of the Andes because of expanded ice-caps (Kilian and Lamy, 2012; Wille *et al.*, 2007). During glacials the landscape is dominated by grasses, with limited *Nothofagus* stands; *Nothofagus* probably finds refugia along the wetter margins of the east coast and further to the north (Heusser, 1981; Heusser *et al.*, 1999). Forest expansion occurs roughly synchronously between 10–11,000 years B.P. in Tierra del Fuego (Kilian and Lamy, 2012; Fontana and Bennett, 2012), with expansion occuring at different speeds, but often reaching stable concentrations within 1,000 years, where it continues to dominate throughout the Holocene. In more northerly areas the expansion is earlier and more rapid; in the Chonos Archipelago forest expansion starts at 14,700 years B.P. and is stable within 1,000 years of the initial rise (Haberle and Bennett, 2004), although in the nearby Chacabuco Valley on the opposite side of the North Patagonian Icecap forest expansion starts later and takes until 10,000 years B.P. to stabilise (Villa-Martínez *et al.*, 2012).

The dominance of stable *Nothofagus* forest across Patagonia throughout the Holocene makes interpretation of climatic events from the record difficult. Despite this there are a number of potential regional vegetation changes throughout the Holocene, the most consistent and common of which is a switch in regional vegetation from 4,500–5,500 years B.P. onwards. The expression of this climate event varies: in northern Patagonia it is a shift to more humid climates (Heusser, 1982; Vargas-Ramirez *et al.*, 2007; Iglesias *et al.*, 2012, 2011), or an increased seasonality (de Porras *et al.*, 2012), but in southern Patagonia the trend diverges into a cluster of records indicating drier and/or cooler conditions (Ashworth *et al.*, 1991; Sottile *et al.*, 2011; Mancini, 2002) or more humid conditions (Moreno *et al.*, 2009, 2012; Markgraf and Huber, 2010; Heusser, 1995). In northern Patagonia precipitation is linked with the strength of the westerlies, suggesting enhanced westerlies after 5,000 years B.P., but in Tierra del Fuego the results are mixed. Cooler and drier conditions in the eastern region are consistent with polar incursions, suggesting decreased westerly wind strength on the southern margin of the wind belt at

this time, but there are conflicting data that could suggest enhanced winds at this time. Almost all studies make other inferences for additional periods of change — there is no clear pattern across Patagonia.

A pollen transfer function has been developed for the semi-arid Argentinian steppe between 49–54°S in order to interpret the pollen stratigraphy from Laguna Potrok Aike (Schäbitz *et al.*, 2013). The data indicate that *Nothofagus* forest has a strong relationship with annual precipitation, and Schäbitz *et al.* used modern training data to produce precipitation reconstructions. Although pollen derived training sets are problematic, particularly from single site reconstructions (Ohlwein and Wahl, 2012), this is an improvement on previous interpretations of the Potrok Aike pollen stratigraphy (*viz.* Wille *et al.*, 2007). A comparison to the other quantative pollen based reconstruction of precipitation in Tierra del Fuego (Tonello *et al.*, 2009) suggests arid phases centered on 11,000, 8,200 and 6,200 years B.P. in the region, but in the later part of the record there are divergent trends. Schäbitz *et al.* suggest this is representative of opposing regional climate signals, where pollen records north of 50°S decrease in moisture availability during the later part of the Holocene.

These inferences are supported by the fire history of Patagonia, as fire occurence is most strongly linked to aridity (Kitzberger, 1997), although anthropogenic influence may also be significant in increasing occurrence (Veblen *et al.*, 2003). Natural ignition by lightning strike occurs only during spring and summer storms (Lara and Villalba, 1993), so summer aridity could lead to an increase in fire occurence. Charcoal is often studied alongside pollen, and so a number of fire histories are available for the Holocene (Markgraf and Huber, 2010). The climate change centered on or around 5,000 years B.P. is also apparent in the charcoal records, where in some areas a reduction in charcoal abundance suggests more humid conditions during the later Holocene; in the early Holocene, despite increasing precipitation, summers must have been relatively dry as fire occurence is high (Markgraf *et al.*, 2007; Markgraf and Huber, 2010; Iglesias *et al.*, 2011; Villa-Martínez *et al.*, 2012; Williams *et al.*, 2012; Huber *et al.*, 2004), although this may be due to increased fuel availability due to expansion of forest at this time (de Porras *et al.*, 2012). The importance of human interference cannot be discounted when interpreting charcoal records from Patagonia (Holz and Veblen, 2011; Kilian and Lamy, 2012), and some reduction in forest density in the late Holocene may be maintained by anthropogenic fire (*e.g.* Urrego *et al.*, 2011), although in natural regimes some fire disturbance may actually promote higher densities of forest (Iglesias *et al.*, 2012).

3.3.3.1 Glacier Fluctuations Driven by Precipitation Change

Glaciers in areas of high precipitation where snowlines are at or below the 0°C isotherm are likely to be especially sensitive to temperature change and insensitive to changes in precipitation (Rodbell *et al.*, 2009) — this encompasses much of the Andes, so Patagonian glaciers can be considered sensitive to Holocene climate change. There are a

number of moraine systems younger than those dated to the Last Glacial Maximum but older than those relating to Little Ice Age re-advance (*e.g.* Glasser *et al.*, 2008, 2004). Rodbell *et al.* (2009) suggest three to four moraine building events in Patagonia over the past 5,000 years:

- the Little Ice Age (*c.*350 years B.P., but temporally variable in Patagonia)
- around 2,500 years B.P.
- two older events that are spatially and temporally variable.

Of these, the 2,500 year B.P. cluster is syncronous with a number of other climate changes across Patagonia; for example, at Laguna Potrok Aike increased humidity around 2,500 years (Schäbitz *et al.*, 2013; Wille *et al.*, 2007), and similar changes are seen elsewhere in Patagonia (*e.g.* Massaferro and Brooks, 2002) at this time, contradicting Rodbell *et al.* (2009) by suggesting precipitation rather than temperature best explains glacier expansion at this time.

3.3.4 Holocene Fluctuations in the Southern Westerly Winds

3.3.4.1 Introduction

The link between the position and intensity of the westerly winds has been established in Section 3.2. What follows is a summary of the Holocene palaeoclimatic histories of northern, central and southern Patagonia; primarily changes in precipitation and temperatures are presented, which are inferred to be reflective of the position and/or intensity of the westerlies.

3.3.4.2 Northern Patagonia

In the northern region between 35–45°S, particularly in and around the Chilean Lake District and the Nahuel Huapi National Park, lake archives have been examined particularly for geochemical proxies used to infer catchment conditions. Northern Patagonia has been a focus of research into Holocene climate, including well characterised ocean cores that have yielded particularly good records of Holocene sea surface temperature (Heusser *et al.*, 2006; Lamy *et al.*, 2002), and lake sediments that have provided the first quantitative reconstructions of Holocene precipitation in Patagonia (Jenny, 2002).

Both records infer periods of change during the Holocene, and in Laguna Facil a shift in the chironomid fauna at 7,200 years B.P. occurs in advance of a shift in vegetation, demonstrating the utility of chironomids over vegetation, as the lagged response to climate is evident in the pollen record (Massaferro *et al.*, 2005).

The well-studied Lago Puyehue (Bertrand *et al.*, 2007; Batist *et al.*, 2007; Bertrand *et al.*, 2008; Charlet *et al.*, 2007; Sterken *et al.*, 2007) presents a full Holocene record that indicates an early Holocene optimum in productivity, followed by lower and highly variable productivity between 6–3,500 years B.P., and also indicates a "cold and/or humid event between 3,400–2,900 [years B.P.]" (Bertrand *et al.*, 2007, p.191), although this is not present in the pollen stratigraphy (Sterken *et al.*, 2007). Other pollen studies from the region do not reflect this change either (Bianchi and Ariztegui, 2011), but a mid-Holocene shift in climate around 5,000 years B.P. is observed at a number of sites in the north (Bianchi and Ariztegui, 2011; Iglesias *et al.*, 2011; Haberle and Bennett, 2004; Iglesias *et al.*, 2011; Jenny, 2002; Ortega *et al.*, 2012; Riquelme *et al.*, 2011; Sterken *et al.*, 2007), considered to be a result of stabilisation of the modern ENSO regime and stronger westerlies (Fletcher and Moreno, 2012a; Ortega *et al.*, 2012). Changes around 3,000 years B.P. are observed in a number of records, but the nature of changes varies: Jenny (2002) and Sterken *et al.* (2007) find wetter conditions, but Marcos *et al.* (2012) infer semi-arid conditions at the same time in northern Patagonia.

3.3.4.3 Central Patagonia

In central Patagonia the few palaeoclimate reconstructions are from the Chonos Archipelago, the vicinity of Coyhaique and, noteably, from Lago Cardiel in Argentina. As previously discussed, central Patagonia (between 45–50°S) has the fewest palaeoclimatic studies of Holocene environments in Patagonia. Almost all studies suggest precipitation and temperature equivalent to modern conditions from between 7,500–8,000 years B.P. onwards (*e.g.* Wille and Schäbitz, 2008; Villa-Martínez *et al.*, 2012; Haberle and Bennett, 2004; Massaferro *et al.*, 2005; Markgraf *et al.*, 2007; de Porras *et al.*, 2012; Ashworth *et al.*, 1991), although slightly earlier dates are found by Bennett *et al.* (2000); Massaferro and Brooks (2002).

Many records suggest stable conditions throughout the Holocene, possibly due to the lack of sensitivity of pollen records (Section 3.3.3), for example Villa-Martínez *et al.* (2012); Wille and Schäbitz (2008). There is some evidence of the mid-Holocene shift in climate, better represented in more northerly regions described previously; Sottile *et al.* (2011) suggested increasing occurence of polar incursions from 5,000 years B.P. onwards at a site on the eastern margin of the south Patagonian icecap, and mid-Holocene climate shifts are also suggested further north in the Chonos Archipelago (Bennett *et al.*, 2000; Massaferro and Brooks, 2002; Haberle and Bennett, 2004). A common feature of records in this region is a shift from moisture conditions equivalent to the modern towards drier conditions from *c.*3,000 years B.P. to around 1,000 years B.P. (*e.g.* Massaferro and Brooks, 2002; Markgraf *et al.*, 2007; de Porras *et al.*, 2012), and quantitative reconstructions suggest peak precipitation at 3,000 years B.P., subsequently decreasing (Tonello *et al.* 2009, shown in Figure 3.6). Older insect-based palaeoclimate records suggest the opposite of this trend — Ashworth *et al.* (1991) suggest drier

conditions from 3,000 years B.P. onwards compared to the previous 3,000 years. The chironomid stratigraphy from Laguna Stibnite indicates drier conditions between 10,500–7,100 and 2,400–1,450 years B.P (Massaferro and Brooks, 2002), broadly consistent with other data for the region.

For Lago Cardiel, located at 49°S in the Argentine steppe, Markgraf *et al.* (2003) use a multiproxy sedimentological and palaeoenvironmental data to register the inception of a wind-driven depositional lake current from 6,800 years B.P. onwards (see also Gilli *et al.*, 2005), and a reduction in lake level from 6,000 years B.P.

3.3.4.4 Southern Patagonia

In southern Patagonia, palaeoclimatic data have mainly been derived from peatland archives such as macrofossil stratigraphy, or occasionally peat macrofossil stable isotopes (Pendall *et al.*, 2001). Laguna Potrok Aike (the focus of the PASADO research project, Recasens *et al.* 2011) is a noteable exception, as the long record from the lake has been extensively studied. Because southern Patagonia has been a focus of research, enough data has been produced to allow Kilian and Lamy (2012) to review the palaeoclimatological history of the region. They concluded there was evidence for an early Holocene thermal maxima (11,500–8,500 years B.P.) and a brief period of increased westerly wind strength from 5,500 years B.P. in the southern region. Like nothern and central regions, there is extensive pollen-based evidence for a mid-Holocene climate shift in this region (*e.g.* Markgraf and Huber, 2010; Markgraf *et al.*, 2003).

A chironomid training set developed for Laguna Potrok Aike and its surrounding region indicates that mean annual temperature is a high-order control on chironomid fauna. This allowed Massaferro and Larocque-Tobler (2013) to infer temperatures for the past 15,000 years at the site. They found temperatures were generally low until around 10,500 years B.P., where temperatures increase gradually until peaking around 7,000 years B.P., followed by a slow decline until around 3,500 years B.P., followed by stabilisation until present. There is further evidence from Laguna Potrok Aike that supports the chironomid record; a drop in the shoreline at the site around 6,590 years B.P. is consistent with peak temperatures around 7,000 years B.P. at the site, but the severity of the shoreline drop (33m below present-day) cannot be explained by increased evaporative losses alone, suggesting more arid conditions in the steppe at this time; this is in keeping with the pollen record from the site (Wille *et al.*, 2007). The lake level drop was accompanied by increased incision and soil deposition to the lake as reflected in $\delta^{13}C$ values in the sediment (Mayr *et al.*, 2008), although the quantitative pollen-based precipitation proxy indicates reduced rainfall at the site from 8,000–2,500 years B.P (Schäbitz *et al.*, 2013). These pollen records are similar to those presented for the northern sector, *e.g.* Fontana and Bennett (2012).

Compared to Lago Cardiel (49°S), conflicting climate signals are recorded in that drier,

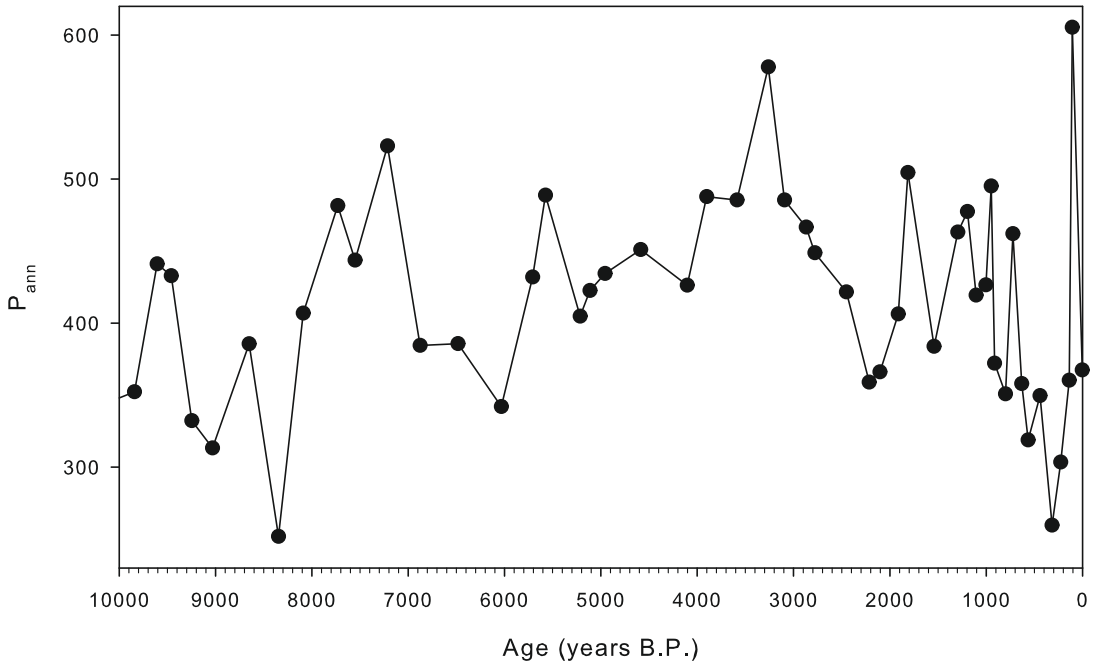

FIGURE 3.6: Inferred Palaeoprecipitation for central Patagonia, redrawn from Tonello *et al.* (2009).

more variable conditions are inferred from 6,000 years B.P. onwards (Markgraf *et al.*, 2003), although changes are also inferred at 6,800 years B.P., where wind conditions changed to a roughly modern configuration, as reflected in the sediment stratigraphy of Lago Cardiel (Anselmetti *et al.*, 2009; Gilli *et al.*, 2005).

A late-Holocene climate shift is suggested in fewer records than for northern and central regions, but Markgraf and Huber (2010) do find evidence for cooler conditions between 2,400–400 years B.P., and Pendall *et al.* (2001) infer a cold period around 2,000 years B.P. on the basis of δ^2H of plant macrofossils, that is noteably absent from their adjoining pollen stratigraphy.

3.3.4.5 Summary

The extensive pollen-based palaeoenvironmental reconstructions are largely equivocal when it comes to reconstructing changes in the southern westerly winds, in part because pollen proxies are subject to confounding lags, forest development and anthropogenic modification. It is also difficult to discern between changes in temperature and changes in precipitation using vegetation proxies alone. Although regional pollen training sets go some way towards solving these problems, other proxies have been explored to provide palaeoclimatic data.

Across Patagonia, many pollen records infer a climate shift around 5,000 years B.P. they

attribute to the southern westerly winds and the El Niño Southern Oscillation reaching broadly modern positions at this time, but other non-pollen records suggest an earlier change, around 6,500–7,000 years B.P.; for example, at Laguna Potrok Aike pollen records suggest a shift to drier conditions at 6,000 years B.P. (Markgraf *et al.*, 2003), but a drop in lake volume at the same site has the earlier date of 6,600 years B.P. and the chironomid stratigraphy suggests changes earlier still at 7,000 years B.P. It is possible that the lag and insensitivity of pollen palaeoclimate proxies (Section 3.3.3) means that widespread climate shift at 5,000 years B.P. actually occurs earlier — poor chronological control may play a part in explaining this temporal variability.

Unlike the widespread evidence for an early Holocene climatic optimum and a mid-Holocene climate shift, there is some evidence for an early Holocene event around 7,000 years B.P., as well as widespread but conflicting evidence for a late-Holocene event around 3,000 years B.P., where not only does the timing for the event vary by up to 500 years between records, but has been variously ascribed to cooler, warmer, wetter and drier conditions.

3.3.4.6 Consistency and Causation of Shifting Southern Westerlies

Although the southern westerly winds are invariably invoked as the cause of inferred palaeoclimatic changes in Patagonia, the explanations between studies are as contradictory as the palaeoclimatic records themselves. The climatology of Patagonia and the anatomy of the southern westerly winds is discussed fully in Section 3.2, but essentially their spatial extent is modulated on the southern margin by the position of the the polar front, on the northern margin by the sub-tropical anti-cyclone, and the vigour of the westerlies is determined by the latitudinal pressure gradient. A number of ad-hoc explanations have been formulated to explain observed patterns in individual sites or localities, but no explanation can accomodate all of the palaeoclimatic records; for example, shifts in climate in the mid to late Holocene have been variously attributed to:

- enhanced southern westerly winds north of 50°S as a result of a 1–3° shift in the maximum wind speed (de Porras *et al.*, 2012; Rojas *et al.*, 2008), that cause increased precipitation over central and northern Patagonia,
- enhanced westerly winds (Iglesias *et al.*, 2011),
- changes in ENSO events (Iglesias *et al.*, 2012; Sottile *et al.*, 2011),
- southward shift in the southern westerly winds bringing more rainfall (Heusser, 1982),
- general northward shift in the westerlies throughout the Holocene (Heusser, 1995),
- cycling wetter/drier episodes due to latitudinal shifts in the westerly storm tracks (Ashworth *et al.*, 1991),

- increased vigour of southern westerly winds that push humid air further east (ibid),
- polar air-mass intrusions to the continent (Sottile *et al.*, 2011),
- weakened westerly winds allowing easterly air mass incursions on Tierra del Fuego, increasing precipitation (ibid),
- stepwise shifts in the latitudinal position of the westerlies throughout the Holocene towards their modern positions (Moreno *et al.*, 1999),
- stabilisation of the westerlies in the mid-Holocene (Markgraf and Huber, 2010),
- weakening and southward shift of westerlies during early Holocene and strengthening during the mid-Holocene (Tonello *et al.*, 2009),
- a weakened tropical high pressure cell leading to northward expansion of the westerlies (Jenny, 2002).

These are obviously inharmonious at best. Some of the confusion arises from an inconsiderate and/or inconsistent approach to comparisons between climatic zones in Patagonia: east of the Andes in steppe environments the southern westerly winds have a drying effect, as they reduce the incidence of Atlantic-derived precipitation in the region. In the southernmost regions of Tierra del Fuego the westerlies reduce the number, duration and severity of polar incursions, and thus effectively increase precipitation. However, in the western parts of Tierra del Fuego stronger westerly winds will carry more moist air further into the region, bring more storm tracks and thus have the effect of increasing precipitation. In the north Patagonian sector near the limit of the influence of the westerlies, both shifts in the strength and position of the westerlies are likely to register; strengthening would lead to increased maritime conditions, but weakening or a poleward shift would allow weak anticyclonic circulation to the north to shift subtropical airmasses across northern Patagonia.

In central Patagonia, which encompasses the region of strongest zonal flow, shifts in the westerlies would have little effect, unless subjected to a modified meridional pressure gradient, increasing the strength of the westerlies and increasing precipitation quantity and pushing maritime airmasses further into the Argentinian steppe. It follows that the same change in the nature of the westerlies will have radically different, sometimes completely opposite effects in different areas of Patagonia.

3.3.5 Summary

The current palaeoclimate data for Patagonia is spatially inadequate, in terms of density and distribution of study sites, and temporally inadequate in terms of the number of records presenting a full Holocene record, to answer many of the pertinent research questions for Holocene-epoch Patagonia. The main proxy used, vegetation inferred from

pollen analysis, offers limited scope for answering questions of potentially small, cyclical shifts in Patagonian climate when most pollen records from the region are dominated by either forest or grasses. Despite these limitations, there are clear indications that the Holocene has seen considerable climate change, most noteably a shift around 5,000 years B.P. to generally more humid conditions in the northern sector, and lower winds in the southern sector, leading to increasing humidity in the west but allowing increased frequency of polar airmass incursions towards the east. This is in keeping with the findings of Fletcher and Moreno (2012a) who suggest westerly winds reaching their modern configuration around 5,000 years B.P. However, where Fletcher and Moreno suggest zonal asymmetry develops with modern ENSO conditions around 5,000 years B.P., there also appears to be considerable heterogeneity in regional climate changes in the early Holocene.

There is also a pattern emerging of a very different climatic history in the central region between *c.*44–48°S, where climate changes seem to occur around 7,000 and 2,500 years B.P. in a number of records. The paucity of data from the region makes these changes difficult to characterise with any certainty, and better records from central Patagonia is key to addressing these questions.

3.4 Recent Climate Change in Patagonia

3.4.1 Introduction

A number of climatic processes have been identified as modulating small-magnitude decadal-scale climate variations observed in southernmost South America, including El Niño Southern Oscillation, Southern Annular Mode and the Antarctic Oscillation (Garreaud *et al.*, 2009), anthropogenic global warming (Rabassa, 2009) and teleconnections to the tropics (Vimeux *et al.*, 2009). However the instrumental data are problematic in both temporal and spatial extent (Prieto and García Herrera, 2009), and many of the available palaeoclimatic reconstructions are either qualitative, dimensionless or have poor accuracy; this limits our ability to identify the relative importance and differentiate the effects of specific climatic processes from one another. Better characterising the climate history of southernmost South America is essential to understanding the hemispheric and global scale processes that modulate the regions climate, essential in further testing and refining the global climate models on which our predictions of future climate scenarios are developed (Caseldine *et al.*, 2010), and in interpreting longer palaeoclimatic archives in terms of climate processes.

Records of instrumental climate data covering the 20$^{\text{th}}$ century and parts of the 19$^{\text{th}}$ century exist for a small number of regions located predominately in Europe, but for southernmost South America only limited data are available (Prieto and García Herrera, 2009). It is now possible to infer palaeoclimatic changes with a temporal accuracy of

decades to years using tree-rings, varved sediments and short-lived radionuclide dating, but the climate proxies (usually for temperature or precipitation) used are limited to qualitative inferences or to a limited number of quantitative proxies, often derived from calibration-in-time approaches.

The recent (<200 years B.P.) palaeoclimatic knowledge currently available for Patagonia is based predominately on tree rings, geochemical/geophysical proxies and chironomids from lake sediments. Chironomids have been used as quantitative indicators of palaeoclimate in the polar regions (Langdon *et al.*, 2011), Europe (Bitušík *et al.*, 2009; Plociennik *et al.*, 2011; Watson *et al.*, 2010; Heiri, 2007), North America (Lotter *et al.*, 1999), Canada (Porinchu *et al.*, 2008), New Zealand (Woodward and Shulmeister, 2007) and Australia (Rees *et al.*, 2008) with considerable success, and in northern Patagonia qualitatively (Guilizzoni *et al.*, 2009; Massaferro and Brooks, 2002; Massaferro *et al.*, 2005, 2009), offering considerable insight into terrestrial climate changes during the Lateglacial in particular, but there have only recently been attempts at quantative analysis for recent sediments in Patagonia (Massaferro and Larocque-Tobler, 2013; Massaferro *et al.*, 2014). The utility of qualitative and descriptive climate proxies outside of palaeoclimate reconstructions (*e.g.* global climate model development) is limited; quantitative estimates are desirable for Patagonia and given the success elsewhere in the southern hemisphere (*e.g.* Verschuren and Eggermont, 2006), should be a possibility.

The following section reviews the available instrumental (Section 3.4.2) and palaeoclimatic proxy data (Section 3.4.3) for Patagonia, including the hemispheric and global scale processes that have been implicated in modulating climate in the region. The following sections are broadly structured by region and conclude with a summary of quantitative climate records for central Patagonia, a statement of the hemispheric-scale processes that influence the region and a synthesis of the most important observed changes in climate during the past 200 years, focussing on the central region.

3.4.2 Instrumental Records

3.4.2.1 Gridded Data

There is little observational data available for the region, and station data is discontinuous, with the earliest records going back to the early 1950's (Garreaud *et al.*, 2009). The gridded CRU-TS climatological data (New *et al.*, 2002; Mitchell and Jones, 2005) provide something of a solution to these spatial and temporal discontinuities; the gridded data for the 0.5x0.5° cell covering the Chacabuco Valley has been extracted (Figure 3.7), normalised and the mean austral summer temperatures and precipitation (T_{DJF} and P_{DJF}) were compared to the nearest available station data from Puerto Aysen (Figure 3.8). Although strongly and significantly correlated (Table 3.1) there is a danger of circularity as these station data have almost certainly formed part of the original data from which the CRU-TS data are derived, although the raw data are unavailable to

confirm this (see Figure 3.8 for a detailed comparison). Nevertheless the CRU-TS gridded data for the region are the most suitable substitute for station data as it fills gaps in the record, and it is preferable to alternative datasets (*e.g.* NCAR reanalysis data; Kalnay *et al.*, 1996) owing to its better spatial resolution. The mountainous topography and the climatic effects of the North Patagonian Icecap could be expected to lead to considerable variation in temperature and precipitation at scales smaller than that resolved by the CRU-TS grid, and thus gridded data could be considered problematic when used at anything less than regional scale.

3.4.2.2 Climate Indices

Climate in the region is linked to hemispheric and global climate via the El-Niño Southern Oscillation (ENSO), Pacific-Decadal Oscillation (PDO) and Southern Annular mode (SAM) (Vimeux *et al.*, 2009), which is also known as the Antarctic Oscillation (AO). ENSO plays an important role in modulating precipitation and temperature across much of South America; in Patagonia positive (warm) El Niño events are related to drier and cooler summer conditions in central Chile (Montecinos *et al.*, 2000). The PDO has a similar pattern of change to the ENSO-related changes although of smaller amplitude, and the northerly climate shift in the mid 1970's is coincident with a change in state of the PDO from cold to warm mode (Garreaud *et al.*, 2009). The SAM/AO (Figure 3.9) is defined as a pressure anomaly of one sign centred on the Antarctic that causes changes of the opposite sign in a band between 40–50°S; in southernmost South America it is the dominant inter-annual control on temperature (ibid). In the past 50 years there has been a trend towards increased frequency of positive Antarctic Oscillation Index (AAO; Marshall 2003) linked with a decrease in ozone (Arblaster, 2006) which would cause summer warming in Patagonia (Gillett *et al.*, 2006), although there is considerable inter-annual variance (Garreaud *et al.*, 2009). This trend has also been linked to positive summer temperature anomalies in Patagonia in the past decade by Thompson and Solomon (2002). Silvestri and Vera (2009) outline the mechanism by which the SAM/AO impacts Patagonian climate during the two most recent positive

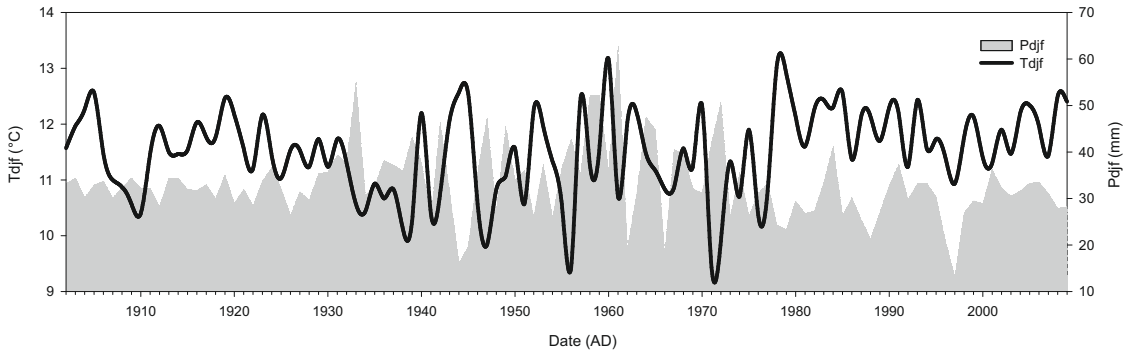

FIGURE 3.7: CRU-TS 3.1 temperature and precipitation for Austral Summer (DJF) for the grid cell covering the Chacabuco Valley (C86/R216).

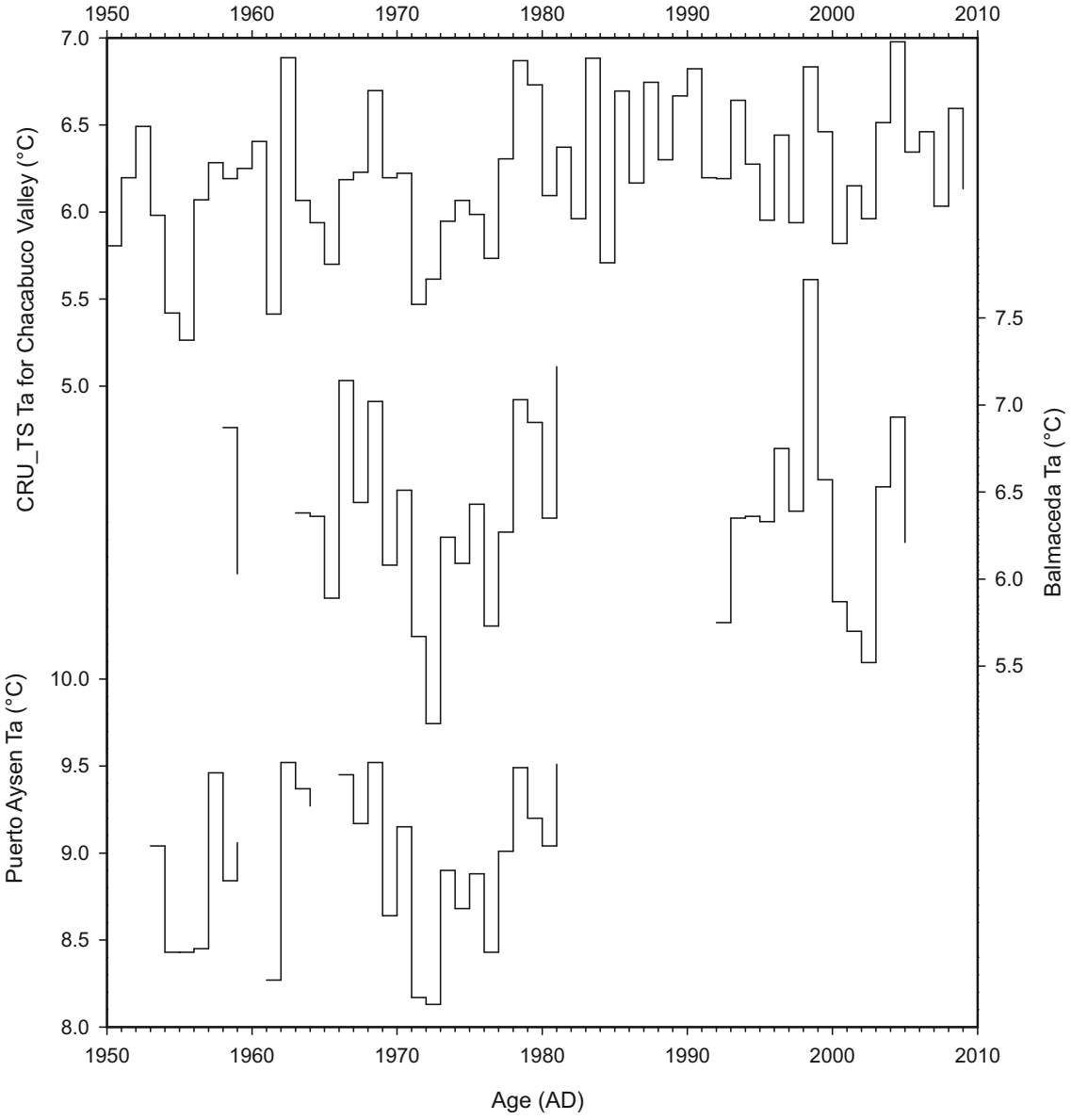

FIGURE 3.8: CRU-TS mean annual temperature (Ta) for the grid cell covering the Chacabuco Valley and observational data from the three nearest meteorological stations. See Table 3.1 for statistical analysis.

	Puerto Aysen Ta (°C)	Balmaceda Ta (°C)
CRU-TS (Chacabuco) Ta (°C)	$\rho = 0.783$, $n = 27$	$\rho = 0.689$, $n = 35$
Puerto Aysen Ta (°C)	—	$\rho = 8.26$, $n = 20$

TABLE 3.1: Correlation statistics for CRU and nearest available observation data for the Chacabuco Valley. Spearmans Rank is used as a linear relationship is expected. All relationships are signficant at $\alpha =< 0.01$; see Figure 3.8.

phases (1958–1979 & 1983–2004), where there is anomalous anticyclonic circulation in the southwestern suptropical Atlantic, promoting increased precipitation in Patagonia due to enhanced moisture advection.

3.4.3 Palaeoclimatic Reconstructions

3.4.3.1 Lake Records: Northern & Central Patagonia

The quantitative summer temperature proxy record from Laguna Aculeo (von Gunten *et al.*, 2009) shown in Figure 3.10 is unusual in that it exploits reflectance properties of the sediment, related to primary production in the lake, and uses a linear scaled calibration-in-time approach to produce quantative estimates. The model presented has a maximum possible temporal resolution of *c.*5 years and r^2 values of up to 0.34°C. Although the site is located at the northerly limits of Patagonia it is within the climate space of strongly, significantly correlated summer temperatures and thus suitable for comparison with climate records from the central region (ibid). The Laguna Aculeo record suggests a period of stable, low temperatures between *c.*AD1400–1800 co-incident with the Little Ice Age. Notably, the data suggest an overall recent warming trend from *c.*1965 onwards, a common feature in instrumental records from Patagonia. There is also a general warming trend from AD1930 to 1955 in the Laguna Aculeo reconstruction, co-incident with an increase in running-variance (not shown).

Urrutia *et al.* (2010) present a combined chironomid, pollen and diatom record extending to *c.*2,000 years B.P. for the Chilean Andes *c.*36°S. Their main finding was a pronounced cooling co-incident with the Little Ice Age (AD1500–1900), reflected by a profound change in the chironomid fauna, specifically an increase in *Macropelopia*, *Parachironomus* and to a lesser extent *Parapsectrocladius* and *Cricotopus* for this period, indicative of colder and possibly drier conditions. They found no evidence of climate change during the Medieval Climate Anomaly (AD950–1250) and suggest that this was because the event was either not of global extent or of insignificant magnitude locally, or that the chironomid proxy is insufficiently sensitive to respond to climate change of that magnitude. Urrutia *et al.* reserve judgement on the ability of chironomid proxies to reflect small magnitude climate events, and note the importance of using a multi-proxy approach to palaeoenvironmental research due to the complex relationship between environmental variables and organisms. The strong volcanic influence on the sedimentology in the region is potentially problematic as there are good grounds for suspecting a chironomid response to tephra deposition, albeit short-lived (<10 years; Urrutia *et al.*, 2007).

Further south a chironomid record from Lake Hess near the Chile/Argentinian border (41°S) inferred low water level and thus precipitation for the pre-AD1800 part of the sequence (Guilizzoni *et al.*, 2009), followed by intermediate environmental conditions associated with relatively cold temperatures for the period from AD1800 to AD1840. For

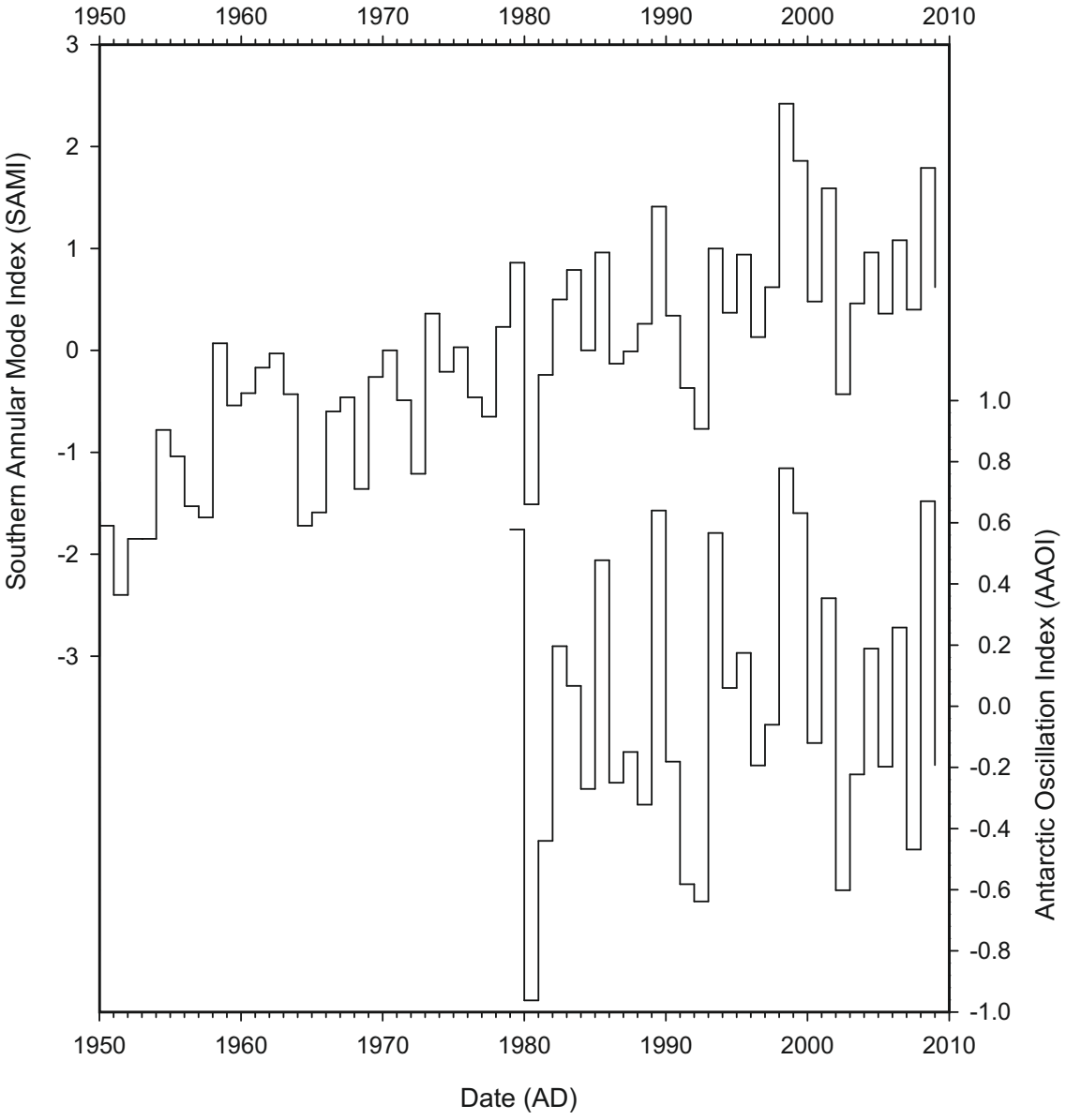

FIGURE 3.9: SAM (AAO) Index at annual resolution. $\rho = 0.921$, $\alpha =< 0.01$, $n = 33$ SAMI is the difference in normalised zonal-mean sea level pressure between 40-70°S, from Nan and Li (2003). AAO the leading mode of EOF analysis of monthly mean 700hPa height during the AD1979–2000 period (data from NOAA).

the last fifty years they suggest decreasing precipitation and possible recent warming, linked with nutrient increases. They found chironomids confirmed the diatom analysis findings of recent wet/dry episodes as they reflected these changes in the relative abundance of profundal/littoral taxa.

Changes in the strength of the westerlies in northern Patagonia during the past 200 years have also been inferred from lake varve thicknesses by Boës and Fagel (2007a), who demonstrated a strong correlation between the strength of the westerlies and ENSO cycles; this study not only identified higher precipitation during the Little Ice Age, but also inferred higher lake levels between AD1920–1950, and decreasing precipitation from AD1950 onwards.

FIGURE 3.10: Temperature reconstruction for northern Patagonia from Laguna Aculeo von Gunten *et al.* (2009)

An annual precipitation reconstruction for AD1530–2002 has been constructed by calibrating varve thickness with the CRU-TS precipitation data (see Section 3.4.2.1) for central Patagonia (Elbert *et al.*, 2011) using a calibration-in-time approach. Because the varves are formed from runoff during austral summer, the reconstruction is of summer precipitation (P_{DJF}), with a RMSEP=13.3mm/month. The record identified a number of wetter periods (Figure 3.11), the latest being during the Little Ice Age between AD1780–1850. From *c.*AD1800 onwards there is a general trend of increasing precipitation.

3.4.3.2 Argentinian Steppe and Tierra del Fuego

There are no lacustrine quantitative palaeoclimate reconstructions for southern Patagonia; those interpretative palaeoclimate studies that do exist are based primarily on diatom, x-ray fluorescence and magnetic susceptibility data. Concluding multi-proxy analysis of a cirque lake located in Argentine Patagonia at *c.*51°S, Fey *et al.* (2009) suggest coldest conditions of the past 1,600 years during the period from the mid-15th to the mid-17th century, followed by warmest conditions from the mid-17th to mid-18th

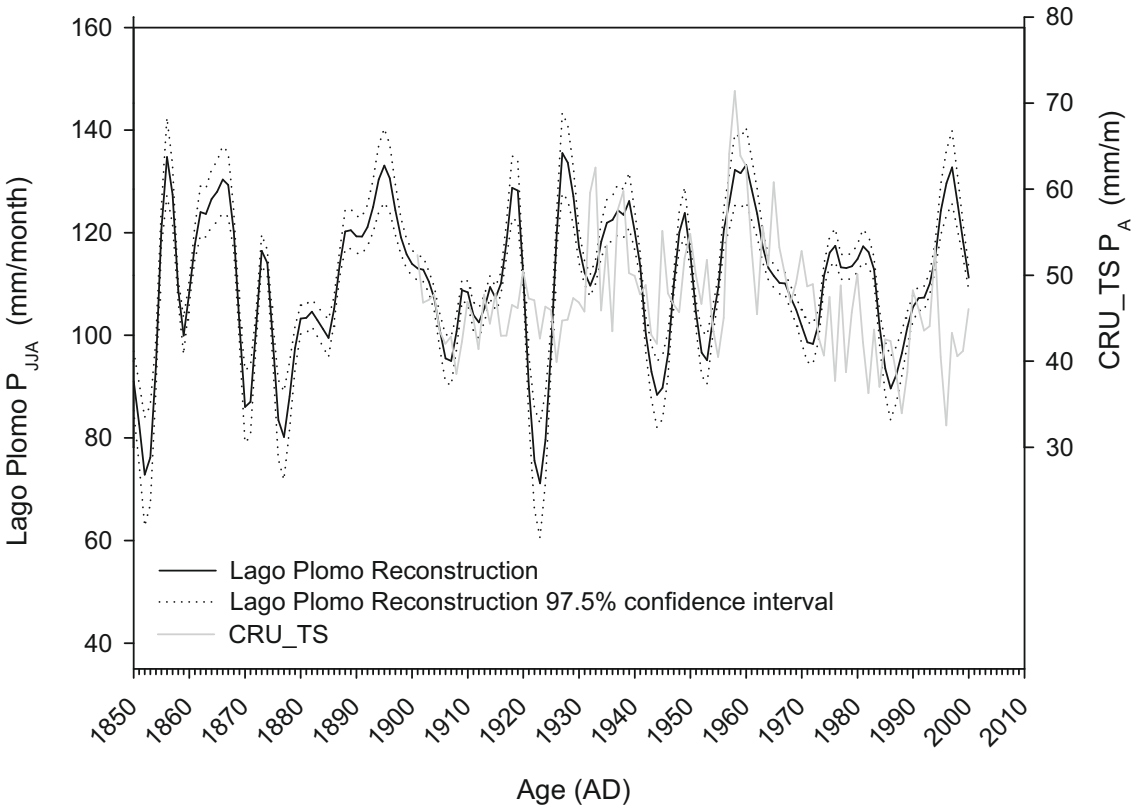

FIGURE 3.11: Precipitation reconstruction from Lago Plomo (Elbert *et al.*, 2011), also showing CRU-TS precipitation data (see Section 3.4.2).

century; this was inferred on the basis of diatom assemblages. This is in considerable discord with the Little Ice Age timing of cooling in the northern sector palaeoclimate records (Section 3.4.3.1) and is difficult to reconcile with the regional Little Ice Age signal.

The well-studied Laguna Potrok Aike also offers some evidence of opposite directions of change around AD1500–1900 compared to northern Patagonia; data from Mayr *et al.* (2008) indicate a lake high stand during the Little Ice Age, suggesting increased precipitation on the basis of stable isotope modelling, and diatom evidence from the same site suggests a decrease in moisture in the 20th century (Wille *et al.*, 2007), but for both studies the sampling resolution is low and the radiocarbon dating resolution for the tops of the cores is too poorly constrained to accept the interpretations with any certainty. Markgraf *et al.* (2003) present a Holocene climate record from Lago Cardiel, a similar lake to Laguna Potrok Aike, and concluded that the modern precipitation patterns that control the lake levels in the semi-arid steppe to the east of the Andes became established around 5,000 years B.P. when seasonally shifting westerly storm tracks and the importance of the ENSO contributed to a considerably more variable precipitation regime. This suggests that closed lakes in the semi-arid regions are primarily archives of changes in precipitation/atmospheric moisture availability. As such neither record provides any robust information on recent temperature change, partly because of the choice of proxies employed and partly because the emphasis of both

studies were on precipitation and the westerlies.

The focus of recent palaeoclimate research in Tierra del Fuego has been on the extent and timing of the Little Ice Age. Waldmann *et al.* (2009) suggest increased precipitation during the Little Ice Age on the basis of lacustrine geochemical and sedimentological changes at Laguna Fagano, consistent with nearby peat stratigraphy from Isla Grande (Mauquoy *et al.*, 2004) and glacial evidence of recent advance offering further support (Planas *et al.*, 2002); other regional peat records support this (*e.g.* Borromei *et al.*, 2010) although the high-resolution stalagmite records presented by Schimpf *et al.* (2011) provide the most robust evidence for the Little Ice Age. As the focus of research in the region has been on the Little Ice Age and older events, more limited data exist on recent climate change.

3.4.3.3 Tree Rings

Tree-ring width, density and isotopic composition have yielded a number of climate reconstructions of precipitation and hydrological variables along with temperature and atmospheric circulation (Boninsegna *et al.*, 2009). Differences in species and regional climate mean that tree-rings provide different climate proxies in different situations, but good results have been obtained for both precipitation and temperature in various settings. Tree rings offer the best current palaeoclimate proxies for local conditions at inter-annual scale for the recent past, and have been used in Patagonia with calibration-in-time techniques to provide quantitative temperature estimates. A significant problem is that tree-ring reconstructions do not typically detect low-frequency changes well because these signals can be removed during de-trending (Esper and Frank, 2009).

Investigations into tree-ring width and climate in the semi-arid Andes in the north of Chile (34–27°S) find a positive relationship between annual precipitation and tree-ring width, strongly associated with ENSO forcing of precipitation in the region (Barichivich *et al.*, 2009; Le Quesne *et al.*, 2009). Tree-ring width was not correlated with an index of Pacific-Decadal Oscillation and showed only weak correlation with summer air temperatures. Similar conclusions were drawn from low latitude, high elevation sites in the Andes (Christie *et al.*, 2009). An annually resolved δ^{18}O record from tree rings in the semi-arid Chile/Argentinian border region of northern Patagonia (36°S) extends back to AD1890 (Roig *et al.*, 2006) and demonstrated summer air temperatures were positively but weakly correlated with tree ring width — they found the strongest correlations with the southern oscillation index, suggesting that ENSO events result in δ^{18}O depleted tree rings. Tree ring δ^{18}O reflected both high-frequency (annual-scale) changes in southern oscillation index along with a long term shift since AD1970 to generally lower δ^{18}O values, reflective of the same shift in ENSO indices. This is unsurprising as at this latitude ENSO is the dominant control on inter-annual precipitation variability, and precipitation is the limiting factor in forest growth. This situation does not hold for

more southern Andean tree-ring records, which can be sensitive indicators of temperature because it is temperature, not moisture availability that limits growth.

For the wetter Patagonian Andes temperature is the limiting factor in tree growth and thus quantitative temperature estimates can be obtained from tree ring width calibrated with meteorological data (Lara and Villalba, 1993). Villalba *et al.* (2003) present an analysis of meteorological and tree-ring temperature reconstruction data, split into northern (38–41°S) and southern (46–52°S) Andean regions. The southern region dataset (covering central Patagonia) is composed of five records from between 47–49°S including two from the Cerro Tamango range, within 20km of Laguna Meche & Edita (the field sites in this study), thus they are the most appropriate palaeoclimate data for comparison in this study. Although the decadal and sub-decadal trends correlate well with the meteorological data for the period of available data (Figure 3.12), longer term trends are not necessarily resolved due to de-trending. Their conclusions pertinent to this study might be summarised as follows:

- There is surface warming between 46–55°S from 1950/60 to *c.*AD1990. It is restricted to the higher latitudes of the southern hemisphere (no such signal is seen in the Andes north of 41°S) and focussed on the Pacific side. The rise in annual temperatures is mainly driven by summer temperature increases rather than increases in winter; this becomes increasingly obvious further south. Villalba *et al.* associate the warming with hemispheric ENSO-like circulatory changes and increases in sea surface temperatures in the Pacific Ocean, although given the latitudes involved the Antarctic Oscillation is perhaps better implicated.
- The case for pronounced climatic cooling in Patagonia around AD1976, already well established by other studies is emphasised.
- Lower temparatures between *c.*AD1600 and AD1850 is equated with the Little Ice Age, adding to the growing body of evidence of such a cooling both in the locale (Araneda *et al.*, 2007) and across vast swathes of South America (Meyer and Wagner, 2008; Koch and Kilian, 2005; Araneda *et al.*, 2009; Masiokas *et al.*, 2009; Espizua and Pitte, 2009).

3.4.3.4 Ice-cores and Moraines

The Little Ice Age is well observed in Patagonian glaciers, indicating the ice-sheets and mountain glaciers are sensitive to changes in global climate (Harrison *et al.*, 2007; Araneda *et al.*, 2007; Fernandez *et al.*, 2011; Araneda *et al.*, 2009; Koch and Kilian, 2005), although the temperature and/or precipitation response in the southern hemisphere may opposite to those observed in the northern hemisphere (Meyer and Wagner, 2008), although glacial dynamics in the region are complex due to the very

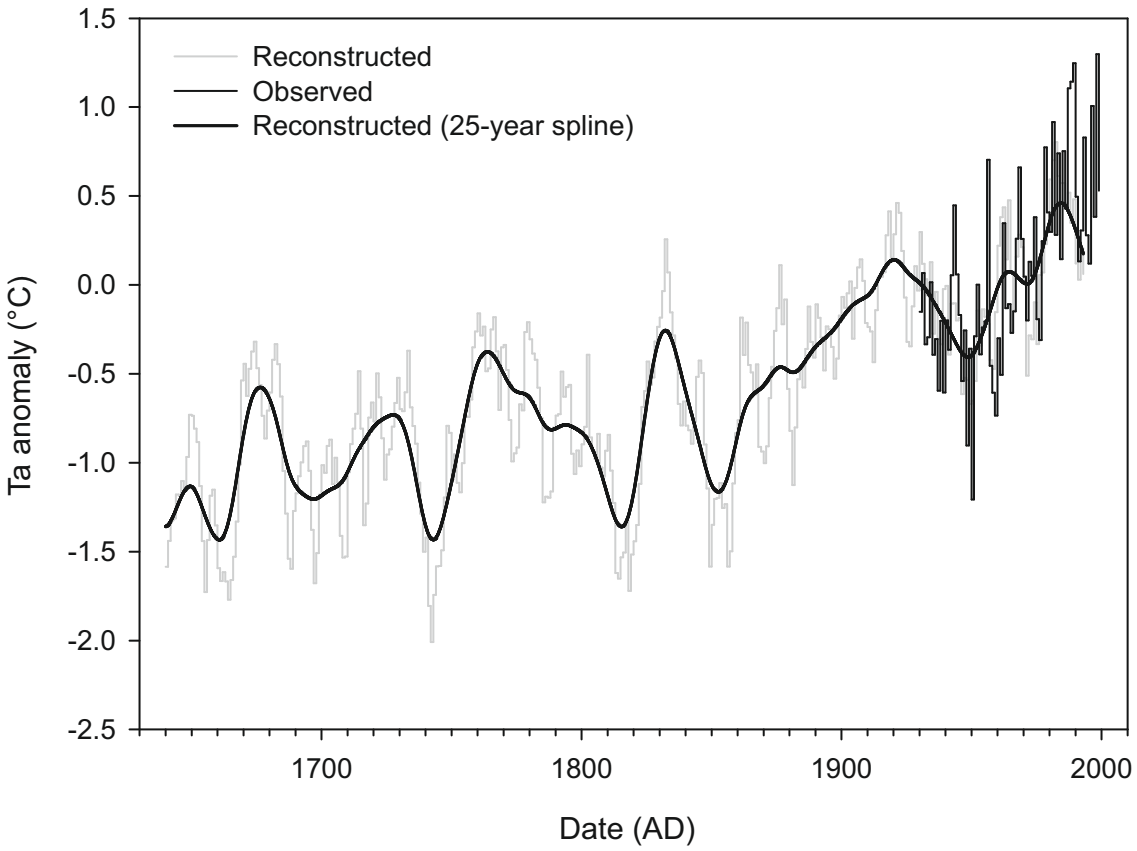

FIGURE 3.12: Tree-ring inferred temperatures from Villalba *et al.* (2003), including the observational data used for calibration (nearest station). Temperatures are inferred from ring-width calibrated against instrumental data. Note that although detrending can obscure low-resolution information, a general warming trend can be inferred from the data.

strong orographic effects (Holmlund and Fuenzalida, 1995); as such the response in the southern hemisphere may be quite different from that in the northern hemisphere.

The North Patagonian Icecap is thinning and outlet glaciers have been retreating as part of the global pattern of glacial thinning and retreat from AD1850 onwards, associated with the termination of the Little Ice Age (*c.*AD1600–1850; Glasser *et al.*, 2011). The rate of shrinkage of the North Patagonian Icecap is increasing, and although the South Patagonian Icecap shares this general trend some outlet glaciers have fluctuated considerably with a net increase in size. Moraines that date to the end of the Little Ice Age are found across Patagonia including on the eastern margin of the north Patagonian Icecap (Harrison *et al.*, 2007).

A short ice-core from the North Patagonian Icecap (46°S; Vimeux *et al.* 2008) emphasise the importance of the influence of easterly and polar-derived air masses on the region, although the westerlies are dominant. The δ^{18}O record is argued to be representative of temperature but shows considerable changes that cannot be explained by temperature alone; the authors argue that an unknown feedback process causes δ^{18}O to amplify the temperature signal. Thus they observe unusually warm conditions in the 1980's but

conclude little else. Historical records also suggest advances of North Patagonian Icecap outlet glaciers coincident with the Little Ice Age (Araneda *et al.*, 2007). A latitudinal transect of ice-cores from the Andes offers a little more insight, identifying isotopic depletion in a number of ice-cores co-incident with the Little Ice Age (Vimeux *et al.*, 2009), consistent with observed recession of glaciers in the northern Andes (Araneda *et al.*, 2009). To conclude, there is good evidence of a Little Ice Age advance of glaciers across Patagonia, and the combination of narrower tree rings and expanded ice sheets point to a cooling rather than a change in precipitation during this time.

3.4.4 Synthesis of Recent Climate Change in Central Patagonia

It seems self-evident that given the latitudinal range and size of southern South America a common, in-phase and synchronous annual to decadal scale climate signal for the whole of Patagonia is difficult to conceive, and yet it is not unusual for distal records to be compared without regard to the wildly different teleconnections between areas. It seems clear that the central region has quite different climatic teleconnections (and thus potentially a different climate history) of the Andes north and south of the site (see Figures 3.14 & 3.15), thus the reference conditions for palaeoclimatic investigations in central Patagonia must be derived from palaeoclimate data specific to the central region. The central Patagonian area differs considerably from the southern zone, where the polar influence is more important, and the northern zone, where ENSO and PDO cycles are the most important inter-annual climate modulators. In addition, the relationship between different elements of the climate is spatially heterogenous — this is shown in Figure 3.13, where northern and southern Patagonia show opposing correlations between annual precipitation and temperature. The positive correlation in the northerly region is due to moisture delivered via storm fronts tracking from the Pacific, bringing warm air from lower latitudes. The detailed nature of climate in the central region is unclear due to the paucity of palaeo/instrumental climate data for the region, but given the importance of the AAO/SAM at these latitudes, it is likely to have a considerably different recent climate history compared with the rest of Patagonia. The key events during the past 150 years are summarised as follows:

- Extensive evidence of a Little Ice Age characterised by cooler temperatures and more humid conditions due to an intensification of the westerly winds, leading to glacial advance between *c.*AD1600 and AD1850.
- Warming from 1950– mid-1970's below 46°S, but no such temperature trend to the north, and northerly stations (37–43°S) show cooling during this period. These trends are driven primarily by austral summer temperature (Villalba *et al.*, 2003).
- A general warming trend between AD1970–1990 across Patagonia of up to 1°C.
- Cooling from AD1990 to AD2000 of around 0.5°C, followed by a general plateaux in temperatures until present.

3.5 Conclusions

The climate in Patagonia is influenced by hemispheric scale processes driven from the sub-tropics (*e.g.* El Niño) and from the pole (*e.g.* the Antarctic Oscillation). The climate across much of Patagonia is characterised by very strong zonal precipitation gradients, and temperature is largely a function of latitude and altitude. It has been demonstrated that different parts of Patagonia can be sub-divided into distinct climatic spaces, where even if mean climate does not differ significantly, the controls on climate differ by area. On the broadest scale, the higher latitudes are more affected by polar climate and the lower latitudes are more affected by sub-tropical climate, but the exact divisions between these zones are indistinct and may change over time. Although the southern westerly winds are the dominant control on climate, particularly precipitation, across the whole of Patagonia, the effect of changes in the westerlies can have different, sometimes opposite effects in each of the different climate spaces. The central region is of particular interest because there are indications from recent data that the Antarctic Oscillation is teleconnected to the region. In addition, the region is relatively insensitive to anything but the greatest changes in the position of the westerlies, but the transitional zone between the forest and steppe ecotones is particularly sensitive to the strength of the westerlies.

Central Patagonian climate has been demonstrated to be sensitive to both recent and long-term climate change, and there is some concensus on the character of recent events, particularly the Little Ice Age. Research interest has focussed on Lateglacial climate and although the Holocene climate has received some research interest, the central region is under-represented in the palaeoclimatic literature. This is problematic because most research interest has focussed on areas near the margins of the southern westerly winds, and thus changes in the strength *vs.* changes in the position of the westerlies are difficult to disentangle. However, the central region at the core of the westerlies is less sensitive to changes in the position and more sensitive to changes in the strength of the westerlies.

Although the palaeoclimate data for the region is largely equivocal, there are some tentative conclusions that can be drawn. The most recent climate changes are reasonably well understood, and the Little Ice Age is well characterised. The termination of the last glacial is also well documented, and although there is still no clear pattern during the Lateglacial, a pattern of small-scale regionally distinct climate reversal during the Lateglacial is emerging. For the Holocene, a picture of mid-Holocene change is emerging, but there are regionally distinct timings and nature of Holocene change that require further consideration.

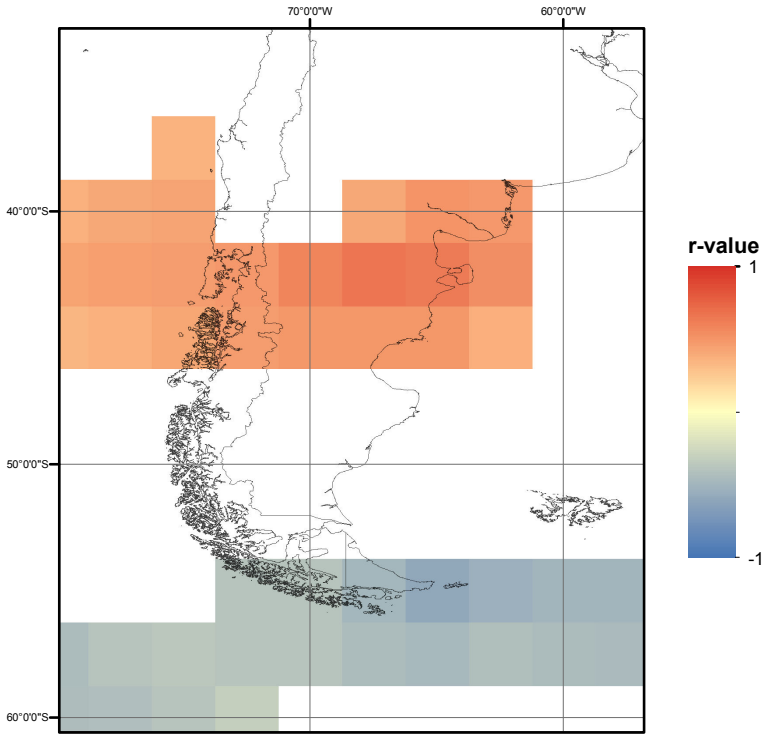

FIGURE 3.13: Map showing correlation coefficient of mean annual precipitation and mean annual temperatures in southernmost South America for the period AD1950–2000 from NCAR reanalysis data (Kalnay *et al.*, 1996). Areas with $p > 0.01$ are not shown.

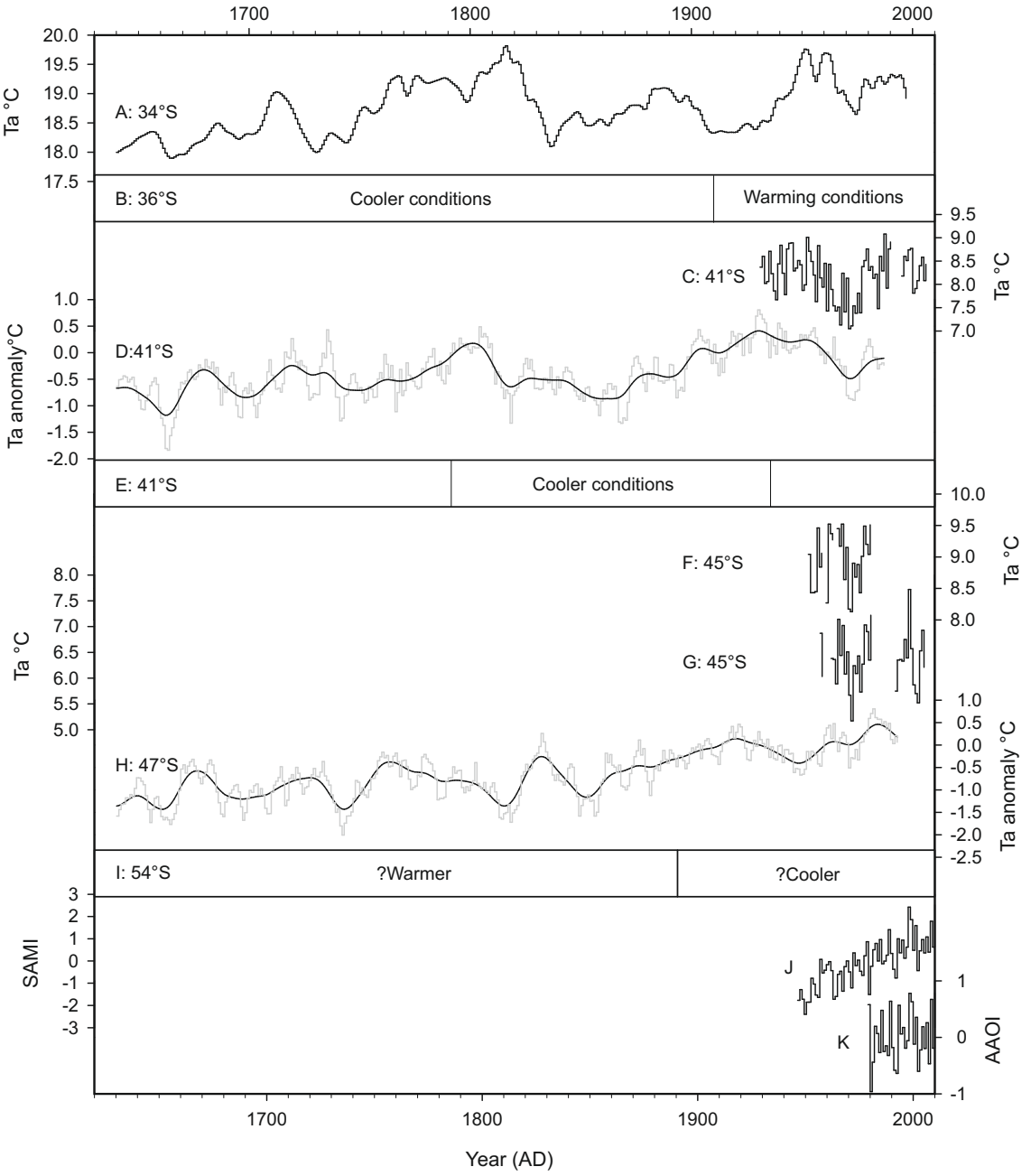

FIGURE 3.14: Observational and palaeo-proxy temperature data mentioned in the text, arranged in order of increasing latitude from top to bottom, along with SAMI and AAOI from Figure 3.9. Sources: A: von Gunten *et al.* (2009), shown as a fourier 5-yr function. B: Urrutia *et al.* (2010). C, F & G: From the Dirección Meteorológica de Chile. D and H: Villalba *et al.* (2003) northern and southern datasets respectively, shown with a 25-year spline in black. E: Guilizzoni *et al.* (2009). I: Mauquoy *et al.* (2004). J & K: NOAA.

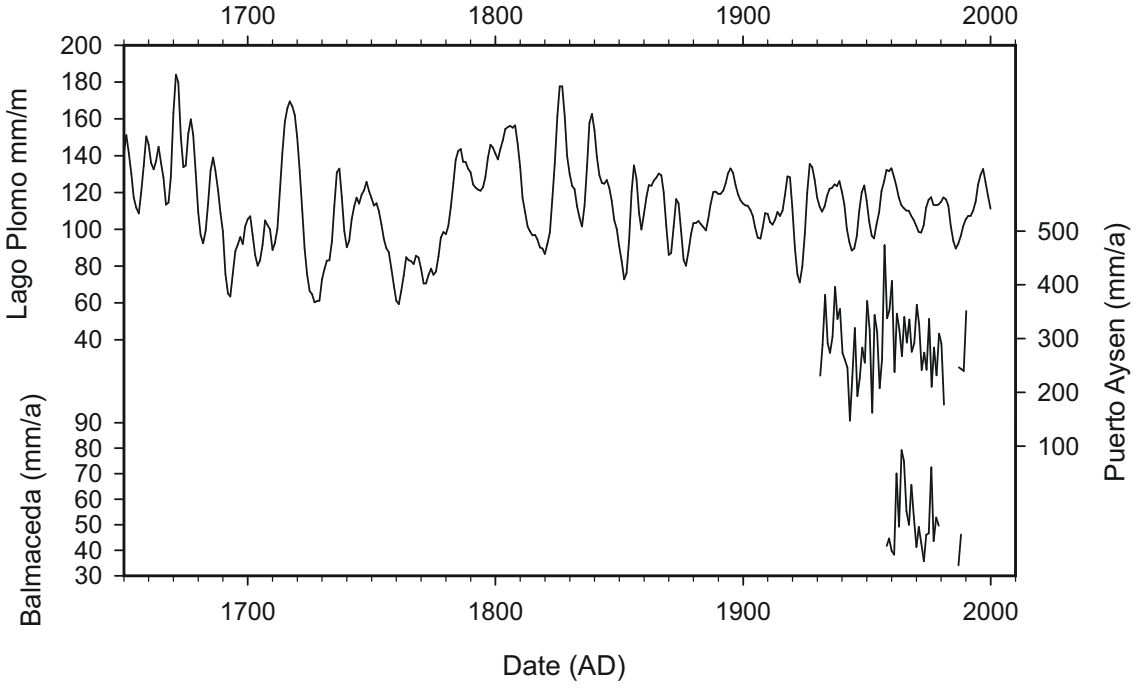

FIGURE 3.15: Observational and palaeo-proxy precipitation data mentioned in the text, arranged in order of increasing latitude from top to bottom. Lago Plomo from Elbert *et al.* (2011), Puerto Aysen and Balmaceda observational data from Directión Meteorológica de Chile.

Chapter 4

Site Descriptions

4.1 Central Patagonia

4.1.1 Physical Geography

Central Patagonia is the region surrounding the North Patagonian Icecap (Campo de Heilo Patagónico Norte), between 45–48°S in South America; the northern icecap currently covers an area of 3,953km^2 and is retreating from the "Little Ice Age" positions (Masiokas *et al.*, 2009) at a rate of *c.*6.3km^2/year (Rivera *et al.*, 2007). A series of outlet glaciers drains into the Hudson River on the eastern flank and terminates in or near to the Pacific Ocean to the west (Turner *et al.*, 2005). The two large lakes to the east of the icecap, Lago Buenos Aires (Lago General Carréra) and Lago Pueyrredón (Lago Cochrane) occupy primarily geologically controlled east–west trending valleys over-deepened by glacial erosion (Glasser and Ghiglione, 2009; Rabassa, 2008).

4.1.2 Climate

The climate is dominated by the southern westerly winds, the main source of precipitation in the Pacific and Andean regions at this latitude, although in Patagonia polar advections are also an important component (Vimeux *et al.*, 2009). The westerlies are driven by the latitudinal pressure gradient between the polar low and the high pressure south Atlantic convergence zone (Vimeux *et al.*, 2009). These meridional winds bring high (<4000mm/year) rainfall with a strong east-west gradient; east of the icecap, precipitation is reduced to around 700mm/year in the Chacabuco Valley (estimated). The North Patagonian Icecap is sustained by high precipitation (1000–4000cm/year), but the Föhn Effect over the North Patagonian Icecap and the Andean foothills east of the icecap reduces precipitation to semi-arid levels (around 20cm/year) within 30km of the mountain front (Hein *et al.*, 2010). There is a strong positive correlation between

zonal wind speed and precipitation on the eastern seaboard, although this relationship breaks down to the east in the Argentinian steppe (Moy *et al.*, 2009).

Positive El-Niño Southern Oscillation (ENSO) Index events are associated with an overall decrease in the wind field and thus a decrease in precipitation, and NCAR re-analysis data indicate high correlation between wind speed, precipitation and air temperature in much of Patagonia (Moy *et al.*, 2009). The Southern Annular Mode (SAM) and Antarctic Oscillation (AO) affect seasonality and climate on inter-annual timescales. These linked features are under-discussed agents of climate change in the region. In its positive phase the SAM/AO is linked with a poleward shift in the position and intensity of the westerlies, particularly in central and southern Patagonia (ibid). The importance of decadal/hemispheric scale climate processes is discussed fully in Section 3.2.

4.1.3 Vegetation

The strong precipitation gradients and latitudinal temperature gradients lead to clearly defined and often sharply contrasting vegetation zones, from evergreen rainforest on the Chilean coast to steppe/half-dessert in Argentina (Gut, 2008). The Chacabuco Valley encompasses the eastern sector of the *c.*50km west-to-east distance in which the *Nothofagus* rainforest gives way to steppe (Veblen and Lorenz, 1988). The vegetation can be divided into the five main zones described in Table 4.1. In regions that have been cleared for ranching there are effectively two tree-lines, the natural tree-line and a lower tree-line that lies where lower areas have been cleared for ranching.

4.2 Chacabuco Valley

4.2.1 Introduction

The Chacabuco Valley is a glacially deepened valley between the Tamango and Jeinimeni ranges (peak elevations 1800m a.s.l.), located *c.*40km east of the North Patagonian Icecap (Figure 4.1) and was a former outlet lobe of the central-east portion of the icecap during the last glaciation. The Rio Chacabuco runs west down valley to meet the Rio Baker, draining to the Pacific. The vegetation is dominated by *Nothofagus pumilio*, characteristic of winter deciduous forest, with steppe/high Andean vegetation at higher altitudes; at the eastern mouth of the valley the forest is almost entirely absent due to reduced precipitation (Gut, 2008) as the valley opens out into Argentinian Steppe. There are several small and medium sized lakes throughout the valley at altitudes from *c.*300m to 1600m a.s.l. The Chacabuco Valley sits *c.*150m higher than its neighbouring outlet valleys, increasing in altitude towards the east. The area was previously ranched in the 20^{th} century, but is now owned and managed as a private nature reserve by Conservatión Patagonia with the aim of uniting the adjoining Jeinimeni and Tamango National Parks.

Zone	Description	Climatic Parameters
Magellanic Moorland Complex	Cushion forming plants	MAT=5–7°C P=3000–4000mm/year
Evergreen rainforest	*Nothofagus* spp.	MAT=12–13°C P=1500–3000mm/year
Winter deciduous forest	*Nothofagus pumilio* dominates	Elevations of 500-1250m a.s.l, T=5–8°C MAT P=400–1000mm/year
Patagonian steppe	Species rich, bunchgrasses, shrubs & herbs	MAT=8–15°C P=<500m/year
High Andean vegetation	Alpine type herbs & shrubs, bare ground	elevations of 900–1500m a.s.l, P=400–1500mm/year

TABLE 4.1: Vegetation zones in central Patagonia. MAT=mean annual precipitation, P=annual precipitation

The natural tree-line is around 1300m a.s.l., although locally there is a lower tree-line that delineates the areas cleared for ranching.

4.2.2 Geomorphology and Palaeoclimatic History

The last glacial maximium moraines in the region have been well dated by Hein *et al.* (2010) along with the associated moraine systems in the outlet valley to the south. Hubbard *et al.* (2005) present a model of glaciation in the vicinity of the North Patagonian Icecap that suggests the entire valley would have been overrun by ice at the time of the last glacial maximum. During deglaciation the highest parts of the Tamango range would have become ice-free between 17,000–15,000 years B.P., and the highest parts of the Oportus range would have become a nunatak; this meant that ice would have overrun the topographic low between the two, flowing south-east in what is now Lago Cochrane. Ice sheet modelling suggests this situation continued until between 14,000–13,500 years B.P., after which the valley was free of ice. Trimlines on Cerro Colorado (around 40km east of the valley) indicate the mountain was a nunatuk during the last glacial maximum (Hein *et al.*, 2010).

At the eastern end of the Chacabuco Valley a large moraine complex was identified by Glasser *et al.* (2012); although it has eroded on the south side it appears to be arcuate and substantial, approximately 60m proud of the base of the valley. The genesis of this moraine is unclear; its position inside of the Rio Blanco moraine (last glacial maximum) and Lago Columna moraine (16,500–15,000 years B.P.; Hein *et al.*, 2010) constrains the age to under 15,000 years B.P. Dates from near the North Patagonian Icecap constrain it to pre-Holocene (Masiokas *et al.*, 2009; Harrison *et al.*, 2007). Given that Hein *et al.*

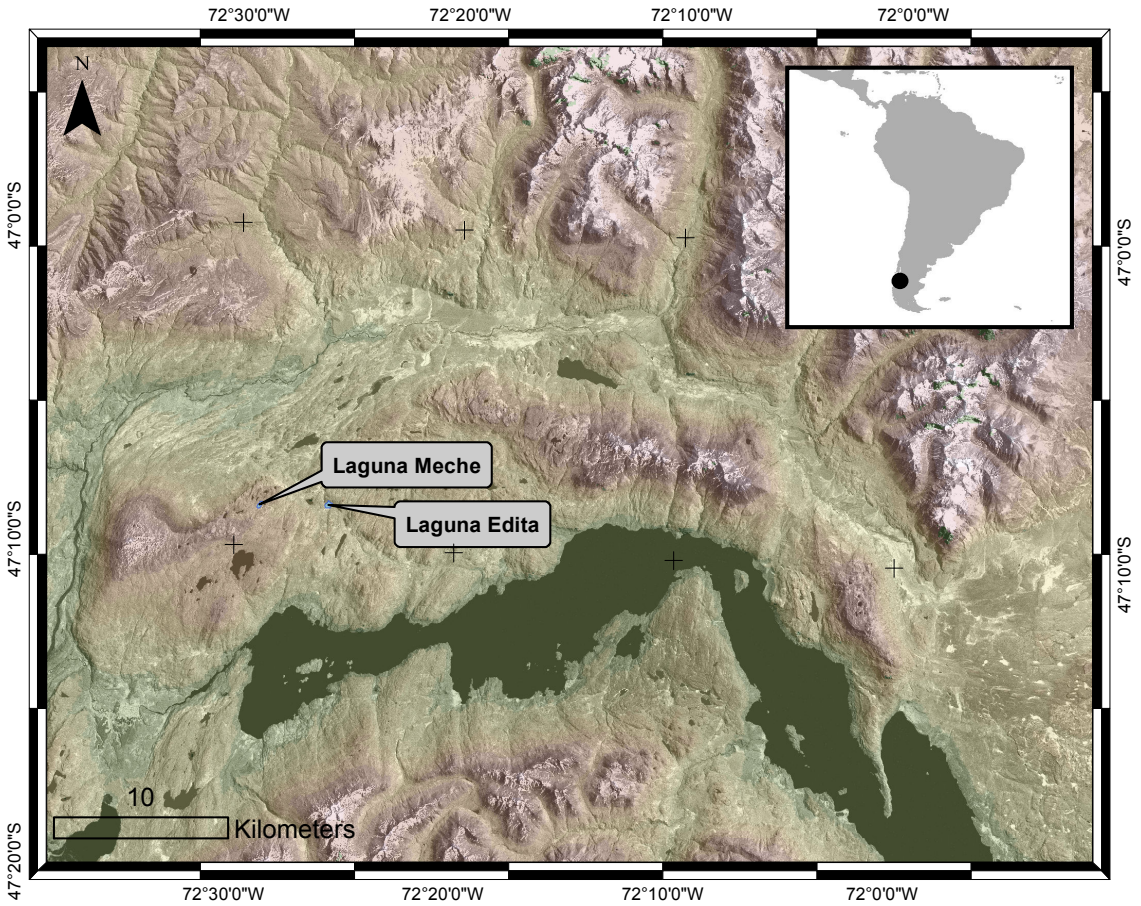

FIGURE 4.1: Map of the Chacabuco Valley. Elevation and imagery as per Figure 4.2. Colour represents altitude in this image.

(2010) correlate the Lago Columna moraines with a partly submerged moraine feature that separates Lago Cochrane and Lago Posadas, it would be worthwhile to examine the bathymetry of Lago Cochrane to identify a possible inner moraine therein, equivalent to those in the Chacabuco Valley. Glasser *et al.* (2008) have also identified glacial lineations in the west of the valley, indicating previous glaciation was warm-based.

Evidence exists suggesting the existence of a series of large pro-glacial lakes formed following deglaciation of the eastern flank of the North Patagonian Icecap. At present the eastern flank of the ice sheets drains to the Pacific via the Rio Baker between the Northern and Southern Ice Fields; during previous glaciations this route would have been blocked and all drainage would have been via the Rio Desceado to the Atlantic. Most recently Hein *et al.* (2010) put forward a modified version of the palaeolake history posed by Turner *et al.* (2005), in which four main stages are outlined:

16,500 to 15,000 years B.P. "Upper Palaeolake 505-470m a.s.l.": A re-advance deposits the Menucos and Lago Columna moraines; an upper palaeolake forms south-east of the Lago Columna moraines (shown in Figure 4.2), draining via the Canadon Caracoles/Rio Deseado to the east. Hubbard *et al.* (2005) interpret this as showing the ice stabilisation during the Antarctic Cold Reversal.

15,000 to 14,000 years B.P. "Upper United Palaeolake 400-370m a.s.l.": The outlet glaciers rapidly retreat to expose the valley linking the two basins; the lake unites, draining via the Rio Deseado.

14,000 to 13,500 years B.P. "Lower United Palaeolake 300-270m a.s.l.": North and South Patagonian icecaps retreat sufficiently to allow drainage to the west (Pacific Ocean).

13,500 to between 12,800 and 6,200 years B.P. "Present day situation": An ice-free Rio Baker draining freely into the Pacific Ocean.

The only published palaeoclimatic work from the valley is the pollen stratigraphy from a valley floor carbonate lake dating back to *c.*16,000 years B.P. (Villa-Martínez *et al.*, 2012). The stratigraphy and radiocarbon dating support the existing glacial chronology and the late glacial chronology of Hein *et al.* (2010) for the valley, although Villa-Martínez *et al.* suggest a temperature decline and/or a deepened proglacial lake as a result of glacial readvance between 14,200 and 15,200 years B.P. From 10,000–11,000 years B.P. to present the pollen record is dominated by *Nothofagus dombeyi*-type, with vegetation before this characterised by herbs, shrubs and ferns indicative of an steppe/alpine open landscape environment; the transition is gradual and interrupted at times. Villa-Martínez *et al.* interpret their record as suggesting temperature increase and precipitation decline between 9,900–11,800 years B.P. consistent with a number of other records suggesting reduced westerly wind strength in Patagonia at this time (see Section 3.3.1). They also suggest a high lake level phase between 7,500 and 11,000 years B.P.

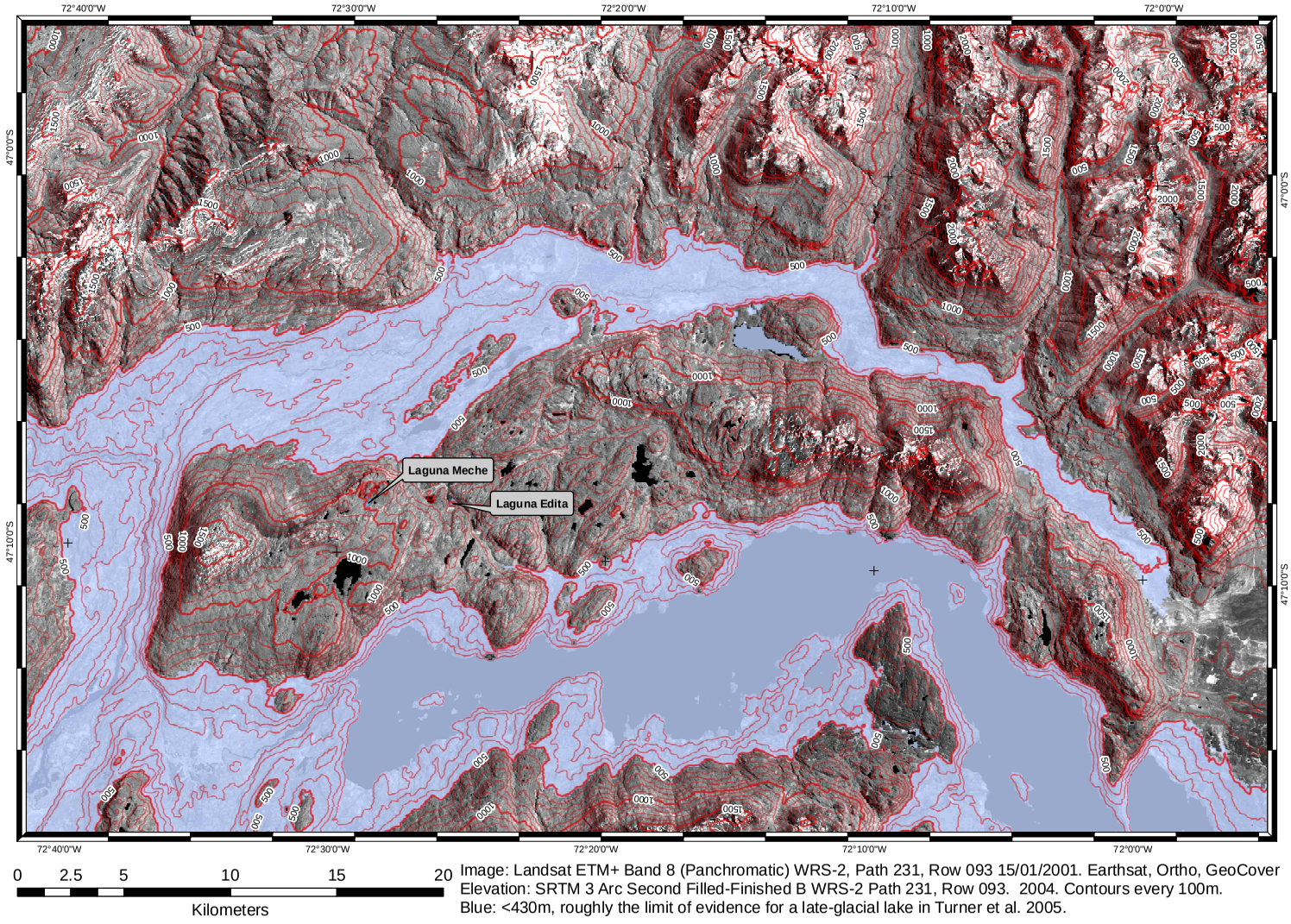

FIGURE 4.2: Map of palaeolake in the Chacabuco Valley proposed by Hein *et al.* (2010), created using a digital elevation model derived from the NASA Shuttle Radar Topography Mission.

which they attribute to weakened westerly winds allowing westward incursions of Atlantic air-masses to deliver increased moisture to the site.

4.3 Site Selection

This project targets sites located east of the North Patagonian Icecap, between the foci of previous research around 42 and 52°S. Chosen sites should be comparable with the published literature in the region as well as fitting the common requirements of sites of palaeolimnological investigation; the key criteria for this study are as follows:

- small ($<2km^2$) basin with a small catchment, preferably with a closed basin,
- deep ($>10m$),
- permanent,
- rainwater/runoff/groundwater fed, and specifically not fed from glacial melt water, and possessing an
- uninterrupted and undisturbed sedimentary sequence.

Section 3.2 discussed the longitudinal precipitation gradient in the region that leads to rapid ecotonal sucession along the same axis. This combined with the altitudinal temperature gradients caused by the valleys dissecting the eastern massifs, generates considerable hydrological heterogeneity in the region. In general terms the numerous small lakes in the Argentinian steppe are unsuitable because they are ephemeral, highly saline lakes prone to desiccation. Along the eastern margin of the icecap the lakes are proglacial and as such are unsuitable for chironomid inferred temperature reconstructions (see Section 5.6.2 for a full discussion), and closed, shallow lakes at low altitudes are known to be periodically dry in summer months even in the wetter Chilean areas, but higher and/or larger closed lakes are permanent. To define lakes between these limits a preliminary survey was conducted using Landsat and aerial photography of the region — the areas considered are described in Table 4.2.

4.4 Lake Site Descriptions

4.4.1 Preliminary Investigations

A large number of small lakes ($<2km^2$) are situated in the Andes east of the icecap from valley floors up to 1600m a.s.l., located in topographic depressions or areas over-deepened by glacial scouring.

Area	Description	Suitability
Argentinian steppe between 45–49°S	Hundreds of small ephemeral lakes with a small number of larger permanent lakes that have previously been studied	Unsuitable — the larger lakes are too big to core, and the smaller lakes are not permanent.
Massif between North & South Patagonian Icecaps	A number of proglacial lakes at the termini of glaciers	Unsuitable — conditions in proglacial lakes are largely controlled by the condition of the glacier
Vicinity of Coyhaique	A number of small/medium lakes in the lowlands	Mixed — some lakes are part of an extensive river drainage system
Southern side of Chacabuco Valley	A number of small lakes in a mountainous environment	Suitable — small lakes across an altitudinal gradient, near to a zone of rapid ecological transition
Vicinity of Cerro Castillo	A small number of remote lakes both above and below the tree line	Mixed — these lakes could be good candidates but are quite inaccessible because of a lack of infrastructure and dense forest

TABLE 4.2: Description of regions considered as study sites.

In 2009 multiple short cores were extracted from a number of lakes in the valley, along with surface and bottom water samples; this was followed by a 2010 coring campaign to extract long overlapping sequences from Laguna Edita and Laguna Meche and a continuation of lake water sampling. Full details are given in Table 4.3.

4.4.2 Laguna Edita

This lake (Figure 4.3) is on the southern side of the south-east aligned valley between the Oportus and Tamango ranges. There is a plain to the south-east side that it was hypothesised could be a former extension of the lake, although it is currently around 5m higher than the current lake level. However, small changes in lake level could cause the north-west margin to become an outlet, draining into the valley to the north. This makes the lake potentially sensitive to changes in precipitation/evaporation balance, as it offers a possible range of lake levels from −12m to +2m of the current level. The catchment vegetation is predominately open herb/grass vegetation with some small stands of *Nothofagus dombeyi* surrounding a palaeochannel draining what is now possibly an in-filled lake a short distance away (shown in Figure 4.4). The limit of evidence for the palaeo-shoreline of the Lateglacial palaeo-lake in the Chacabuco Valley is 430m a.s.l. (Turner *et al.*, 2005) and as such Laguna Edita would have been a separate water body during this time.

4.4.3 Laguna Meche

This lake (Figure 4.5) sits on a small plateau on the north side of the Tamango range, and is the largest of a number of small, isolated lakes on the plateau. It has a small, slow flowing outflow draining to a number of lower lakes and no obvious flowing inputs (Figure 4.6). The bathymetry shows two small basins with a maximum depth of 10m. The lake is surrounded by *Nothofagus dombeyi*, and is *c.*50m below the treeline altitude. The evidence summarised in Section 4.2.2 suggest all but the highest peaks in the Tamango range would have been overrun by the ice sheet during the last glaciation in the area, but the persistence or otherwise of ice in the difficult to reconstruct; there are no geomorphological data to suggest ice persisted in the mountainous areas surrounding the valley following the retreat of the icecap, thus the lake has the potential for a sedimentary record going back to the Lateglacial. The site cored was in the northern basin where the bathymetry has a relatively flat base.

FIGURE 4.3: Photograph of Laguna Edita, taken facing south-east.

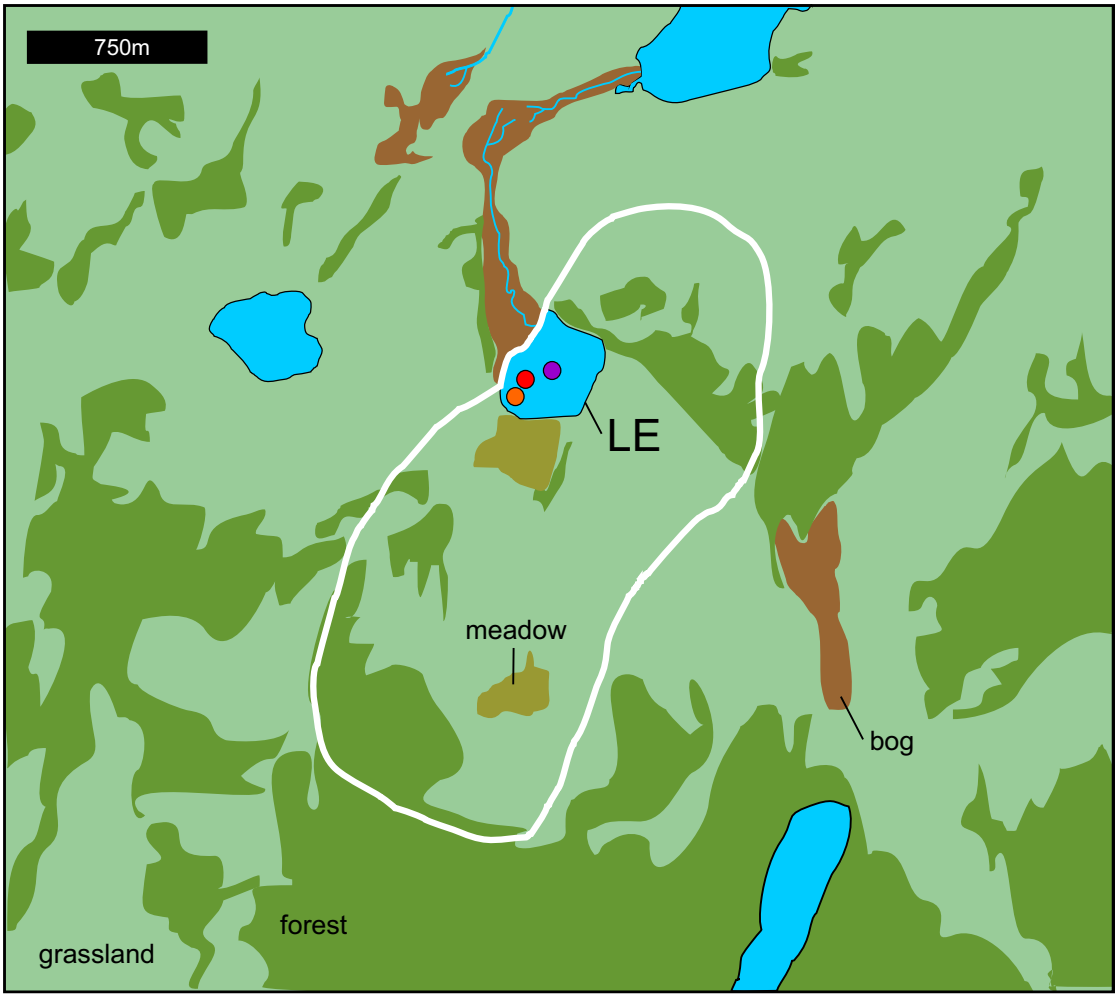

FIGURE 4.4: Sketch of Laguna Edita (LE) and catchment, showing vegetation and watershed (white line). Red dot marks the long core location code EDI-2010. Purple and orange dots mark the short core locations codes EDI-2009-1 and EDI-2009-3 respectively.

FIGURE 4.5: Photograph of Laguna Meche, taken facing south-west.

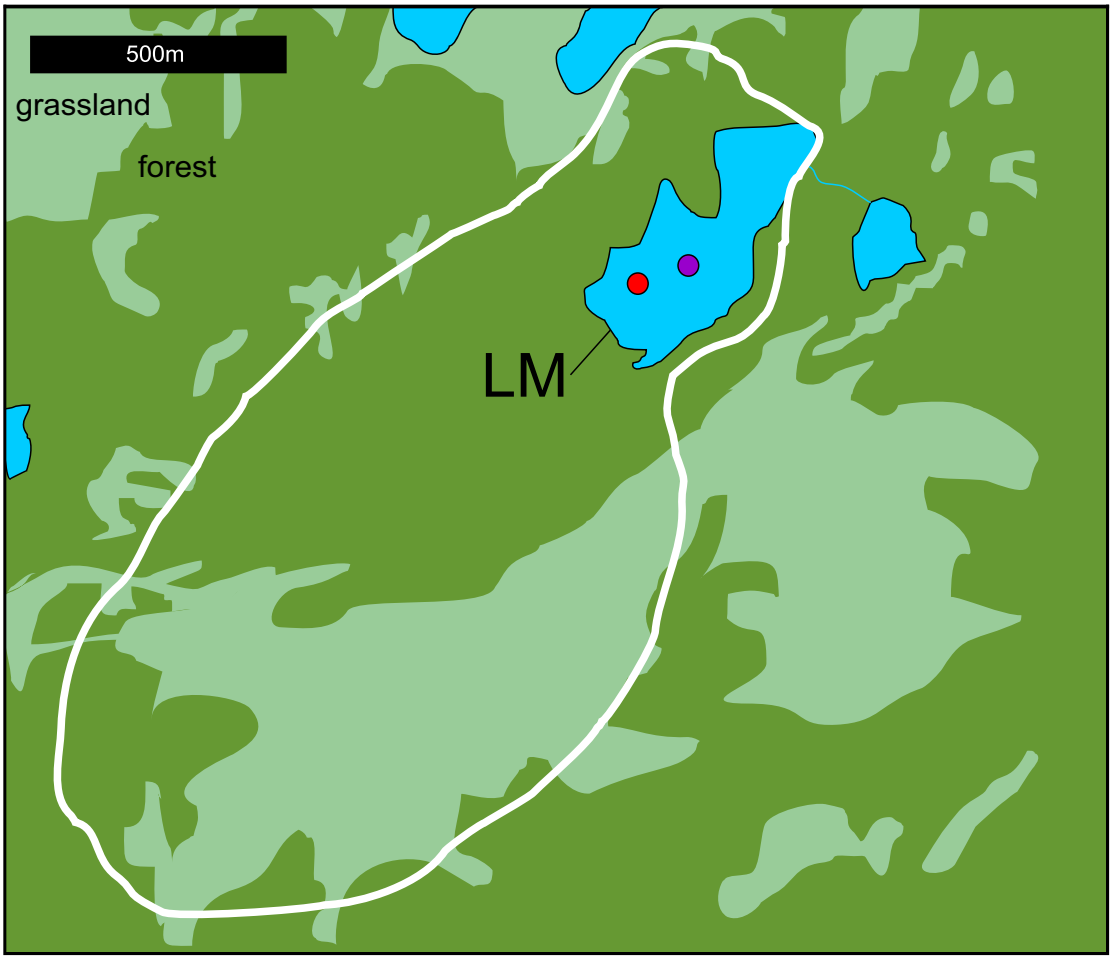

FIGURE 4.6: Sketch of Laguna Meche (LM) and catchment, showing vegetation and watershed (white line). Red dot marks the long core location code MEC-2010. Purple dot marks the short core location code MEC-2009.

Site Name	Location	Altitude	Coring Water Depth	Sediment Length Cored	Sample Codes
Laguna Edita	47°08'44.2"S 72°25'50.8"W	582m a.s.l	7.7m	5.76m	EDI1-9 inc. 1A
Laguna Meche	47°08'48.4"S 72°28'56.8"W	994m a.s.l	7.2m	4.96m	MEC1-6 inc. 1&3A
Dry Lake "Maria Elena"	47°04'06.8"S 72°21'29.7"W	475m a.s.l	n/a	0.87m	OP1
Laguna Espejo	45°42'54"S 71°54'31"W	725m a.s.l	6.5m	0.35m	OP2 1-2
Laguna Cea	45°40'19.5"S 72°14'13.3"W	287m a.s.l	8.5m	5.49	C1-8
Laguna Burgos	45°42'24.1"S 72°12'52.8"W	373m a.s.l	5.5m	4.18m	B2-7

TABLE 4.3: Locations and details of all sites from which material was retrieved in January 2010.

Chapter 5

Methods

5.1 Introduction & Overview

This chapter outlines the technical details of the analytical methods employed in subsequent chapters. It explains the background of the methods and their suitability to address the aims (in Section 2). The first section details the coring technique, sub-sampling strategy and storage of samples. The following section details the different dating methods used to derive the age/depth models. The three following sections deal with the geochemical, modern water and biological proxy analyses respectively.

5.2 Coring & Sample Treatment

5.2.1 Overview

Sediment sequences need to be extracted intact, without contamination. Because of accessibility and transport limitations the equipment employed is necessarily portable and hand-powered. Both gravity and rod-driven devices are used in this study, and cores were subsampled in the field and freeze-dried on their return.

5.2.2 Short Cores

For <100cm long cores gravity driven devices are usually employed because the chambers are capable of capturing the sediment-water interface. In this study a UWITEC gravity-type corer was employed with a barrel length of *c.*60cm, and employing the bottom seal mechanism to prevent loss of sediment during retrieval. Cores were extruded and sub-sampled in the field at 1cm intervals and treated identically to long core material when returned to the laboratory.

5.2.3 Long Cores

In this study a Livingstone-type 100cm long, 5cm gauge stainless steel corer was used to retrieve overlapping core sections (Glew *et al.*, 2001; Wright *et al.*, 1984). Cores were extruded immediately into cleaned PVC guttering and covered with cling-film for stowage during coring. Core logging, photography and sub-sampling at contiguous 1cm intervals was carried out on-site under canvas, and u-channel impressions were taken where particularly complex stratigraphy presented. Samples were transported in airtight barrels and placed in cold storage (+4°C). Samples were freeze-dried because magnetic susceptability measurements using wet samples can hinder detection of magnetic properies (Walden, 1999). Freeze drying was performed using a Heto Freeze Drier at 22\-50°C without sample heating as this can affect the magnetic properties of the sample (ibid).

5.3 Dating Techniques

5.3.1 ^{210}Pb and ^{137}Cs Dating

5.3.1.1 Analytical Procedures

All ^{210}Pb and ^{137}Cs assay were performed at the Geosciences Advisory Unit (GAU) at the National Oceanographic Centre (NOCS), Southampton (UK). ^{210}Pb was measured by alpha spectroscopy of samples spiked with ^{210}Po. ^{137}Cs was measured by gamma spectroscopy.

5.3.1.2 ^{210}Pb age/depth models

^{210}Pb is a naturally occurring isotope resident in the atmosphere. It is deposited in lake sediments primarily as a particulate in rainfall, but can also be transported from sediment within the catchment. It is also produced in-situ as a product of decay of naturally occurring ^{226}Ra. There are a number of age/depth models that utilise the reducing trend in ^{210}Pb activity down-core caused by its decay over time.

Arnaud *et al.* (2006) caution against over-interpretation of radionuclide derived age models in Patagonia because of low radionuclide concentrations in the region and the active geodynamic setting which can cause sediment reworking both within catchments and lake sediment. The importance of tephra deposition when considering choice of model was also emphasised. The necessity of combining ^{210}Pb modelling with both ^{137}Cs derived chronological markers and non-radionuclide derived chronological markers was emphasised by von Gunten *et al.* (2008), who suggest that the best age models can be derived by constraining age/depth models using chronological markers independent of

the ^{210}Pb. The choice of model is dependent on the nature of deposition in the lake, most importantly whether an assumption of a constant rate of ^{210}Pb delivery and/or a constant sedimentation rate can be made (see Table 5.1). Reasons this second assumption may not be valid in this study could include tephra deposition that would increase the sedimentation rate in both volume and mass, thus diluting the ^{210}Pb concentration, or vegetation clearance and burning associated with ranching in the area that could have destabilised the catchment and increased recent sediment flux to the lake. The assumption of constant supply is more difficult to test, as the supply of ^{210}Pb is primarily from rainfall, although there may also be a terrestrial detrital component. Variations in rainfall may thus influence the ^{210}Pb concentration, although on decadal averages the variability in the instrumental record suggests this is unlikely to be a significant limitation. As such, a constant rate of supply of ^{210}Pb is assumed for these lakes and thus the CRS and CIC models are deemed the most appropriate; these models and this assumption is explored and tested in Section 6.2 and summarised in Table 5.1. Although the SIT method is also suitable as it has no *a priori* assumptions, it is not possible to verify the reliability of the model using independent age markers and so was not employed here.

5.3.1.3 ^{137}Cs Age/Depth Models

Smith (2001) propose a protocol for the peer-review of papers utilising ^{210}Pb dating which includes the use of "at least one independent tracer which separately provides an unambiguous time-stratigraphic horizon" (Smith, 2001, p.122). ^{137}Cs is commonly used to provide this independent marker, although some workers have asserted that for CRS and SIT chronologies they cannot provide definitive support, and suggest the IMZ is the only suitable alternative (Abril, 2004, see Table 5.1), although these restrictions apply primarily to mixed sediments. ^{137}Cs was created and released in large quantities into the atmosphere during atmospheric nuclear weapons testing — fallout of ^{137}Cs was incorporated into lake sediments and can thus be used as an independent chronological marker. These markers can be used to assess the accuracy of the age/depth model used to date a sediment sequence.

There is some debate as to the interpretation of ^{137}Cs curves in South America. The long standing interpretation, based on the data from the northern hemisphere is that an initial steep rise in ^{137}Cs represents the start of atmospheric testing in AD1953 and the decline in ^{137}Cs concentration is reflective of the cessation of testing associated the AD1963 Partial Nuclear Test Ban Treaty (peak atmospheric values occurred immediately prior to the treaty). This chronological interpretation has been utilised with satisfactory results in Patagonia (Arnaud *et al.*, 2006), although ^{137}Cs activity data from South America (from Cow's milk, a convenient and sensitive measure of environmental ^{137}Cs due to bioaccumulation) suggests that the history of ^{137}Cs may be quite different in South America (Guevara and Arribére, 2002) with most intense fallout between AD1964–6 with

Model	Description\Assumptions	Reference
SIT	Sediment Isotope Tomography: Inductive model, using independent age markers to constrain the model rather than verify it. Has no assumptions, and can account for mixing, changing initial concentrations and sedimentation rate.	Carroll and Lerche (2003)
CIC	Constant Initial Concentration: assumes both a constant accumulation rate and no changes in supply of ^{210}Pb to the sediment (thus the initial concentration remains constant).	Appleby and Oldfield (1978)
CRS	Constant Rate of Supply: Assumes that the supply of ^{210}Pb remains constant and there is no mixing, but allows for changing accumulation rates.	Appleby and Oldfield (1978)
CFCS	Constant Flux Constant Sedimentation: An early model that assumes both a constant flux and a constant sedimentation rate.	Krishnaswamy *et al.* (1971)
IMZ	Incomplete Mixing Zone: Assumes a mobile radionuclide fraction in the sediment.	Abril *et al.* (1991)

TABLE 5.1: Summary of ^{210}Pb models (excluding ad hoc models) used to date sediments.

a secondary peak from AD1970–72 (Guevara and Arribére, 2007), coincident with French and Chinese atmospheric test periods. This chronology has been used elsewhere in Patagonia (*e.g.* Guilizzoni *et al.*, 2009) although it remains controversial as it is unsupported by direct fallout measurements which indicate the intense testing periods between AD1956–1962 saw the highest ^{137}Cs deposition at monitoring stations (Magand and Arnaud, 2007). This study accepts a ^{137}Cs fallout peak of AD1964±1.

5.3.2 ^{14}C Dating

5.3.2.1 Introduction

All radiogenic dating techniques are based on the predictable decay of unstable radiocarbon atoms (^{14}C) over time and the ability to accurately quantify the current level of decay of a sample, thus obtaining an age estimate. The level of decay is measured using either gas scintillation counting, or using accelerator mass spectrometry (of particular use in small samples). The proportion of the stable ^{12}C/^{13}C is used to calculate the original amount of ^{14}C and through comparison with current activity the level of decay is obtained (Sheridan, 1990).

Variation in atmospheric ^{14}C levels violates the assumption of a constant relationship between stable isotopes ^{12}C/^{13}C and ^{14}C over time, so ages as calculated from radiocarbon dating will be more or less than the true calendar ages (Guilderson *et al.*, 2005). Independent age control on past atmospheric ^{14}C concentrations can provide a method for calibrating radiocarbon ages with calendar ages. Annually resolved tree rings

and U-series dated corals have both been used to model this ^{14}C/calendar year relationship for the past 50,000 calendar years B.P. (Reimer *et al.*, 2009). As the northern and southern hemispheric atmospheric circulatory systems are to some extent independent, separate calibration curves are used for both (Hogg *et al.*, 2009; McCormac *et al.*, 2004). This variation is particularly important for certain periods during the Late Glacial as it has been proposed that deep sea ventilation caused an increased flux of ^{14}C depleted carbon at this time, associated with increased vigour of upwelling as a consequence of the changes in thermohaline circulation that occur during glacial transitions (Fairbanks *et al.*, 2005). This causes radiocarbon "plateaux", where the errors in calibration can be very wide (Reimer *et al.*, 2009). Wiggle matching can help (Bronk-Ramsey *et al.*, 2001; Blaauw *et al.*, 2003), alongside modelling with alternative isochrons *e.g.* tephra layers.

5.3.2.2 Choice of Material & Analytical Procedures

Where there is a mixture of auto– and allochthonous material preserved there are problems with the assumption that both are living contemporaneously and that both are in equilibrium with the atmospheric radiocarbon content at the time of deposition. For autochthonous carbon, organisms will be in equilibrium with the radiocarbon content of their food source; this may or may not be the same as atmospheric ^{14}C concentration (Fallu *et al.*, 2004). The presence of carbonate within lakes is possible in areas where geological carbon is present, and will cause radiocarbon ages of aquatic material to be over estimates of the calendar age of a sample because the inorganic carbon fraction will have an infinite radiocarbon age determination; this is the well established "hard water error effect" (Grimm *et al.*, 2009). Within the catchment, terrestrial material will be in equilibrium with atmospheric ^{14}C at the time the organism was alive (Shotton, 1972), but may be stored for an unknown length of time before being transported to the lake. Allochthonous material can be problematic as it is not necessarily living contemporaneously with the associated autochthonous material; it may have been integrated into the lake sediment sometime after the organism died, being stored in the catchment.

The use of bulk dates can complicate interpretation because of the different radiocarbon sources in the catchment (Blaauw *et al.*, 2004). This has been shown to be a problem in central Patagonia because of the in-wash of Holocene soils (Bertrand *et al.*, 2012), yielding radiocarbon ages 300 to 1100 years too old. Although Bertrand *et al.* attempt to correct for this effect using C/N as a proxy for terrestrial/autogenic carbon this is unlikely to be effective for long sequences where the ^{14}C of soil almost certainly changes through time, and C/N ratios cannot be interpreted purely in terms of carbon source.

As Bertrand *et al.* suggest the ideal sample material is short-lived terrestrial macrofossils; this negates any hard-water effect, and because of the short-lived nature of the fabric of plant leaves, twigs *etc.* there is little possibility of long-term storage *and* preservation

within the catchment. If such material is not present and the lake is known to have no hard-water offset, then aquatic macrofossils may be used, although carbon cycling within the lake means aquatic carbon may yield ages systematically too old. If aquatic material is not appropriate or available and large terrestrial macrofossils are not present, charcoal fragments may be appropriate; they have the benefit of certain terrestrial origin and the preservation of the delicate nature of such material suggests low residence times in the catchment. There is potential in using chironomid head capsules for dating (Fallu *et al.*, 2004; Jones *et al.*, 1993), but problems remain in current understanding of chironomid feeding habits (Grey *et al.*, 2004). There may also be some potential in using pollen concentrates for ^{14}C dates (see Newnham *et al.*, 2007), but the technique remains in an early stage of development and is not appropriate in routine age/depth modelling.

Material was prepared by rehydrating freeze-dried material with de-ionised water using equipment cleaned with 10% HCl, and sieved at 90μm. Material was picked in the following order of preference:

1. terrestrial plant material *e.g.* wood fragments,
2. small particles of charred material or
3. aquatic plant material.

AMS radiocarbon determinations were performed at the Scottish Universities Environmental Research Centre. Pre-treatment of plant remains and charcoal followed the acid-alkali-acid method, specifically digesting in 1M HCl (80°C, 30 minutes), washing free from mineral acid with de-ionised water and digesting in 0.2M KOH (80°C, $\leq$20 minutes). The residue was then rinsed free of alkali, digested in 1M HCl (80°C, 60 minutes) then rinsed free of acid and transferred wet to a silver capsule before freeze-drying. Large woody fragments were processes using the same basic method but with stronger acid and digestion times — 2M HCl (80°C, 8 hours) followed by 1M KOH (80°C, 2 hours), then 1M HCl (80°C, 1 hour). Total carbon is a known weight of the sample recovered as CO_2 by heating with CuO in a sealed quartz tube. Dates are reported in conventional radiocarbon years before AD1950 and analytical confidence expressed at the $\pm 1\sigma$ interval, and calibrated using OxCal v4.1 (Bronk Ramsey, 2009; Ramsey, 2008) using the southern-hemisphere specific calibration data SHCAL04 (McCormac *et al.*, 2004). All dates expressed in this text are calibrated unless otherwise noted.

5.3.3 Tephrochronology

5.3.3.1 Utility of Tephrochronology in Dating

Tephra is fallout from volcanic eruptions, and in the context of tephrochronology in sedimentary environments distal to the source, usually referring to volcanic glass shards.

Most eruptions tend to span weeks or months at most, and are spread across large areas of land and sea. This leaves a marker in sedimentary environments laid down simultaneously (unless reworked). Where tephra layers found in separate sedimentary environments can be matched by their chemical composition, age-equivilence can be established (Alloway *et al.*, 2008). Multiple isochrons can be used to tie sedimentary archives together, and where absolute dating methods constrain the age of a tephra, this date may be transferred to any site where that tephra layer is identified (Lowe, 2011). This is useful in the context of this study for two reasons:

1. Where known and previously dated tephra is identified, well-constrained dates for those eruptions can be integrated into the age/depth model.
2. Where unknown tephra layers are identified in both cores, radiocarbon ages can be integrated and the resolution and/or certainty can be increased; a Bayesian approach to age/depth modelling is particularly appropriate in this context (Wohlfarth *et al.*, 2006).

In the Patagonian Andes a large number of volcanoes are currently active or are known to have been active during the Holocene (see Figure 5.1). The largest Holocene eruptions in Patagonia are well documented, dated and chemically characterised (*e.g.* Stern, 2007), but recent data from the region indicates a large number of previously undocumented ashes (Langdon & Blockley, *pers. comm.*). The geological differences between the Central (basaltic) and Austral (andesitic and rhyolitic) Volcanic Zones mean that it is relatively straightforward to differentiate between volcanic sources by way of elemental analysis of volcanic glass.

In lake sediments tephra is delivered via both direct atmospheric deposition and in-wash of material deposited from the catchment, although in lakes with no significant inflow or outflow and stable catchments the situation is simplified considerably to predominately direct atmospheric fallout. Large quantities of tephra delivery to the lake will dilute the overall organic/inorganic composition of the lake, and thus possible tephra deposits can be identified on the basis of sharp reductions in organic content and confirmed using scanning XRF (Itrax) and microscopic inspection. Depending on the level of delivery of tephra from the catchment to the lake via aeolian and hydrological pathways these sudden dips in organic content may be followed by a gradual recovery (reworking of material) or more simply a sudden recovery as direct deposition ceases.

5.3.3.2 Preparation and Analysis

Volcanic glass shard extraction was attempted using flotation extraction following Blockley *et al.* (2005), but results were unsatisfactory, so acid digestion was used. This method risks chemical modification of the tephra shards, particularly through sodium

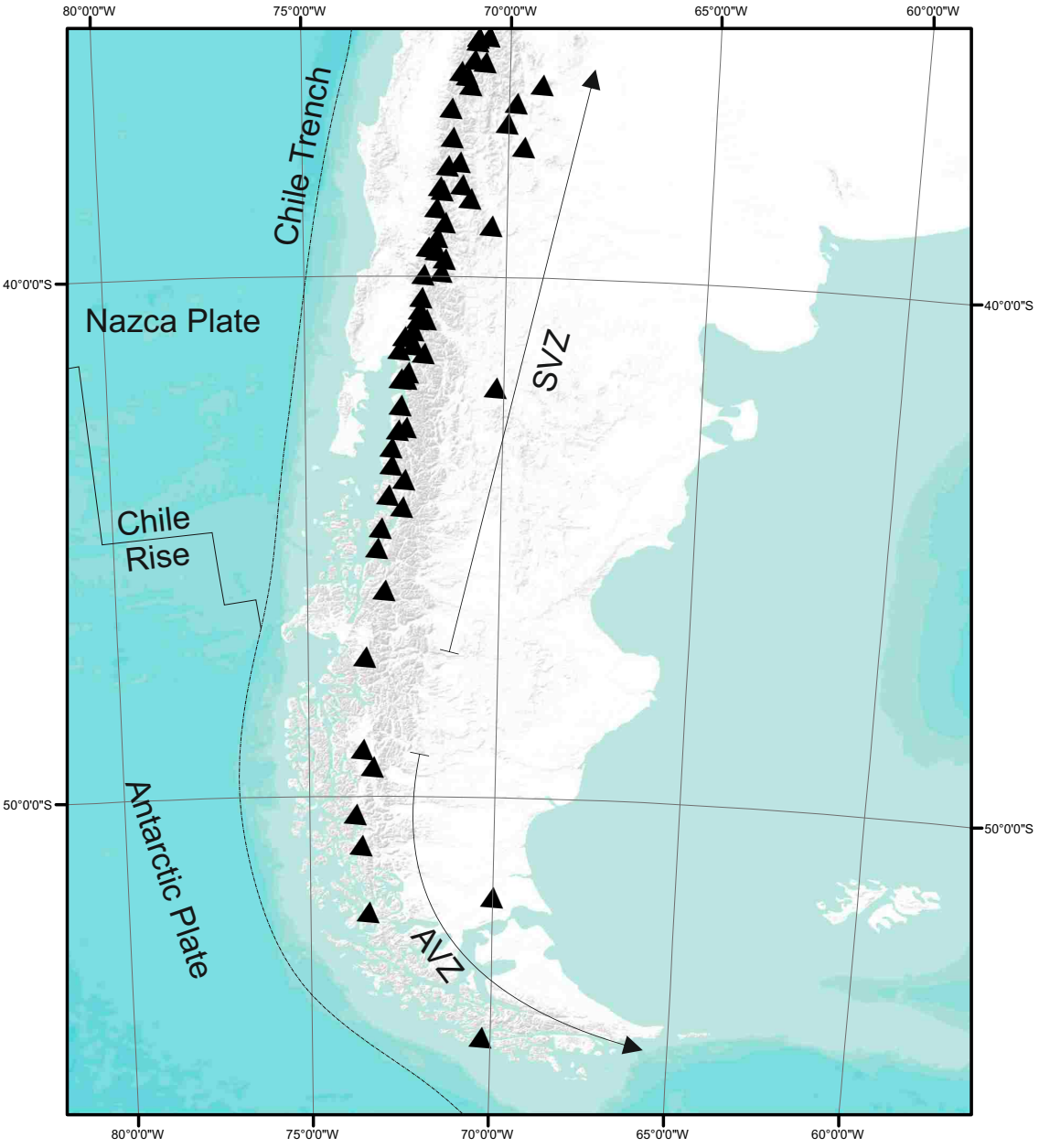

FIGURE 5.1: Map of volcanoes in southern South America known to have been active during the Holocene. Volcano location data from the Smithsonian Global Volcanism Program, geological information simplified from Naranjo and Stern (2004).

migration, although the analyses will be inter-comparable and remain comparable with the published data for elsewhere in South America (*e.g.* Stern, 2007). Acid digestion was performed as follows:

1. add 50ml H_2SO_4 (98%) and agitate,
2. add 15ml of HNO_3 (68%) and agitate,
3. boil until the liquid is clear or yellow,
4. cool the samples and add water,

5. pipette the liquid out, leaving the sediment,
6. decant into a 50ml centrifuge tube, top up with water and centrifuge at 3000 r.p.m.,
7. repeat three times and check the solution is neutral.

Slides for microscopic examination were prepared by drying tephra onto the surface of a glass slide and mounting in Hydromatrix. Tephra stubs for chemical analysis were prepared by placing freeze-dried concentrated tephra in a epoxy stub, conducted by technicians at the University of Edinburgh Tephra Analytical Unit. Chemical analysis by electron microprobe took place at the Tephra Analytical Unit (University of Edinburgh) using a Cameca SX100 and Cameca Peak Sight software. Shards were selected following inspection under reflected light and scanning electron microscopy for the presence of inclusions. The instrument was configured with 5μm electron beam size and a current of 2 and 80KeV, as per Hayward (2011). Secondary standards were analysed every twelve hours (the results are shown in Table 5.2).

5.4 Geochemical Proxy Analyses

5.4.1 Carbon

The total organic carbon (%TOC) is a fundamental measure of the proportion of organic matter in sediments, and is widely employed in palaeolimnology. TOC is a function of within-lake biogenic activity and terrigenous inputs of organic matter, and so gives a catchment-wide indicator of biota and associated transport mechanisms. In this study the loss-on-ignition (LOI) method was used to estimate TOC and $CaCO_3$ following the method of Bengtsson and Enell (1986). The bulk carbon content (organic carbon and $CaCO_3$) can be estimated using weight loss-on-ignition followed by a correction factor based on molecular weight (Lamb, 2004). Although more reliable methods like elemental analysis or "direct-determination" exist, loss-on-ignition is cheap and quick to implement and is considered standard procedure before stable isotope analysis. Percentage content of organic carbon and $CaCO_3$ were measured on contiguous 1cm sub-samples, following freeze-drying. Sub-samples (>0.3g) were weighed to 100μg and heated to 550°C for 2

Standard	n	Na_2O	Al_2O_3	K_2O	CaO	FeO	SiO_2	P_2O_5	TiO_2	MnO	Total
Lipari[(a)]		4.07	13.1	5.11	0.73	1.55	74.1	0.010	0.074	0.065	100.03
1SD		(0.22)	(0.5)	(0.27)	(0.06)	(0.05)	(1.4)	(0.02)	(0.02)	(0.031)	(0.45)
Lipari	48	4.34	13.00	5.19	0.74	1.55	74.68	0.006	0.076	0.061	99.67
1SD		(0.19)	(0.21)	(0.10)	(0.03)	(0.10)	(0.38)	(0.005)	(0.004)	(0.012)	(0.44)
BCR2G	51	3.44	13.48	1.80	7.17	12.52	54.94	0.33	2.25	0.20	99.89
1SD		(0.10)	(0.18)	(0.06)	(0.11)	(0.22)	(0.39)	(0.015)	(0.015)	(0.015)	(0.53)

TABLE 5.2: [(a)]Recommended values for the Lipari glass standard quoted from Kuehn *et al.* (2011). Standard values and standard deviations for the secondary standards used in SEM-WDS analysis of tephra shards. Values are given as wt. %, with their respective standard deviations.

hours, re-weighed and re-heated to 950°C for 4 hours to ascertain the percentage loss of organic carbon and calcium carbonate respectively. In addition, total organic carbon (TOC) was also analysed as part of C/N analysis (described fully in Section 5.4.2), where a direct comparison of measurements validated the method and suggested an appropriate linear conversion factor between LOI and elemental analyser derived measurements, shown in Figure 5.2.

The loss-on-ignition method of estimation was first presented by Dean (1974). Subsequent tests by Heiri *et al.* (2001) demonstrated that variations in inter and intra-laboratory results were present and suggested a standard method be used; this has not been widely adopted. They also concluded that within laboratory range of measurements was generally small, and thus loss-on-ignition remains "a useful tool in for correlating different sediment cores with a distinct LOI signature" (Heiri *et al.*, 2001, p.109). It should not, however, be considered a strictly quantitative method (Dabrio *et al.*, 2004). It has been used to correlate distinct loss-on-ignition profiles between sites (*e.g.* Nesje and Dahl, 2001), and between cores (*e.g.* Virkanen *et al.*, 1997; Walker *et al.*, 1993; Watson *et al.*, 2010). Loss-on-ignition is routinely used as a proxy for the organic/minerogenic content of sediments in lacustrine environments (*e.g.* Massaferro *et al.*, 2005; Langdon *et al.*, 2004) and is sometimes interpreted as an environmental proxy (*e.g.* Nesje and Dahl, 2001; Tingstad *et al.*, 2010), although their utility is much increased where C/N and δ^{13}C data are also available.

5.4.2 C/N Ratios & Stable Carbon Isotopes

5.4.2.1 Scientific Principles

Organic nitrogen forms a greater proportion of lower plants (predominately algal) biomass because of increased abundance of particular proteins and nucleic acids compared to higher plants. Thus different organisms have different C/N ratios; terrestrial organisms have higher C/N ratios (25-50) than aquatic organisms (8-12), which again have a different C/N ratio range to marine organisms (6-8). As such, the origin of deposited organic matter can be ascertained from the C/N ratio (Leng *et al.*, 2006). Although global inventories exist these have been augmented in this study with C/N ratios from modern material throughout the study catchments and locale.

Carbon has two stable isotopes, ^{12}C (98.93%) and ^{13}C (1.07%), and naturally occurring values of δ^{13}C range from $>+20‰$ to $<-100‰$ (Hoefs, 2009). Kinetic isotope effects during photosynthesis concentrate ^{12}C in organic material; the differences between the photosynthetic pathways in C3 and C4 plants mean CO_2 is fractionated differently between them, meaning C3 plants have lower δ^{13}C than C4 plants relative to atmospheric CO_2. The interpretation of stable carbon isotope ratios of the organic carbon depends on the source of the carbon in question — information often derived from C/N ratio. Where the organic material is dominated by aquatic material aquatic

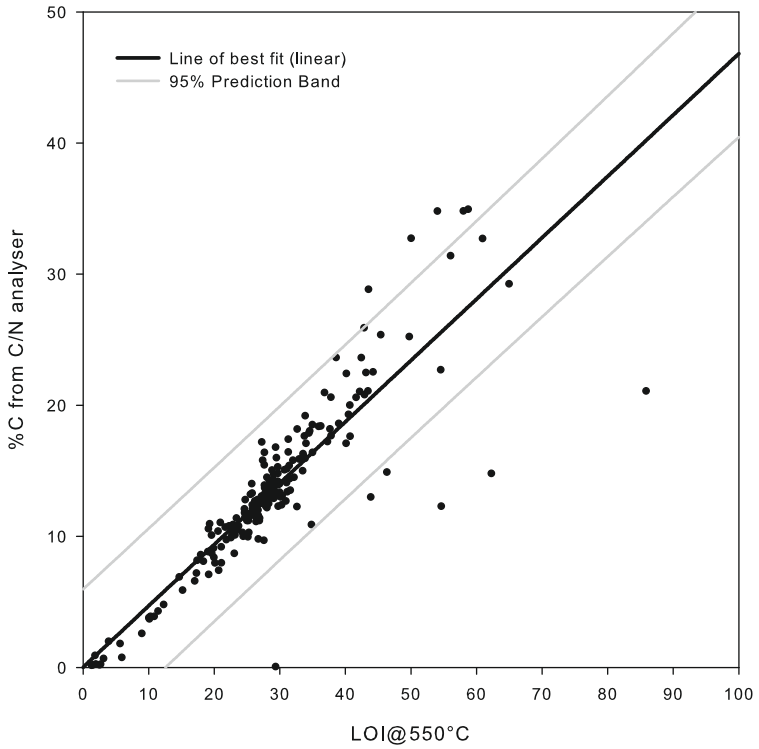

FIGURE 5.2: The relationship between loss-on-ignition and elemental analyser derived %C, showing the conversion factor.

productivity exerts the primary control on δ^{13}C values (Wolfe *et al.*, 2001) via changes in available CO_2. Where the organic carbon is predominately terrestrial in origin δ^{13}C values reflect the surrounding vegetation composition.

Carbon isotopes and C/N ratios have been used extensively in a number of palaeoecological contexts, although the application has been limited in Patagonia: C/N ratios in lake sediments from the central Patagonian region have been reported (Bertrand *et al.*, 2012), and carbon isotopes have been reported for lake sediments for the past 2,000 years which were linked to lake level changes in the Argentine steppe (Mayr *et al.*, 2005). Moy *et al.* (2008) reported productivity changes in Torres del Paine region that they linked to temperature changes in the past 1,000 years.

5.4.2.2 Analytical Methods

Samples were initially treated with 5% HCl for 12 hours to remove carbonate, followed by rinsing using 300ml of de-ionised water through Whatman no.41 filter paper using a vacuum line. Sediment on filter paper was then dried at 50°C in a drying cabinet and the remaining sediment was powdered using a pestle and mortar. Small (<1g) sub-samples provided large quantities of carbon for analysis. Analyses were performed using equipment at the NERC Isotope Geophysical Laboratory. Sub-samples of powdered samples *c.*50μg were placed in tin capsules which were folded and crushed by hand and weighed before combustion and C/N analysis using a Thermo Finnegan Delta

+XL followed by $^{12}C/^{13}C$ analysis using a VG Optima with Carlo Erba NA1500. Appropriate in-house standards were used throughout and the values corrected to the $\delta^{13}C_{PDB}$ (Pee Dee Belemnite) standard. Errors are not reported as analysis of standards measured during analysis show very low analytical error (see Figures 5.3 & 5.4).

5.4.3 Scanning x-ray Fluorescence

5.4.3.1 Scanning x-radiography in Palaeoecology

The application of micro-radiographic imaging and elemental analysis in lacustrine sedimentology has been of use in identifying annually laminated layers (Ojala, 2004), but the techniques are also particularly applicable where clast sizes are >2mm (Principato, 2004), as is the case for parts of the early sediments in this study. The use of flat-beam radiography overcomes many of the limitations of traditional radiographic methods and allows radiographic analysis at intervals of between 20–100μm. The method could be considered semi-quantative and there are problems with normalising data, discussed in Weltje and Tjallingii (2008); Löwemark *et al.* (2011).

To date scanning x-ray fluorescence (XRF) has been applied mainly in marine sediment sequences (*e.g.* Hibbert *et al.*, 2009; Cronan *et al.*, 2010), and has had more limited application in lacustrine sediments (Cuven *et al.*, 2010; Metcalfe *et al.*, 2010). The continuous core scanning feature of these systems has not been fully exploited in sediment sequences from southernmost South America (Kastner *et al.* 2010 used >1cm stepped analysis). In limnological studies that have used scanning XRF the data has been used to interpret changes in sedimentology, and as a precipitation proxy (ibid) linked to catchment runoff and erosion. Often individual elements or pairs of elements are used as environmental proxies, some of which are summarised in Table 5.3. Elemental profiles in combination with imaging may allow for the detection of indicators of tephra deposition (Fe, Ti, Si) along with elements representative of erosion in the catchment (Fe, Mn). This is a novel use of the technique, as the usual method for detecting tephra is ashing samples and visually checking (Pilcher and Hall, 1992) which is time consuming. The method also has the potential to provide a very high resolution alternative to magnetic susceptibility, which is essentially a proxy measure of Fe and Mn in sediments.

5.4.3.2 Analytical Procedure

The Itrax core scanner (Cox Analytical Systems) is a relatively new core scanning system that combines x-radiography and x-ray fluorescence scanning to a resolution as low as 200μm (Croudace *et al.*, 2006). The scanner has the ability to assay major and trace elements in continuous cores, non-destructively, unlike conventional WD-XRF which is destructive and can only sample single aliquots. Core material was sampled into u-channels in the field and stored sealed in cold storage at +4°C prior to scanning.

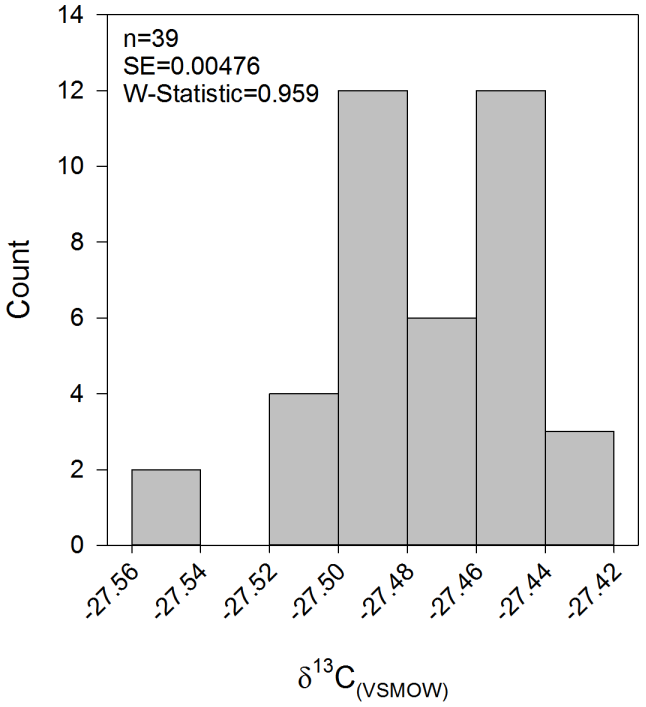

FIGURE 5.3: δ^{13}C measurements of internal laboratory standard BROC2 and standard deviations of the same. Note that normality is assumed due to the sample size.

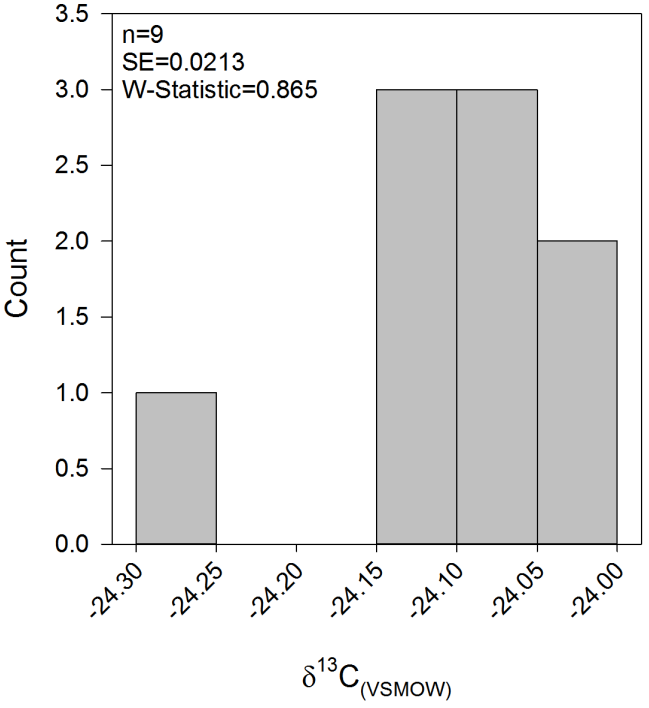

FIGURE 5.4: δ^{13}C measurements of internal laboratory standard SOIL and standard deviations of the same. Note that normality is assumed due to the sample size.

Element	Interpretation
Si	Tephra deposition, diatoms abundance. Grain size.
Ti	Tephra deposition
Fe	Erosion in catchment
Mn	Erosion in catchment
Fe:Mn	Redox conditions
Ca:Fe	Biogenic carbonate: detrital clay ratio. Sediment source relationships.
Sr:Ca	Affected by sediment porosity and grain size. Can indicate high Sr, indicative of shallow water.
K:Rb	K is associated with detrital clay.
Zr:Rb & Ti:Rb	Useful as sediment source indicators.
Fe:Ti	Fe is mobilised during redox diagenesis so elevated Fe associated with oxic conditions.
Mn:Ti	Indicator of redox-related processes.
Ba:Ti	Productivity indicator.
Zr	Grain size.
Ti, K, Rb, Zr & Si	Detrital inputs.
Ca, Sr, Mn, Si	Lake productivity indicators.
All	Correlation matrices allow for unit identification.

TABLE 5.3: Summary of common palaeolimnological interpretations of elements in scanning XRF profiles.

Photographic and x-radiographic images were aquired at high resolution followed by XRF scanning at a resolution of 400μm; full analytical conditions are presented in Table 5.4. Analysis was performed using equipment at the National Oceanography Centre, Southampton.

5.4.4 Magnetic Susceptibility

5.4.4.1 Environmental Magnetism in Palaeoecology

The influx (and thus concentration) of magnetic minerals to lake sediment is modified by various erosional, depositional and transport processes within the catchment which can be summarised as follows:

Allogenic: Atmospheric (wind erosion, tephra), fluvially borne minerals,

Authigenic: Bacterial magnetosomes, authigenic iron sulphides, reductive diagenesis.

These are controlled partly by climate (temperature, rainfall, seasonality) along with pedogenic processes and atmospheric deposition, particularly from volcanic ash deposition. The concentration of magnetic minerals can be monitored by measuring the magnetic susceptibility of sediments; the material is subjected to a low magnetic field inducing a small magnetisation that disappears when the field is switched off. The proportional factor between magnetic field and magnetisation is the magnetic susceptibility.

It is for these reasons the logging of magnetic susceptibility of lake cores has become a standard method in lacustrine studies. Magnetic susceptibility has been measured in lake sediments from Tierra del Fuego, where Waldmann *et al.* (2009) concluded that it was correlated with regional climate changes throughout the Holocene, and interpreted the record as representative of humidity in the region, further suggesting that distinctive climate events could be recognised in the record, including the "Little Ice Age" (higher values) and Medieval Warm Period (lower values). Although plausible, the dating control (4 chronostratigraphic markers for >11,000 years of accumulation) for this record precludes a confident correlation with these events. Magnetic susceptibility was also measured in lake sediments from Lago Puyehue, where it was interpreted as representing

Parameter	Setting
Tube	Mo
Voltage	30kV
Current	30mA
Exposure time	30s
Step size	400μm

TABLE 5.4: Summary of parameters used in Itrax XRF data aquisition.

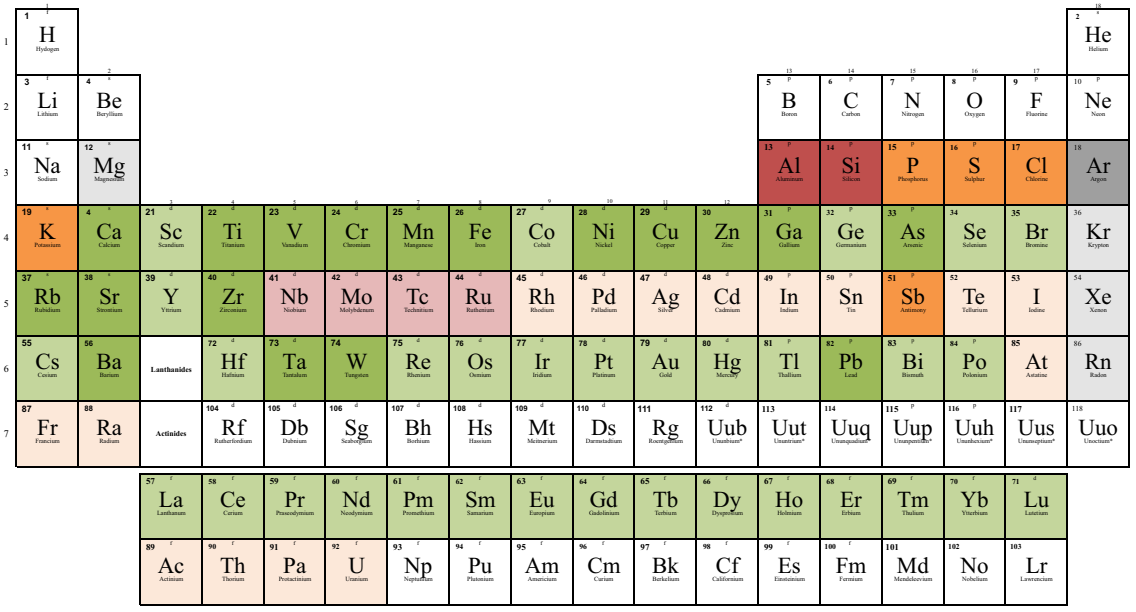

FIGURE 5.5: Table of the elements, showing the detection capabilities of the Itrax system, coloured in order of descending sensitivity: green, orange and red. Elements in bold are those for which data was collected in this study. Noble gas data was collected as it provides useful information on sediment density and instrument configuration.

changes in productivity and rate of detrital supply (Bertrand *et al.*, 2007). In both records the highest values correspond to layers of tephra, and as such the method has utility in identifying tephra layers in the sediment. In this study the magnetic susceptibility measurements have two main uses — the first is to identify potential tephra deposits for further analysis, and the second is to construct a history of terrigenous detrital input to the lake. In addition the data will allow for cross-correlation of the cores in conjunction with other proxies.

5.4.4.2 Analytical Procedure

Although whole-core logging is often employed, in this study contiguous discreet 1cm sub-sampled aliquots were employed as the cores were previously sub-sampled in the field. Volume specific magnetic susceptibility measurements were taken from 10ml sub-samples using a Bartington Instruments MS-2 aliquot sampler at both high and low frequency. Magnetic susceptibility is measured against a background of ambient magnetism that is subtracted from the reading — where background variation was >0.2 S.I units measurements were rejected.

5.5 Modern Water Isotopes (δ^2H & δ^{18}O)

5.5.1 Utility of Modern Water Isotopes in Palaeoecology

The analysis of the stable isotopes of H and O is important is understanding the hydrology of the catchments being studied, particularly the state of the evaporative conditions at the sites. Precipitation will plot on a global and locally offset meteorological water line which is a linear relationship between δ^2H and δ^{18}O (Leng *et al.*, 2006). Where surface waters diverge from this line by way of reduced δ^2H, kinetic fractionation has taken place. This occurs during the processes of water evaporating to vapour, because $^1H_2{}^{16}O$ has a higher diffusivity than $^2H^1H^{16}O$ or $^1H_2{}^{18}O$; this leads to enrichment of the remaining water (Hoefs, 2009). Lakes with very high evaporative losses will have waters with low δ^2H, whereas those that have no evaporative loss and are open and groundwater fed will have δ^2H/δ^{18}O in balance with local meteoric waters (Leng, 2004).

The most extensive study of surface waters in Patagonia constructed local meteoric waterlines and local evaporation lines for an area of semi-arid Patagonia in the region surrounding Laguna Potrok Aike (Mayr *et al.*, 2007). They found that the isotopic composition of precipitation was dependent on wind direction, where air masses from the west were more depleted in δ^2H and δ^{18}O than those from the east. As isotopic composition of precipitation is influenced by temperature during condensation in clouds, subsequent evaporation processes, as well as the origin of source precipitation. Ascent of westerly air-masses over the Andes causes rain-out; this leads to $\delta^{18}O_{VMOW}$ values of -8 to -13 to the west and -12 to -16 east of the Andes (Stern and Blisniuk, 2002).

5.5.2 Analytical Procedure

Modern waters were collected from surface waters directly and stored in double-sealed plastic containers. Abyssal waters were sampled using an remotely operated sampler. Samples were stored at 4°C before analysis at the Natural Environment Research Council Isotope Geosciences Facility using a GV Isoprime with Multiprep and EuroPyrOH and reported as $\delta^{18}O_{VMOW}$ and δ^2H_{VSMOW} (relative to the Vienna Standard Mean Ocean Water) with reference to appropriate in-house standards.

5.6 Chironomid Analysis

5.6.1 Ecology, Physiology & Lifecycle

Chironomids grow from eggs, where they develop through five juvenile stages; four larval instars, the pupa and the adult imago. Importantly, the juvenile stages are split into four

instars and the head capsule is shed at each stage. The larval stages are either free-living, or more commonly encountered in tubes made from detritus. Feeding habits are more or less species or genus specific and include a variety of material including organic detritus, woody debris, diatoms and predation including cannibalism. Chironomids are encountered in the littoral, profundal and semi-terrestrial zones, with individual species (sometimes genera) usually specific to one such region; some profundal species are adapted to low-oxygen conditions via haemoglobin-like compounds in the blood. The pupal stage is brief, and the metamorphosis to adult imago takes place during this time. The adult stage is usually short-lived; the majority of species do not feed at all, and once mating and oviposition occurs the adult dies. Most larvae are multi-modal feeders, and the mode can change thorough larval development. For tube-dwelling species the foraging area is restricting to the area immediately surrounding the tube. They usually utilise some combination of collector-gathering, collector filtering, scraping, shredding, engulfing and piercing. Food sources can be broadly classified as algae, detritus, macrophytes, woody debris and invertebrates but taxa are rarely limited to one such group. A fuller description of the general biology and ecology on the Chironomidae can be found in Armitage *et al.* (1995).

5.6.2 Development of Chironomid Inferred Proxies

These characteristics were first exploited in the limnological classification of lacustrine environments (see Porinchu and Macdonald, 2003) where indicator species were used as measures of trophic status (*e.g.* Wiederholm, 1979; Wiederholm and Eriksson, 1978) and in monitoring pollution (*e.g.* McGill *et al.*, 1979; Kansanen, 1985); these studies were by their nature qualitative and limited by the ecological data available at the time. The relationship between chironomid population and environment has been explored in a number of regional "training sets", where a number of lakes across an environmental gradient are sampled for both physical properties and contemporary chironomid populations. From this the important environmental variables are defined and the specific climatic/population relationship for individual species can be calculated; this is ideally a normal or skewed-normal distribution. Most chironomid transfer functions utilise weighed average transfer functions, sometimes with additional partial least squares regression (WA-PLS), using the modern population training sets to calculate the optimum value and tolerance range of a particular taxa in relation to the environmental variable of interest (ter Braak and Juggins, 1993). The sensitivity of the proxy response to environmental variables is tested using jackknifing and bootstrapping; similar methods have been used in palaeolimnology for several years (see Battarbee, 1994).

Subsequent advances in statistical techniques have allowed for the use of chironomid-based techniques in quantitative reconstruction of a number of lacustrine environment variables including salinity (Mousavi, 2002), trophic status (Langdon *et al.*, 2004), acidification (Brodin and Gransberg, 1993), oxygen supply (Clerk *et al.*, 2000),

total phosphorus (Brooks *et al.*, 2001), chlorophyll a (Brodersen and Lindegaard, 1999) and lake level (Kurek and Cwynar, 2008b; Luoto, 2009b). Of particular interest to climatologists is the use of chironomids to reconstruct past lake surface temperatures (Olander *et al.*, 1999; Brooks and Birks, 2001; Luoto, 2009a; Larocque *et al.*, 2001). It has been demonstrated that lake surface temperatures are usually directly related to air temperature, and that chironomid populations are sensitive to changes in water temperature. The early criticisms of Hann *et al.* (1992) who argued that the influence of depth, transparency and substrate were more important in explaining population have been largely overshadowed by subsequent studies suggesting that air temperature is often the most powerful variable in controlling chironomid assemblage (Boggero *et al.*, 2006; Lotter *et al.*, 1997; Walker *et al.*, 1991), at least in the northern hemsiphere. Most studies now use the average temperature of the three warmest months (June, July & August in the North; December, January & February in the South), usually interpolated from local weather stations, although a single site measurement has been shown to be adequate (Walker *et al.*, 1992). Populations are to a far lesser extent affected by winter temperatures, although it seems likely that seasonality plays a role in influencing the length of the breeding season for some species (Tokeshi, 1995).

Regional temperature-transfer functions have been constructed for the European palaeoarctic (Lotter *et al.*, 1999), Russia (Nazarova *et al.*, 2010), New Zealand (Verschuren and Eggermont, 2006), Australia (Rees *et al.*, 2008) and for South America (Massaferro and Larocque-Tobler, 2013). A number of studies have shown that chironomid populations in north-western Europe respond to previously known changes in climate throughout the Lateglacial and Holocene for both millennial and sub-millennial scale events (Brooks and Birks, 2001; Langdon *et al.*, 2011, 2004; Watson *et al.*, 2010; Luoto *et al.*, 2010). However, "chironomid palaeoecology in north-temperate regions has made tremendous progress over the past decade, but studies in tropical and southern hemisphere regions remain relatively scarce" (Verschuren and Eggermont, 2006, p.1926). Although there has been limited success in combining training sets from a wide area (see Lotter *et al.*, 1999) usually regional training sets are necessary (Larocque-Tobler, 2009), and for Patagonia these are in early stages of development.

The chironomid based qualitative studies for South America that have already been published have provided considerable insight. The first application was in the Taitao Peninsula where Massaferro and Brooks (2002) identified, on the basis of the chironomid evidence, a number of cooling/drying episodes throughout the Lateglacial/Holocene. Subsequent work in the Chonos Archipelago (Massaferro *et al.*, 2005) identified a number of changes inconsistent with those identified in the Taitao Peninsula. Chironomid records from the Huelmo site again identify a number of climate changes consistent with previous work on the site. The lack of a quantitative element to these chironomid analyses means there is considerably more potential in these archives, but these three studies have proved that chironomid based climate proxies are sensitive and provide useful climate information in the region.

Vandergoes *et al.* (2008) presented the first quantitative chironomid-inferred temperatures for the Lateglacial in the southern hemisphere (New Zealand), suggesting a temperature depression of *c.*2–3°C during a 700 year period during the Antarctic Cold Reversal, along with generally unstable temperatures during this period; although the chironomid stratigraphy shows significant excursions from the long term warming trend during the Lateglacial, the pollen stratigraphy does not reflect this to such an extent; this suggests the chironomid proxies are most sensitive to these changes at the time. Chironomid-based quantitative temperature reconstructions in New Zealand have been extended as far back as MIS 2/3 (Woodward and Shulmeister, 2007). Massaferro and Larocque-Tobler (2013) demonstrate the utility of the first transfer function for Patagonia, presenting a temperature record for 15,000 years of palaeoclimate at Laguna Potrok Aike, suggesting highest temperatures between 10,500–3,500 years B.P. and the possibility of depressed temperatures during the period of the Antarctic Cold Reversal.

5.6.3 Problems with Chironomid Proxies

Chironomid populations respond to a number of factors that potentially confound the climatic variable being reconstructed. Chemical factors (*e.g.* oxygen availability), food quality and availability, changes in substrate (*e.g.* tephra deposition) and lake level can all influence chironomid populations and confound climate reconstructions. There is some within lake variation of chironomid populations (Heiri, 2004) associated with water depth (Kurek and Cwynar, 2008a). Sediment coring position has not been found to radically change the palaeoclimate reconstructions (Heiri *et al.*, 2003), but may be significant when attempting to reconstruct chironomid inferred temperature where there have been lake level or bathymetric changes; some studies have exploited this relationship between chironomid populations and water depth to reconstruct lake level using both within-lake and local training sets (Kurek and Cwynar, 2008b).

The inter-play between regional climate variables and catchment or local scale variability can cause problems in the interpretation of chironomid based reconstructions (Velle *et al.*, 2010), but by using multiple sites with different conditions (*e.g.* altitudinal differences) a consensus can be built on the timing of change. When considering the building of training sets, there are still problems in obtaining accurate temperature data for remote sites. Interpolated or modelled average temperatures from nearby metrological stations have been used in most studies over single point measurements and found to be satisfactory. Calibration-in-time offers a means of constructing training sets from recent palaeolimnological data which can be very precisely correlated with appropriate meteorological data (Larocque-Tobler *et al.*, 2011; Larocque *et al.*, 2008). Gridded data combined with GIS modelling can suffice where there are no suitable meteorological stations to interpolate from (Porinchu *et al.*, 2008; Rolland *et al.*, 2008). The sample specific errors in some chironomid-inferred temperature transfer functions are still high enough to preclude a robust interpretation of small climate changes,

although it should be noted that the reporting of uncertainties at all is a significant improvement on other methods.

There have been relatively few studies of chironomid ecology in South America (aside from the northern sector, see Donato *et al.*, 2008), thus the taxon-specific autoecology and indicative value of chironomids in South America is relatively poorly understood compared to the data for the northern hemisphere; even some of those taxa that are present in the better understood European, North American and Canadian faunas seem to have radically different ecological preferences in a South American context (Verschuren and Eggermont, 2006). Many of the taxa present in South America are also present in New Zealand and to a lesser extent Australia.

5.6.4 Preparation, Extraction & Taxonomy

The preparation of samples for chironomid analysis is always based on the Walker and Paterson (1985) methodology of treatment with KOH, sieving and manually sorting under magnification. There are variations and allowances for differing sediment types, including ultrasonic treatment (Lang *et al.*, 2003) and staining (Larocque-Tobler and Oberli, 2010). Rolland and Larocque (2006) demonstrated the use of heavy liquid flotation of head capsules and suggested it may represent an alternative, more rapid method similar to that described by Fast (1970). This is advantageous as the current methods are labour intensive and time-consuming; they are however very robust and are well proven to have little species bias, and as such the following methodology was employed:

1. *c.*0.3g of freeze-dried sediment sub-sampled.
2. Sub-sample placed in 15ml 10% KOH preheated to 65°C.
3. Sample immersed for 240 seconds, with 10 seconds agitation by magnetic stirrer repeated every 50 seconds.
4. Samples sieved using de-ionised water to 180μm and 90μm fractions.
5. Samples transferred to airtight vials for processing within 24 hours; stored at 4°C.
6. All specimens picked using fine forceps from Borgorov sorting chamber under low power magnification (x4–30).
7. Specimens mounted using Euparal on 6mm circular cover slips ($<$2 specimens per cover slip, 12 cover slips per slide).
8. Specimens identified to lowest taxonomic level under high power microscope (x100–1000).

Digestion time and agitation should be as short and gentle as possible to minimise chemical and mechanical damage to chironomid head capsules; freeze drying was found the reduce the digestion and agitation time, possibly due to the release of water held in mineral structure by polar attraction. The ultrasonic bath processing to clean dirty specimens (Lang *et al.*, 2003), particularly of Tanypodinae proved ineffective. The blue staining described by Larocque-Tobler and Oberli (2010) also proved unnecessary as the sediment could be diluted prior to sorting to reduce the density of material during picking; this proved sufficient to reveal all of the specimens. Small meshes were used because larger mesh sizes have had mixed results (Larocque *et al.*, 2009).

A minimum of around 30–50 head capsules is considered the minimum sample size to be considered statistically robust sample of the population (Heiri and Lotter, 2001; Quinlan and Smol, 2001), and in keeping with most other studies half head capsules split along the medial suture were counted as such. This presents a potential source of bias in the Tanypodinae, because unlike all other sub-families of Chironomidae they have no medial suture, but are liable to tear irregularly, preventing fair assessment of the amount of head capsule remaining. There is no obvious solution to this problem and so fragments smaller than half of Tanypodinae specimens were excluded, whereas fragments over half were counted as complete. The entire sample was picked and counted as although Velle and Larocque (2007) propose the use of exotic markers to enable sub-samples to be processed, the method they present does not guarantee the sample to be free from bias caused by the preferential settling of specimens when decanted.

Although many species are only described from the adult stages, cladistic analysis from all life stages supports the assertion that the larval characters differentiate according to phylogeny (Armitage *et al.*, 1995). Diagnosis is usually possible to genus or below, but diagnosis to genus level is usually sufficient to produce accurate temperature estimates (Heiri and Lotter, 2010). Chironomid identification is based mainly on the morphology of the mentum, ventromental plates and the number and condition of teeth on the manibles. A number of Tanypodinae can also be differentiated on the basis of the arrangement of the cephalic setae (Rieradevall and Brooks, 2001). Chironomid taxonomy is far from harmonious between workers, and the guides published focus on the palaearctic, and few focus specifically on features present in sub-fossil specimens. This is problematic for work in the southern hemisphere because parts of the fauna are considerably different. Taxonomic work is on-going in South America (Donato *et al.*, 2008), and this investigation presents an opportunity to test and enhance the taxonomic work in the area. The statement "some subfamilies are better understood than others, and the Orthocladiinae [are] probably the least understood" (Armitage *et al.*, 1995, p.49) is true of the South American fauna and the sub-family are given special treatment here.

The published chironomid taxonomy for South America is limited, but the extensive guides for northwest Europe and North America, along with working taxonomies from New Zealand and South America provide the basis of the taxonomy used in this study (see Appendix A for a complete description of taxonomic sources). Although taxonomic

harmony between all studies is always desirable, the compatibility with the taxonomy used in transfer functions is absolutely essential to robust application of transfer functions outside of the training set. As such, this taxonomy has been designed to function with the transfer functions applicable to the area and for completeness is described in Appendix A. For the sake of clarity, in-line citations to sources of ecological interpretations of individual taxa have largely been omitted but complete reference lists are given in the relevant taxonomic entry in Appendix A. Non-chironomid Dipteran taxa were described as a percentage of the total chironomid sum, following Woodward and Shulmeister (2007).

5.6.5 Transfer Function

Transfer functions from the northern hemisphere are likely to be ineffectual and inaccurate for application in the southern hemisphere; a number of genus level taxa show radically different habitat preferences and there is a high risk of poor representation of taxa because of the number of species endemic to the southern hemisphere (*c.f.* Woodward and Shulmeister, 2006). This has led to the development of training sets for both southern South America and New Zealand. The transfer function used in this study was developed and published by Massaferro and Larocque-Tobler (2013). It uses a 63-lake, 44-taxa training set covering much of central Patagonia (the locations are shown in Figure 5.6). They found that Secchi depth, conductivity, depth, mean annual temperature and water temperature explained 41% of the variance in the chironomid assemblage, and 21% of the variance was explained by mean annual temperature alone. The resulting performance statistics for the WA-PLS 3-component model are given and compared to other transfer functions in Table 5.5.

The mean annual temperature optima are given in Figure 5.7, showing patterns of temperature distribution of key taxa seen supposed elsewhere in the current literature — for example, *Parochlus*, *P.fennica* and *Corynoneura* as cool indicators. This transfer function overestimates temperatures at the lower end and underestimates temperatures at higher temperatures (see Figure 5.8).

5.7 Summary and Conclusions

This study uses a number of methods with established applications in predominantly northern European contexts, but which have not yet been widely applied in southernmost South America. They have been shown to have potential to answer the research questions set out in Chapter 2, but will require careful appraisal to test their

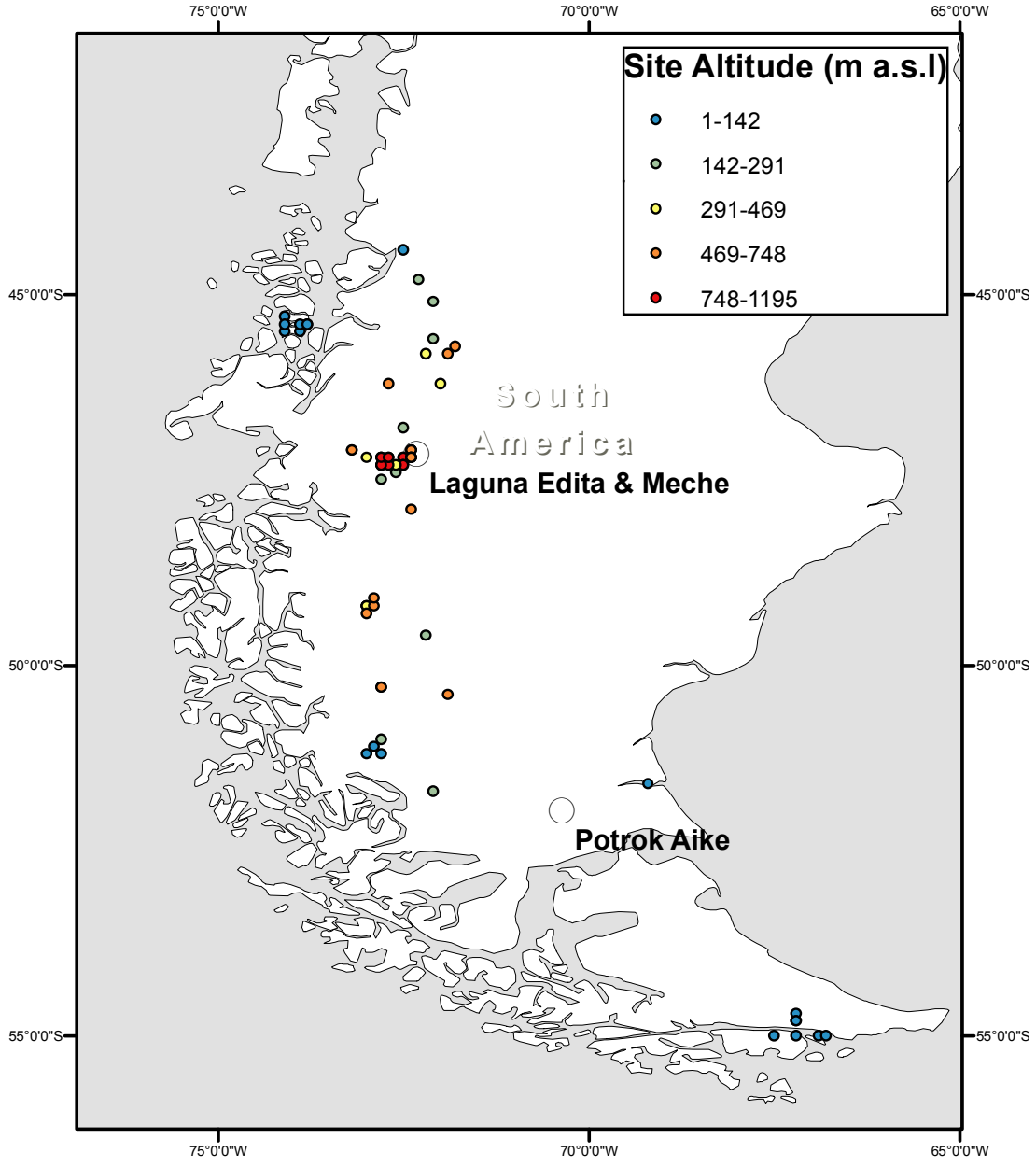

FIGURE 5.6: Map of sites included in the training set for the transfer function presented by Massaferro and Larocque-Tobler (2013) with Laguna Potrok Aike and the sites used in this study also marked.

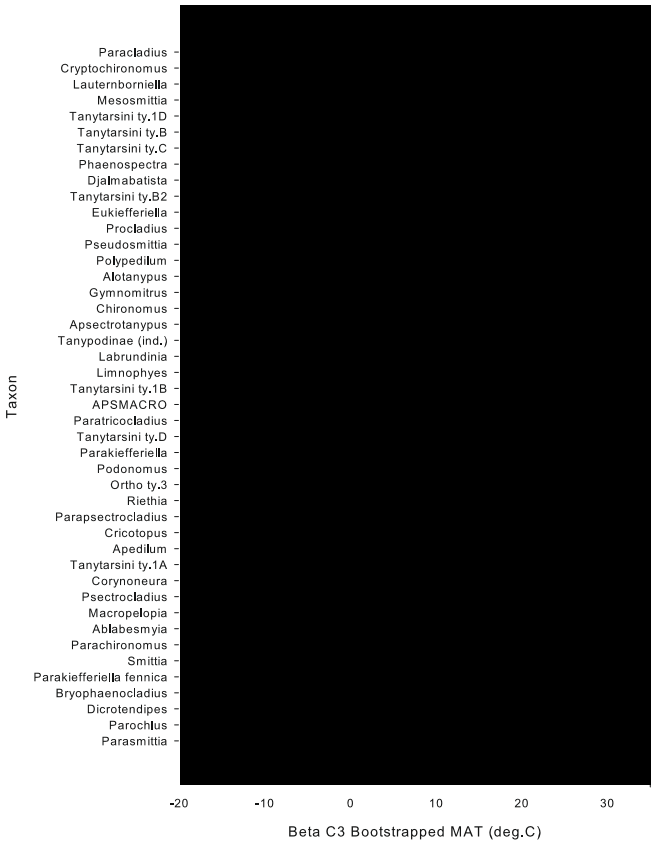

FIGURE 5.7: WA-PLS beta 3rd component bootstrapped mean annual temperatures of all taxa in the Massaferro and Larocque-Tobler (2013), shown with standard deviations from jackknifing.

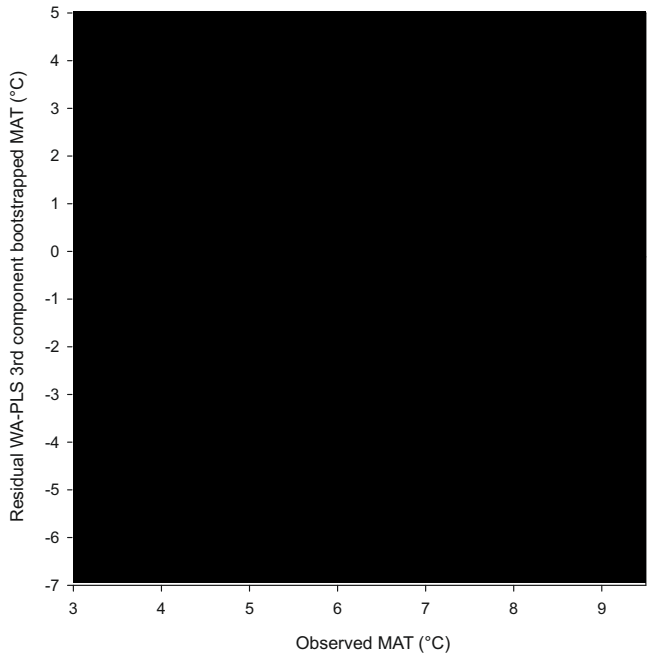

FIGURE 5.8: Residuals of the WA-PLS 3rd component temperatures plotted against observed temperatures in the transfer function of Massaferro and Larocque-Tobler (2013).

Region	r^2	RMSE (°C)	Max. bias (°C)
Patagonia[a]	0.64	0.83	1.81
Combined[b]	0.794	1.82	4.92
NE Russia[c]	0.87	7.93	2.17
Australia[d]	0.72	0.94	1.35
Fennoscandia[e]	0.37	1.53	3.88
Norway[f]	0.86	2.13	2.84
Finland[g]	0.78	0.72	0.79
Lapland[h]	0.65	1.13	2.1

TABLE 5.5: Performance statistics for the chironomid inferred mean annual temperature inference model. [a]Massaferro and Larocque-Tobler 2013, [b]Lotter *et al.* 1999, [c]Nazarova *et al.* 2010, [d]Rees *et al.* 2008, [e]Olander *et al.* 1999, [f]Brooks and Birks 2001, [g]Luoto *et al.* 2010, [h]Larocque *et al.* 2001.

ability to produce palaeoclimatological data for the study sites introduced in Chapter 4. As such, Chapter 8 will test the proxies for cores covering the past *c.*100 years for which instrumental and high resolution quantitative palaeo-environmental data are available from sites proximal to the study area. This will inform the interpretation and inferences made from data from longer cores presented in Chapters 9 and 10. The following chapter presents the chronological framework for this study.

Chapter 6

Chronologies

6.1 Introduction

This chapter presents and analyses the results of ^{210}Pb, ^{137}Cs, ^{14}C and tephrochronological data from both short and long cores. The age/depth models used when presenting the data in subsequent chapters are also presented, along with dates and geochemical analyses for a number of unknown or poorly described eruptive events. A full analysis and discussion of the choice of ^{210}Pb model is also presented.

6.2 Short Cores

6.2.1 ^{210}Pb Dating Using the CIC and CRS Model

^{210}Pb analysis was performed as described in Section 5.3.1. Levels of ^{210}Pb at the base of the cores from Laguna Edita and Laguna Meche are comparable to those in other lakes in the region (see Table 6.1), indicating that the ^{210}Pb activity at the bottom of the cores is indicative of ^{210}Pb supported by in-situ decay from ^{226}Ra, referred to as $^{210}\text{Pb}_{\text{supported}}$. All ^{210}Pb in excess of this amount has been deposited as a result of deposition from decay of ^{222}Rn in the air or water column, and is referred to as $^{210}\text{Pb}_{\text{unsupported}}$. Figures 6.1 & 6.2 show the raw data and the $^{210}\text{Pb}_{\text{supported}}$ level for each core is shown.

Both cores show a good fit to the expected natural logarithmic decay curve, although both cores contain layers where ^{210}Pb is less than the expected amount given the levels in surrounding samples; some of these reductions are caused by tephra deposits in the sediments and where appropriate these samples are excluded from the CIC modelling calculations. Although deletion of some data points is common in the literature there is little consistency (or even explanation) when deletion occurs; here deletion only occurs when it makes a noteable difference to the resulting age determinations. This strategy avoids deleting data to simply improve the r^2 score, which would have to effect of

reducing the sample specific errors. The log transformed data and the data used for CIC modelling calculations are shown in Figures 6.3 and 6.4. For both cores r^2 scores >0.8 were obtained and the resulting CIC model returned accumulation rates of 0.28cm/year for Laguna Edita and 0.12cm/year for Laguna Meche. The errors include the analytical error, goodness-of-fit of the CIC model, and down-core error propogation and are expressed at the 1σ level. The CIC models used are unconstrained by tephrochronology or ^{137}Cs chronology as these are intended to be used as independent verification of the performance of the ^{210}Pb based model. Where the 1σ errors are considered the CIC models perform adequately in both Laguna Edita and Laguna Meche; this suggests that the changes in accumulation rate are within the errors presented for the model.

The CRS model was also applied to the ^{210}Pb data without excluding data points, as the assumptions for this model allow for variations in the rate of deposition and assume a fixed rate of supply of ^{210}Pb to the sediment. In Laguna Meche the lowest obtained value was used (^{210}Pb=0.003115 Bq/g) as the model does not allow $^{210}\mathrm{Pb}_{\mathrm{supported}} > {}^{210}\mathrm{Pb}_{\mathrm{unsupported}}$; for Laguna Edita this was not an issue as the lowest values were found at the bottom of the core. The gross accumulation rates from both the CIC and CRS models are comparable and shown in Table 6.2. Although the CRS model allows for changes in accumulation rates the models return age/depth profiles that are largely within the errors of the CIC model; as both models give age/depth profiles that are indistinguishable when sample-specific errors are considered, the CIC model is used in the spirit of *lex parsimoniae*.

$^{210}Pb_{supported}$ (Bq/g)	Location	Reference
0.00044	Laguna Edita, Chacabuco Valley	this study
0.0033	Laguna Meche, Chacabuco Valley	this study
1 & 2	Lago Puyehue, bet. Puerto Montt & Concepcion	Arnaud *et al.* 2006
1 & 1.6	Lago Icalma, bet. Puerto Montt & Concepcion	Arnaud *et al.* 2006
0.001	Lago Morenito, Nahuel Huapi Park	Guevara *et al.* 2010
0.025	Lago Tonĉek, Nahuel Huapi Park	Guevara *et al.* 2010
0.015	Laguna Negra, nr. Santiago	von Gunten *et al.* 2008
0.04	Laguna el Ocho, nr. Santiago	von Gunten *et al.* 2008
0.008	Lago Gulletué, nr. Lonquimay	Urrutia *et al.* 2007

TABLE 6.1: $^{210}Pb_{supported}$ levels in lake sediments in southernmost South America from the available literature.

Site	Model	Accumulation Rate (cm/year)	r^2
Laguna Edita	CIC	0.28	0.86
Laguna Edita	CRS	0.20 (average)	0.98
Laguna Meche	CIC	0.12	0.83
Laguna Meche	CRS	0.14 (average)	0.96

TABLE 6.2: Accumulation rates derived from CIC and CRS models for Laguna Edita and Laguna Meche. The CRS data are average accumulation rates over the whole sequence.

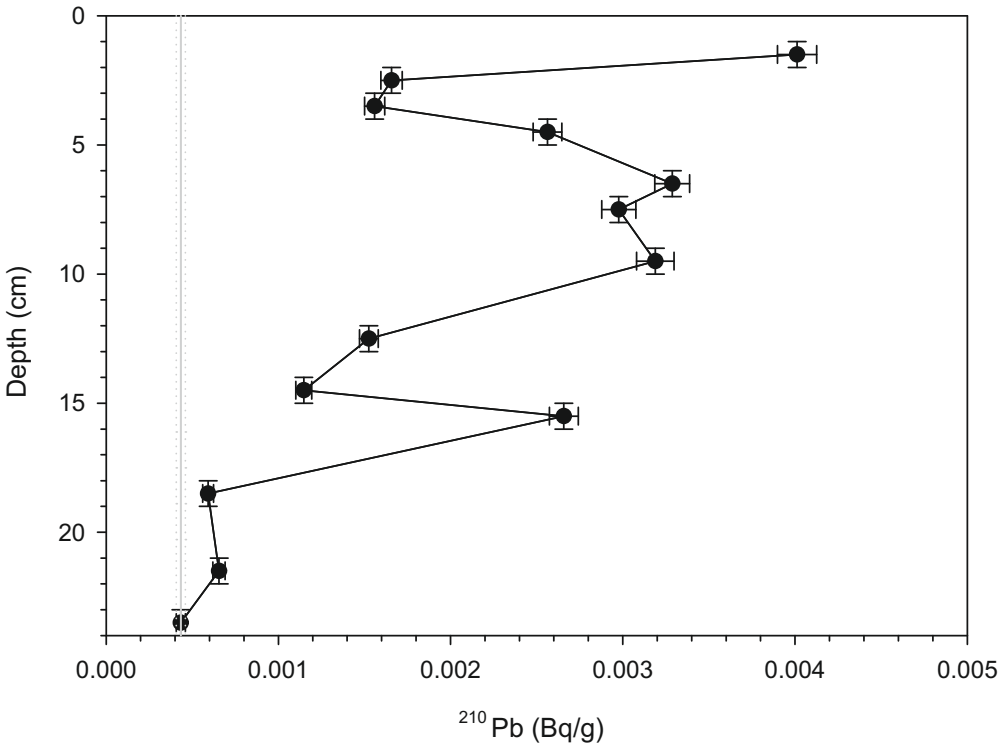

FIGURE 6.1: ^{210}Pb in Laguna Edita, showing the supported ^{210}Pb level used in the CIC modelling in grey, with the 1σ propogated error shown with dotted lines. Vertical error bars show the sample depth range, horizontal bars show the analytical error.

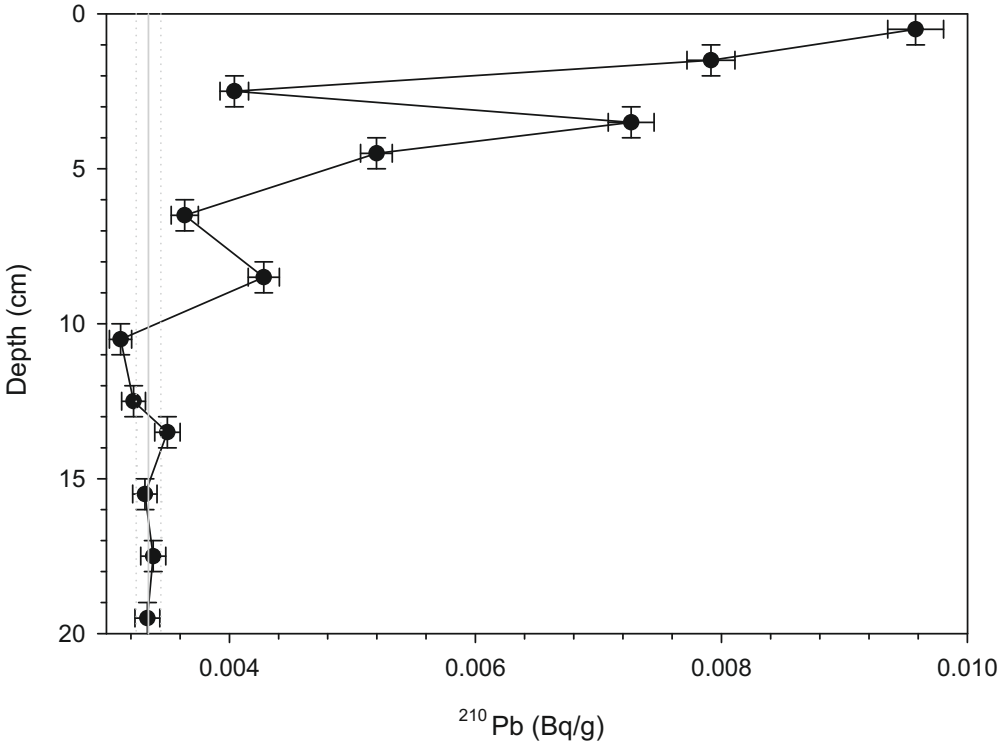

FIGURE 6.2: ^{210}Pb in Laguna Meche, showing the supported ^{210}Pb level used in the CIC model in grey, with the 1σ propogated error shown with dotted lines. Vertical error bars show the sample depth range, horizontal bars show the analytical error.

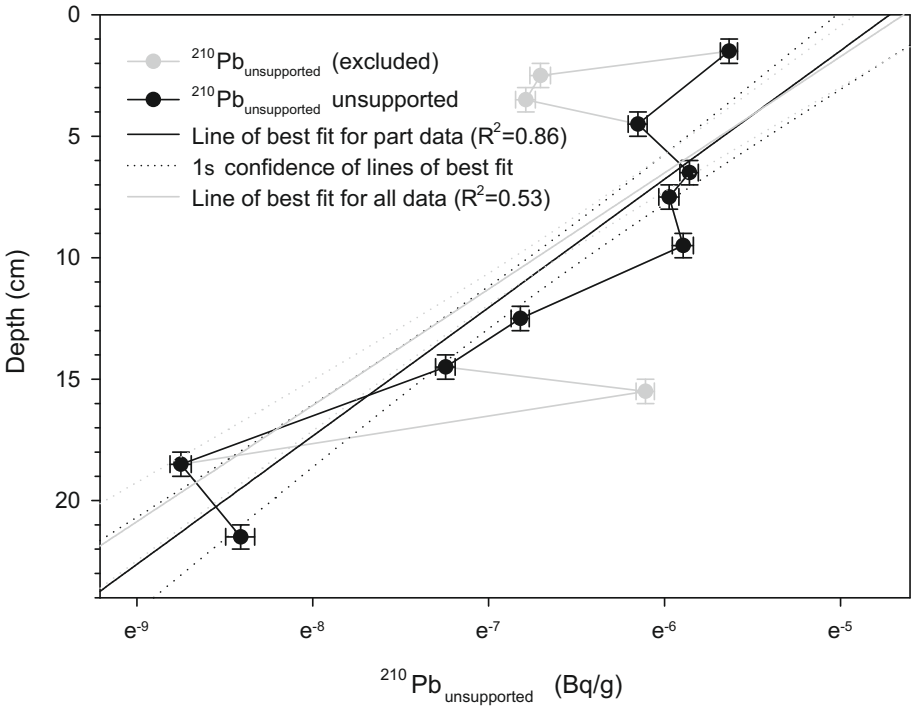

FIGURE 6.3: $^{210}Pb_{unsupported}$ in Laguna Edita showing lines of best fit for all (solid black) and selected (solid grey) data. Note the log scale (ln). r^2 values are given for a natural log fit, and the 1σ lines of confidence are shown for the regression (dotted lines). The data points removed are those that gave the largest change in age determinations by deleting the fewest number of points, and the point removed are very likely to represent dilution of ^{210}Pb by tephra deposition.

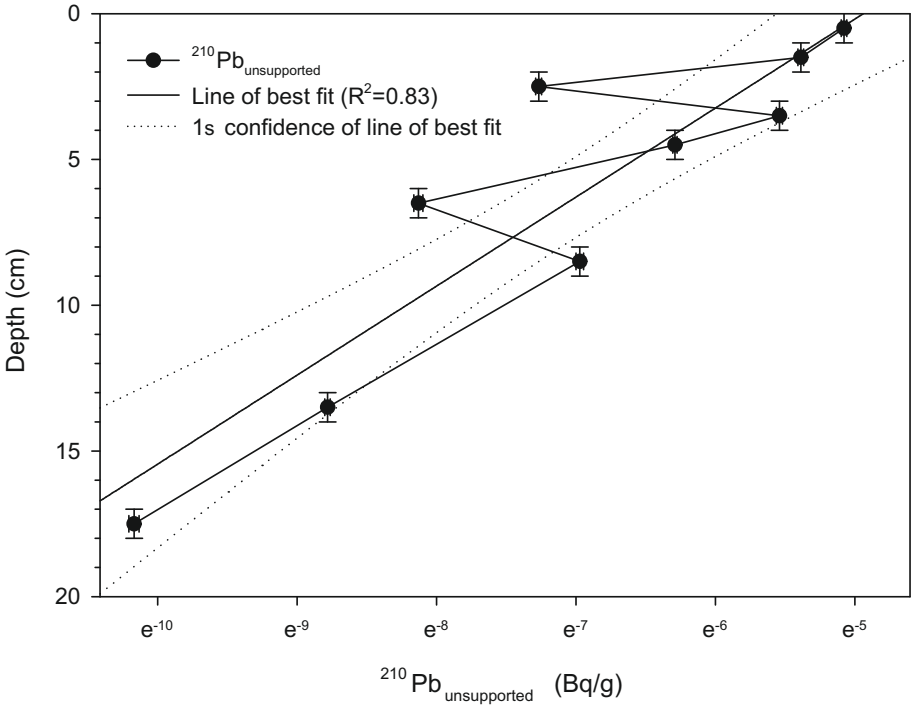

FIGURE 6.4: $^{210}Pb_{unsupported}$ in Laguna Meche showing lines of best fit for all and selected data. Note the log scale (ln). r^2 values are given for a natural log fit, and the 1σ lines of confidence are shown for the regression (dotted lines). Removing outliers did not signficantly change the final age estimates.

6.2.2 ^{137}Cs Dating

The ability to pinpoint the year AD1964±1 using ^{137}Cs created and released into the atmosphere during atmospheric nuclear testing is described fully in Section 5.3.1. The concentrations in Laguna Edita and Laguna Meche are consistent with peak values obtained elsewhere in southernmost South America (Table 6.3) and the curves show the expected pattern of deposition (Figures 6.5 & 6.6), with zero levels at the bottom of the core, a gradual rise to peak values and a subsequent decline towards the top of the core. Both cores show small peaks after the main peak in the curve related to the dilution of ^{137}Cs by tephra deposition in the top 2–4cm of the sequences, which causes artificially depressed levels of ^{137}Cs near the tops of the cores. These data indicate accumulation rates for the tops of the cores of around 0.16cm/year for Laguna Edita and around 0.08cm/year for Laguna Meche; both of these estimates are slightly lower than the rates derived from ^{210}Pb modelling (see Table 6.2) but are consistent given the sample specific age errors of those models. As such the age/depth models derived from ^{210}Pb can be used with confidence as they are supported by the independent ^{137}Cs age.

Peak ^{137}Cs (Bq/g)	Location	Reference
0.035	Laguna Edita, Chacabuco Valley	this study
0.027	Laguna Meche, Chacabuco Valley	this study
0.0105 & 0.012	Lago Puyehue, bet. Puerto Montt & Concepcion	Arnaud *et al.* 2006
0.012 & 0.015	Lago Icalma, bet. Puerto Montt & Concepcion	Arnaud *et al.* 2006
0.05	Lago Nahuel Huapi, Nahuel Huapi Park	Guevara and Arribére 2002
0.028	Lago Morenito, Nahuel Huapi Park	Guevara *et al.* 2010
0.048	Lago Tonĉek, Nahuel Huapi Park	Guevara *et al.* 2010
0.1	Laguna Negra, nr. Santiago	von Gunten *et al.* 2008
0.009	Laguna el Ocho, nr. Santiago	von Gunten *et al.* 2008
0.04	Lago Gulletué, nr. Lonquimay	Urrutia *et al.* 2007

TABLE 6.3: Peak values of ^{137}Cs in southernmost South America.

6.2.3 Tephrochronology

6.2.3.1 Identification & Aims

Two layers of potential tephra deposits were identified by stratigraphic changes, low organic contents (shown in Figures 6.7 & 6.8) and by Itrax core scans (see Section 5.4.3) from nearby cores in both lakes (listed in Table 6.4). Shard counts revealed very high concentrations of tephra (>1000 shards/g) in these layers. On the basis of the ^{210}Pb

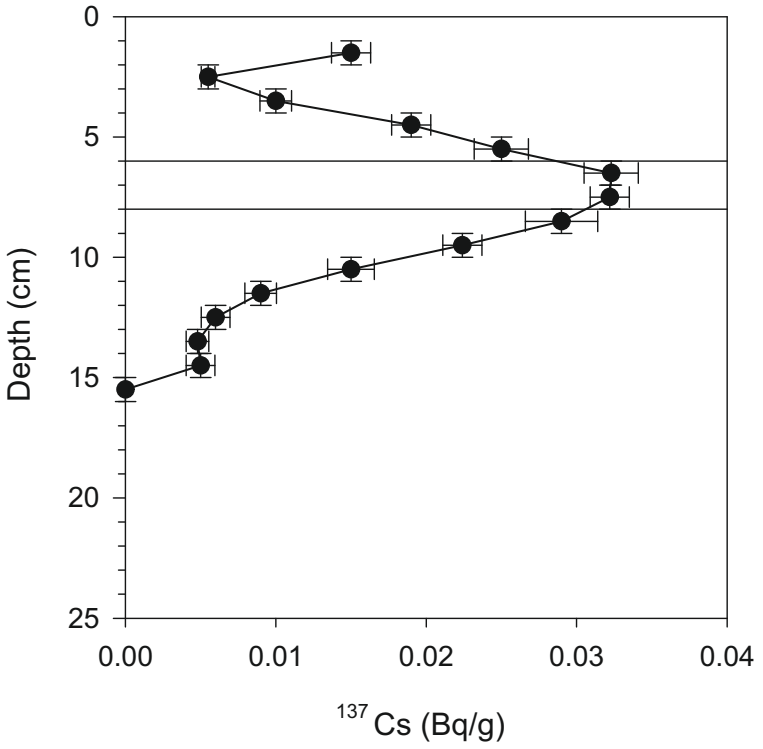

FIGURE 6.5: ^{137}Cs profile for Laguna Edita. Dilution by tephra deposition is apparent between 2–4cm, and the peak centered on AD1964±1 is shown by a pair of horizontal lines.

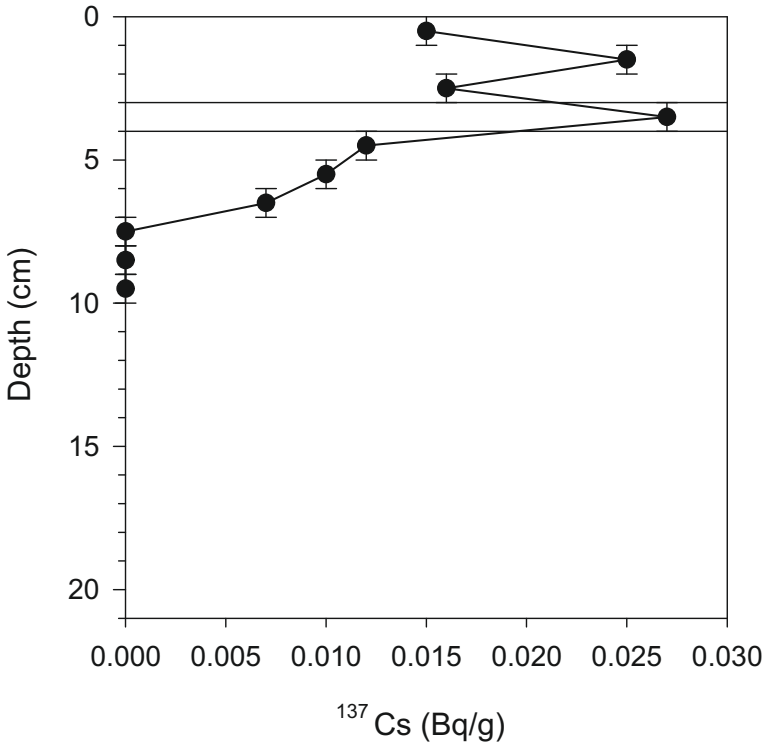

FIGURE 6.6: ^{137}Cs profile for Laguna Meche. Dilution by tephra is apparent between 2–3cm. The peak centered on AD1964±1 is shown by a pair of horizontal lines.

chronology it was hypothesised that the upper and lower tephra layers in each core were deposited synchronously, that the uppermost tephra layers were deposited during the AD1991 explosive (VEI=5) eruption of Mt. Hudson and the lower tephra layers were deposited during the AD1891 eruption of Mt. Hudson. Chemical analysis was sucessfully performed on the four tephra layers with a mimimum of 40 shards analysed for each layer, with the aim of answering the following:

1. Are the upper and lower layers chemically similar or distinct? Can they be ascribed to the same eruption?
2. Using chemical composition data, can the ash layers be ascribed to a particular source (*e.g.* Mt. Hudson?)

6.2.3.2 Chemical Analysis

All four layers fall within the published chemical ranges for Mt. Hudson (see Figure 6.9). Layers S02 and S03 show a bimodal distribution, with a minor component of high SiO_2 & K_2O beyond the documented ranges of tephras in South America. These minor bimodal components differ in a number of ways to the majority of the data, being noteably enriched in SiO_2, Na_2O and K_2O and deficient in CaO, FeO, TiO_2 and P_2O_5 (shown in Figure 6.10). The uppermost layers, S01 and S03 plot closely to one another with a high-K dacite composition, whereas the lower layers S02 and S04 are basaltic andesites (full chemistries are given in Table 6.5). The upper and lower tephra layers in Laguna Edita and Laguna Meche can thus be matched to one another. The ^{210}Pb modelling dates the uppermost eruption in the last two decades in both lakes; on the basis that the source of this tephra can be attributed to Mt. Hudson, and that there is widespread documentary evidence for a large eruption at this time, it seems clear that this layer represents the large AD1991 eruption of Mt. Hudson and thus constrains the $^{210}Pb/^{137}Cs$ chronology. The ^{210}Pb modelling dates the lower tephra layer as occuring near the turn of the century in Laguna Edita and Laguna Meche; given the documentary evidence for an eruption of Mt. Hudson AD1891 (Siebert *et al.*, 2010), this eruption can also be used to constrain the chronology.

Lab ID	Core	Depth	Date
S1	EDI-2009-01	01–02cm	AD1991±20
S2	EDI-2009-01	22–23cm	AD1991±20
S3	MEC-2009-03	01–02cm	AD1891±20
S4	MEC-2009-03	16–17cm	AD1891±20

TABLE 6.4: List of identified tephra layers in short cores.

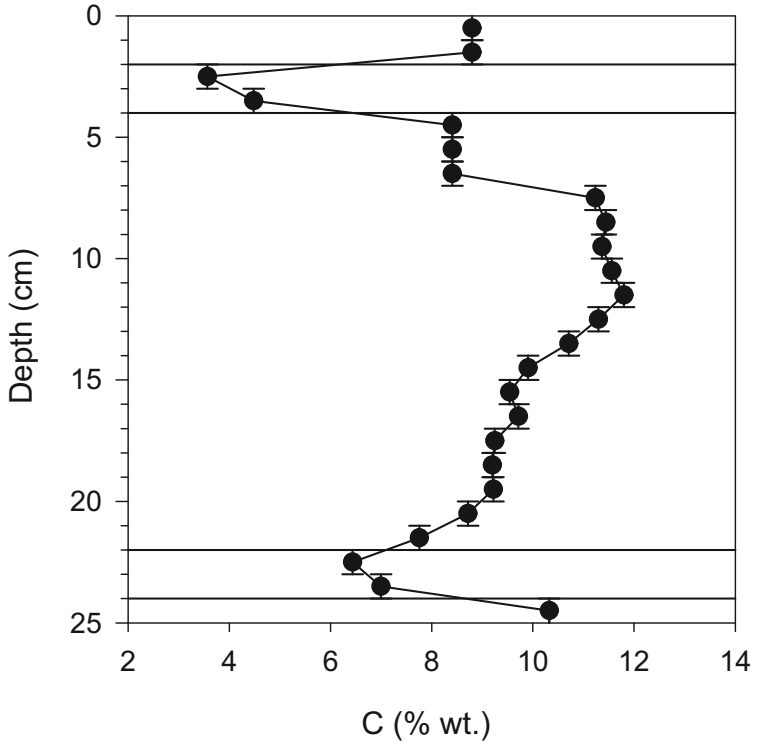

FIGURE 6.7: %C profile for Laguna Edita. Suspected dilution by tephra deposition is shown by pairs of horizontal lines.

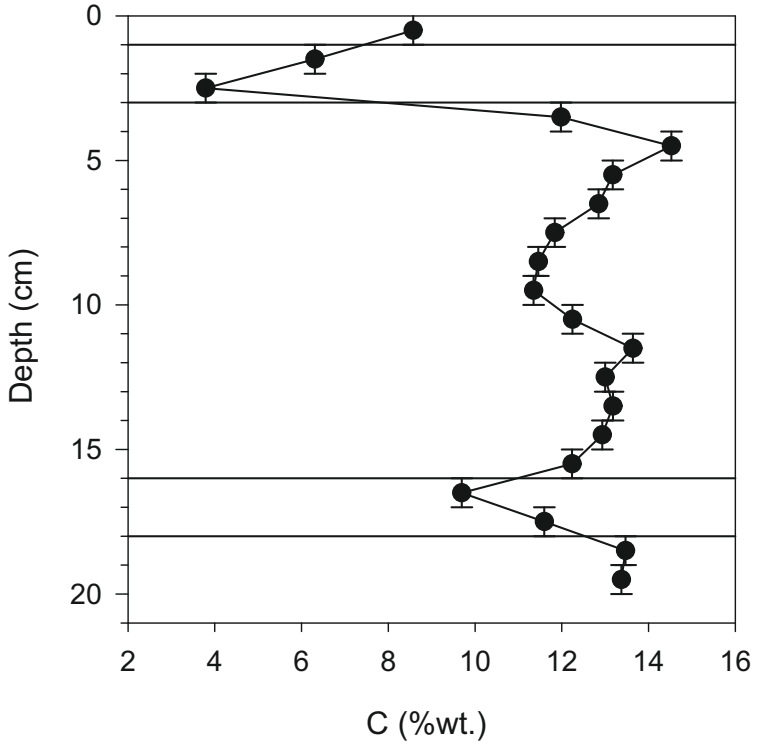

FIGURE 6.8: %C profile for Laguna Meche. Suspected dilution by tephra deposition is shown by pairs of horizontal lines.

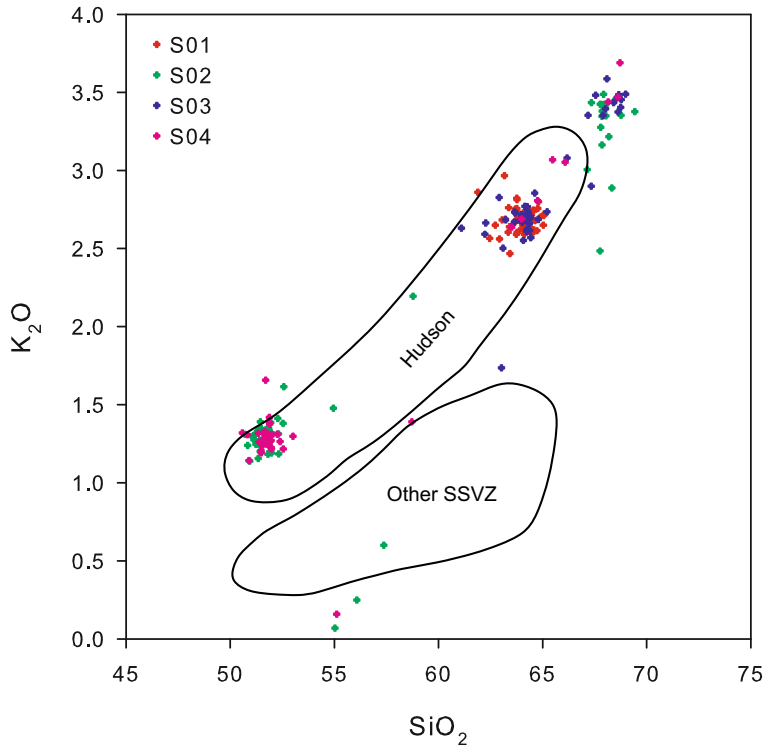

(a) K_2O vs. SiO_2 composition of short core tephra layers.

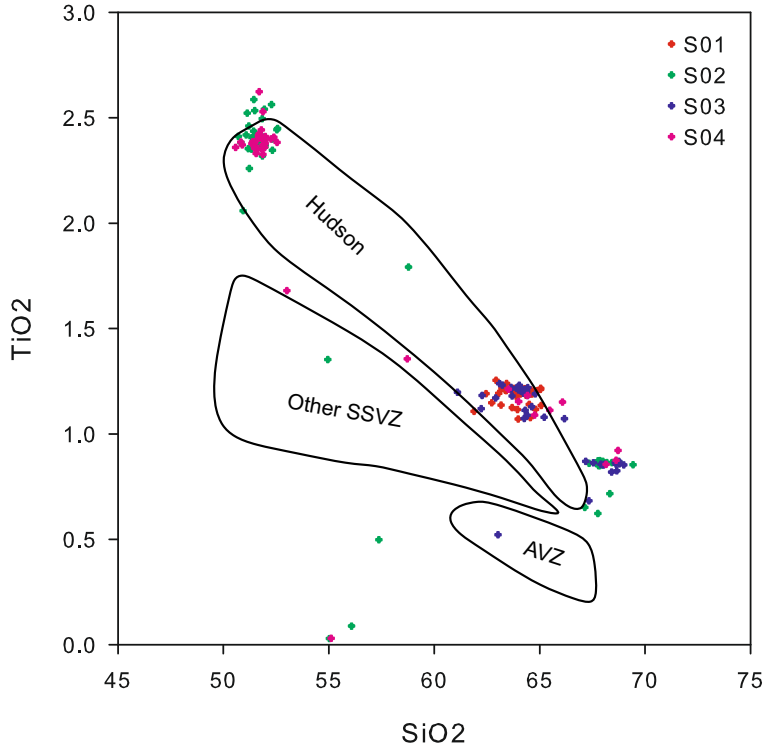

(b) TiO_2 vs. SiO_2 composition of short core tephra layers.

FIGURE 6.9: Chemical composition of short core tephra layers, showing the ranges for Mt. Hudson, other southern volcanic zone (SSVZ) and Andean Volcanic Zone (AVZ) volcanic chemistries redrawn from Naranjo and Stern (1998).

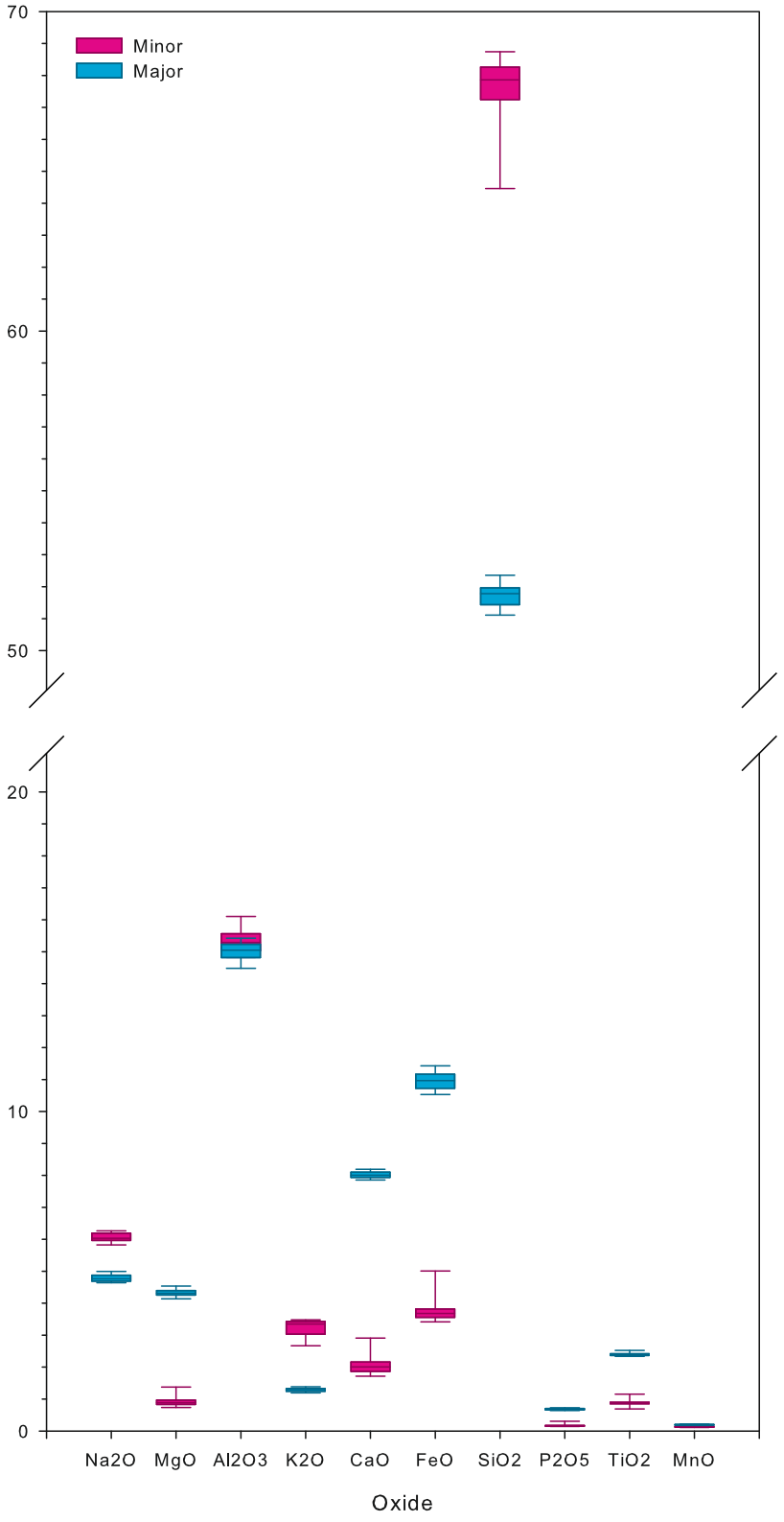

FIGURE 6.10: Chemical composition data for bimodal tephras in the short cores (S02 and S03); results are grouped as the major and minor component in both samples. It is clear from this data that whilst the major component in both S02 and S03 have differing chemical compositions, the minor component is both distinct and similar between sites. Box represents the limits of the 25th and 75th percentile; the lines represent the 10th and 90th percentile.

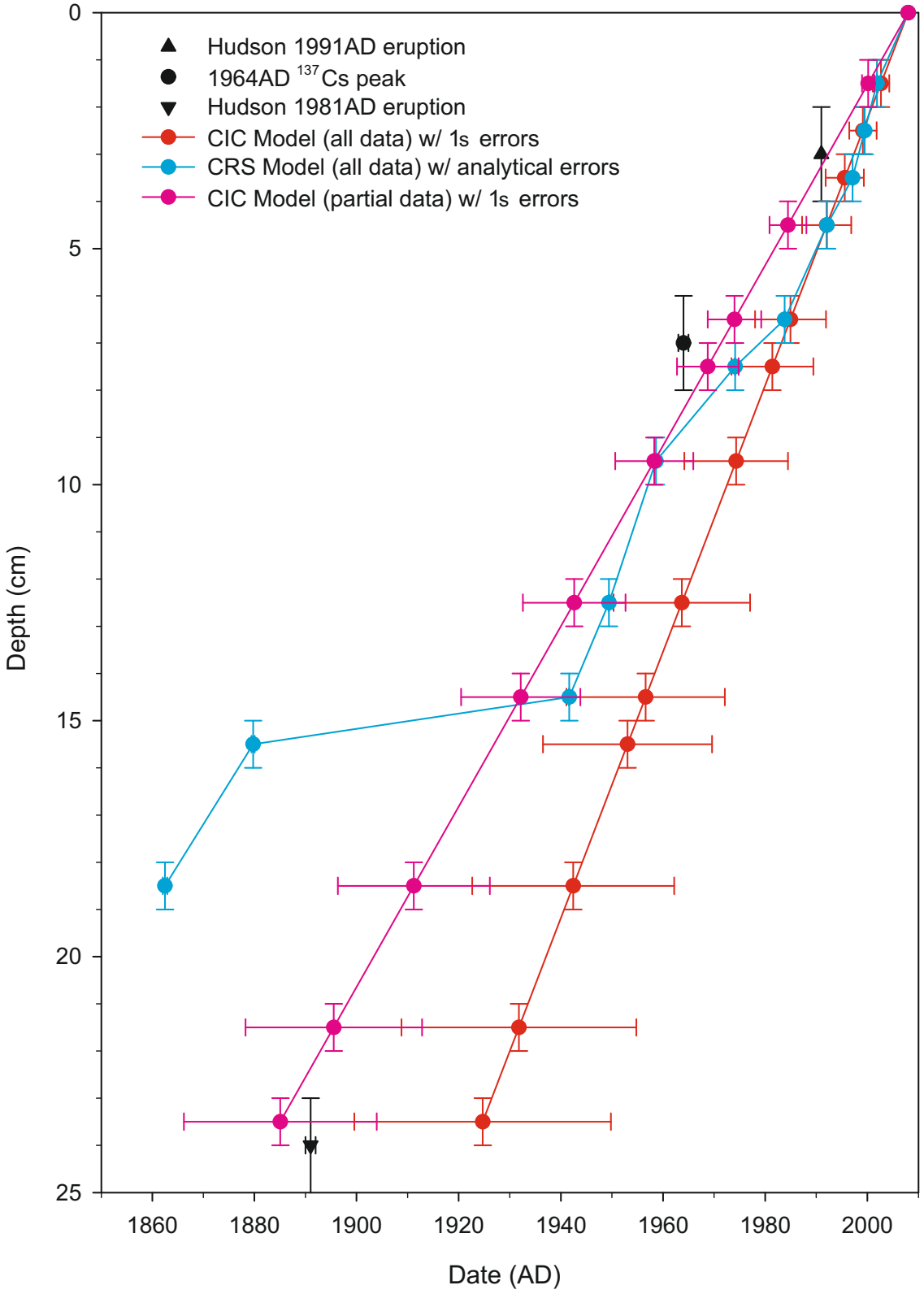

FIGURE 6.11: Age/depth models for Laguna Edita short core. The CIC model with some data removed (pink) gives the accumulation rate that fit best with the independent age markers (black), and is the chronology used to present the data.

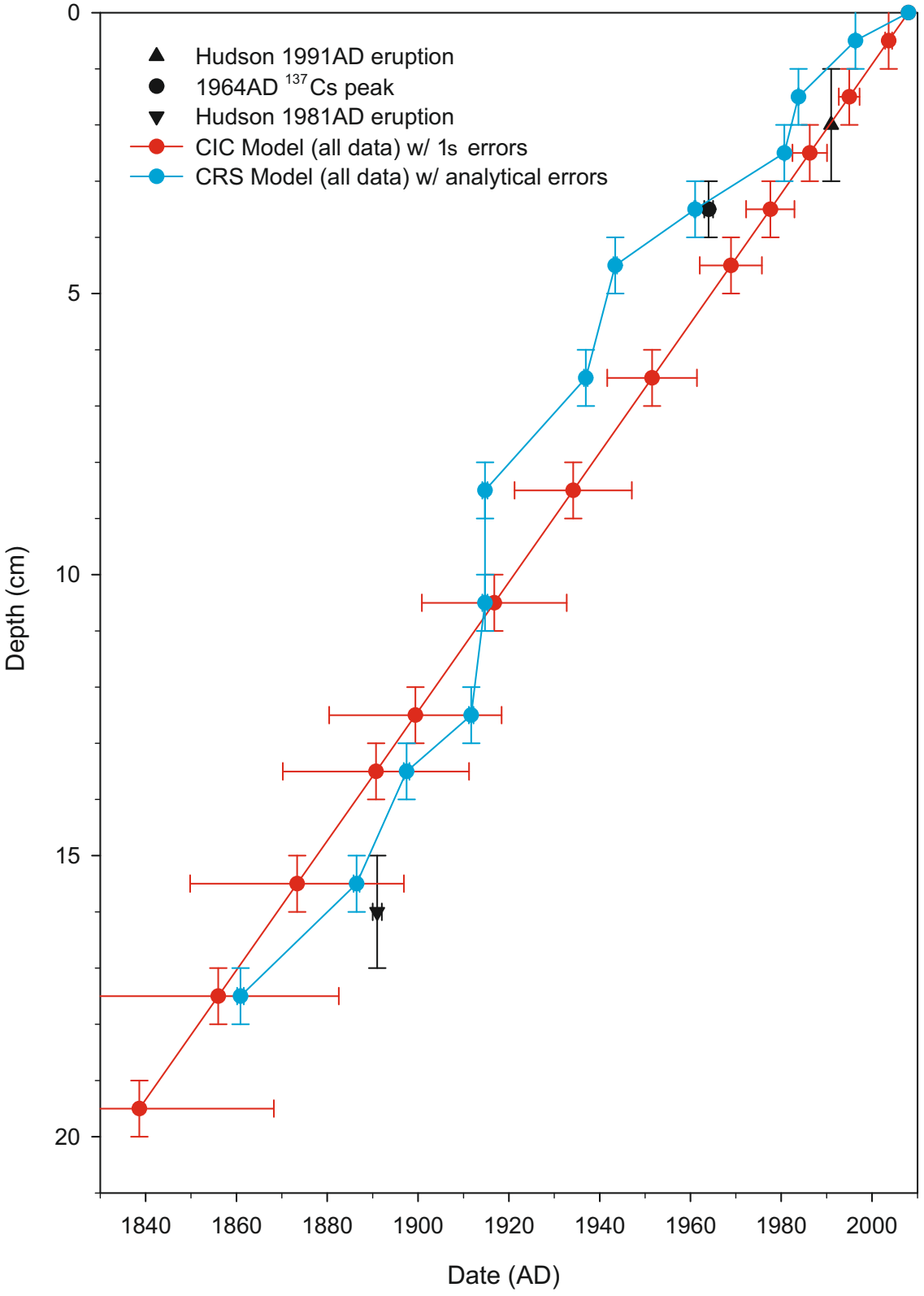

FIGURE 6.12: Age/depth models for Laguna Meche short core. The CIC model (red) gives the accumulation rate that is closest to the independent age markers (black), although neither model is completely accurate when compared to these markers. The CIC model is the chronology used to present the data.

		Na_2O	MgO	Al_2O_3	K_2O	CaO	FeO	SiO_2	P_2O_5	TiO_2	MnO	Total
S1	Mean	6.30	1.49	16.06	2.69	3.06	5.00	63.99	0.34	1.19	0.18	100.29
	1SD	(0.16)	(0.07)	(0.22)	(0.08)	(0.15)	(0.18)	(0.68)	(0.02)	(0.04)	(0.02)	(0.96)
S3	Mean	6.20	1.27	15.98	2.88	2.80	4.43	65.18	0.28	1.07	0.16	100.23
	1SD	(0.27)	(0.32)	(0.83)	(0.38)	(0.60)	(0.83)	(2.14)	(0.09)	(0.18)	(0.03)	(0.97)
S2	Mean	4.78	4.34	14.94	1.30	8.02	11.04	51.65	0.69	2.41	0.20	99.37
	1SD	(0.13)	(0.14)	(0.41)	(0.09)	(0.11)	(0.36)	(0.45)	(0.03)	(0.07)	(0.01)	(0.62)
S4	Mean	4.81	4.17	15.47	1.26	8.08	10.50	52.08	0.64	2.27	0.19	99.46
	1SD	(0.24)	(0.81)	(2.39)	(0.22)	(0.78)	(1.93)	(1.43)	(0.13)	(0.47)	(0.04)	(0.74)

TABLE 6.5: Chemical composition of tephra layers S1, S2, S3 & S4. Only the major component data from layers S2 and S4 are given.

6.3 Long Cores

6.3.1 Core Correlation

The overlapping core sequences from Laguna Edita and Laguna Meche were correlated on the basis of coring depth, with adjustments for errors in measurement of coring depth, variation in sedimentary structure and compression during coring. These adjustments were made by cross-correlating overlapping drives using loss-on-ignition, magnetic, and where available, Itrax data. The core depths were then re-mapped onto a single depth model that is used for age/depth modelling; this depth mapping is shown in Figure 6.13.

6.3.2 ^{14}C Dating

The radiocarbon dating strategy (see Section 5.3.2) necessitated the use of some very small samples of charcoal which must be analysed at low current by AMS with additional standards, and thus in terms of analytical errors these samples may be considered less robust than those from larger samples. The use of small samples often means that δ^{13}C values cannot be obtained directly from some samples and are thus estimated. In addition, carbon content could not be estimated from some samples because of the small sample size. Calibration and age/depth modelling was performed using CLAM v2.1 (Blaauw, 2010) using ShCal04 (McCormac *et al.*, 2004) where possible, otherwise IntCal09 (Reimer *et al.*, 2009) with a 50 year offset (*c.f.* Hogg *et al.*, 2009). Age/depth models were generated using both standard and Bayesian techniques (using Oxcal v4.2, Ramsey 2008; Bronk Ramsey 2009), but because of the resolution of the dating effort an entirely Bayesian approach yields very similar age/depth models when compared to other methods, and thus the simplest model has been chosen (a linear interpolation, shown in Figure 6.15). It should be noted however that Bayesian models do produce different estimates of interpolation errors, although these are similarly centennial in scale.

6.3.2.1 Laguna Edita

A total of 8 AMS ^{14}C dates were sent for analysis from the Laguna Edita long core sequence, although the basal sample failed due to the low carbon content; the complete data are given in Table 6.6. The last *c.*4,000 years of deposition appear to be relatively consistent, but three radiocarbon dates (SUERC-44366, 43343 and 46350) cluster around 3,800 years B.P. Assuming this is not slumping or disturbance of the core, there would remain the problem of selecting the best radiocarbon date. However, the presence of a tephra layer (S11) at a depth of 268cm that is correlated with a layer in Laguna Meche (S14) with an interpolated age of 4,686±83 years B.P. means that the most appropriate age determination can be selected. This allows selection of SUERC-46350 and rejection of the other two dates as the most appropriate and harmonious solution; using this

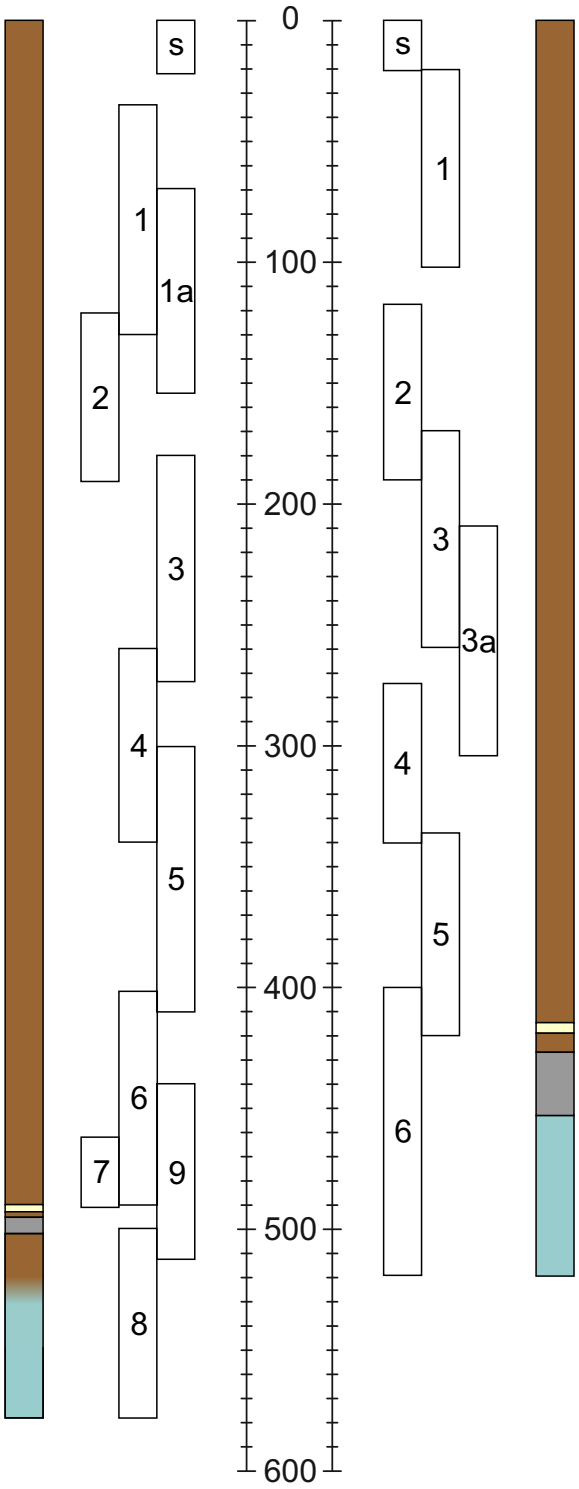

FIGURE 6.13: Core correlations for both Laguna Edita and Laguna Meche. Units are in centimeters below the seidment-water interface. Core ID's are given — 's' represents the surface cores. In the stratigraphic diagrams, brown is gyttja, cream is a cream coloured ash, grey is a grey coloured ash and blue is blue-grey glacial clay.

chronology the date for the tephra layer in Laguna Edita is given as 4,810±208 years B.P., and is thus in agreement with the tephrochronological correlation with Laguna Meche. Because of the failure of the basal sample, dates have been extrapolated beyond the age/depth model, although these dates are used with caution.

6.3.2.2 Laguna Meche

A total of 7 AMS ^{14}C determinations were analysed from the Laguna Meche sequence; the complete data are given in Table 6.7. One of the first (rangefinder) dates, SUERC-33512, was confirmed to be anomalous following analysis of an alternative sample (SUERC-44365). SUERC-44360 could be considered slightly too old; it is identified as a poor fit and has therefore been omitted. The cream tephra layer at the base of Laguna Edita, constrained by two bounding dates in the Laguna Edita sequence (SUERC-34432 & SUERC-34431) is chemically and stratigraphically identical to a layer in Laguna Meche, and this has been used as an additional chronological marker in this stratigraphy (see Section 6.3.3.3).

At the base of the sequence the accumulation rate is relatively low, which is usual in lake sediments and is likely a result of low productivity at the inception of the lake as well as compression under the weight of accumulated sediment. Overall the accumulation rate appears to be relatively stable, at around 20 years/cm throughout the rest of the sequence.

Lab ID	Sample ID	Sample Depth (cm)	Material Used	C content	Conventional ^{14}C age (years B.P.$\pm 1\sigma$)	$\delta^{13}C_{VPDB}‰$
SUERC-43343	EDI-4 41–42cm	300	charcoal fragments	112μg	3824±69	-40.3±4.6
SUERC-34432	EDI-9 29–30cm	488	charcoal fragments	143μg	7380±113	-38.7±1.7
SUERC-34431	EDI-9 33–34cm	491	charcoal fragments	96μg	7171±77	-44.5±3.1
SUERC-46348	EDI-1 44–47cm	81	charcoal fragments	268μg	1460±77	-31.8
SUERC-46349	EDI-2 10–13cm	139	charcoal fragments	107μg	2181±77	-26.6
SUERC-46350	EDI-3 55–56cm	234	charcoal fragments	54μg	3957±82	-0.3
SUERC-44366	EDI-6 20–23cm	423	charcoal fragments	n/a	3581±38	-29.7±0.1
FAILED	EDI-8 20–21cm	522	charcoal fragments			

TABLE 6.6: ^{14}C determinations from Laguna Edita. δ^{13}C is expressed as relative to the VPDB standard ($\delta^{13}C_{VPDB}$, and conventional dates are expressed as ^{14}C years before AD1950.

Lab ID	Sample ID	Sample Depth (cm)	Material Used	C content	Conventional ^{14}C age (years B.P.$\pm 1\sigma$)	$\delta^{13}C_{VPDB}‰$
SUERC-33512	MEC-4 59–60cm	338	wood fragments	n/a	3177±37	-25*(est.)*
SUERC-34433	MEC-6 45–46cm	476	plant material	127μg	10919±86	-48.9±1.7
SUERC-44360	MEC-1 63–64cm	83	wood fragments	52μg	2314±37	-29*(est.)*
SUERC-44367	MEC-2 35–36cm	155	wood fragments	55μg	2271±37	-29.4±0.1
SUERC-44361	MEC-3 30–31cm	201	wood fragments	44μg	2972±38	-29*(est.)*
SUERC-44364	MEC-3 70–71cm	241	wood fragments	52μg	3723±36	-29*(est.)*
SUERC-44365	MEC-4 50–51cm	328	plant material	45μg	4861±38	-35.4±0.1

TABLE 6.7: ^{14}C determinations from Laguna Meche. δ^{13}C is expressed as relative to the VPDB standard ($\delta^{13}C_{VPDB}$, and conventional dates are expressed as ^{14}C years before AD1950.

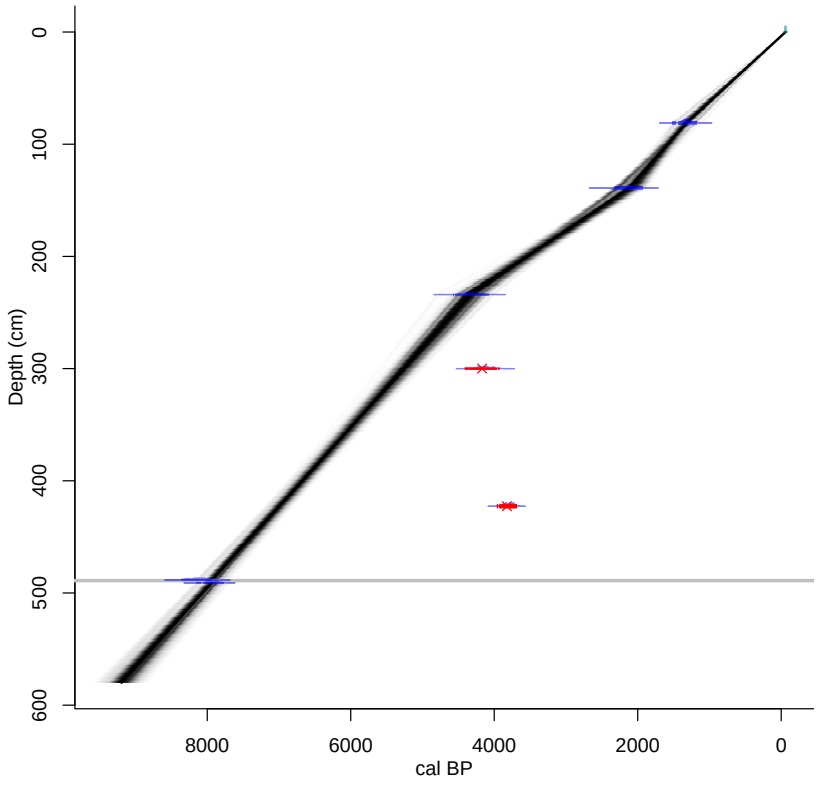

FIGURE 6.14: Age/depth model for Laguna Edita, generated using linear interpolation in CLAM v2.1, using 10,000 interations. Red dates are those not included in the age/depth model, and the grey line represents the tephra layer that cross-correlates the two sequences — see Section 6.3.3.5 for further explanation.

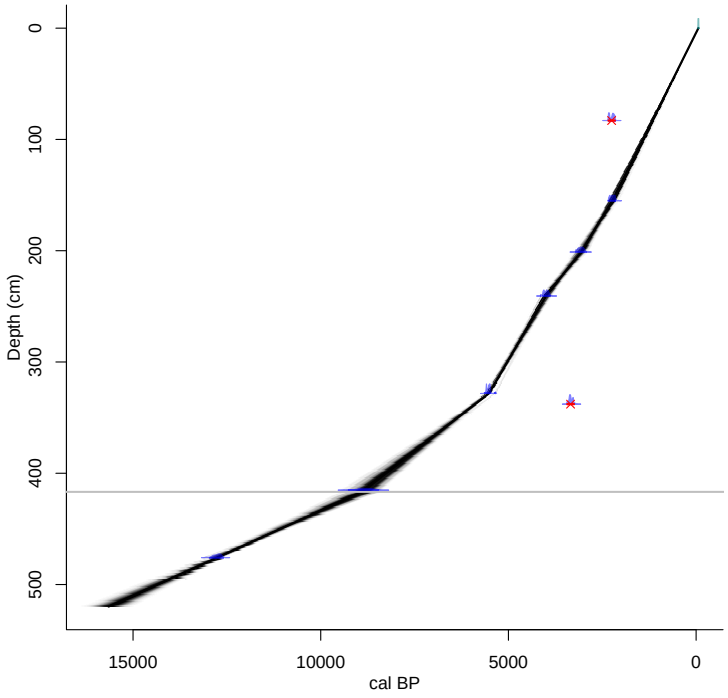

FIGURE 6.15: Age/depth model for Laguna Meche, generated using linear interpolation in CLAM v2.1, using 10,000 interations. Red dates are those not included in the age/depth model, and the grey line represents the tephra layer that cross-correlates the two sequences — see Section 6.3.3.5 for further explanation.

6.3.3 Tephrochronology

6.3.3.1 Identification

Four tephras were identified visually at the base of the sequences. In both sites discreet layers of very high minerogenic content were identified. These layers were identified as tephras by Itrax elemental analysis followed by microscopic inspection. A further eight possible tephras were identified from intervals of low organic content and high magnetic susceptability, and presence of tephra was confirmed by microscopic inspection. Identified possible tephras are detailed in Table 6.8.

6.3.3.2 Chemical Analysis

Six tephras were analysed from each site; two were the visible tephra layers at the bottom of the cores, and the remaining four were identified from proxy data. In addition to a number of basaltic to rhyolitic tephras, mineral material was also present, likely as a result of catchment erosion. Previous powder-XRD spectroscopy identified the presence of plagioclase feldspar (given the WDS analysis, probably Andesine), quartz, and Mica (following WDS analysis this seems likely to be Illite) in both lakes. Powder-XRD spectroscopy also identified the possible presence of Amphiboles (given the local geology, likely to be Hornblende) in Laguna Edita. These minerals have been excluded from the chemical analysis — only the tephra glass shards have been included. Analyses were considered acceptable where at least 30 analyses achieved oxide percentages of 98–102%. Outliers have not been reported, but bimodal and other complex assemblages are represented in full.

ID No.	Sample	Depth	^{14}C Age	Notes
S5	EDI-2010-07 047-048	488cm	7917±184 yrs. B.P.	White ash
S6	EDI-2010-07 055-056	496cm	8038±191 yrs. B.P.	Coarse grey ash
S7	MEC-2010-05 036-037	373cm	7247±214 yrs. B.P.	White ash
S8	MEC-2010-05 049-050	385cm	7701±282 yrs. B.P.	Coarse grey ash
S9	EDI-2010-02 003-004	127cm	1955±160 yrs. B.P.	
S10	MEC-2010-01 063-064	083cm	1166±53 yrs. B.P.	
S11	EDI-2010-03 090-091	268cm	4810±208 yrs. B.P.	
S12	EDI-2010-04 061-062	320cm	5540±173 yrs. B.P.	
S13	MEC-2010-03 075-076	246cm	4086±125 yrs. B.P.	
S14	MEC-2010-08 069-070	280cm	4686±83 yrs. B.P.	
S15	EDI-2010-05 068-069	395cm	6608±144 yrs. B.P.	
S16	MEC-2010-04 046-047	324cm	5448±90 yrs. B.P.	

TABLE 6.8: List of identified tephra layers and interpolated ages.

6.3.3.3 Visible Tephra Layers

Both sequences exhibit two visible tephra layers (see Figure 6.13) at their base. The lower, larger visible unit (S6 & S8) is the lowermost tephra unit analysed; the chemistry indicates the ash is consistent with a Mt. Hudson source. Given the radiocarbon date directly above the tephra (7,171±77 ^{14}C years B.P.), and given the size of the ash this layer is likely to have been deposited during the H1 eruption (dated to 6,850±120 ^{14}C years B.P. by Wastegard *et al.* 2013). Figure 6.16 shows the results from the unit in both Laguna Edita and Laguna Meche plotted against available published chemical analyses for the H1 ash (Table 6.9 gives a comparison of the complete chemistries).

The upper visible unit is clearly distinct from many of the other tephras observed in the sequence and the chemistry is indicative of a source in the Austral Volcanic Zone (AVZ); the tephra is rhyolitic, distinguishing it from the Southern Volcanic Zone basaltic character (the full chemistry is given in Table 6.10). Of the known AVZ sources this tephra fits the geochemical envolope of Mt. Burney, and can be distinguished from other northern AVZ sources (Viedma, Lautaro & Aguilera) due to a higher Ti content, and from Reclus due to a lower K content (Wastegard *et al.*, 2013, fig.3). Two radiocarbon dates from directly above and below the tephra layer in Laguna Edita indicate the date of deposition is between 7,868–8,169 years B.P. (Section 6.3.2.1).

Although the geochemistry suggests the most likely source of the ash is Mt. Burney, with the study site being located 580km north of the volcano only the largest of eruptions from Mt. Burney could be considered possible sources, as the tephra is 2cm thick in both cores. Given the early Holocene dates for the deposition of this tephra, MB1 could be considered the only likely previously documented eruption. However, MB1 has recently been dated to between 8,851–9,949 (Stern 2008) and 8,851–10,238 (Wastegard *et al.*, 2013) years B.P. This is clearly incompatable with both the bounding radiocarbon dates for the ash obtained from Laguna Edita, and the identification of a tephra matching H1 (dated to 7,329–7,918 years B.P.) below this ash. Given the quantity of material deposited, the distance from any known Holocene volcanic source in this zone and the constraining radiocarbon dates, this tephra is highly unlikely to have been deposited during any of the documented major Holocene eruptions from the AVZ. As such, it may represent a more proximal eruption of a previously unknown Holocene volcanic source in the AVZ. The nearest active volcanic source to the study site is Arenales, a volcano on the eastern margin of the North Patagonian Icecap first identified in 1958 by a Japanese scientific expedition. It was identified as being active when ash was observed on the

		Na_2O	MgO	Al_2O_3	K_2O	CaO	FeO	SiO_2	P_2O_5	TiO_2	MnO	Total
S6	Mean	6.09	1.37	15.52	2.93	2.77	4.73	65.32	0.28	1.15	0.16	100.32
	1SD	(0.18)	(0.24)	(0.24)	(0.18)	(0.44)	(0.49)	(1.23)	(0.48)	(0.10)	(0.02)	(0.66)
S8	Mean	6.06	1.39	15.48	2.94	2.85	4.72	65.03	0.29	1.16	0.16	100.65
	1SD	(0.19)	(0.26)	(0.27)	(0.15)	(0.43)	(0.39)	(1.06)	(0.03)	(0.70)	(0.01)	(0.82)

TABLE 6.9: Chemical composition of tephra layers S6 and S8 (white ash layer at base of the cores), showing that the chemical composition is identical in both cores.

icecap surrounding the volcano on a Landsat image from AD1979 (Figure 6.17); ash was also observed surrounding Lautaro (located on the northern tip of the South Patagonian Icecap) at the same time, suggesting the two systems may be linked. Although nothing is known of the geology of Arenales, given the link with Lautaro it is at least possible that the volcano is part of the Austral Volcanic Zone. The study site is 78km downwind of Arenales, and as such a minor eruption of the volcano could cause localised ash deposits across the region to the east of the icecap without the ash being present elsewhere.

6.3.3.4 H2 & Other Tephra Layers

A further eight possible layers of tephra were identified in the record from drops in the proportion of carbon and increases in magnetic susceptibility. All but two of these layers have a considerable range of chemical compositions (see Figure 6.19(b)). Two layers (S11 and S14) have relatively homogeneous chemistry that match closely (shown in Figure 6.19(a)); these are likely to have the same source. Given the chemistry, this eruption matches most closely published chemistries from Mt. Hudson 'H2', distinguished from other Mt. Hudson eruptions on the basis of its relatively low TiO_2 and high K_2O and SiO_2 content (see Figures 6.18(a) & 6.18(b)). The tephra has previously been dated to between 3,452–4,094 years B.P. (calibrated from data in Naranjo and Stern 1998), and in this study is dated to 4,810±208 & 4,686±83 years B.P. in Laguna Edita and Meche respectively. Some studies (*e.g.* Elbert *et al.*, 2013) use Naranjo and Stern's date of eruption (3,600 ^{14}C years B.P. or 3,860 years B.P.) as the date for H2, but both chronologies from this site support an earlier date of the eruption — this date is recommended as an improvement on the previously published dates.

Although the remaining layers (S09, 10, 12, 13, 15 & 16) have a varied chemistry, there are indications that the remaining number are pairs as the majority of the populations cluster. However, due to the considerable spread of chemistries within the individual populations, this cannot be certain and matching the tephras has not been attempted. These spreads of chemical compositions are not uncommon in South American tephras and are possibly a product of distal or weak eruptive sources combined with high background tephra deposition (Alison MacLeod, *pers. comm.*). They may even be the result of reworking of volcanic ash from within the catchment. Further work on the morphology and size distribution in combination with chemical analysis can assist in discriminating primary and catchment-derived sources.

		Na_2O	MgO	Al_2O_3	K_2O	CaO	FeO	SiO_2	P_2O_5	TiO_2	MnO	Total
S5	Mean	5.28	0.42	13.31	1.45	1.90	1.80	75.10	0.039	0.31	0.10	99.63
	1SD	(0.18)	(0.05)	(0.40)	(0.08)	(0.15)	(0.14)	(1.18)	(0.01)	(0.02)	(0.01)	(1.43)
S7	Mean	5.27	0.41	13.30	1.45	1.90	1.78	75.01	0.04	0.30	0.10	99.56
	1SD	(0.16)	(0.05)	(0.53)	(0.07)	(0.24)	(0.13)	(1.15)	(0.01)	(0.02)	(0.02)	(1.70)

TABLE 6.10: Chemical composition of tephra layers S5 and S7 (white ash layer at base of the cores), showing that the chemical composition is identical in both cores.

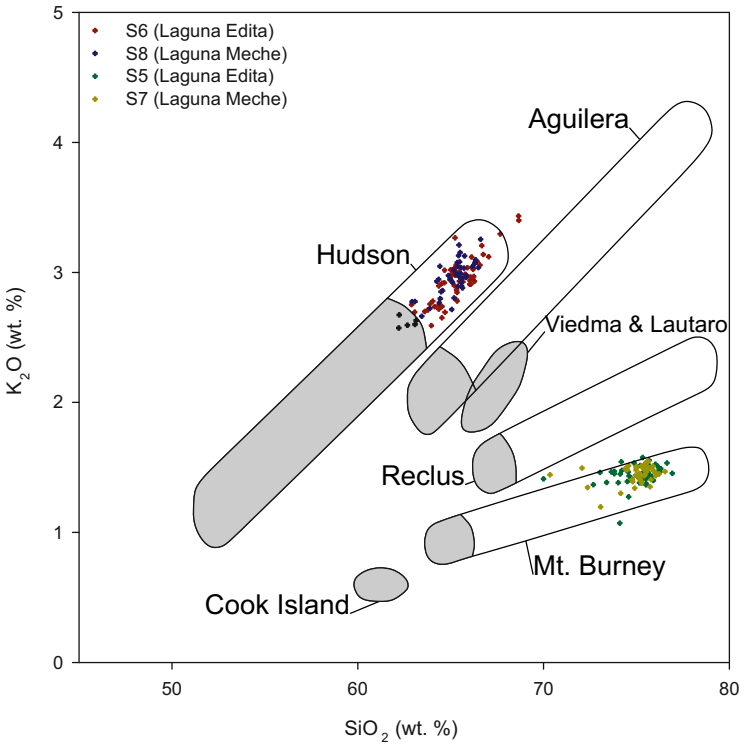

FIGURE 6.16: Visible tephra layers S05–S08, showing SiO_2 and K_2O envolopes for major Holocene eruptions (redrawn from Stern 2007, Figure 3a). The shaded areas are for bulk tephra, the unshaded areas for glasses.

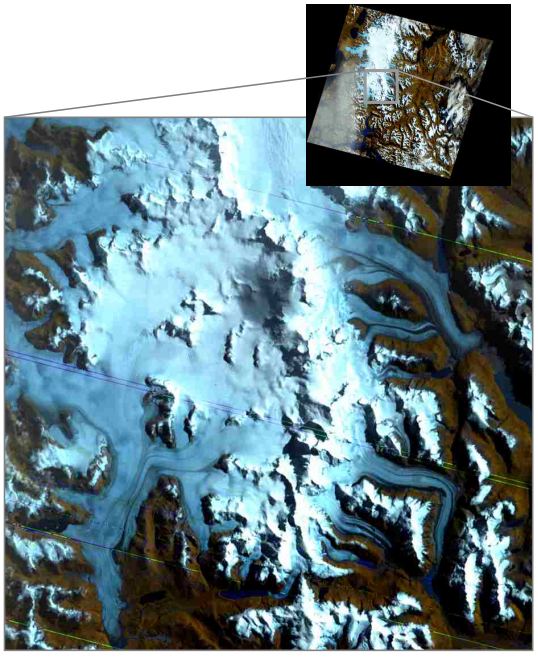

FIGURE 6.17: Landsat image showing Arenales ash deposits on the North Patagonian Icecap. Arenales is the conical peak in the centre of the image; the ash cloud can be seen on the south-west flank of the volcano. The image is a colour-composite of Landsat imagery aquired on the 8th March, 1979 (path 248, row 93).

		Na_2O	MgO	Al_2O_3	K_2O	CaO	FeO	SiO_2	P_2O_5	TiO_2	MnO	Total
S11	Mean	6.03	0.88	15.54	3.27	2.17	3.47	67.36	0.169	0.84	0.12	99.86
	1SD	(0.55)	(0.30)	(1.34)	(0.44)	(0.73)	(0.75)	(1.40)	(0.07)	(0.20)	(0.03)	(1.40)
S14	Mean	6.12	0.77	16.80	2.99	2.81	3.10	66.77	0.145	0.75	0.11	100.37
	1SD	(0.52)	(0.28)	(3.51)	(0.99)	(2.09)	(0.98)	(3.25)	(0.05)	(0.26)	(0.04)	(0.64)

TABLE 6.11: Chemical composition of tephra layers S11 and S14, showing that the chemical composition is identical in both cores given the analytical errors.

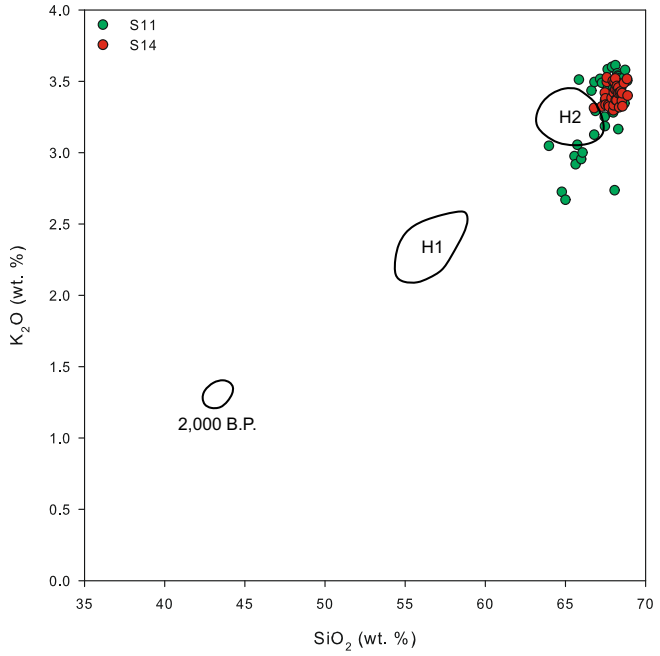

(a) K_2O vs. SiO_2 composition of tephra layers S11 and S14.

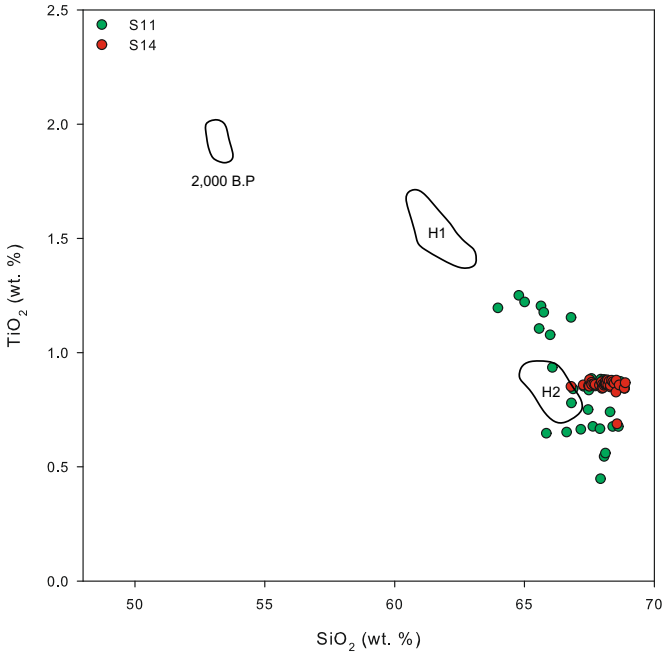

(b) TiO_2 vs. SiO_2 composition of tephra layers S11 and S14.

FIGURE 6.18: Chemical composition of tephra layers S11 and S14, also showing the ranges for H1, H2 and an un-named eruption around 2,200 ^{14}C years B.P. redrawn from Naranjo and Stern (1998).

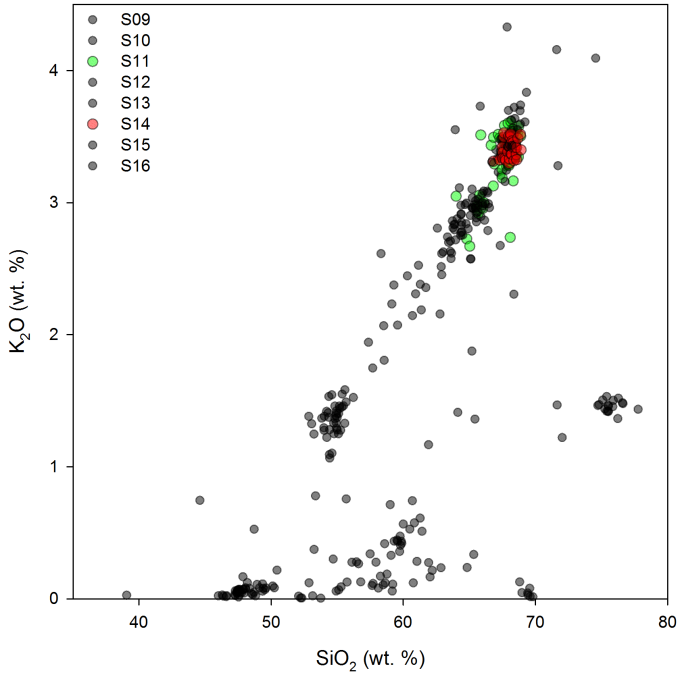

(a) Chemical composition of tephras S11 and S14 in comparison to the other six Holocene tephras. It is clear that the population ranges are considerably smaller than other tephra layers.

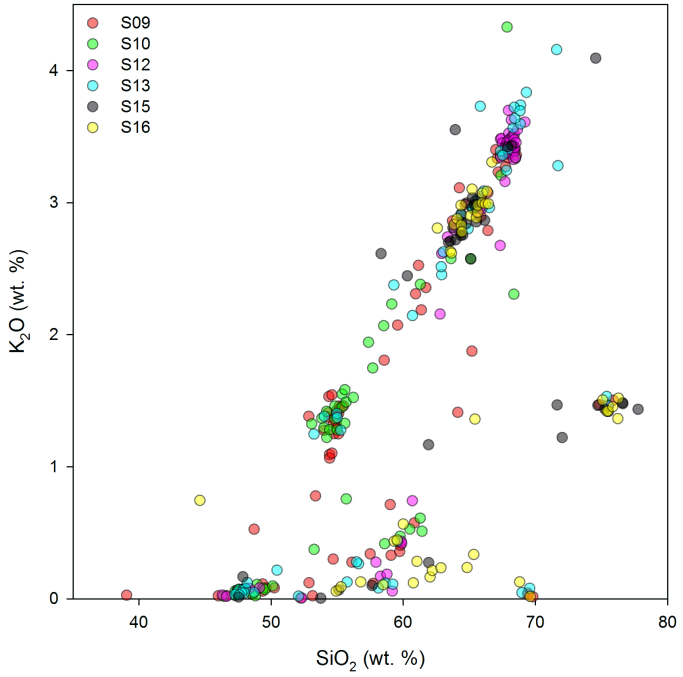

(b) Chemical composition of tephras S09, 10, 12, 13, 15 & 16. Given the majority chemistry of the populations, a number of possible matches can be identified: S09 & S10, S12 & S13, S15 & S16, but given the chemical range of the populations this cannot be certain.

FIGURE 6.19: Chemical composition of non-visible tephras.

6.3.3.5 Improvements From Tephrochronology

The most profound effect of utilising a tephrochronological approach is on the quality of the short core chronologies, where the identification of the AD1991 and AD1891 Hudson eruptions allow the ^{210}Pb chronology to be constrained at the base of the sequence, where the errors of the model are greatest. The approach has also improved the ^{14}C chronologies for the long cores. The ability to cross-correlate the two sequences at three points (see Figure 6.20) means fewer radiocarbon analyses are necessary and the chronologies are more reliable. Tephrochronology informed the decision on which radiocarbon dates to delete at Laguna Edita, where no date was obviously erroneous. The H2 tephra identified the date that contributed to the chronology best matching Laguna Meche. This would not have been possible without the use of tephrochronology, and would have otherwise required further dating effort. The tephra derived core correlations with radiocarbon dates are summarised in Figure 6.20. In addition this study has provided new dates from know tephras and bounding dates for a previously unreported tephra. This will lead to future improvements in dating efforts in the region.

6.4 Summary and Conclusions

This chapter has presented multiple, independent data sets and used those to construct age/depth models for two short and two long cores. In addition to providing an absolute dating framework for the presented in Chapters 7, 9 and 10, improved geochemical data is presented for the H1 eruption and the first glass shard geochemical data is presented for the two recent eruptions of Mt. Hudson. Geochemical data and a precise radiocarbon date is also presented for a previously undescribed ash present throughout the Chacabuco Valley. The key conclusions are:

- Short cores from Laguna Edita and Laguna Meche have been dated using ^{210}Pb verified with ^{137}Cs and tephrochronological markers.
- Long cores from Laguna Edita and Laguna Meche have been dated using ^{14}C verified with tephrochronological markers.
- The AD1891 eruption of Mt. Hudson is present in the stratigraphic record in Patagonia.
- There is a tephra widespread in the Chacabuco Valley deposited 7,868–8,169 years B.P. that cannot be ascribed to any previously described ash.

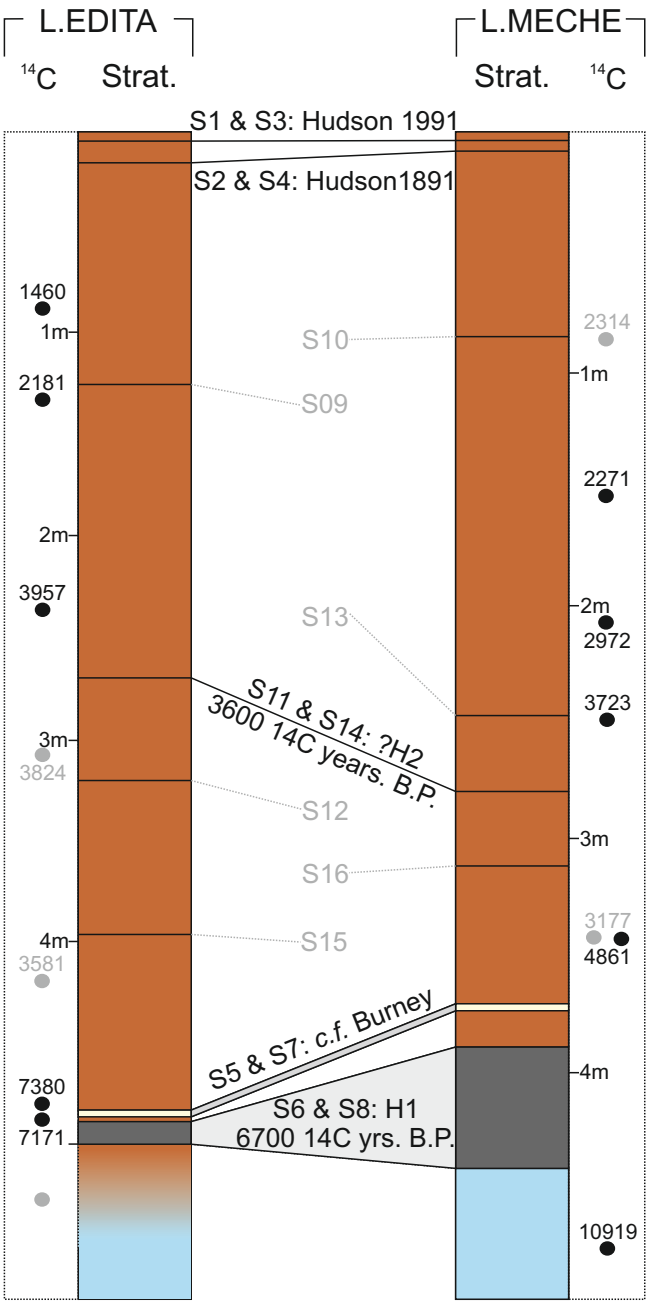

FIGURE 6.20: Stratigraphic diagram showing tephra correlation points and radiocarbon dates for both sites. Note that all ages are in radiocarbon years. The dates used for H1 and H2 eruptions were from (from Naranjo and Stern, 1998).

Chapter 7

Results from Modern Samples and Short Cores

7.1 Introduction

This chapter presents data for modern samples and short cores obtained from both study sites. The first part presents the results of stable isotope analysis of modern surface waters and modern vegetation carbon. The purpose of modern water isotope analysis is to understand local hydrology and lake status. The purpose of isotope analysis of modern vegetation carbon is to understand the properties of potential sources of carbon to the lake. The methods employed are described more fully in Sections 5.5 & 5.4.2. The second part presents analysis of carbon (%TOC, δ^{13}C and C/N) and chironomids (stratigraphy and transfer function) of the short cores, for which chronologies were presented in Section 6.2.

7.2 Modern Samples

7.2.1 δ^{2}H and δ^{18}O of Modern Lake Water

The surface water δ^{2}H and δ^{18}O in the region have a linear relationship between altitude and isotopic fractionation (shown in Figure 7.1(a), where higher altitudes are more fractionated) with the exception of Laguna Edita which has stable isotope values usually found at higher altitudes in the valley. This reflects the increase in humidity (Leng, 2004) as temperature drops with altitude (Mayr *et al.*, 2007). The intersection of the line of best fit for these data with the Global Meteorologic and Local Meteorologic Water Lines for the Argentinian steppe indicates that the altitude at which lakes in the region cease to be predominantly evaporative is somewhere around 980m a.s.l.; below this altitude the lakes can be strongly evaporative (Darling *et al.*, 2005), defining a local

evaporation line for the valley (shown in Figure 7.1(a)). It differs from the local evaporation line for the semi-Arid Argentine steppe because of the higher humidity in the Chacabuco Valley; humidity is higher as it is more proximal to the dominant and humid source of orographic rainfall from the Pacific coast (Mayr *et al.*, 2007). There is no indication of prolonged stratification in these lakes as samples from surface, basal and littoral zone waters show no significant differences from one another. The data do indicate small shifts between sampling seasons (see Figure 7.1(b)), although further long-term data are required to ascertain if there is a seasonal pattern; the pattern observed here is most likely reflective of local weather conditions and source airmass at the time of collection (Darling *et al.*, 2005; Mayr *et al.*, 2007).

7.2.2 δ^{13}C and C/N of Modern Vegetation

The δ^{13}C and C/N ratios of modern plant and soil material were sampled to contextualise the down-core δ^{13}C and C/N data. The terrestrial vegetation C/N *vs.* δ^{13}C plots largely within the generalised limits for C_3 land plants presented by Meyers and Teranes (2001), whereas the vast majority of terrestrial vegetation and soil samples fall within δ^{13}C values of between -30 to -25‰ (shown in Figure 7.2(a)).

C/N ratios are largely confined to values between 15–110, although the two terrestrial grass samples were considerably higher (145 & 208). There is a wide range of δ^{13}C values of aquatic plants, from as high as -12 to as low as -37‰. The lowest aquatic macrophyte δ^{13}C values are from deeper parts of lakes, around 7–8m, where macrophytes are likely utilising within lake (recycled) CO_2, whereas the highest values tend to be from marginal or littoral zones where macrophytes could be emergent and utilising atmospheric CO_2 (shown in Figure 7.2(b)).

The C/N ratios show a relationship between lower and higher plants (lower and higher C/N ratios respectively); for these data an aquatic/terrestrial divide at a C/N ratio of 20 is appropriate as a generalisation of the data. Although the δ^{13}C values of C_3 terrestrial plants plot well within the limits of Meyers and Teranes (2001) of *c.*-25 to -30‰, but the wide range of δ^{13}C values of aquatic plants, particularly those below *c.*-27‰ is atypical (Meyers and Teranes, 2001).

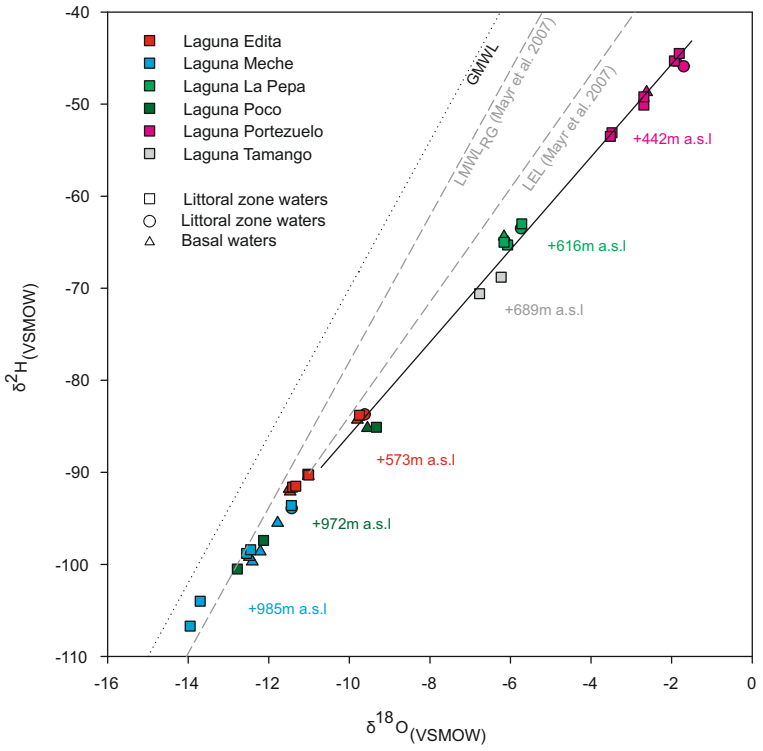

(a) δ^2H and δ^{18}O of surface water in the Chacabuco Valley, shown with the line of best fit (in solid black), the global meteoric water line (dotted black) and the local meteorological water line and local evaporation line for semi-arid Argentinia from Mayr *et al.* (2007). The altitude above sea level for each site is also marked.

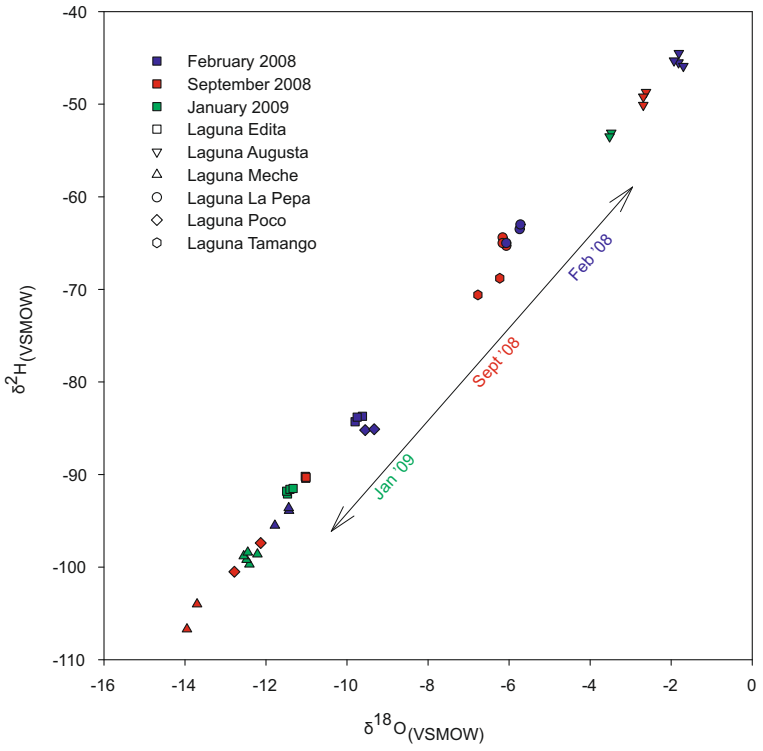

(b) As for 7.1(a), but labelled to show the differences between sampling seasons. Samples from each of the three sampling seasons are colour coded and the general trend is represented by the arrow.

FIGURE 7.1: δ^2H and δ^{18}O of surface water in the Chacabuco Valley.

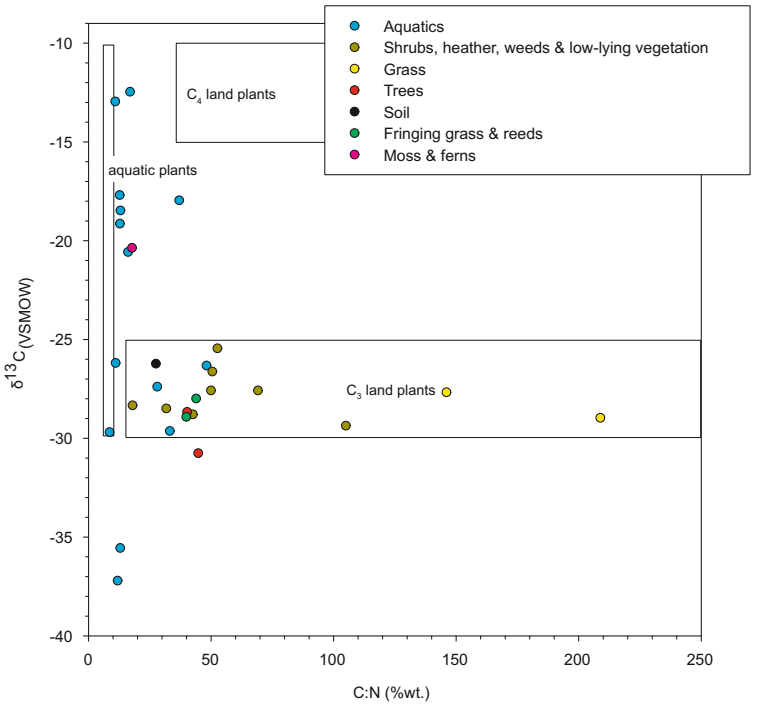

(a) δ^{13}C and C/N ratio of all sampled modern vegetation in the Chacabuco Valley. Colours represent different types of vegetation, and the generalised values from Meyers and Teranes (2001) are shown as rectangles.

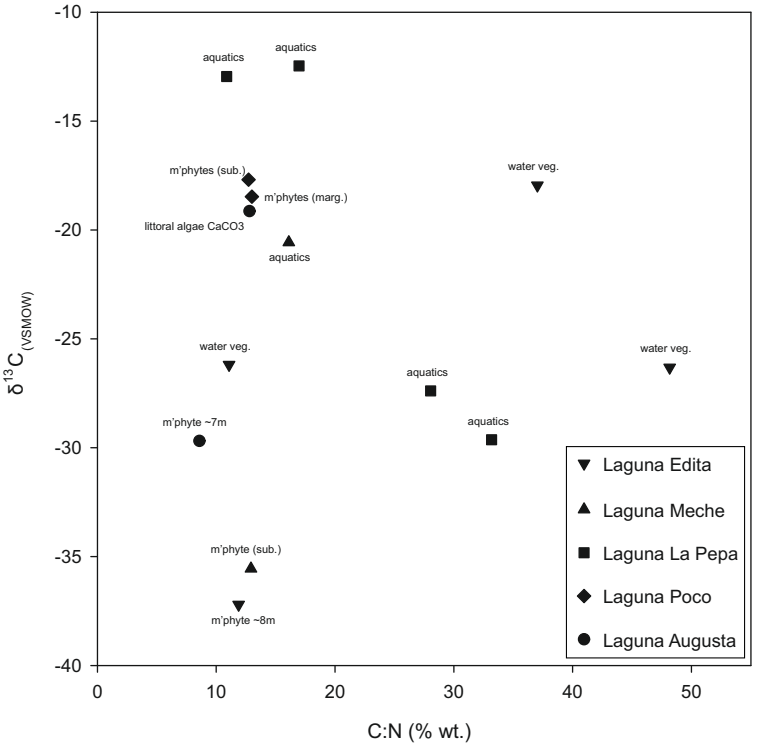

(b) δ^{13}C and C/N ratio of aquatic vegetation in the Chacabuco Valley; symbols represent the sample site, and the original sample labels are shown.

FIGURE 7.2: δ^{13}C and C/N ratio of modern vegetation in the Chacabuco Valley.

7.3 Laguna Edita and Laguna Meche Short Core Results

7.3.1 Cores Analysed and Results Obtained

A 26cm long core (EDI-1) was retrieved from the central part of Laguna Edita and a 20cm long core was obtained from the central part of Laguna Meche (MEC-3). An additional 20cm long core from a shallower, more marginal location in Laguna Edita (EDI-3) was also obtained and analysed to investigate any spatial differences in the modern chironomid compositions. All cores were sub-sampled in the field at 1cm intervals and subsequently freeze-dried before analysis. The cores were sampled for dating (described in Section 6.2), loss-on-ignition, chironomid, carbon isotope and C/N analysis at contiguous 1cm intervals, although some samples were exausted before all analyses could be performed. Two additional cores (EDI-2 and MEC-2) proximal to the primary research cores (EDI-1 and MEC-3) were returned intact for Itrax scanning to determine the recent sedimentary history of the two lakes (a summary of material obtained and analyses performed is given in Table 7.1). A second undated sequence (EDI-3) from a more marginal position in Laguna Edita is included for comparison.

Site Code	Core Code	Length	Analysis Performed
EDI-2009	EDI-1	26cm	^{210}Pb, ^{137}Cs, δ^{13}C, C/N, chironomids, %TOC
EDI-2009	EDI-2	28cm	Itrax scanning
EDI-2009	EDI-3	20cm	Chironomids, %TOC
MEC-2009	MEC-2	40cm	Itrax scanning
MEC-2009	MEC-3	20cm	^{210}Pb, ^{137}Cs, δ^{13}C, C/N, chironomids, %TOC

Table 7.1: List of short core material obtained and analyses performed.

7.3.2 Laguna Edita

7.3.2.1 Itrax Analysis

Core EDI-2 (Figure 4.4) was collected for Itrax analysis. The radiograph indicates a dense layer at the top of the core that scanning x-ray fluorescence analysis (XRF) showed was rich in Fe, Ti, Ca, Zr, Mn, K and Si amongst other elements (Figure 7.3), and microscope smear slides confirms this layer is rich in tephra shards (concentrations >1000/g). There is another less discrete layer with a similar chemical composition at the base of the core, in which peaks in Fe, Ti, Ca and Mn are present.

7.3.2.2 %TOC, δ^{13}C and C/N

Total organic carbon content measurements (%TOC, shown in Figure 7.4) show a large decline in %TOC between AD1990 to AD2000, and there is also a less pronounced decrease in organic content centred on AD1885, due to tephra input previously described

in Section 6.2.3. There is a rise in %TOC between AD1930–1970, but otherwise carbon content is stable at 8–10%TOC. The ratio of C/N shows little variation given the range of values in modern plants, varying between 8.3–11.5 in three main trends: from AD1880–1910 a downward trend from 11.5 to 9.5, followed by a 20 year rising trend to around 11, where it remains for a decade before a decline from AD1940 onwards to the lowest values observed at present. Values are stable between AD1958–1973. δ^{13}C declines until AD1920, where there is a small peak of around 1‰, followed by a further decline from AD1940 onwards concurrent with the declining C/N ratio.

7.3.2.3 Chironomid Analysis

The samples were generally rich in chironomids, with average concentrations of 82 head capsules/g of dry sediment. Five of the samples had total chironomid head capsule counts <40. The fauna comprised 21 chironomid taxa and a small number of Simuliidae head capsules were also encountered. The chironomid stratigraphy is generally dominated by Tanytarsini, *Ablabesmyia*, nr.*Macropelopia* and *Chironomus*. There is also a minor component of *Riethia* and *Alotanypus*. Throughout the record there are low levels of a range of Orthocladiinae. The following bio-stratigraphic zones are based on constrained cluster analysis:

EDI-1 Zone 1 (AD1875–1895) This zone is dominated by *Chironomus*, nr.*Macropelopia*, *Ablabesmyia*, and Tanytarsini, along with a small number of *Dicrotendipes*. A number of taxa present elsewhere in the fauna are absent at the bottom of the sequence, and as such the diversity is relatively low.

EDI-1 Zone 2 (AD1895–1930) This zone features the reduction, complete disappearance and re-appearance of *Chironomus*, centred on AD1920 and spanning the entire zone. *Chironomus* is replaced by Tanytarsini, with much smaller increases in a number of other taxa including *Ablabesmyia*, *Dicrotendipes* and *Reithia*. There is also the first appearance of *Parapsectrocladius*, *Thienemanniella*, *Labrundinia* and *Alotanypus* in this zone, although individually they make up a small part of the fauna.

EDI-1 Zone 3 (AD1930–1991) This zone is diverse and populations are relatively stable. Although dominated by *Chironomus*, Tanytarsini, *Ablabesmyia* and nr.*Macropelopia*, there are small but persistent occurences of *Dicrotendipes*, *Polypedilum*, *Riethia*, *Alotanypus* and *Labrundinia*. There are the first appearances of *Apedilum* and *Parakeifferiella*, which occur occasionally at low levels throughout the zone. A number of new taxa appear at very low levels (*e.g. Stictocladius*, Orthoclad. "wood miner" & *Eukiefferiella*), and the occurence of *Parochlus* increases.

EDI-1 Zone 4 (AD1990–present) At or immediately following tephra deposition, Tanytarsini proportions expand while those of *Ablabesmyia* are reduced.

Alotanypus increases from previously low levels, and some very minor Orthocladiinae proportions increase slightly (*e.g. Limnophyes*, *Cricotopus*, *Parapsectrocladius*), although overall the fauna does not change radically.

7.3.2.4 Additional Chironomid Stratigraphy

An additional chironomid-only stratigraphy from Laguna Edita (EDI-3) allows for the discrimination of spatial differences in the chironomid fauna (shown in Figure 7.6). The EDI-3 core is more marginal than the EDI-1 core and in shallower water. Because the core does not have an age-depth model it is not possible to compare the stratigraphy through time, but the overall similarity of the chironomid faunas can be compared. The fauna is similarly dominated by *Chironomus*, Tanytarsini, *Ablabesmyia* and nr.*Macropelopia*. The Orthocladinae fauna is slightly more diverse. Numbers of *Labrundinia* are slightly higher in EDI-3 than in EDI-1.

7.3.2.5 Ordination and Transfer Function

Detrended correspondence analysis of the chironomid data yielded an axis 1 eigenvalue of <0.2 and so the data are best treated as linear. Principle components analysis (PCA) yielded an axis 1 eigenvalue of 0.22; the second axis has an eigenvalue of 0.16 (both axes are shown in Figure 7.7). These variable data could be in part due to the large number of rare taxa whose proportions are often at or near zero; this is particularly the case for the 8 taxa within the Orthocladiinae (this is the case even though rare taxa were downweighted in the calculations).

The transfer function described in Section 5.6.5 was applied to these data and is shown in Figure 7.7. Over 98% of taxa in the fossil data were present in the training set, so the training set is representative of the fauna of this site. It correlates well with the PCA axis 1 scores (Section 7.3.2.6). The range of inferred temperature values produced varies from 3.5 to almost 9.5°C; this range is unrealistically too large.

7.3.2.6 Correlation Matrix

Table 7.2 shows that there are a number of significant relationship between the datasets presented for Laguna Edita. The relationship between PCA axis 1 scores and CI-MAT indicates that CI-MAT (chironomid-inferred mean annual temperature) reconstructions from these data may be valid, although there are other reasons for not accepting these data (see Section 7.3.2.5). The relationship between PCA axis 2 of the PCA with tree rings ($\rho = 0.48$) and PCA axis 1 and CI-MAT ($\rho = 0.72$) is significant. There are significant correlations between C, C/N and δ^{13}C. %TOC has significant relationships with PCA axis 1 scores and chironomid-inferred temperature.

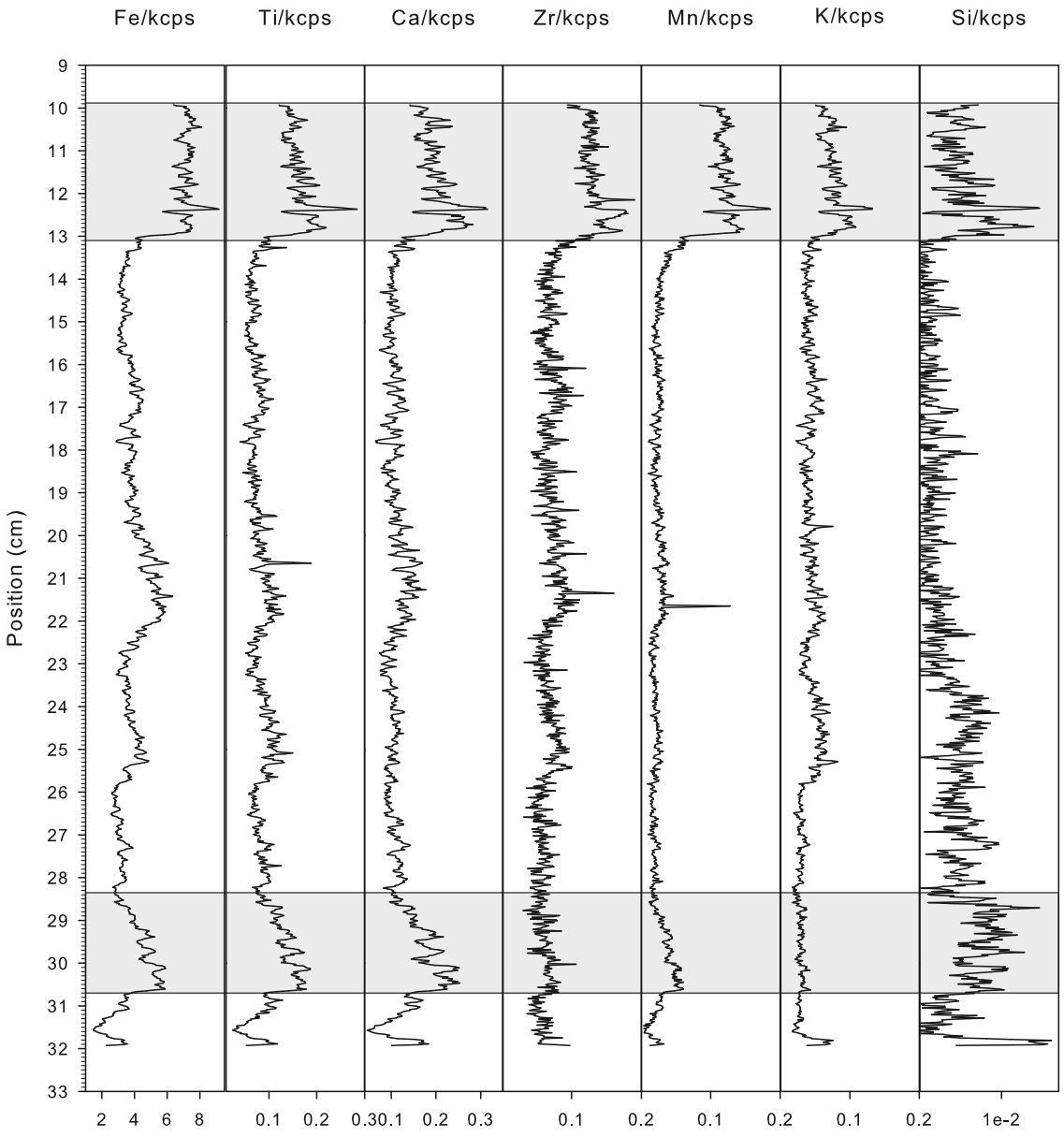

FIGURE 7.3: Itrax scan data from EDI-2, showing selected data divided by the count rate. The tephra layers mentioned in the text are highlighted in grey — the upper layer being the AD1991 and the lower layer being the AD1891 eruptions of Mt. Hudson.

	C	δ^{13}C	C/N	PCA axis 1	PCA axis 2	CI-MAT	Tree Rings
%TOC	**0.58**	0.23	-0.03	**-0.52**	0.02	**-0.56**	-0.20
C		**-0.50**	**0.74**	-0.32	0.10	-0.22	-0.26
δ^{13}C			**-0.79**	-0.16	0.16	-0.18	-0.09
C/N				-1.80	0.20	0.05	-0.20
PCA axis 1					0.00	**0.72**	0.11
PCA axis 2						0.29	**-0.48**
CI-MAT							0.05

TABLE 7.2: Correlation matrix for Laguna Edita short core data. Pearsons correlation coefficients (ρ) shown, calculated using normalised data. **Bold type** denotes significance $\sigma \leq 0.05$ ($n = 26$). Tree ring temperature inference data resampled to match time intervals for other data from Villalba *et al.* (2003). %TOC are corrected loss-on-igntion measurements and C are total C determinations from elemental analysis (Section 5.4.1).

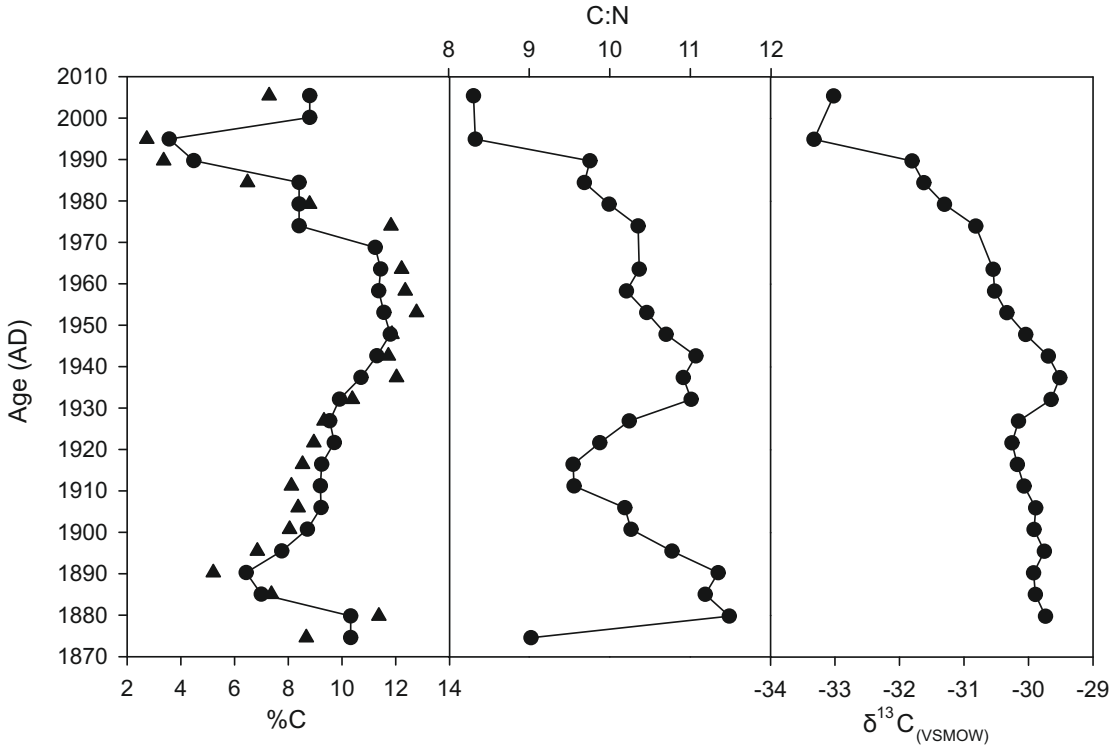

FIGURE 7.4: %C, δ^{13}C and C/N of EDI-1 short core. In the %C column circles represent the adjusted loss-on-ignition data and triangles represent elemental analyser data.

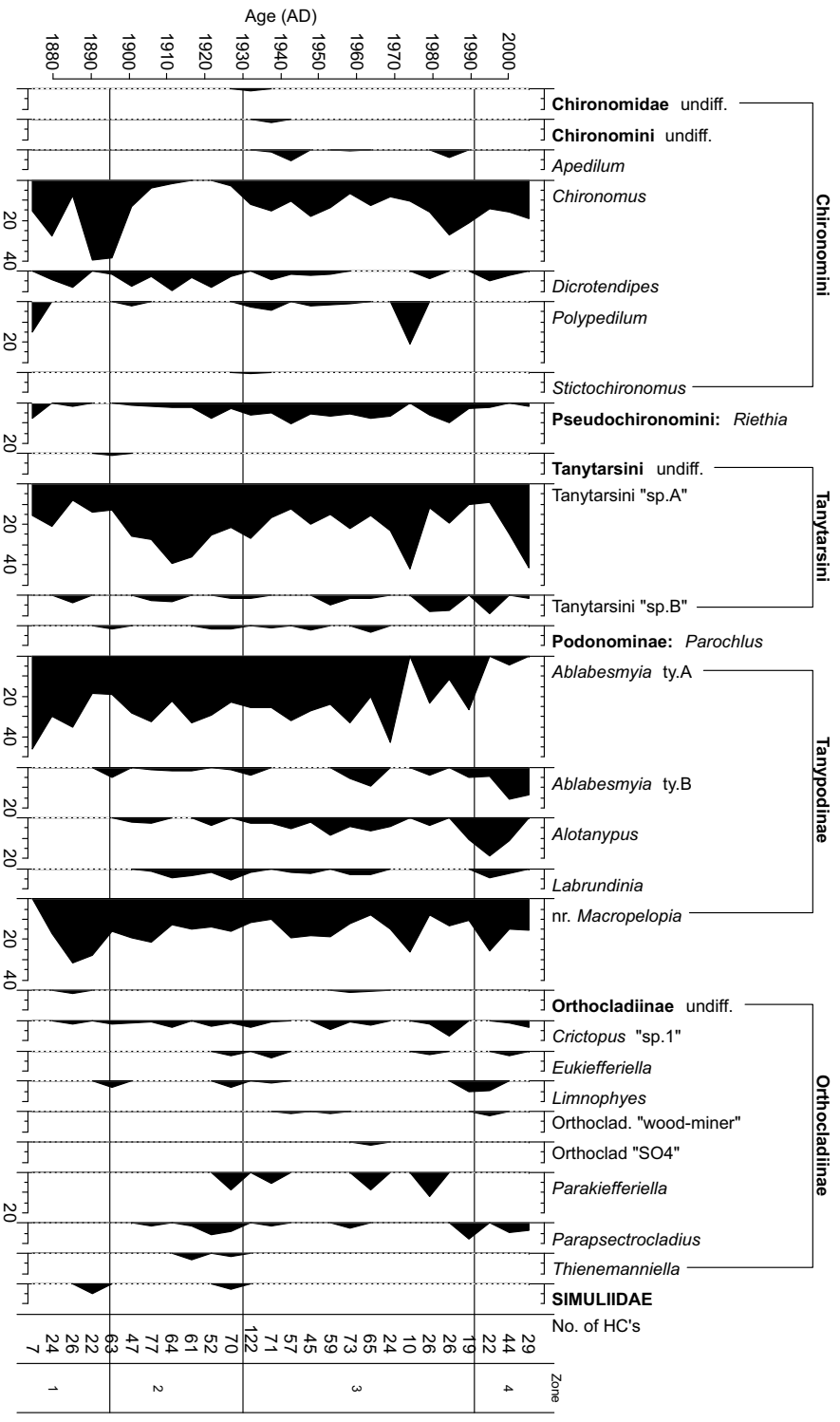

FIGURE 7.5: Chironomid diagram for EDI-1 short core. Sub-families are shown in bold, genera and species in italics. The 'no. of head capsules' figure does not include those taxa outside of the Chironomidae. In calculating the percentage abundance diagrams taxa from other families (*e.g.* Simuliidae) were not included in the calculation, and their percentages have been plotted relative to the total number of chironomids. Zones refer to those described in Section 7.3.2.3.

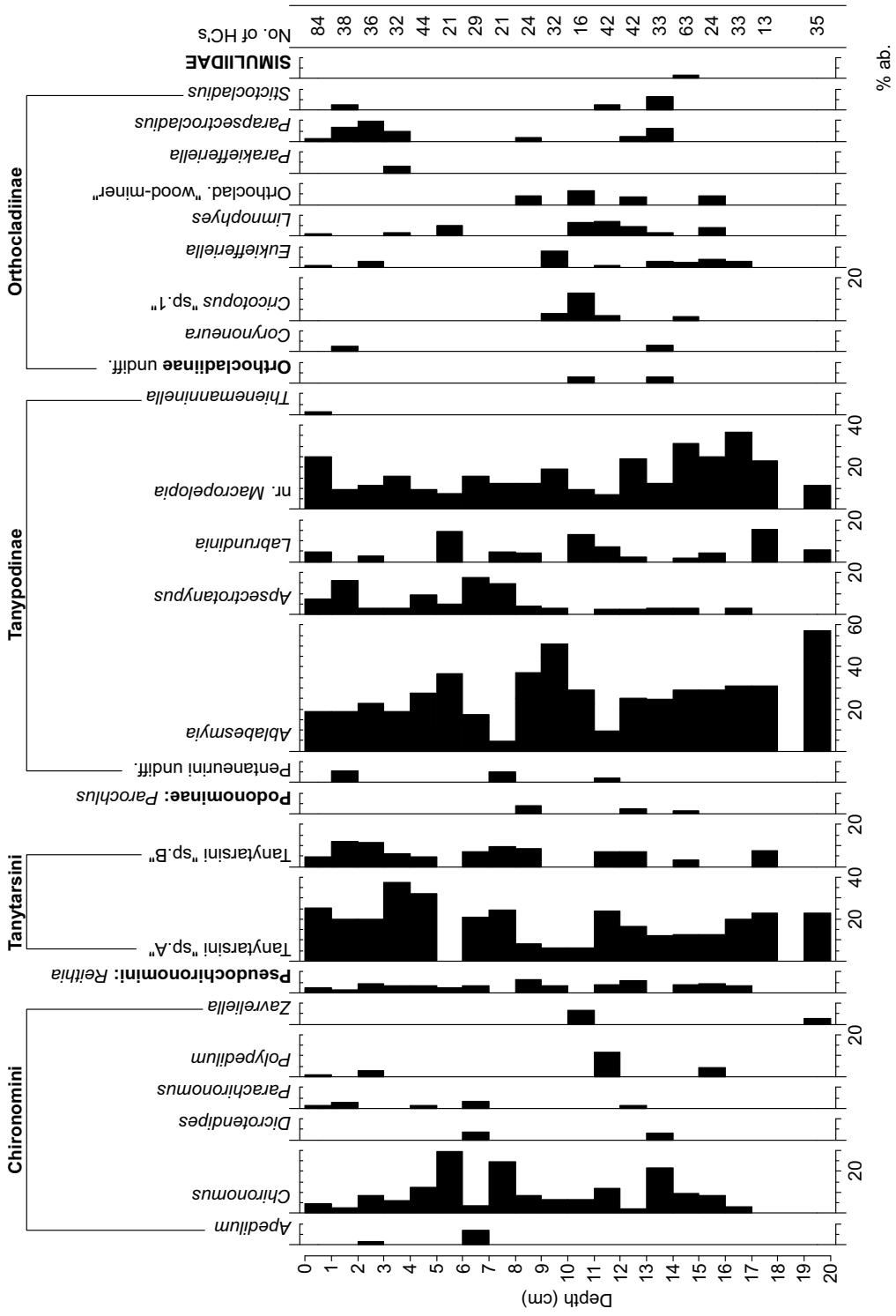

FIGURE 7.6: Chironomid diagram for EDI-3 short core. Sub-families are shown in bold, genera and species in italics. The 'no. of head capsules' figure does not include those taxa outside of the Chironomidae. In calculating the percentage abundance diagrams taxa from other families (*e.g.* Simuliidae) were not included in the calculation, and their percentages have been plotted relative to the total number of chironomids.

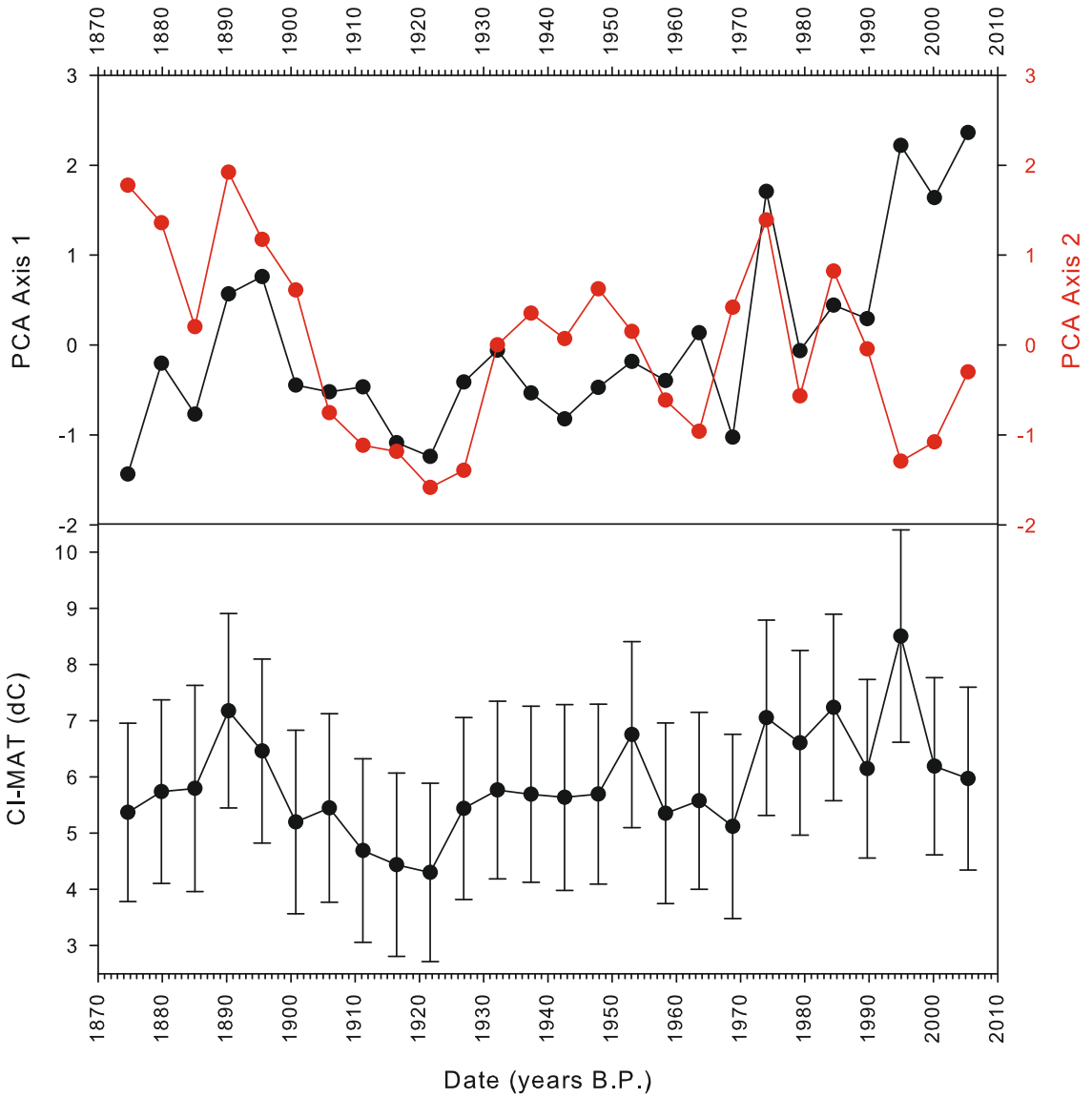

FIGURE 7.7: PCA axes 1 and 2 scores and chironomid-inferred mean annual temperature (CI-MAT) for Laguna Edita short core. PCA axes 1 and 2 have eigenvalues of 0.22 and 0.16 respectively. CI-MAT was calculated using the transfer-function presented in Massaferro and Larocque-Tobler (2013).

7.3.3 Laguna Meche

7.3.3.1 Itrax Analysis

Core MEC-2 was collected for Itrax analysis. This indicated a layer of tephra at the top of the core enriched in Si, K, Ti, Mn and Fe, amongst other elements (Figure 7.8). An additional layer at around 27cm was also identified that was enriched in Ti and Ca.

7.3.3.2 %TOC, δ^{13}C and C/N

The %TOC data (Figure 7.9) shows a period of decreased organic content around AD1991. C/N remains relatively stable throughout the core until this event, where values fall from 12.5 to 8.5 and do not recover. There are small-scale variations in δ^{13}C in the order of 1‰, and two zones of lower and two zones of higher δ^{13}C, the more depleted zones being between AD1880–1910 and from AD1950 onwards. There is a general trend towards lower C/N towards the top of the core, and no clear correlation between C/N and δ^{13}C.

7.3.3.3 Chironomid Analysis

The samples were generally rich in chironomids, with concentrations of around 124 head capsules/g of dry sediment. Six of the samples had total chironomid head capsule counts $<$40; these samples should be treated with caution. The fauna comprised of 26 chironomid taxa and a small number of Simuliidae and Ceratopoginae head capsules. The fauna is dominated by *Parakiefferiella* for much of the sequence, with a diverse fauna of minor taxa, the most numerous of which are *Limnophyes* and *Eukiefferiella*. The following two zones are based on the results of constrained cluster analysis:

MEC-3 Zone 1 (AD1840–1991) The bulk of the chironomid record is dominated by *Parakiefferiella*, although the fauna is diverse. From AD1890 onwards nr.*Macropelopia* gradually increases, along with *Cricotopus*, although the overall contributions from these two taxa are still under 15%.

MEC-3 Zone 2 (1991–present) There is a sudden dramatic drop in the *Parakiefferiella* population, and a syncronous expansion of Tanytarsini. There is also the first appearance of *Dicrotendipes* at proportions as high as 20%. In addition, *Corynoneura*, *Eukiefferiella* and *Polypedilum*, previously present at low levels throughout Zone 1, disappear completely. There are small expansions in some minor taxa, including *Parapsectrocladius*, *Ablabesmyia* and *Riethia*.

7.3.3.4 Ordination and Transfer Function

Principle components analysis gives an eigenvalue of 0.48, and this axis is dominated by the *Parakifferiella*/Tanytarsini shift that defines the transition between Zones 1 and 2, and the appearance of *Dicrotendipes* during this transition. While the first axis explains much of the variance in the data, the second PCA axis explains a much smaller proportion (eigenvalue of 0.11); Figure 7.11 shows both axes.

The first axis scores show good agreement with the chironomid-inferred mean annual temperatures (Figure 7.11, see also Section 7.3.3.5), although it is to be expected for the transfer function to reflect this complete re-organisation of the chironomid fauna at the top of the core at the same time as tephra deposition. The dominance of *Parakiefferiella* is also likely to reduce the sensitivity of the transfer function to climate osillations as the reconstruction will be heavily weighted towards to optimum of this taxon (7±2°C).

7.3.3.5 Correlation Matrix

Table 7.3 shows that there are a number of significant relationship between the datasets presented for Laguna Meche. There are significant relationships between C/N, %TOC and δ^{13}C. The PCA axis 1 scores and %TOC & C are correlated, as discussed previously due to the re-organisation of the chironomid fauna following tephra deposition. PCA axis 1 scores are also correlated with local tree-ring temperature reconstructions.

	C	δ^{13}C	C/N	PCA axis 1	CI-MAT	Tree Rings
%TOC	**0.59**	-0.29	0.41	**-0.88**	0.05	-0.432
C		**-0.87**	**0.92**	**-0.50**	0.06	-0.33
δ^{13}C			**-0.96**	-0.22	-0.37	0.28
C/N				-0.39	0.22	0.40
PCA axis 1					0.05	**0.49**
CI-MAT						-0.05

TABLE 7.3: Correlation matrix for Laguna Meche short core data. Pearsons correlation coefficients (ρ) shown, calculated using normalised data. **Bold type** denotes significance $\sigma \leq 0.05$ ($n = 20$). Tree ring data resampled at appropriate time intervals from Villalba *et al.* (2003).

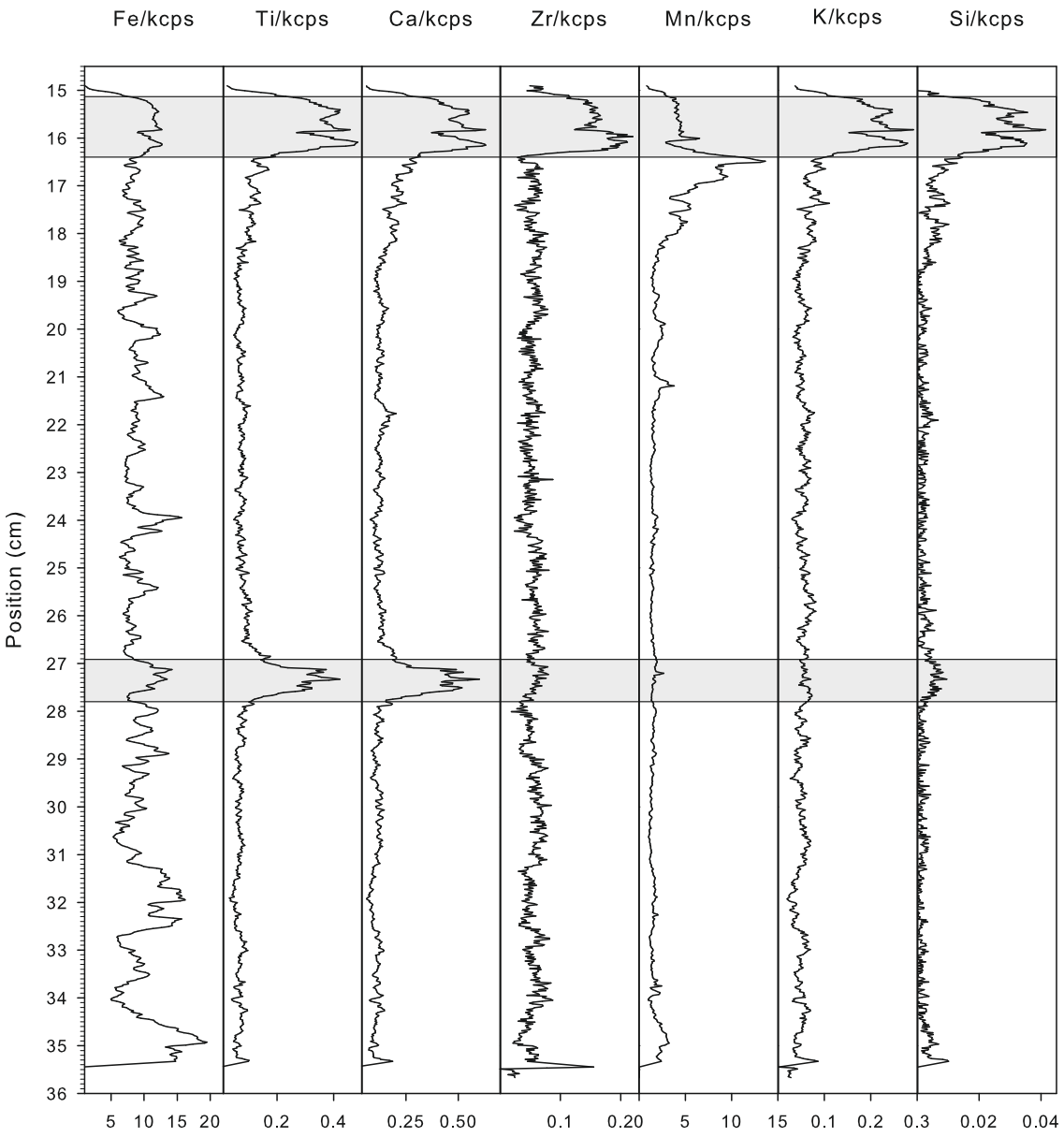

FIGURE 7.8: Itrax scan data from MEC-2, showing selected data divided by count rate. The tephra layers mentioned in the text are highlighted in grey, the upper being the AD1991 and the lower being the AD1891 eruption of Mt. Hudson.

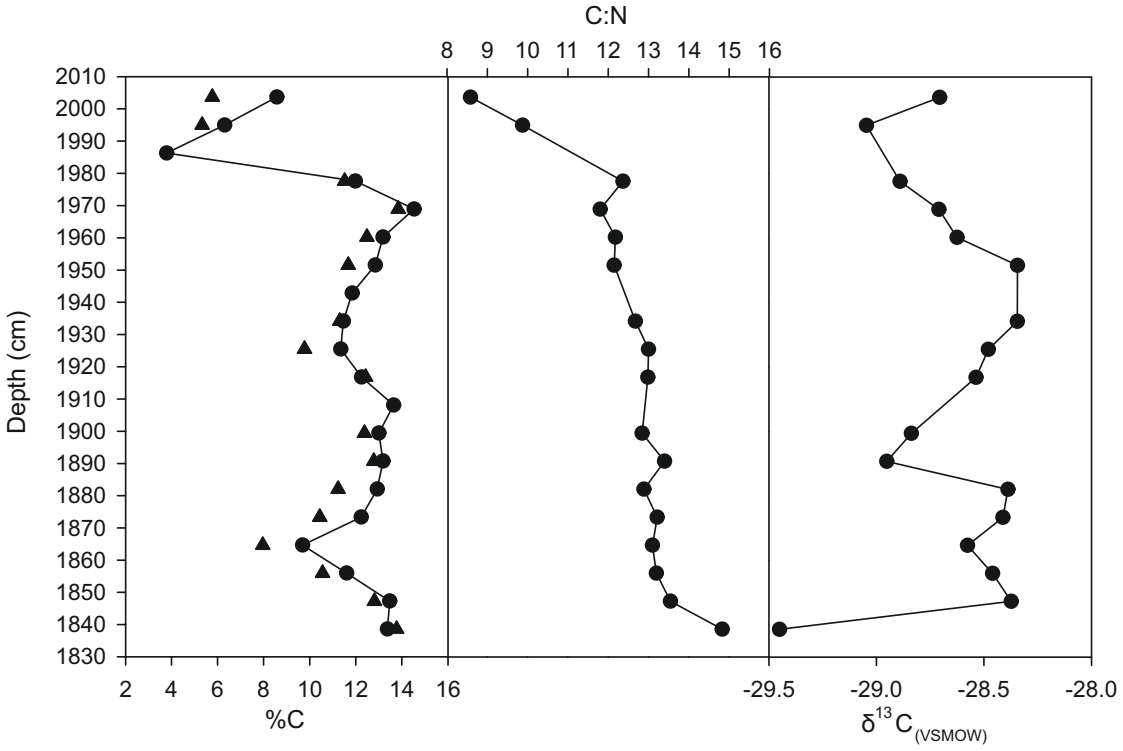

FIGURE 7.9: %C, δ^{13}C and C/N of MEC-3 short core. In the %C column circles represent the adjusted loss-on-ignition data (see Section 5.4.1) and triangles represent the elemental analyser data (%TOC).

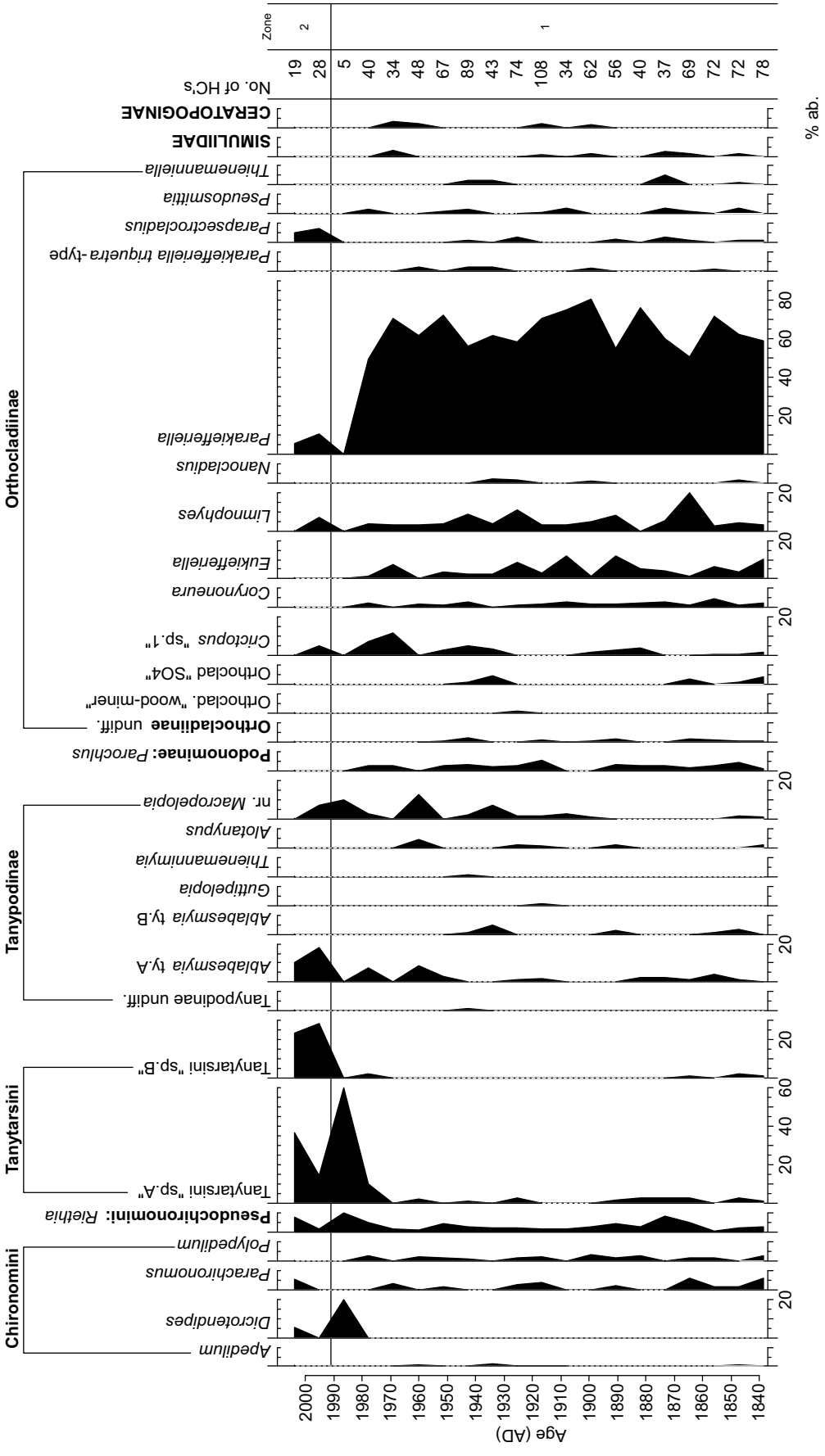

FIGURE 7.10: Chironomid diagram for MEC-3 short core. Sub-families are shown in bold, genera and species in italics. The 'no. of head capsules' figure does not include those taxa outside of the Chironomidae. In calculating the percentage abundance diagrams taxa from other families (*e.g.* Simuliidae) were not included in the calculation, and their percentages have been plotted relative to the total number of chironomids. Zones refer to those described in Section 7.3.3.3.

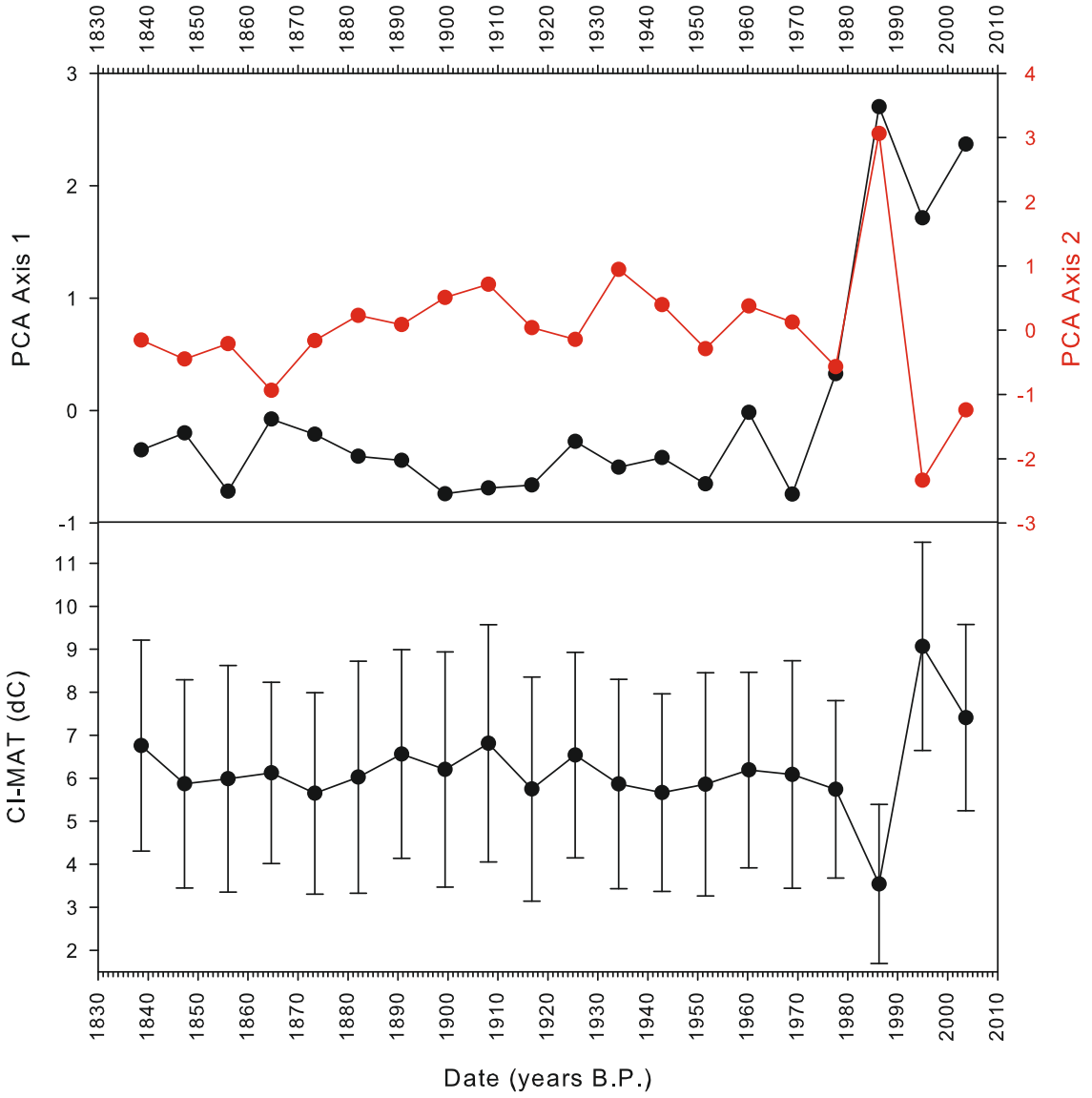

FIGURE 7.11: DCA axis 1 scores and CI-MAT for Laguna Meche short core. CI-MAT was calculated using the transfer-function presented in Massaferro and Larocque-Tobler (2013).

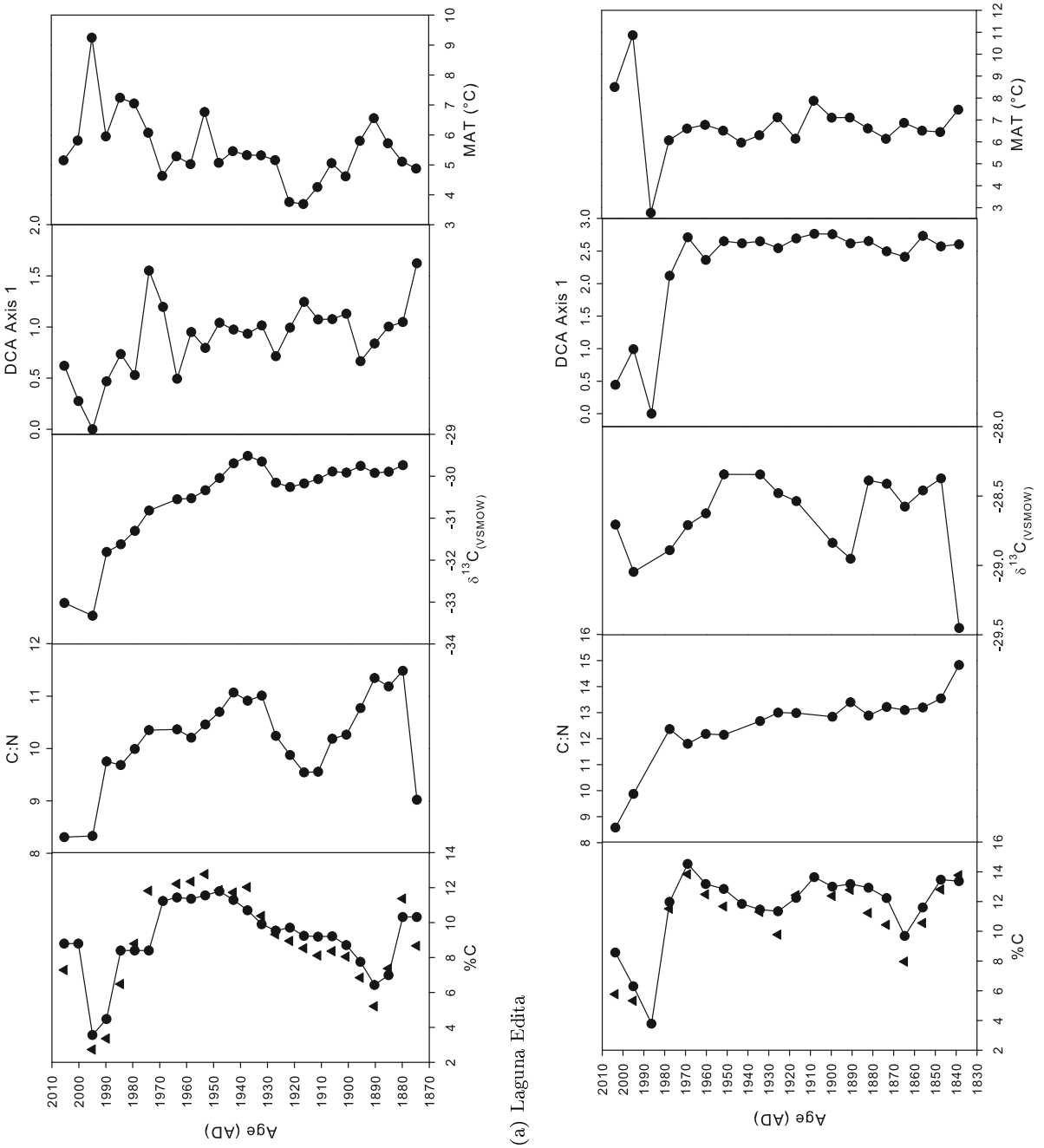

(a) Laguna Edita

(b) Laguna Meche

FIGURE 7.12: Summary diagrams of the short core data from Laguna Edita and Meche, showing the carbon and chironomid data. For %TOC, triangles represent elemental analyser determinations, circles represent corrected %LOI data.

Chapter 8

Discussion of Modern Sample and Short Core Data

8.1 Introduction

This chapter analyses the results presented in Chapter 7, presenting a hydrological model for the lakes in the Chacabuco Valley as well as simplified version of the Leng (2004) model of carbon isotopes in lake systems. It goes on to analyse the short-core data in the context of known environmental change in the Chacabuco Valley, presented in Chapter 3.

8.2 Hydrological Regime in the Chacabuco Valley

The $\delta^{18}O$ data in the non-evaporating lakes match predicted isotope values based on the Isomap project modelling (Figure 8.1). The $\delta^{2}H/\delta^{18}O$ values form a line ($r^2 = 0.99$) with a slope value of 1:5.04; slopes of 1:5 are given as typical of evaporative lake waters (Darling *et al.*, 2005) and are consistent with values seen elsewhere in the region (Aravena *et al.*, 1999; Mayr *et al.*, 2007). Most of the lakes waters plot on the Local Evaporation Line (LEL), indicating that all but the highest altitude lakes are evaporative (Darling *et al.*, 2005; Gibson *et al.*, 2002). The lowest lakes are highly evaporative and likely only maintained by seasonal precipitation, spring meltwater, groundwater and inflows from higher lakes (ibid). All three sampling seasons plot on the LEL, indicating that there is no seasonal variation in the relationship between humidity and altitude, and the offset of isotope values between seasons is likely a reflection of variations in source rainfall composition; the primary airmasses affecting the region (described fully in Section 4.1.2) have distinctive isotopic compositions described by Stern and Blisniuk (2002).

The relatively low $\delta^{18}O/\delta^{2}H$ values of Laguna Edita waters are unexpected given the lake's altitude, but suggests it is probably recharged by ground water (Krabbenhoft

et al., 1990) or a higher altitude source. The possibility that Laguna Edita has a much higher surface water inflow rate (as the isotopic composition is strictly reflective of evaporation to inflow rates (E/I) as per Gibson *et al.* 2002) can be discounted as the difference in lake area to catchment ratio is not anomolous compared to other lakes in this dataset (see Section 4.4). The 2‰ offset between austral summer and winter $\delta^{18}O/\delta^{2}H$ from this lake suggests the recharge may be seasonal, for example from meltwater or an ephemeral fluvial source. The relatively low $\delta^{18}O/\delta^{2}H$ values of Laguna Meche are in keeping with the altitudinal gradient and indicate the lake has limited evaporation. The systematic offsets between sampling seasons indicates that residence times are seasonal or less, and the indistinguishable results from surface and basal waters indicate that all lakes in the valley are well mixed (Darling *et al.*, 2005).

With regard to the interpretation of hydrological change of long-core data, Laguna Meche is effectively a fresh, open system at present, so any inferred lowering of lake level could be due to either any significant reduction in precipitation, an increase in temperature in the order of 1.5°C (estimated from altitudes in Figure 7.1(a) and assuming an environmental lapse rate of 6.5°C/km), thus bringing the lake into the zone of evaporative conditions, or both. As the lake is currently at the level of its overflow, no increase in lake volume is possible.

Laguna Edita is already assumed to be in the evaporating zone but is recharged via an upstream or groundwater source, so the interpretation of lake level changes for the lake is more complex — lake level lowering from present conditions could be due to either reduced precipitation, an increase in temperature, or a reduction in the volume of water delivered from higher altitudes. An increase in lake volume is possible as the lake does not currently drain from its outlet, so an increase in lake level is possible if there were to be an increase in precipitation, cooler temperatures, or an increase in the volume of water delivered from higher altitudes.

In summary, Laguna Meche is only sensitive to reductions in lake volume compared with present, whereas Laguna Edita is sensitive to both increases and reductions but has an unquantified ground or overland water recharge. In addition, a greater temperature shift is required to reduce lake level in Laguna Meche compared to Laguna Edita, which in theory would be sensitive to any increase in temperature.

8.3 Modern and Lake Sediment Carbon

8.3.1 Source Carbon in the Study Catchments

The modern C/N and $\delta^{13}C$ data are generally consistent with established relationships between land plants and aquatic plants, where terrestrial plants have higher C/N ratios, and lower $\delta^{13}C$. Organic matter from grasses in the catchment can be distinguished by

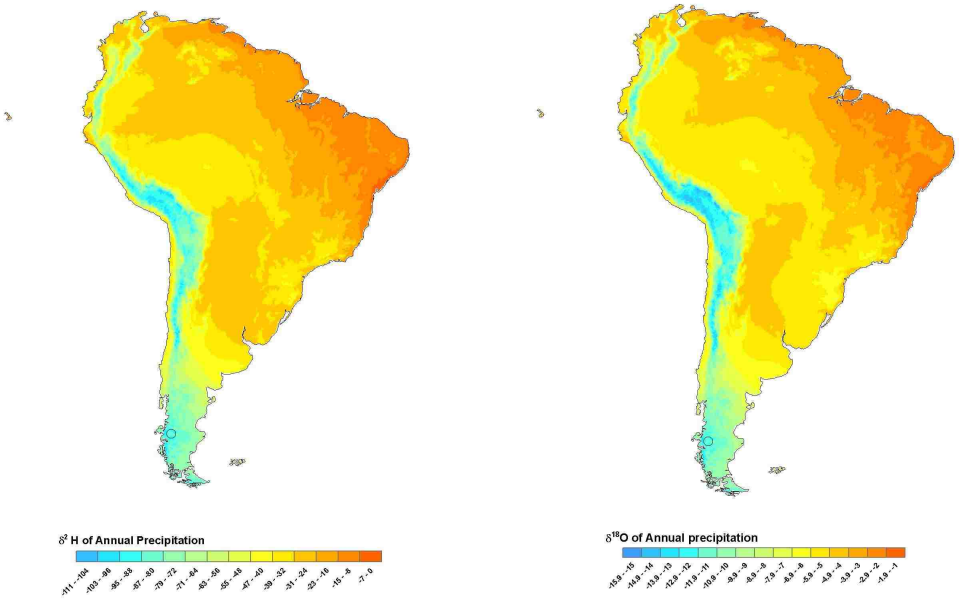

(a) Annual δ^2H (interpolated)

(b) Annual δ^{18}O (interpolated)

FIGURE 8.1: Modern isotope values of precipitation in Patagonia, from (Bowen and Revenaugh, 2003); the location of the Chacabuco Valley has been marked with a blue circle (Source: www.waterisotopes.org).

very high C/N values, although these grasses do not fall into the generalised limits for C_4 plants. There is some overlap between terrestrial vascular plants and submerged macrophytes, but generally terrestrial vegetation has lower $\delta^{13}C$ and higher C/N values compared to macrophytes (Figure 7.2). The aquatic plants have a wide range of $\delta^{13}C$, but generally lower C/N compared to terrestrial vegetation.

Figure 8.2 shows the data in this study compared to the data presented in Mayr *et al.* (2007) for Laguna Potrok Aike and Laguna Azul in the Argentine Steppe. Although those lakes are environmentally and hydrologically different, the results for soils and terrestrial vegetation are comparable, with the notable difference that submerged vegetation in the Chacabuco Valley has a broader range and generally lower $\delta^{13}C$ than in the data presented by Mayr *et al.* (2007). Mayr *et al.* reflect that their high $\delta^{13}C$ value of aquatic macrophytes can be attributed to utilization of bicarbonate HCO_3^- which is "enriched in ^{13}C relative to dissolved CO_2" (Mayr *et al.*, 2007, p.91). In the more acidic, softer waters of the Tamango range there should be more CO_2 and less HCO_3^- than for Laguna Potrok Aike and Laguna Azul (Wetzel, 2001, ch.11). Thus the wide range of $\delta^{13}C$ values for aquatic plants is likely due to a range of aquatic plant species, some of which are fixing CO_2 and others HCO_3^- (Keeley and Sandquist, 1992; Coleman and Fry, 1991), and may also reflect physiological differences between species (O'Leary, 1981). The higher values are consistent with those observed by Mayr *et al.* (2007) for a system dominated by HCO_3^-, and the lower values consistent with values from obligate CO_2 fixers (Keeley and Sandquist, 1992, Table 2). However, these lower values could also reflect source carbon isotopically depleted through recycling of carbon by respiration of uptake by phytoplankton (Leng, 2004).

8.3.2 Interpretation of Carbon Isotopes in Palaeoecological Data

The $\delta^{13}C$ and C/N of bulk organic matter can provide information on the source of the organic matter and productivity in the lake and its catchment, but this is best in conjunction with other indicators of authigenic/allogenic sediment balance (*e.g.* magnetic susceptability) and productivity. Diagenetic effects and basin sediment heterogeneity can affect the interpretation of these results. An assessment of isotopic inhomogeneity is beyond the scope of this study, and diagenetic effects on $\delta^{13}C$ and C/N are likely to be of little concern as they are usually small and the effects are greater in anoxic environments (Lehmann *et al.*, 2002; Best *et al.*, 1990), unlike these well-oxygenated lakes.

C/N values are indicative of source carbon; C/N <11 is commonly considered to be indicative of systems where the dominant source of sedimentary carbon is mixed phytoplankton, whereas C/N >17 is characteristic of terrestrial plants (Leng, 2004; Meyers and Teranes, 2001). In these data a small proportion of aquatic macrophytes have C/N values between 27-46, and these are likely to be seasonally partly submerged terrestrial vegetation rather than truly aquatic. In terrestrial plants $\delta^{13}C$ can be used to differentiate between C_3, C_4 and CAM photosynthetic pathways (O'Leary, 1981), but for

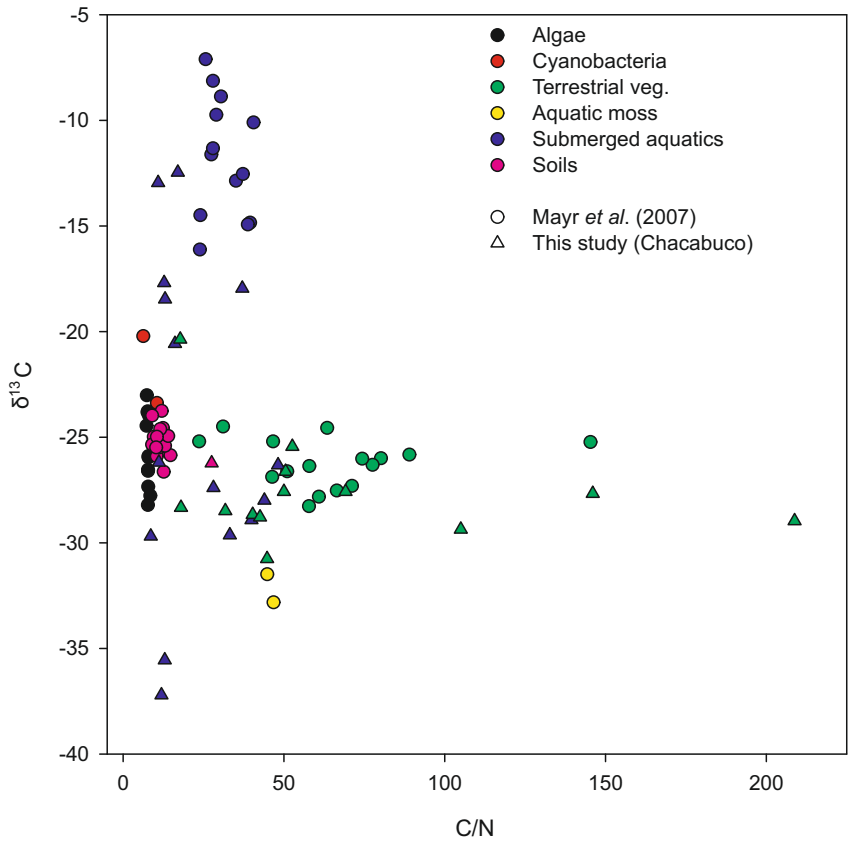

FIGURE 8.2: Modern Source Carbon Isotope Data from Mayr *et al.* (2007) and this Study. Circles are from Mayr *et al.* (2007) and triangles from this study. Data points are colour coded by carbon source.

autochthonous lake carbon, this is not possible because as discussed in Section 8.3.1, δ^{13}C is dependant on the source carbon composition (Keeley and Sandquist, 1992; Coleman and Fry, 1991).

As such, δ^{13}C of autochthonous sediment should reflect isotopic composition at the time of deposition (fractionation and diagenetic effects notwithstanding). Where sediment C and N indicate a predominantly terrestrial (allochthonous) source of organic carbon, isotope values reflect the source of the carbon (*e.g.* C_3, C_4 vegetation). Where the carbon source is a subequal mixture of allo- and autochthonous components (*e.g.* C/N values between 11–17), interpretation of bulk isotope values is difficult to interpret (Leng, 2004).

Figure 8.3 redraws the conceptual model of lake δ^{13}C presented by Leng (2004, Figure 8), replacing the generalised values with values observed in these data and simplifying to remove elements not relevant to these lakes in their modern configuration (*e.g.* marine limestone sources). A summary follows of possible pathways of change in bulk sediment δ^{13}C and C/N for these lakes:

1. changes in the amount of catchment derived terrestrial material, an increase of which will increase C/N, and according to data presented in Figure 8.2, lower δ^{13}C.

2. changes in the abundance and/or activity of macrophytes in the lake, where increased respiration causes a increase of δ^{13}C as sediments lock away isotopically depleted organic matter thus removing ^{12}C from the system and enriching the DIC pool in ^{13}C.

3. a change in the phytoplankton productivity, an increase of which will increase δ^{13}C values and decrease C/N.

4. a change in the oxidation conditions in the lake, which will govern the release of CO_2 from the lake sediment, and lead to decreases in δ^{13}C where anoxic conditions occur.

5. a change in lake volume, and extent of seasonal ice-cover, which will affect the relationship between CO_2 and plant macrophytes.

It follows that where carbon is predominantly autochthonous, pathways 2 and 3 will allow for an interpretation of sedimentary δ^{13}C as a palaeo-productivity indicator (Leng, 2004). Where carbon is predominantly allochthonous, changes in δ^{13}C will be reflective of source carbon (see Section 8.3.2), although practically C/N, %TOC and δ^{13}C are inter-related and will all inform the palaeoclimatic interpretation of the stratigraphies.

8.3.3 Palaeoenvironmental Interpretation of Carbon in the Short Cores

8.3.3.1 Laguna Edita

The average C/N in Laguna Edita is 10, with values as high as 11.7 and as low as 8.2. Values in this range are considered to have a predominantly algal origin (see Section 8.3.2), although as algal sources have C/N $<$10 a small non-algal source must be present. It may still be considered predominately algal (*c.f.* Meyers and Teranes, 2001, Table 2). The variations are small and variation of this magnitude have previously been considered not to represent a significant change of source carbon (Mayr *et al.*, 2005). From AD1940 onwards gradually declining δ^{13}C suggests increasing productivity in the lake. These low values decline further from AD1991 onwards, suggestive of an increase in phytoplankton; this is supported by lower C/N ratios at this time, indicative of an increased proportion of sedimentary carbon sources from phytoplankton in the lake. There is also a small rise in δ^{13}C from AD1930–1950, concurrent with a small positive deviation in C/N, possibly indicative of an increased allochthonous source of carbon to the lake.

It is noteable that the changes appear to take place at around the time that the valley was initially ranched, from the 1930's onwards. This could be co-incidental or a confounding factor in the palaeoenvironmental interpretation of these data. In Chilean Patagonia ranching has historically been initiated by clearing of the forest by burning

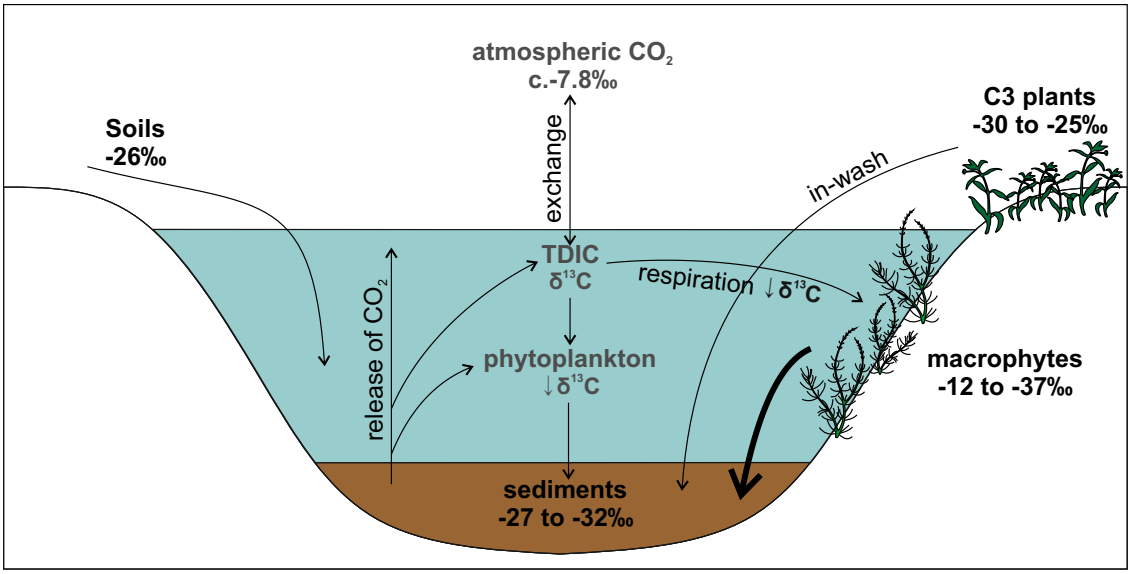

FIGURE 8.3: Simplified concept diagram of carbon cycling in the two study lakes, after Leng. Values in bold are from the observed data.

(Gut, 2008) — this might be expected to cause destabilisation of the soils and a temporary increase in sedimentation, although this does not seem to have been the case in either catchment (sedimentation rates fit a linear model; see Section 6.2). Modern soils from these catchments have similar C/N to that in this record but lighter carbon isotope composition (-26‰), so this would cause the opposite trend to that observed in these data. Bovine faecal carbon matter is similarly isotopically light (Dungait *et al.*, 2010). As such, it seems improbable that the changes seen in both records between AD1930–1970 can be attributed to ranching disturbance in the area.

8.3.3.2 Laguna Meche

C/N in this sediment core indicates that for the majority of the core there is a mixed contribution from allochthonous and autochthonous sources of carbon to the sediment. As previously discussed this means the multitude of possible pathways of change cannot be disentangled. However, the stable values of $\delta^{13}C$ throughout the period of mixed contribution (<1‰) suggest no major changes in carbon source or cycling for this time period. Following tephra deposition C/N values under 10 indicate a mainly algal source for carbon at this time. This could be due to either a reduction in allochthonous carbon or an increase in autochthonous carbon. There is no change in $\delta^{13}C$ to discern between either option, as values are consistent around -28.5‰, where modern values from plant macrofossils and catchment vegetation overlap (shown in Figure 7.2(a)). Percent TOC values drop because of dilution from tephra deposition and thus cannot be used to identify an increase in productivity that could swing the balance between these two options. From the base of the core up until AD1991, C/N values decline gradually (from 15 to 12.5), again suggesting a gradual change in source carbon due to either a reduction

in allochthonous carbon or an increase in autochthonous carbon. Since this area was not cleared for ranching, this long-term trend cannot be related to clearance.

8.3.3.3 Changes in Carbon during Tephra Deposition

The Itrax data from both lakes identify two layers of likely tephra deposition in both lakes, characterised by spikes in Ca and Ti. Itrax analysis was performed on adjacent cores and the %TOC profiles for the analysed cores show reductions in organic content in the same stratigraphic positions. This 2-layer stratigraphy has also been observed in nearby Laguna La Pepa and Laguna Augusta (Langdon & Bishop, in prep.). The top layer is the AD1991 VEI=5 eruption of Cerro Hudson (Scasso *et al.*, 1994), which spread considerable volumes of tephra across Patagonia (Moxey, 2004) and the smaller eruption in AD1891 (Naranjo and Stern, 1998) also explains the lower layer of tephra (see Section 6.2). In both lake stratigraphies the fall in C/N and δ^{13}C indicate a change in the source of carbon following the eruption; in Laguna Edita lake productivity increases, and in Laguna Meche there is an increase in the proportion of autochthonous carbon in the sediment. There is evidence of nutrient increases following recent tephra events in Patagonia (Urrutia *et al.*, 2007) and elsewhere (Eastwood *et al.*, 2002), as well as changes in turbidity, pH, mineral concentrations and silica, all of which can affect algal productivity (ibid).

8.3.3.4 Comparison Between Tree-ring Inferred Temperatures and Carbon Stratigraphy

The key observations from these carbon geochemical data are a general, slow trend towards higher lake productivity in Laguna Edita, and at least the possibility of the same in Laguna Meche from *c.*AD1940 onwards, coupled with a hastening of the same changes following tephra deposition in AD1991. This is consistent with generally warmer temperatures observed in the instrumental and tree ring records at this time (see Figure 8.6) and of the decadal-scale effects of tephra on lake ecosystems, although the latter precludes this part of the core being interpreted palaeoclimatically as this masks any relationship with local climate.

8.4 Interpretation of Chironomid Stratigraphies

8.4.1 Laguna Edita

The fauna is generally profundal, with a minor but diverse littoral component, and the overall fauna is reflective of higher altitude sites (*e.g. Parapsectrocladius*), with warm stenotherms characteristic of mesotrophic conditions, suggesting no indication of a

fundamental reconfiguration of the lakes status in the recent past. The presence of black fly larvae (Simuliidae) indicates a small lotic input to the lake, in keeping with the low-level presence of other lotic taxa (*e.g. Eukiefferiella*, *Limnophyes* and *Parochlus*). Many of the minor taxa are associated with macrophytes, including *Apedilum*, *Dicrotendipes*, *Polypedilum*, *Cricotopus* & *Limnophyes*.

The base of this sequence has a less diverse fauna of generalists like nr.*Macropelopia*, *Ablabesmyia*, Tanytarsini and *Chironomus*. In the deeper EDI-1 core these taxa are present in higher abundance than this core, suggesting the possibility of deeper or colder conditions in the lake between AD1875–1895. Between AD1985–1930 there is a general increase in diversity, although this is most likely a function of increased total head capsule counts (from an average of 20 in Zone 1 to 62 in Zone 2). The decrease in *Chironomus* is suggestive of warmer or shallower conditions at this time. The increase in *Dicrotendipes*, associated with standing water and macrophytes indicates shallower conditions at this time. Between AD1930–1991 *Chironomus* increases to the levels seen in Zone 1 and *Dicrotendipes* suggesting lake levels and/or temperatures rose once more, but the presence of *Polypedilum* indicates increased macropyte abundance in this zone. Following tephra deposition, changes in the abundance of a number of taxa occur, probably as a response to tephra deposition.

8.4.1.1 Within Lake Consistency

The two cores from Laguna Edita offer an opportunity to compare the different faunas for the central study core and a more marginal, shallower coring location. This is important in understanding the ecology of chironomids in this study site because of the importance of littoral/profundal gradients in controlling chironomid faunas (see Section 5.6.2). Generally the faunas are similar, with the key taxa the same which suggests that the non-central coring locations used in the long cores are appropriate in capturing the general lake fauna. There is an expanded fauna of Orthocladiinae, many of which are associated with macrophytes and/or lotic environments, which is explained by the more marginal location of this core. Conversely, the central core has much higher quantities of *Chironomus*, which is adapted to low-oxygen conditions and thus has a competitive advantage in deeper water (Brodersen and Quinlan, 2006).

8.4.2 Laguna Meche

Almost all of the taxa are associated with vegetation and/or the littoral zone of lakes, specifically *Apedilum*, *Dicrotendipes*, *Parachironomus*, *Polypedilum*, *Guttipelopia*, *Cricotopus*, *Corynoneura*, *Limnophyes* and *Pseudosmittia*. Others are indicative of cooler and/or running water (*Thienemanniella*, *Parapsectrocladius* and *Parochlus*). It is clear that the southern basin of the lake has extensive littoral, vegetated areas and there is at least seasonal flow of cool water into this part of lake, probably from spring snowmelt.

The presence of Simuliidae larval head capsules in small quantities confirms the presence of flowing water to the lake.

The dominance of *Parakiefferiella* in Laguna Meche Zone 1 is constant throughout the sequence up until the peturbation by tephra deposition (Zone 2). This dominance does not affect the diversity in the lake, which is relatively high, but around 60% of the fauna is dominated by this morphotype; as such *Parakiefferiella* is very important in controlling the abundance of other taxa in a statistical sense — this is not necessarily true of the ecosystem. All of the described species of *Parakiefferiella* in South America were collected in relatively fast flowing streams, often at high altitudes (Wiedenbrug and Andersen, 2002), but globally *Parakiefferiella* is known to inhabit both running and standing water. In Fennoscandia, lake-dwelling *Parakiefferiella* are often found to be dominant in the shallower parts of oligotrophic lakes, possibly associated with macrophytes, although they are tolerant of a very wide range of trophic and sedimentary conditions (Tuiskunen, 1986); this fits with the situation at Laguna Meche. This tolerance of a variety of conditions may explain how the taxon has come to dominate for much of the sequence, but also means that this chironomid stratigraphy is relatively insensitive to ecological change.

8.4.3 Tephra Deposition and Chironomid Faunas

The most recent Hudson AD1991 eruption clearly effected change across both lake systems. In both Laguna Edita and Laguna Meche total carbon proportion was reduced to $<4\%$, indicating large quantities of tephra were deposited and/or concentrated in both lakes. The disappearance of *Ablabesmyia* from Laguna Edita at this time is similar to results from Lake Galletué (Urrutia *et al.*, 2007), where a similar decline occured during tephra loading events; they suggested that *Ablabesmyia* performs poorly in sediments with a high loading of tephra. *Parakiefferiella* populations are also known to respond badly to catchment burning disturbance events in Patagonia (Araneda *et al.*, 2013); this suggests the taxon is particularly sensitive to rapid-onset catchment disturbance events. This could be associated with changes in plant abundance and re-colonisation due to turbidity and/or nutrient input. The elimination of *Parakiefferiella* and sudden increase in Tanytarsini in Laguna Meche in recent times is co-incident with the tephra loading; the *Parakiefferiella* population reduces from 49% to 0% between the samples 3–4 and 2–3cm, so it seems likely that the tephra loading has some causal effect in the decline of *Parakiefferiella* and the increase in Tanytarsini.

8.4.4 Comparison with Published Palaeoclimatic Data

8.4.4.1 Transfer Function and Chironomid Stratigraphy

Because tree-ring inferred temperatures (Villalba *et al.*, 2003) are available for the period these cores cover, a comparison of chironomid and tree-ring inferred temperatures allows for an assessment of the utility of the chironomid inferred reconstructions. There is no need to further compare the chironomid data to instrumental records as the tree-ring inferred temperatures are tuned to, and thus strongly correlated with, the best available instrumental temperature records for the region. Tree-ring records are preferred because they extend far beyond the short and discontinuous instrumental records presented in Section 3.4.

The key recent climate changes outlined in Section 3.4 are a general warming trend from AD1950–1990 and significant short-term changes around AD1976. When the best available climate data (from both models and tree-rings) are aggregated at the same time intervals as the Laguna Edita chironomid data there is no significant correlation (see Figure 8.4 and Table 7.2). There is a significant correlation between the Laguna Meche data and the tree-ring data, but the CI-MAT from Laguna Meche are compromised due to the extreme response of *Parakiefferiella* to tephra deposition, probably because of the change in substrate.

However, in Laguna Edita chironomids may reflect the major recent warming trend described previously — that is, there is warming trend from AD1970–1995 that is comparable, given sampling uncertainties, to the AD1960–1990 warming trend observed locally. In addition, peak temperatures around AD2000 observed in a number of local climate records are reflected in peak chironomid inferred temperatures at this time. For the Laguna Edita record at least the ability to discern such small temperature variations ($<$1.5°C) is an indicator of the sensitivity of chironomids at this site, however the statistics in Table 7.2 should be considered indicative of the general failure of the temperature transfer function.

8.4.5 Implications for the Interpretation of Long Core Chironomid Stratigraphies

The transfer function fails to reflect the expected temperature difference between the two lakes (the lower lake has lower inferred temperatures than the higher lake in altitude, probably due to the importance of *Parakiefferiella* in Laguna Meche), and the unrealistically high range of temperature change in both reconstructions means that the reconstructions are at best presented as standarized values and interpreted as indicative of direction of change only. The temperature transfer functions offer little more utility than the ordination. The transfer function encompasses all of the taxa present in the short core data, so should be generally applicable to these data, but the failure to

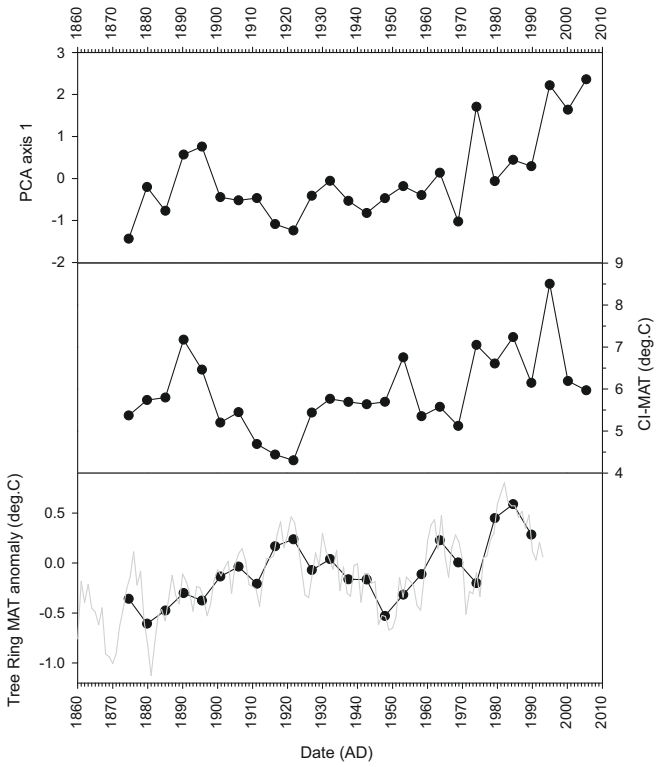

FIGURE 8.4: Laguna Edita short core PCA, chironomid-inferred mean annual temperature and (Villalba *et al.*, 2003) reconstructions. The PCA has an eigenvalue of 0.22. There is no significant correlation between PCA axes and the tree rings.

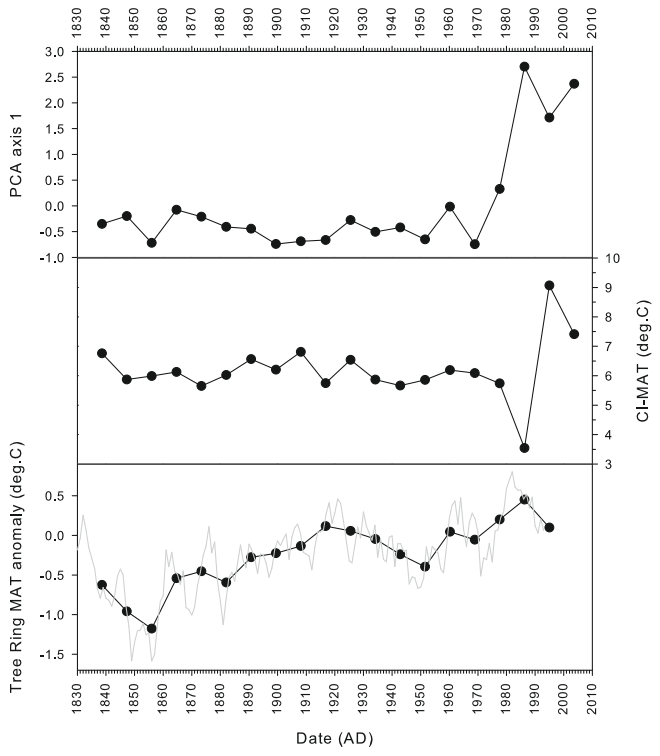

FIGURE 8.5: Laguna Meche short core PCA, chironomid-inferred mean annual temperature and (Villalba *et al.*, 2003) reconstructions. The PCA has an eigenvalue of 0.22. There is a significant correlation between PCA Axis 2 scores and the tree rings ($\rho = -0.48$).

correctly represent the temperature difference between the sites is probably due to the influence of *Parakiefferiella* in Laguna Meche (see also Section 5.6.5). The transfer function performance statistics are comparable to other successful and widely-applied studies (see Section 5.6.5).

The poor results may be in part because the magnitude of temperature change over the last 150 years is less than the errors in the model, but this does not explain why the model fails to reflect the altitudinal differences between the lakes. It may also be due to the primary control on chironomid communities being something other than temperature — as discussed in Section 5.6.2, lake depth and its co-variables precipitation and associated changes in lake chemistry are the most likely possibility, but the small range of precipitation variability over the length of these cores precludes a conclusion from the data presented in this chapter. Alternatively, the problem may lie in generalist fauna of these lakes; the average standard deviation of an individual taxon from its optima is 4.9°C, showing many of the taxa are eurythermic.

Although the development of chironomid transfer functions for Patagonia is at an early stage, these problems may be due to the generally eurythermic tolerances of taxa in the region due to the regional bio-geography; this could limit the utility of chironomid transfer functions in the region (Section 5.6.1 discusses this in more detail). The evolutionary and biogeographical history of the Patagonian chironomid fauna tends to follow two main ideas: the first proposes that much of the fauna is shared with North America via migration through the Andes, the second reasoning that the fauna is a relict of that of the (warmer than present) Gondwanan palaeo-supercontinent (Saether and Ekrem, 2003; Jong *et al.*, 2007). The two are not mutually exclusive, but have important and distinct implications for the kind of fauna that is present in present-day Patagonia. For example, recent taxonomic and phylogentic work across South America, Australia and New Zealand is making clear that at least amongst certain sub-families much of the fauna is shared, split geographically only by the break-up of the supercontinent, *e.g.* *Botryocladius* and *Riethia*, a large genus common to Patagonia and Australia (Krosch *et al.*, 2011; Cranston *et al.*, 2010). However, a large number of taxa are morphologically similar to those recorded in North America and Europe; this could reflect either a global distribution of these taxa (*e.g.* *Chironomus*), or exchange of species to/from North America. This migratory route is only open to those taxa that can withstand migration through environments warmer than those generally encountered in Patagonia.

Although migration through the Andes is possible, the number of natural barriers to migration is high. It is of note that of the taxa exclusive to the Gondwanan-derived continents, those seen in the Andes but not in North America are often cold stenotherms (*e.g.* *Bryophaenocladius* & *Apedilum*) suggesting that migration of cold-stenotherms through the Andean chain has not occured. These biogeographical theories would both have the effect of limiting the number of chironomid species that are cold stenotherms in South America; the limited number of taxa in this niche and the wide temperature tolerances for taxa with warm optima indicate that these factors may exert a

fundamental control on the fauna that affects the efficacy and accuracy of chironomid-inferred palaeotemperature reconstructions.

The data from Laguna Meche show that where large volcanic events occur there can be complete re-organisations of the chironomid fauna, characterised in both lakes by an increase in Tanytarsini, and in Laguna Meche by a decimation of *Parakiefferiella*. As such chironomid proxies of climate may be unreliable surrounding large volcanic ash deposition events.

8.5 Conclusions

The aim of studying the short cores from Laguna Edita and Laguna Meche was to understand the present day catchments and environments and recent palaeoecology in order to inform the interpretation of long core data from the same lakes.

In addition the chironomid stratigraphies were presented and the existing transfer function for the region was subjected to a test against recent palaeoclimate data. Although the interpretation and to some extent the ordination reflects recent climatic trends, the temperature transfer function failed to produce reasonable temperature reconstructions, reflect the temperature difference between the two sites or produce temperature reconstructions that agree with proximal tree-ring inferred palaeo-temperatures.

In summary, the key conclusions from Chapters 7 and 8 with regard to the recent palaeoclimatic history of the valley are summarised in Figure 8.6. With regard to the interpretation of the long core data that will presented in Chapters 9 and 10, the following key conclusions should be considered:

- The temperature inference model of Massaferro and Larocque-Tobler (2013) fails to perform for these short cores and as such is likely to be of limited utility in earlier Holocene reconstructions. However the potential for recent anthropogenic change and the low magnitude of change in these data means that the models may be of some utility for longer time-scales, and as such it is prudent to present the results with a very cautious interpretation and application.
- Carbon isotope, C/N and chironomid data provide information on within-lake processes and conditions in the recent past.
- The C/N and $\delta^{13}C$ have different associations with climate between Laguna Edita and Laguna Meche, depending on their source carbon as elucidated by the modern water isotope data presented in Section 8.2.
- Ti and Ca are the most consistent and reliable of the XRF markers for tephra deposition in these lakes.

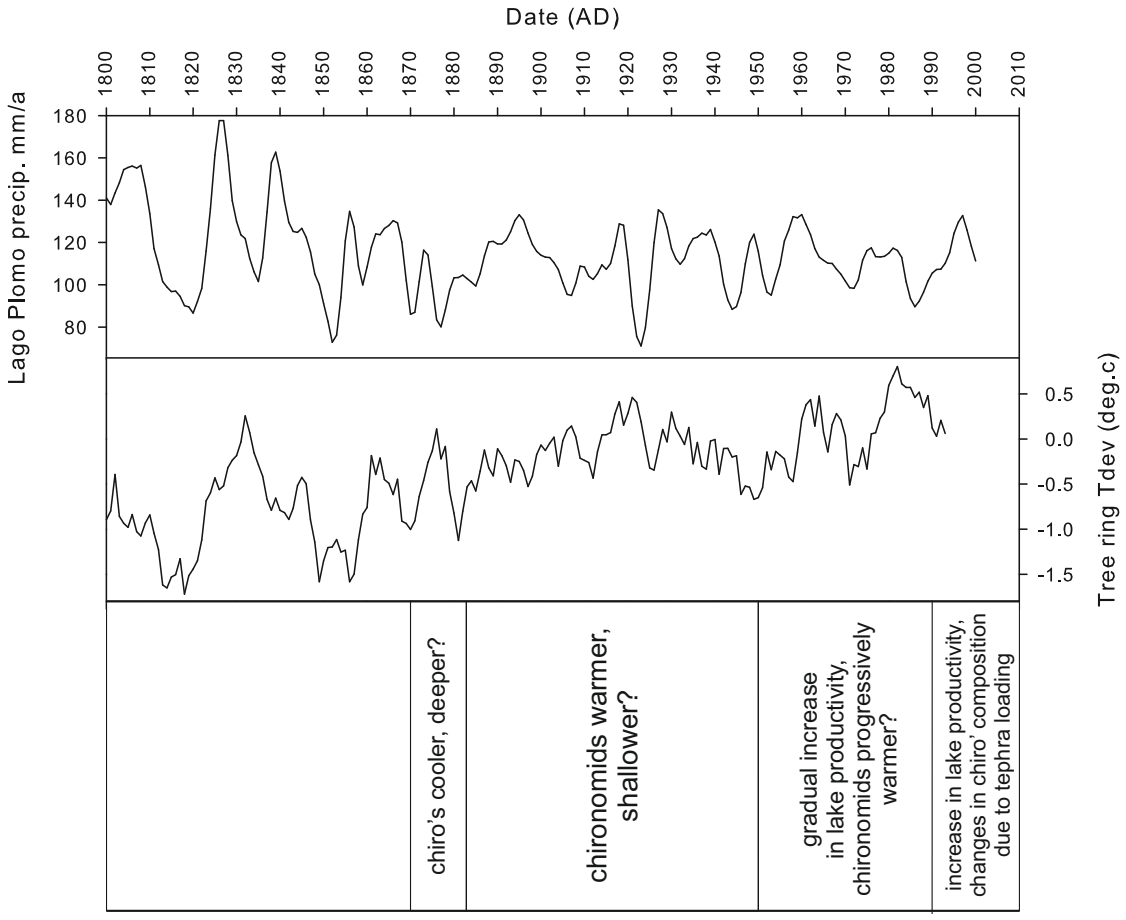

FIGURE 8.6: Recent climate records for the Chacabuco Valley overlaid with a summary of the palaeoclimatic interpretation of short core data.

Chapter 9

Laguna Edita Long Core Results & Proxy Interpretation

9.1 Introduction

This chapter presents the the results for the proxy data for Laguna Edita (magnetic susceptability, total organic content, C/N ratio, δ^{13}C, and chironomids), followed by an interpretation of these data for this lake in a palaeoenvironmental context. The stratigraphic record covers the entire Holocene, and the palaeolimnological proxy data cover the period from around 7,500 years B.P. onwards. The interpretation section discusses the early-Holocene stabilisation of the lake, including the effects of large tephra deposition events on the biostratigraphy. The evidence for a mid-Holocene stabilisation is discussed, and some minor late-Holocene environmental change (2,000 years B.P. onwards) is also identified. Chironomid-inferred temperatures are presented, notwithstanding the caveats elucidated in Section 8.4.5.

9.2 Results

9.2.1 Stratigraphy

An overlapping sequence of lake sediment cores that has a composite depth of 578cm below the sediment/water interface was extracted (the overlapping sequence is shown in Figure 6.13) and dated using radiocarbon and tephrochronology (as per Section 6.3). The sediment is predominately dark brown gyttja, with basal clay and two distinct layers of volcanic ash near the base of the sequence (H1 and an unidentified event described in Section 6.3.3.3). There are few variations in sediment character following the unidentified tephra event at 8,019 years B.P. The average accumulation rate is 0.64mm/year, comparable to other Patagonian lakes (see Section 6.3).

9.2.2 Magnetic Susceptability

Magnetic susceptability measurements at both high and low frequencies were obtained at contiguous 1cm intervals for all retrieved material including overlaps are are shown in Figure 9.2. The highest magnetic susceptability values are found in units of bulk tephra H1 and tephra S5, both of which are high in FeO, with noteably high MnO and TiO components according to scanning (Figure 9.1) and bulk XRF data (see Appendix C).

9.2.3 Organics

Loss-on-ignition measurements (%LOI) calibrated against %TOC were obtained at contiguous 1cm intervals (including overlaps), and δ^{13}C, total organic C (%TOC) and total N measurements totalled 126, spaced evenly through the sequence, giving a sampling resolution of 8cm; these are shown in Figure 9.3.

Prior to 8,300 years B.P. %TOC and δ^{13}C values show considerably lower values from the otherwise relatively stable values from around 7,800 years B.P. onwards. At this early stage of the lake the depleted δ^{13}C values (as low as -33‰) occur concomitantly with generally low %TOC. For the remainder of the sequence, from 7,800 years B.P. to present, δ^{13}C values stabilise at around -29.5‰ and at an average C/N ratio of 12. Ratios of C/N are variable throughout the sequence, between 10–14, although the variability declines and a general lowering trend is seen from around 4,000 years B.P. onwards. This zonation can be summarised as follows:

Carbon Zone 1 9,200–8,200 years B.P.: The δ^{13}C is variable throughout the zone, oscillating between -33 to -29.5‰. The basal part of the zone has low C/N and %TOC which rises rapidly at 8,300 years B.P. to a peak value of 25% TOC at the top of the zone.

Carbon Zone 2 8,200–500 years B.P.: TOC and δ^{13}C are stable around 14% and -29‰ respectively. C/N is highly variable, with a range of 10–14, until 4,000 years B.P., where values stabilise and decline gradually until 2,000 years B.P. to values of 10; values of %TOC and C/N subsequently increase slightly towards the top of the sequence.

9.2.4 Chironomid Analysis

9.2.4.1 Chironomid Stratigraphy

A total of 78 samples for chironomid analysis were prepared, with 69 samples having $\geq$40 head capsules and thus being suitable for inclusion in ordination and transfer function

analysis (Quinlan and Smol 2001, see also Section 5.6.4). Samples were spaced approximately 8cm apart, giving an approximate resolution of *c.*300 years between samples. The fauna can be broadly split into 3 zones (see Figure 9.5):

Chironomid Zone 1 8,400–8,000 years B.P.: This zone is characterised by low concentrations of head capsules. Undifferentiated Orthocladiinae dominate; these taxa are difficult to identify due to the poor state of preservation, and the majority of undifferentiated Orthocladiinae in this zone presented as half head capsules that had curled inward, preventing definative diagnosis; however, this presentation is in common in *Cricotopus*. *Labrundinia* also has maximum abundance (14%) in this zone.

Chironomid Zone 2 8,000–4,200 years B.P.: The dominant taxa in Zone 2 are Tanytarsini, *Ablabesmyia*, nr.*Macropelopia* with minor components of *Dicrotendipes*, Orthocladiinae and *Chironomus*. *Polypedilum* and *Rhiethia* maintain a constant low-level presence and a number of minor taxa appear intermittently. In the dominant taxa there is high variability between samples around a long term mean of 30%, with changes of over 30% and back within a few hundred years.

Chironomid Zone 3 4,200–700 years B.P.: There is a subtle change between Zones 2 and 3; the composition of the fauna remains the same, but the inter-sample variability in the data is greatly reduced. In addition, there is a long-term trend throughout the zone towards lower concentrations of head capsules.

9.2.4.2 Ordination Analyses of Chironomids & Temperature Transfer Function

A preliminary detrended correspondence analysis (DCA) yielded an eigenvalue for the first axis of <0.2, indicating that the data is best treated as linear (Dytham, 2011; Braak and Smilauer, 1998; Lepš and Šmilauer, 1999; Hammer, 2010). Presented in Figure 9.6 are the results of a principle components analysis (PCA). The relationship between the first and second axes changes phase through time: from 7,600–5,000 years B.P. the phase relationship is "positive", but from 5,000 years B.P. onwards, this relationship is reversed. A similar reversal is also present prior to 8,000 years B.P.

The temperature transfer function described in Section 5.6.5 was applied to the down-core assemblage data and the results are shown in Figure 9.7.

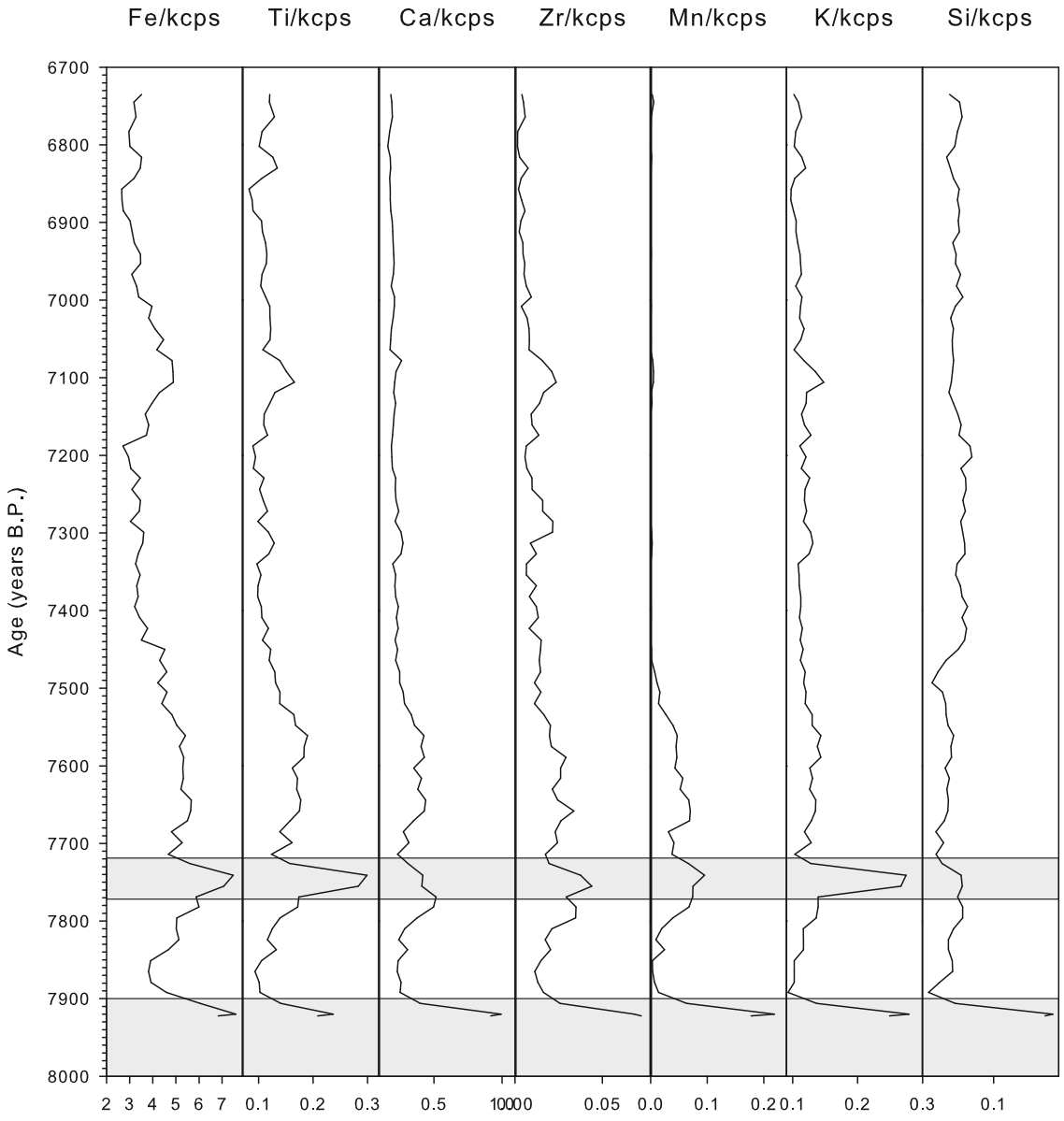

FIGURE 9.1: Itrax data from Laguna Edita, showing selected elements divided by count rate. The tephra layers are shown in grey.

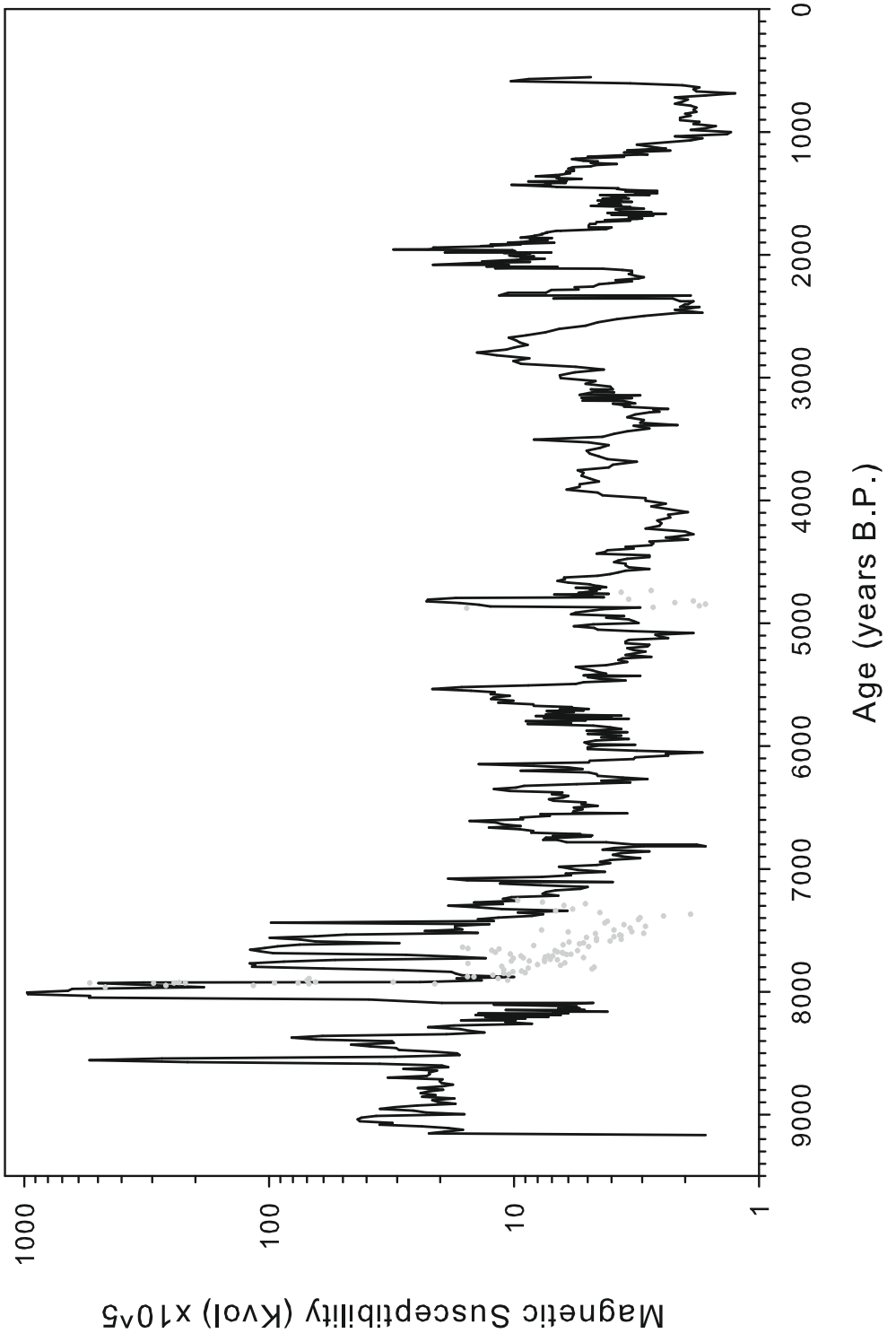

FIGURE 9.2: Volume magnetic susceptability values for Laguna Edita, shown without smoothing but with some data (shown as grey dots) removed. Note the log scale.

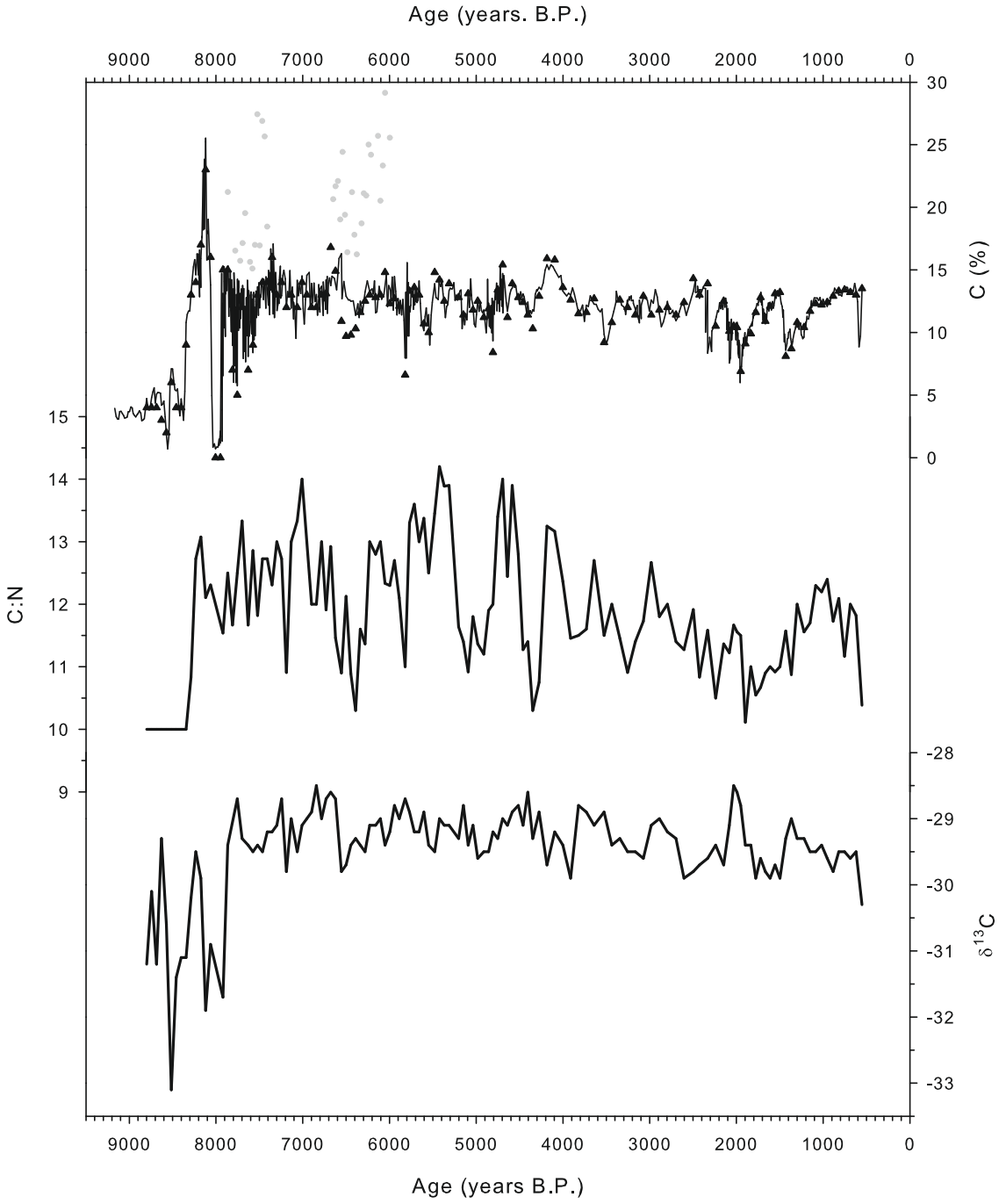

FIGURE 9.3: C:N, C(%) and δ^{13}C values for Laguna Edita. For the graph showing C(%) the triangles represent results obtained using an elemental analyser, and grey circles represent loss-on-ignition points excluded.

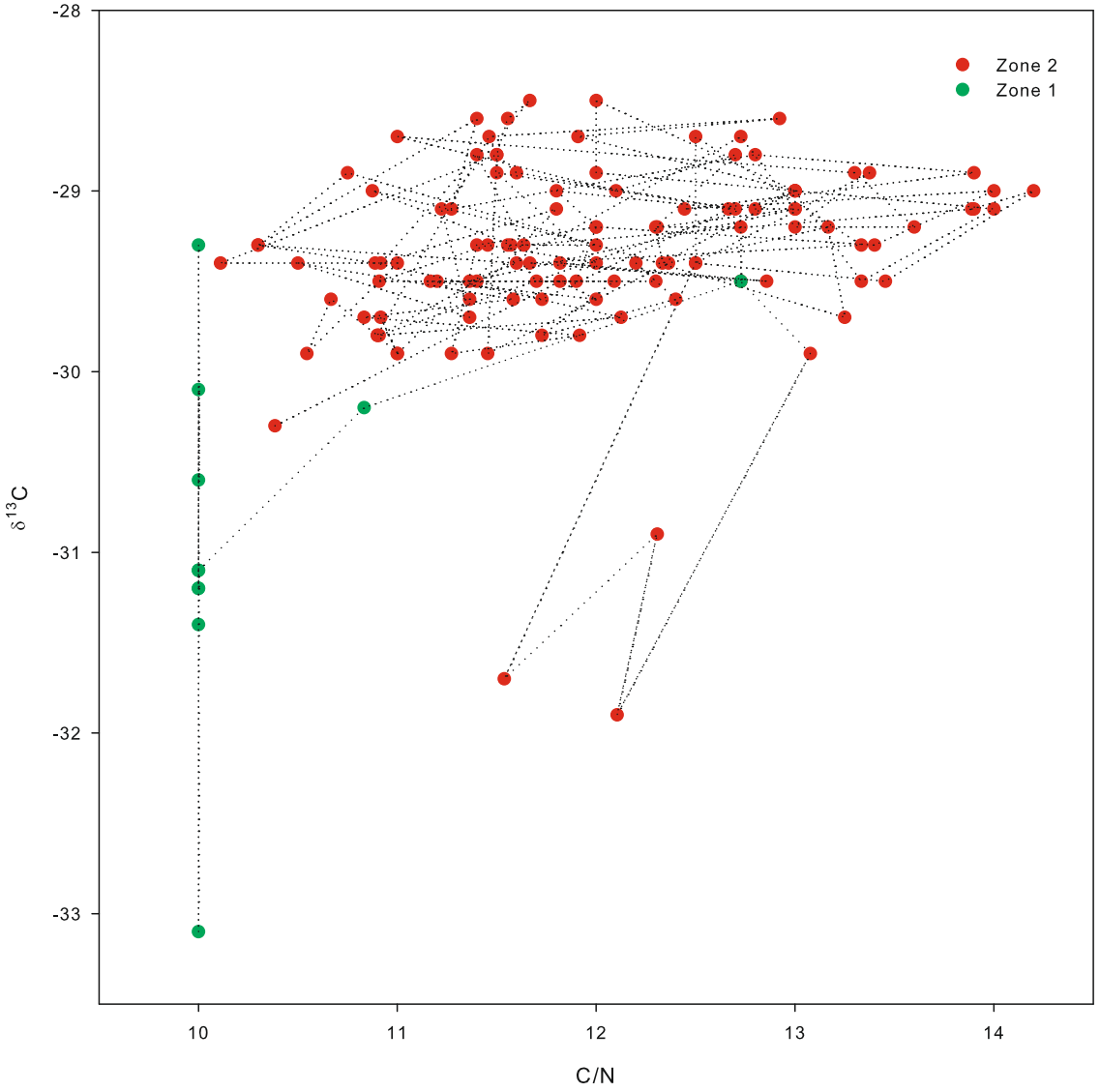

FIGURE 9.4: C:N, and δ^{13}C values for Laguna Edita. Zones are shown in different colours (see legend) and the dotted line joins adjacent samples.

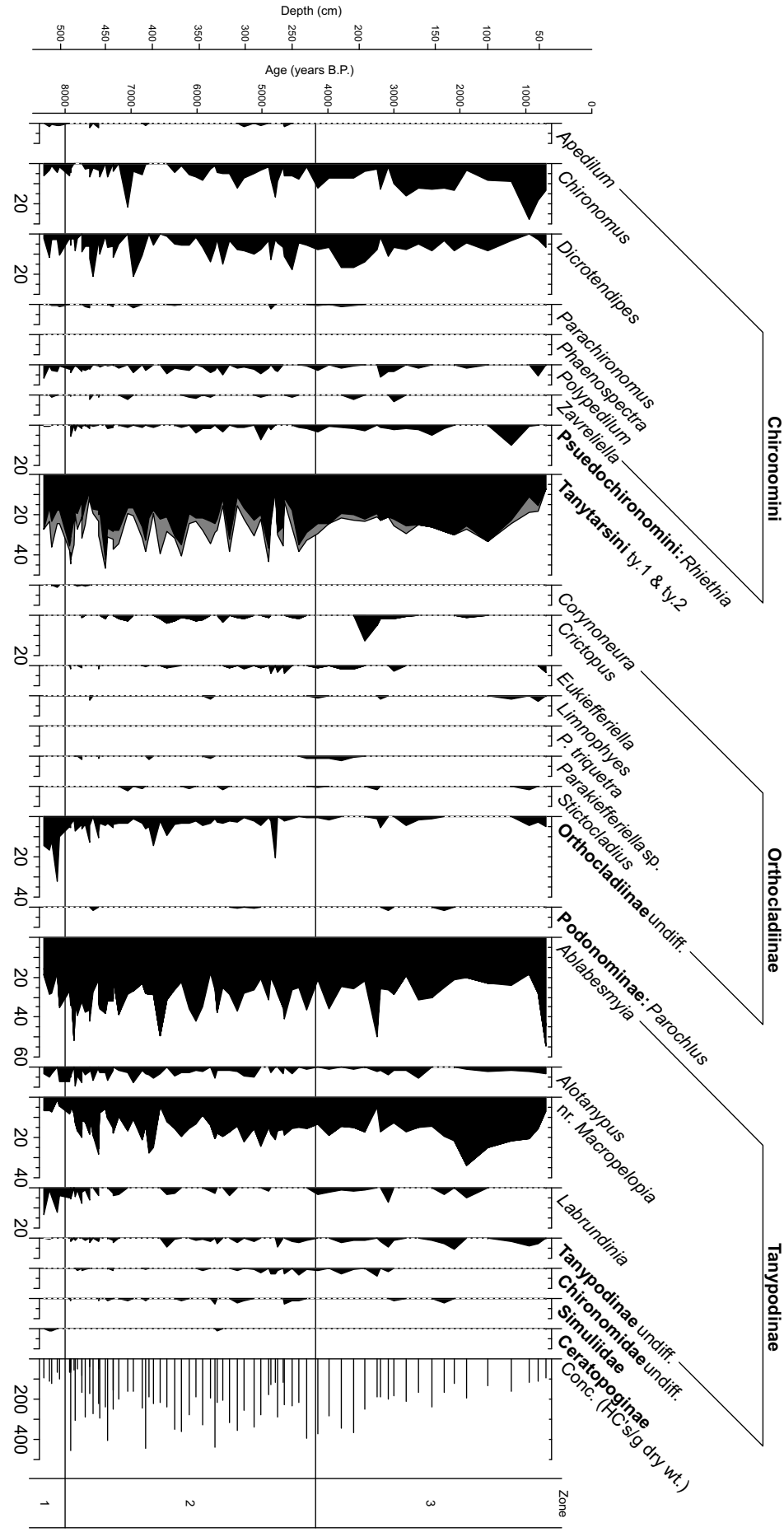

FIGURE 9.5: Chironomid diagram for Laguna Edita, showing the percentage abundance of all taxa. Non-chironomid taxa (Ceratopoginae and Simulidae) are shown as percentages of the sum of the chironomidae. Zones refer to those described in Section 9.2.4.1.

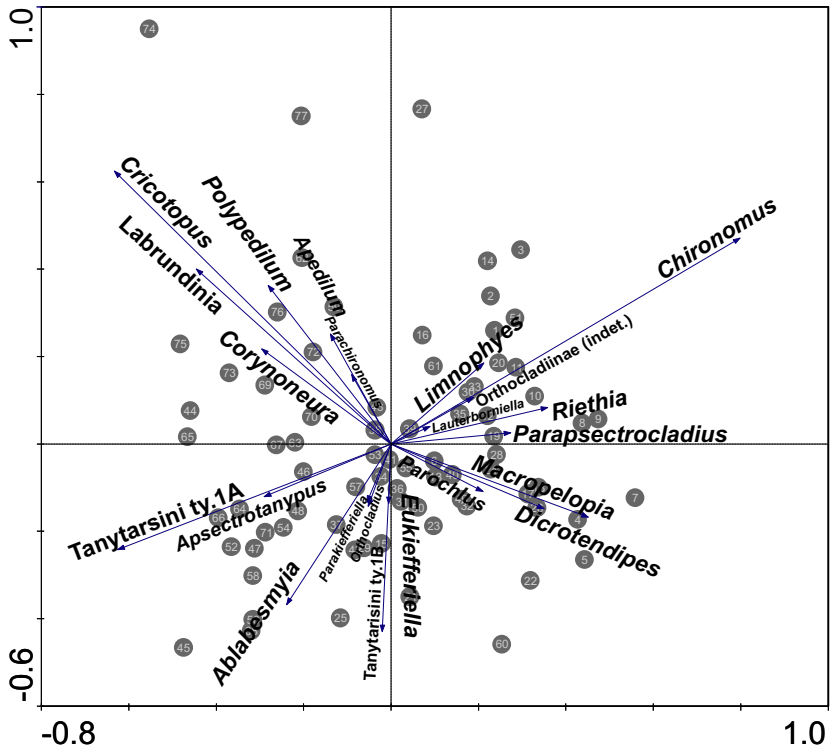

(a) Species and sample scores for axes 1 & 2.

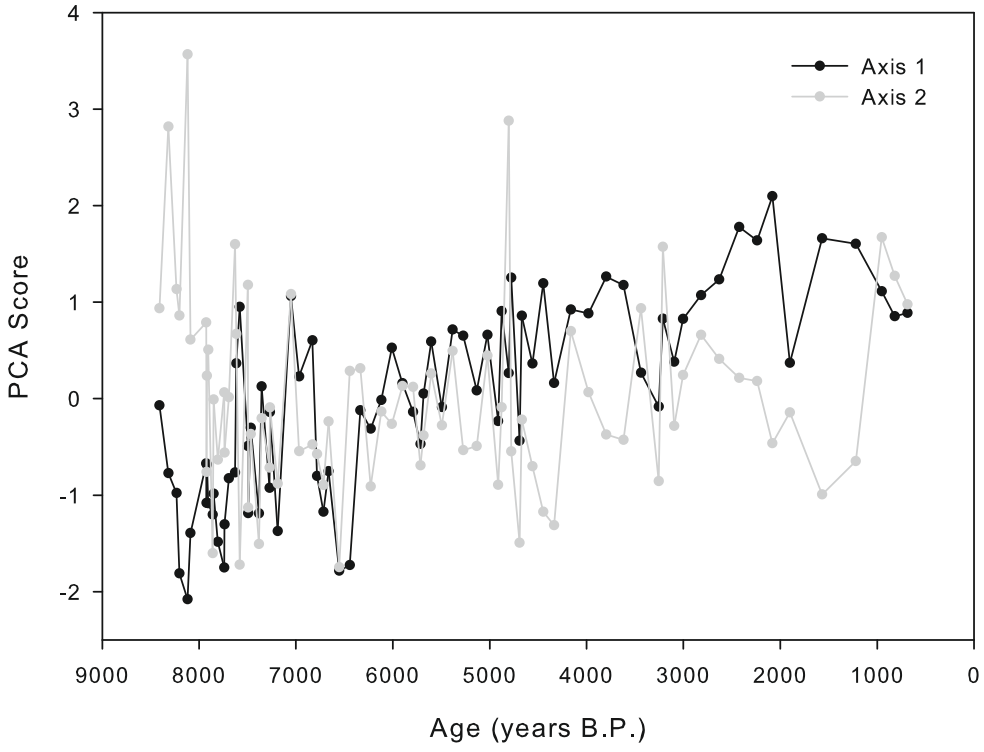

(b) Sample scores for axes 1 & 2.

FIGURE 9.6: Principle component analysis scores for Laguna Edita long core. Calculated using Canoco v.4, using scaling focussed on inter-species correlations, species scores are expressed divided by their standard deviation. Species data were square-root transformed and centred by normalization. The eigenvalues for axis 1 and 2 were 0.23 and 0.12 respectively.

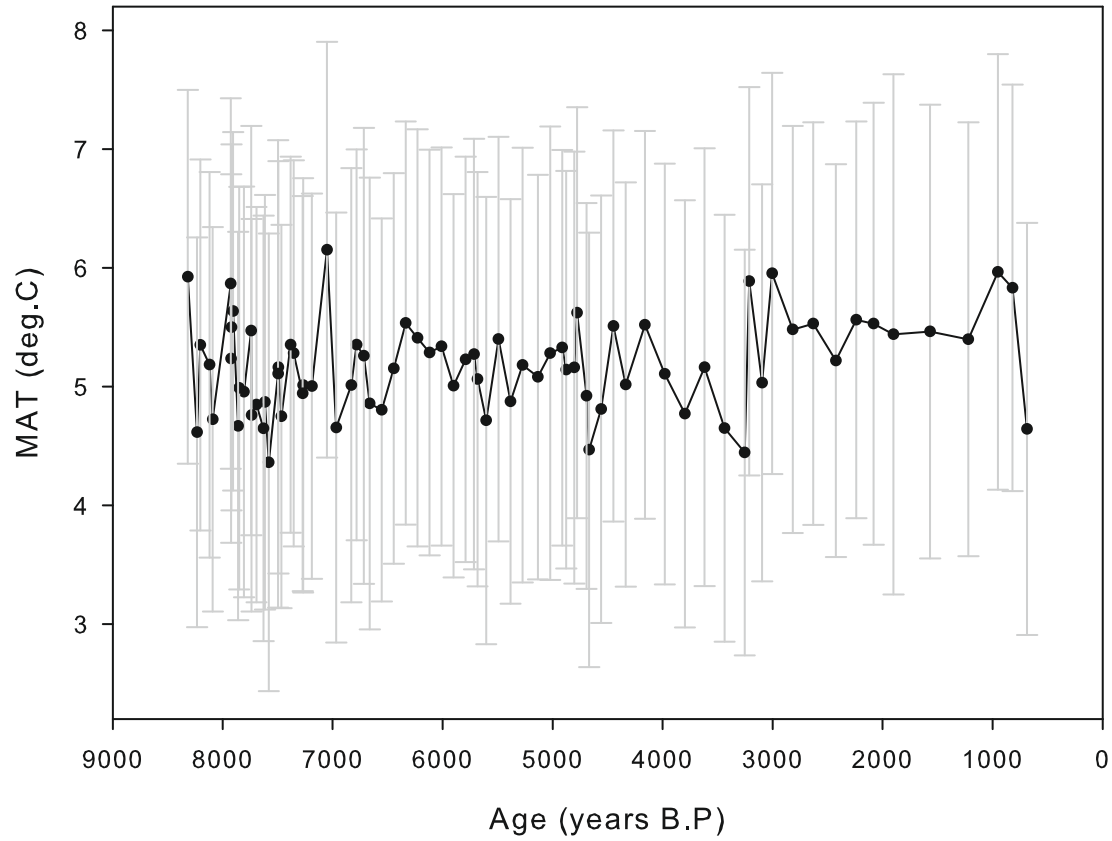

(a) CI-MAT transfer function results, showing bootstrapped estimated standard errors of prediction (SEP's).

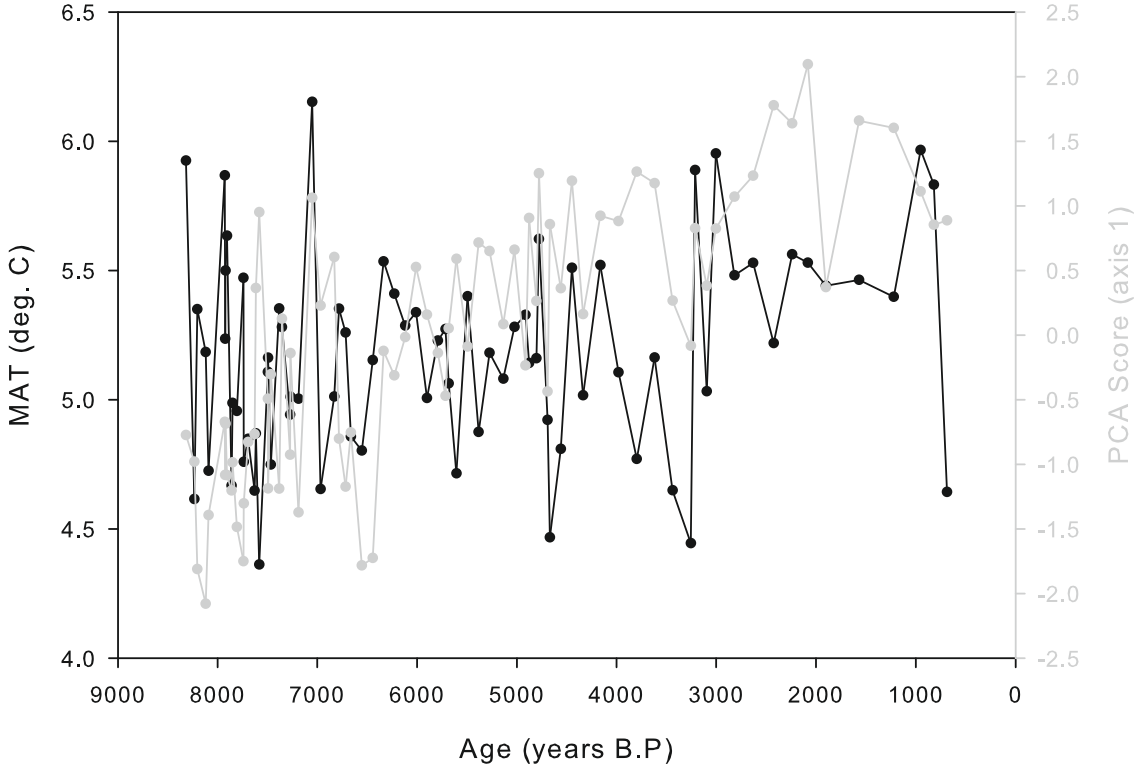

(b) CI-MAT plotted alongside PCA axis 1 scores as shown in Figure 9.6.

FIGURE 9.7: Chironomid inferred mean annual temperature transfer function results for Laguna Edita long core.

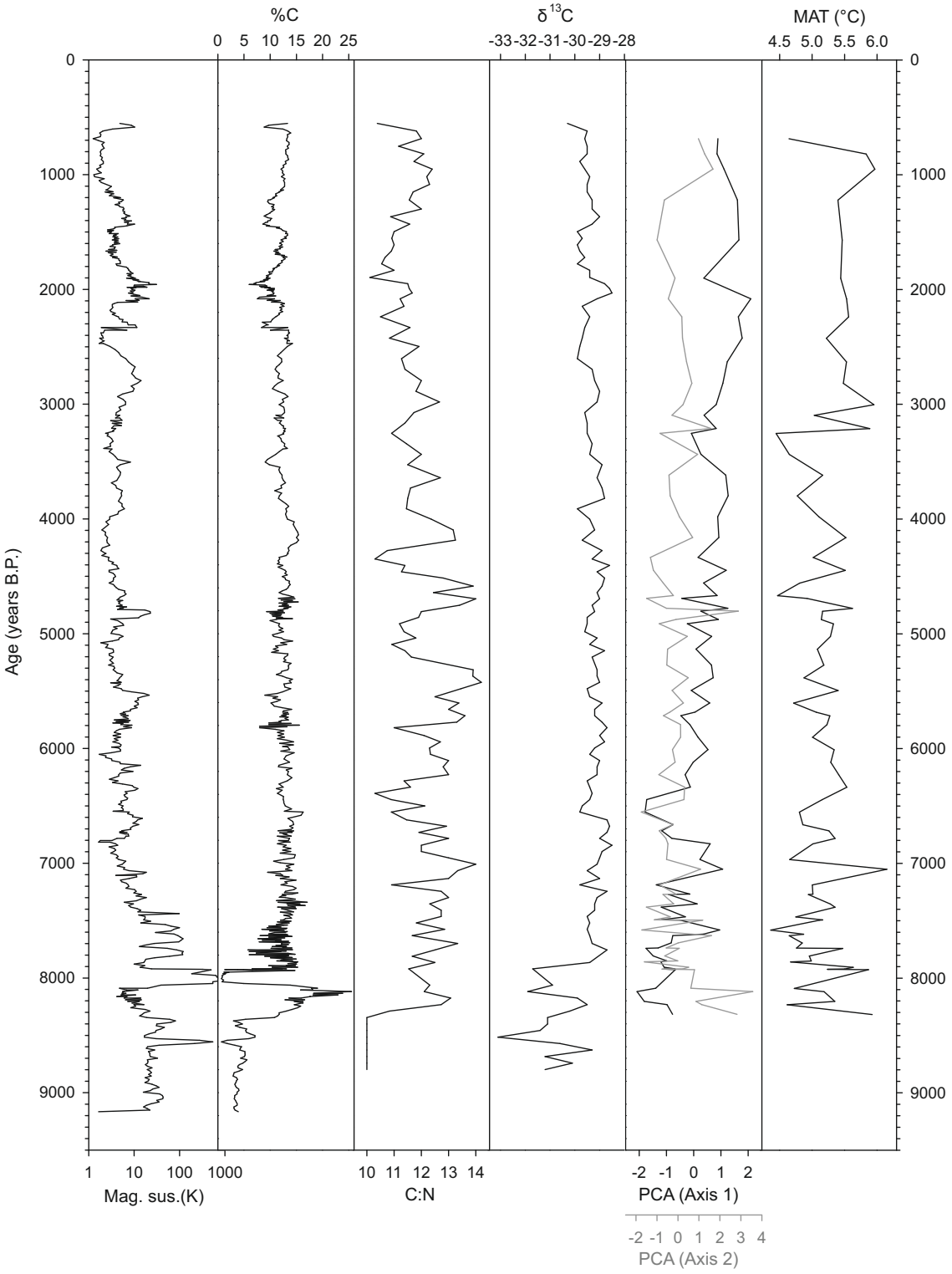

FIGURE 9.8: Summary of available data for Laguna Edita long core, showing magnetic susceptability, organic carbon content, C/N, δ^{13}C, chironomid PCA scores and chironomid-inferred mean annual temperatures.

9.3 Interpretation

9.3.1 Overview

Following early Holocene lake and catchment development and stabilisation, Laguna Edita does not undergo any fundamental changes in configuration. In general the lake appears to be mesotrophic, with relatively shallow (<10m) standing water and a predominantly algal autogenic source of carbon; catchment inputs are low. However, between 4,200–8,000 years B.P. the composition of the chironomid fauna is unstable, suggesting some internal or external forcing that causes rapid oscillations. The interpretations that follow in this section are summarised in Figure 9.9.

The C/N of the entire sequence falls within a range of 10–14.5, a narrow range of low values suggesting a relatively minor contribution from (semi)terrestrial vegetation; C/N of <11 in lake sediments can be considered indicative of a predominately algal source of carbon (Meyers and Teranes, 2001; Leng *et al.*, 2006). In this respect the source carbon is the same as for the short core from Laguna Edita (Section 8.3.3.1). The C/N data follow broadly the outline of the proportion of organic carbon (%TOC), indicating these small changes in carbon source are probably related to variation in productivity rather than sediment source (Leng *et al.*, 2006).

9.3.2 Early Catchment & Lake Development

The basal clays are characteristic of deglacial sedimentation and are common in Late-glacial sediments in this region; the gradual grading from blue-grey clays, largely devoid of organic remains, to organic gyttja is characteristic of basal sediments in the region (*e.g.* Villa-Martínez *et al.*, 2012; Massaferro and Brooks, 2002; Massaferro *et al.*, 2005; Tonello *et al.*, 2009) and interpreted as characteristic of post-glacial catchment development and stabilisation of glacial clay substrates (Hein *et al.*, 2010).

The sources of magnetically susceptible elements to the lake are weathered bedrock material (Dearing, 1999), transported either by aeolian (Bidegain and Rico, 2012) or pluvial mechanisms (Janbu *et al.*, 2011), volcanic ash (Haberle, 1998), deposited either by way of direct atmospheric deposition, or reworking of fallout previously deposited in the catchment, or a composite of fallout and weathered bedrock in soils eroded to the lake.

The very high values of magnetic susceptability at the bottom of the sequence in the clays are likely due to the high input of detrital weathered bedrock material; this is common in lake cores where the basal sediments date to the early Holocene (*e.g.* Gonzalez-Carranza *et al.*, 2012; Seltzer *et al.*, 2000; Araneda *et al.*, 2013; Iglesias *et al.*, 2014) and is indicative of poorly developed soils, sparse vegetation cover and high allochthonous inorganic inputs (Sandgren and Snowball, 2001). The values are also high because of the increased density of this material — values given are volume specific.

High values of magnetic susceptability further indicate the importance of catchment-derived minerogenic input to the lake at this early stage, and the inverse relationship between magnetic susceptability and %TOC prior the H1 tephra suggests both proxies are indicators of the balance of allochthonous and autochthonous inputs to the lake (Dearing, 1999). Initially low values of δ^{13}C and C/N in the early stages of the lake indicates an almost completely algal source of carbon to the sediment, but following the increase in %TOC the mix changes to a dominant phytoplankton source prior to the H1 tephra deposition (Leng, 2004). The absence of chironomid head capsules in these clays is indicative of very low productivity at this time (Schmidt *et al.*, 2011; Holmes *et al.*, 2008).

The gradual increase (decrease) of %TOC (magnetic susceptability) between 8,400–8,100 years B.P. is due to stabilisation of the catchment, and thus a reduction in the supply of glacially reworked material, and generally higher productivity in the catchment and lake (*c.f.* de Porras *et al.*, 2012; Villa-Martínez *et al.*, 2012; Bennett *et al.*, 2000). Higher C/N (from 10 to *c.*13) indicates the carbon source becomes slightly more mixed, although still dominated by phytoplankton, and δ^{13}C becomes less depleted, reflecting a change in carbon source and relatively low productivity at this time (see Section 8.3.2). Relatively low concentrations of chironomid head capsules in the basal gyttja part of the sequence is in keeping with this interpretation.

The undifferentiated Orthocladiinae that dominate this part of the chironomid stratigraphy are mainly composed of half-head capsules split along the medial suture that have curled and as such are impossible to positively identify, but this is characteristic of many of the *Cricotopus* specimens in this sequence. For clarity, these are marked as undifferentiated Orthocladiinae in Figure 9.5, but in this interpretation are tentatively treated as *Cricotopus*. As *Cricotopus* are commonly associated with algae, this supports the interpretation of the C/N and δ^{13}C data of a lake where algae were dominant, but as it includes scrapers, the taxon is also associated with macrophytes (Brodersen *et al.*, 2001). The presence of *Labrundinia* at double the proportion than in the rest of the core is noteworthy as there are indications from other lakes in Patagonia that *Labrundinia* is an indicator of shallow water (Massaferro and Brooks, 2002; Verschuren and Eggermont, 2006), an interpretation consistent with ecological data from the Palaearctic (Millet *et al.*, 2007; Engels *et al.*, 2012). These data combined suggest an initially mostly sterile depositional environment composed mainly of re-worked glacial material until 8,400 years B.P., when there is a stabilisation of the catchment and a general increase in productivity, and the lake is dominanted by algal rather than macrophyte or allochthonous sources of carbon.

More depleted values of δ^{13}C at the base of the sequence, (8,400–8,000 years B.P.), including the lowest values in the sequence could reflect either a different macrophyte vegetation at this time, or isotopic depletion due to recycling of inorganic carbon by phytoplankton (see Section 8.3.2). The lowest C/N values (10), before the start of organic sedimentation indicate lake organic carbon was almost completely algal and thus

the very low δ^{13}C values are reflective of increased cycling of carbon in the lake, possibly due to more anoxic conditions; this could be caused by either extended seasonal ice-cover or summer stratification in ultra-oligotrophic lakes (Wetzel, 2001, ch.9). The more regular interpretation of lower δ^{13}C as a result of increased phytoplankton productivity at this time (*e.g.* Wooller *et al.*, 2007; Leng, 2004) is not supported by the %TOC data, which might be expected to increase if this were the case (Thevenon *et al.*, 2012).

9.3.3 Large Tephra Deposition Events

Two large tephra events in close sucession, one of which has been identified as the H1 tephra (Section 6.3.3.3) punctuate the lower part of the record at 8,000 years B.P. These layers exhibit very high values of K_{HF} due to both the large magnetically susceptible component of volcanic ash and the density of the material — this is also true of the smaller tephra layer just above this and is in keeping with evidence elsewhere in Patagonia of large eruptions having high K_{HF} (Charlet *et al.*, 2007; Guilizzoni *et al.*, 2009; Arnaud *et al.*, 2006).

Peak values of %TOC at 8,100 years B.P., following the H1 tephra layer could be caused by large terrestrial input of organic matter to the lake caused by widespread death of terrestrial plants following the H1 eruption of Mt. Hudson — values above 20% are not observed anywhere else in the sequence. The catastrophic effects of the H1 eruption are alluded to by Prieto *et al.* (2013) in the context of human cultural changes at this time, and the effects of large eruptions on vegetation in the region are well documented (Kilian *et al.*, 2006). This is supported by the decrease in δ^{13}C values by around 2‰ during these large tephra loading events; the modern plant δ^{13}C values for the area presented in Section 8.3.1 demonstrate that lower δ^{13}C values are found in terrestrial plants, compared with aquatic plants (see also Mayr *et al.*, 2008, Table 2). The possibility that tephra deposition acts as a fertiliser for authochthonous algal growth, as proposed by Urrutia *et al.* (2007), is less likely given the contemporaneous increase in C/N and the previously reported changes in δ^{13}C that conflict with this interpretation.

9.3.4 Early-Holocene Stabilisation

Following the unidentified eruption dated to between 7,868–8,169 years B.P., organic sedimentation re-establishes immediately, although Itrax data indicate that elevated metals (Ti, Fe, Mn) and Ca persist for 2–300 years following deposition; this is consistent with magnetic susceptability data. However, in general the organic gyttja has a considerably lower susceptability, indicative of a relatively low input of catchment derived minerogenic material to the lake sediment (*c.f.* Iglesias *et al.*, 2014). The dominance of autogenic material over catchment sources is further supported by the negligible difference between K_{HF} and K_{LF} (the frequency-dependency, or χ_{FD}). High values of χ_{FD} are indicative of a soil-derived allogenic source (Dearing, 1999; Hatfield

and Maher, 2009). Smaller variations in K_{HF} could be due to variations in flux of catchment derived material, or due to supraregional volcanic activity. Without control for either of these factors (*e.g.* tephra shard counts) it is impossible to differentiate between these possible causes, but the frequency of these changes can hint at the causal processes: low frequency increases or decreases are unlikely to be as a result of volcanic activity, which is usually short lived, and so are likely to be caused by variations in the flux of catchment derived material, and *vice versa*.

The transition from Zone 1 to Zone 2 occurs at the point of tephra deposition, where undifferentiated Orthocladiinae (probably *Cricotopus*) begin to decline alongside *Labrundinia*, and *Rhiethia* first appear and persist, alongside the first appearances of a number of other taxa. The generalist fauna makes qualitative interpretation of these relatively minor changes difficult, but the reduction in *Labrundinia* suggests warmer conditions. The abundance of generalist taxa such as Tanytarsini, *Ablabesmyia*, nr.*Macropelopia*, *Chironomus* and *Dicrotendipes* is generally indicative of a mesotrophic, relatively shallow lenic environment not unlike the modern lake conditions (detailed in Section 8.4.1). There is a slow decline of undifferentiated Orthocladiinae, probably *Cricotopus*, suggesting a decline in the importance of algal sources in the ecosystem.

The main taxa exhibit rapid fluctuations of as much as 20% between samples, suggesting the fauna is not stable. This high inter-sample variability is noteworthy — these rapid oscillations occur with the same period as the sampling interval, suggesting there are changes at a higher resolution than this dataset can discern. This variability is also seen in C/N data for this period, although the variations are small enough to be considered noise in the absence of other data. Possible forcing of these rapid fluctuations is discussed in Chapter 11. This high variability in the chironomid taxa suggests a community that lacks stability due to internal or external forcings — given high frequency variation in the C/N data, external forcing seems more likely as carbon source is also affected. There is a long term trend towards lower and more stable values after *c.*4,000 years B.P., possibly due to reduced catchment soil input to the lake as soils stabilise, or possibly due to a shift in the auto/allochthonous productivity importance, albeit minor, given the total reduction is small.

9.3.5 Mid-Holocene Climate Stabilisation

Zone 3 retains the same faunal composition of Zone 2, but without the inter-sample variation of Zone 2. The long-term reduction in chironomid head capsule concentration is probably as a result of an increased sedimentation rate (see Section 6.3).

Lower average C/N values from 4,000 years B.P. onwards suggest a small increase in phytoplankton productivity (Leng *et al.*, 2006), although Mayr *et al.* (2005) might suggest the high-frequency variation within this narrow range of values cannot be interpreted as anything other than noise in the dataset. However, these high frequency

oscillations are also reflected in the chironomid stratigraphy; this noise may be oscillations when sampled at higher resolution.

9.3.6 Minor Late-Holocene Environmental Change

The slight change at 2,000 years B.P., where nr.*Macropelopia* increase by 10% and later *Chironomus* increase by 15%, alongside a reduction in Tanytarsini and *Dicrotendipes*, is noteable, but the fauna is similar to the modern lake composition. The generalist fauna makes interpretation of this minor change difficult, but *Chironomus* is associated with the profundal, so there may have been a deepening of the lake, and both *Chironomus* and *Macropelopia* have been associated with cooler water.

9.3.7 Chironomid Inferred Temperatures

The sample specific errors are high (mean=1.72°C, see Figure 9.7(a)), due to the performance of the transfer function itself, rather than the applicability to this palaeoecological data (Section 5.6.5). The range of values, from 4.4–6.1°C are not unreasonable in the context of the qualitative interpretation of estimates given by Ashworth *et al.* (1991); Hoganson and Ashworth (1992). From the base of the sequence until around 4,000 years B.P. the pattern of changes in inferred temperature is very similar to that of the first PCA axis (Figure 9.7(b)).

These two datasets are not independent: PCA data represent the primary axes of change in faunal data, and the same faunal data drive the temperature reconstruction (ter Braak and Juggins, 1993). As such, if the two datasets show no relationship at all, temperature or a co-variable environmental variable may not be the primary control on chironomid populations (Juggins, 2013). The loss of this relationship at 4,000 years is roughly co-incident with a number of changes in the chironomid and other proxy data, including reduced chironomid concentrations for the remainder of the sequence. The temperature reconstructions, like the chironomid abundances themselves, show a high inter-sample variability, but the record is punctuated by some rapid changes in temperature that persist, the most important of which is a warming at 3,200 years B.P. from 4.4 to 5.9°C, a warming that although rapidly reduces, remains and stabilises at *c.*5.5°C between 1,100–2,900 years B.P.

9.4 Summary

Figure 9.8 summarises the proxy data for Laguna Edita, and Figure 9.9 summarises the interpretation of those data presented in Section 9.3. There are three zones in the lake stratigraphy, separated at 8,200 years and 4,000 years B.P. Immediately following lake formation the lake was relatively shallow and algae was dominant, and possibly

seasonally slightly anoxic. Large volcanic eruptions around 8,000 years B.P. are associated with an influx of allogenic organic matter, possible due to sudden and short-lived de-forestation of the catchment. Following these large eruptions the lake becomes closer to its modern state as a relatively productive, slightly acid lake, although the chironomid populations are variable suggesting an instability or sensitivity to high-frequency climate changes.

After *c.*4,000 years B.P. this inter-sample variation disappears and the phase relationship between the chironomid PCA axes changes; this is interpreted as a stabilisation of the the lake system, either because of a dampening of the sensitivity to high-frequency climate change or because of cessation of that climate forcing. Higher temperatures are also inferred from 4,000 years B.P. onwards — the wider literature on mid-Holocene change is outlined in Section 3.3.1 and the importance of this data in that context is discussed in Section 11.5.2.3.

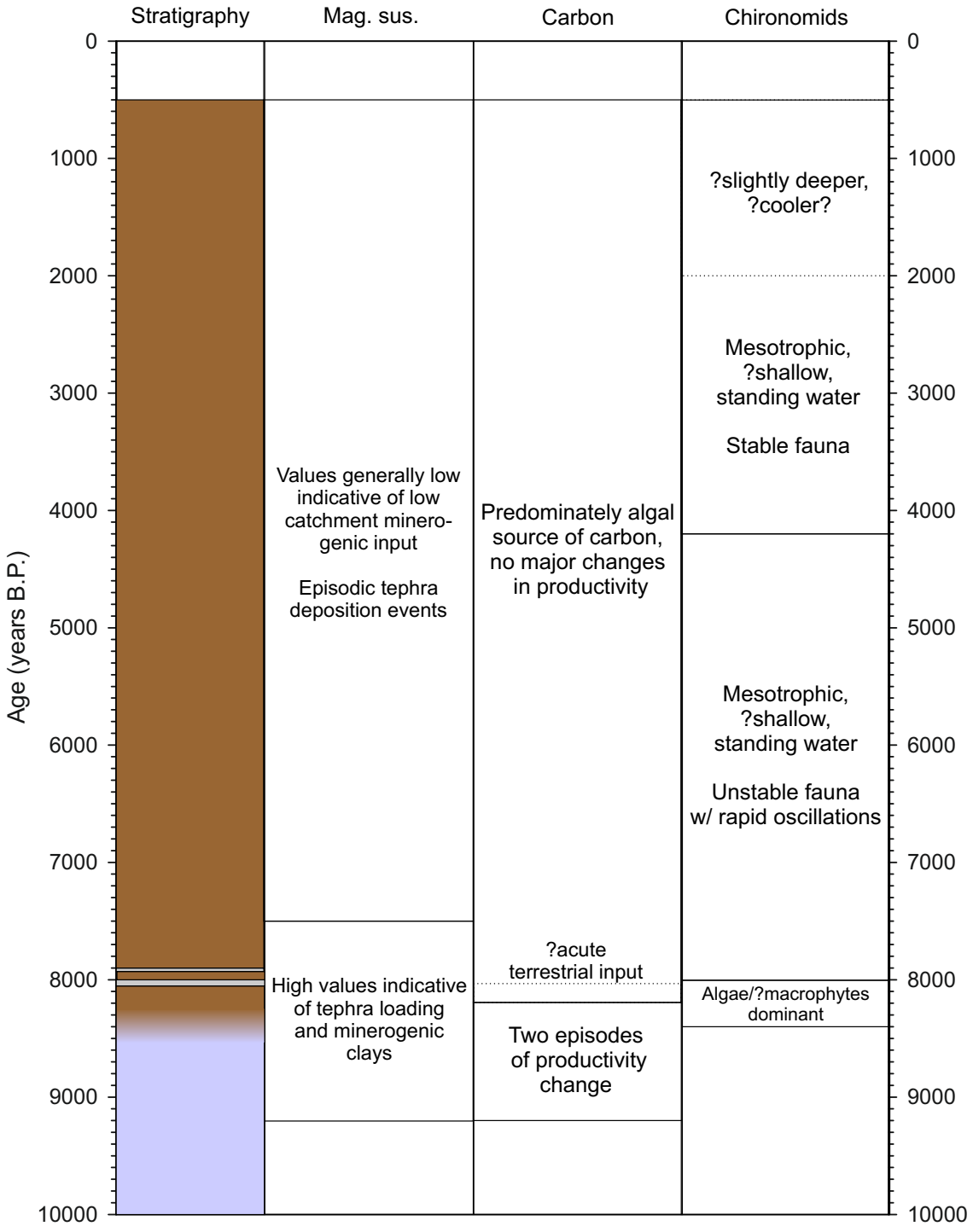

FIGURE 9.9: Summary of interpretation of long core data from Laguna Edita.

Chapter 10

Laguna Meche Long Core Results & Proxy Interpretation

10.1 Introduction

This chapter presents the results for the proxy analysis for Laguna Meche (magnetic susceptibility, total organic content, C/N ratio, δ^{13}C, and chironomids), followed by an interpretation of those data for this lake in a palaeoenvironmental context. A record of Holocene climate change from the H1 tephra onwards is presented, and a number of palaeoclimatic inferences are made, including a late-Holocene aridity event, a mid-Holocene wet/warm event and some late-Holocene changes that are tentatively ascribed to lake productivity changes.

10.2 Results

10.2.1 Stratigraphic Interpretation

An overlapping sequence of cores with a total length of 519cm were retrieved from the lake and is shown in Figure 6.13. It was dated using radiocarbon and tephrochronology as per Section 6.3. From the top down, the core is composed of organic gyttja until 410cm, where a large tephra unit (identified as Hudson H1; see Section 6.3.3.3) lies above grey clays. The grey clays appear to be have been deposited in a lacustrine environment, as evidenced by aquatic macrofossils found in small quantities. The grey clays are likely to be residual material from glacial retreat (Hein *et al.*, 2010, see also Section 4.2.2) and dominate the sediment flux until the development of soils and more organic sedimentation (*c.f.* Villa-Martínez *et al.*, 2012; Massaferro and Brooks, 2002; Massaferro *et al.*, 2005; Tonello *et al.*, 2009). The average accumulation rate in the post-H1 section of the core is 0.04cm/year. Itrax data are presented in Figure 10.1.

10.2.2 Magnetic Susceptibility

A total of 531 magnetic susceptibility measurements at both high and low frequency were obtained at contiguous 1cm intervals for all core sections including overlaps. The highest magnetic susceptability measurements (K_{HF}) are in either tephra layers or clay-rich (inorganic) depositional units because of the higher minerogenic content and the denser material (Dearing, 1999) — although the values presented are volume-specific, mass-specific measurements indicate that correction for density does not change this interpretation. There is a general declining trend in K_{HF} throughout the gytjja unit (8,200 years B.P. onwards; see Figure 10.2).

10.2.3 Organics

Loss-on-ignition measurements were made at contiguous 1cm intervals on all material (including overlaps), giving an average temporal resolution of 22.3 years/sample. A total of 86 samples spaced evenly throughout the sequence were analysed for δ^{13}C, total organic carbon and total nitrogen analysis, giving a resolution of around 8cm for these data (an average temporal resolution of 179 years between samples).

There are considerable variations in all three measures of organic carbon throughout the sequence in six distinct zones:

Carbon Zone 1 8,400–6,500 years B.P.: Depression of δ^{13}C from -28.5 to -30.8‰, and C/N between 12–17 (average of 14.5), reduced from an initial value of 25. Total organic carbon proportion remains stable.

Carbon Zone 2 6,500–6,100 years B.P.: Brief period where δ^{13}C is relatively stable at around -28‰ and C/N is relatively stable at 21.

Carbon Zone 3 6,100–5,100 years B.P.: A sudden reduction in δ^{13}C to values as depleted as -31.9‰, associated with a drop in C/N to as low as 13, following an initial spike of 28.

Carbon Zone 4 5,100–2,800 years B.P.: A prolonged period of stable δ^{13}C (-28.5‰), C/N (18) and TOC (15%).

Carbon Zone 5 2,800–1,300 years B.P.: Peak in C/N values of 35 (from 17), along with a distinct rise in %TOC to ≥35% but no discernable change in δ^{13}C. Brief intermediate reversal with accompanying brief reduction in δ^{13}C to -30‰, which is otherwise stable in this zone at around -28.5‰.

Carbon Zone 6 1,300–200 years B.P.: C/N values stabilise at around 15, but δ^{13}C increase to -26.2‰.

10.2.4 Chironomid Analysis

10.2.4.1 Stratigraphy

A total of 59 samples were analysed for chironomids, giving a sampling resolution of 8cm, or an average temporal resolution of 179 years between samples. Forty samples had total head capsule counts ≥40, the threshold for inclusion in ordination and training set analysis (Quinlan and Smol 2001, see also Section 5.6.4). The stratigraphy can be divided into three major zones:

Chironomid Zone 1: 8,200–6,100 years B.P.: Chironomid concentrations are relatively low. The dominant taxon is Tanytarsini, although *Ablabesmyia*, *P. triquetra* and *Dicrotendipes* are present at low levels.

Chironomid Zone 2: 6,100–2,000 years B.P.: The base of this unit is defined by a drastic reduction in the concentration of Tanytarsini and the replacement of the dominant taxa with *Parakiefferiella*, with concentrations up to 65% (average *c.*40%). A number of taxa appear in this zone to make the fauna more diverse than chironomid Zone 1, including *Parachironomus*, *Corynoneura*, *Nanocladius*, *Paraspectrocladius*, *Paratricocladius*, *Thienemanniella*, Orthocladiinae "wood miner" and Tipulids. The concentration of head capsules rises gradually to a peak at about 4,200 years B.P., where it gradually declines to concentrations comparable to chironomid Zone 1. There is a slight shift in the composition from 2,500–2,000 years B.P. *Parakiefferiella* reduce by around 15%, and there are increases in *Eukiefferiella*, Orthoclad. "wood miner" and there are peak values of Simuliidae. The only presence of Ceratopogoninae head capsules is observed at this time.

Chironomid Zone 3: 2,000–200 years B.P.: Overall chironomid concentrations begin low but suddenly increase at 900 years B.P. *Parakiefferiella* are reduced as Tanytarsini again dominate the fauna, although *Parakiefferiella* remain at around 15%. *Rheithia* disappears initially but briefly reappears at high levels (25%). *Macropelopia*, present at low levels throughout the record, suddenly increases to concentrations of up to 23%, in a similar fashion to *Rheithia*. Non-chironomid Diptera larvae (Ceratpoginae, Simulidae, Tipulidae) all but disappear in this zone. *E. gracei* is also present at its highest abundance in this zone.

10.2.4.2 Ordination Analyses

Detrended correspondence analysis (DCA) of the data indicated the data were better treated as linear (DCA axis 1 eigenvalue <0.2) and thus the results of a principle components analysis (Dytham, 2011; Braak and Smilauer, 1998; Lepš and Šmilauer, 1999; Hammer, 2010) are presented in Figure 10.5. This stratigraphy shows a shift in the

phase relationship between axis 1 and 2 values of the samples, starting positive and becoming negative after 2,500 years B.P.

10.2.4.3 Temperature Transfer Function

The temperature transfer function described in Section 5.6.5 was applied to the down-core assemblage data and the results are shown in Figure 10.7. Although Chapter 8 concluded that there are good reasons that temperature transfer functions may not provide reliable temperature estimates from these lakes, it is at least possible that the long core data can provide more reasonable estimates of palaeo-temperature, not least because they are free of the possibility of confounding anthropogenic factors, and they should be considered with the caveats expressed in Section 8.4.5 in mind. The inferred temperatures can be split into two main zones:

CI-T Zone 1 8,000–6,000 years B.P.: Temperatures gradually rising from as low as 4.2°C to 6.5°C at the end of this zone.

CI-T Zone 2 6,000–300 years B.P.: Stable temperatures of around 6.5°C, with possible short warming events centered on 1,000, 2,000 and 2,500 years B.P.

10.3 Interpretation

10.3.1 Overview & General Remarks

In general terms the C/N and chironomid proxy data indicate a lake with an important allochthonous contribution, including inflow from small streams in the catchment that are not present in the modern lake catchment (compared to data presented in Section 7.3.3.3). Following the onset of organic gytjja deposition after the H1 eruption there are a number of important changes in lake status, including an increase in lotic input from 6,100 to 2,000 years B.P., a significant terrestrial flux to the lake between 1,300–2,800 years B.P., and a number of possible changes in lake/catchment productivity. The palaeoenvironmental interpretations presented in this section are summarised in Figure 10.11.

The rationale behind the interpretation of the magnetic susceptibility data is identical to that given in Section 9 for Laguna Edita. There were no discernable differences between low and high frequency measurements (χ_{FD}), indicative of a neglible input of soil-derived allogenic material (Dearing, 1999; Hatfield and Maher, 2009).

Based on ecological information presented in Appendix A, the chironomid fauna is indicative of a mesotrophic lake, although the temperature range of the fauna is

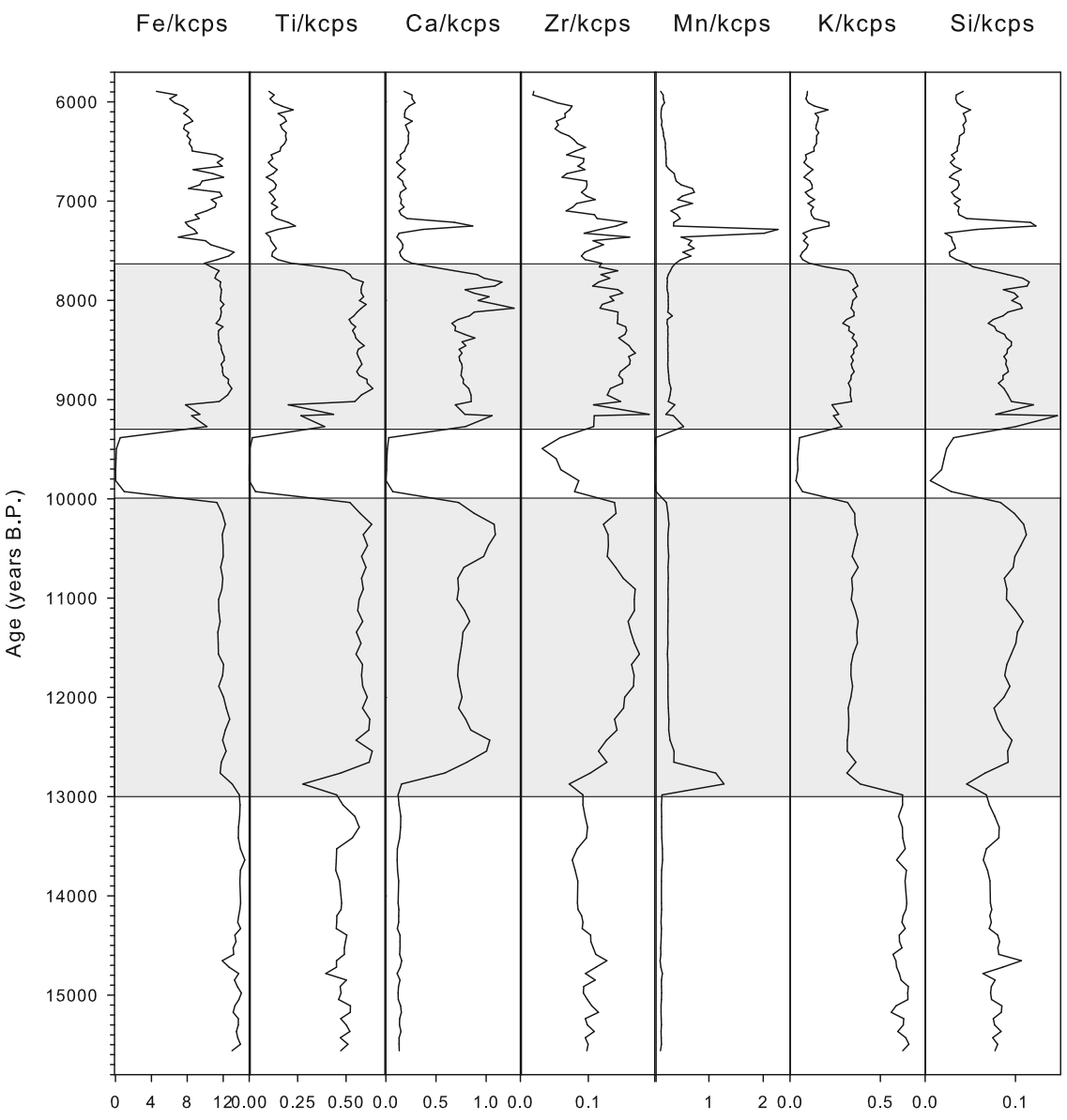

FIGURE 10.1: Itrax data from Laguna Meche, showing selected elements divided by count rate. Zones in grey show H1 tephra (lower) and unidentified tephra layer (upper).

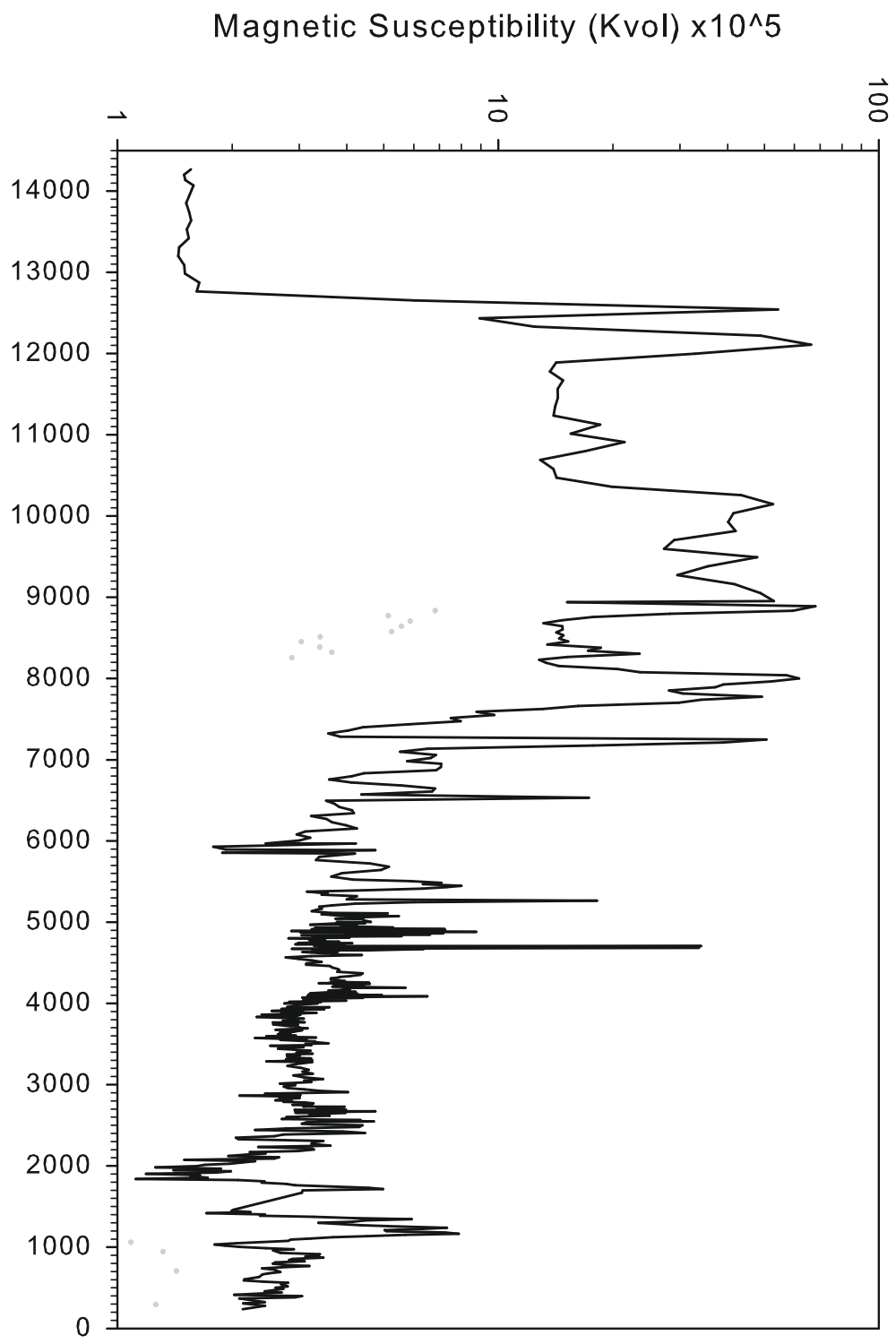

FIGURE 10.2: Volume magnetic susceptibility values for Laguna Meche, shown without smoothing but with some data (shown as grey dots) removed. Note the log scale.

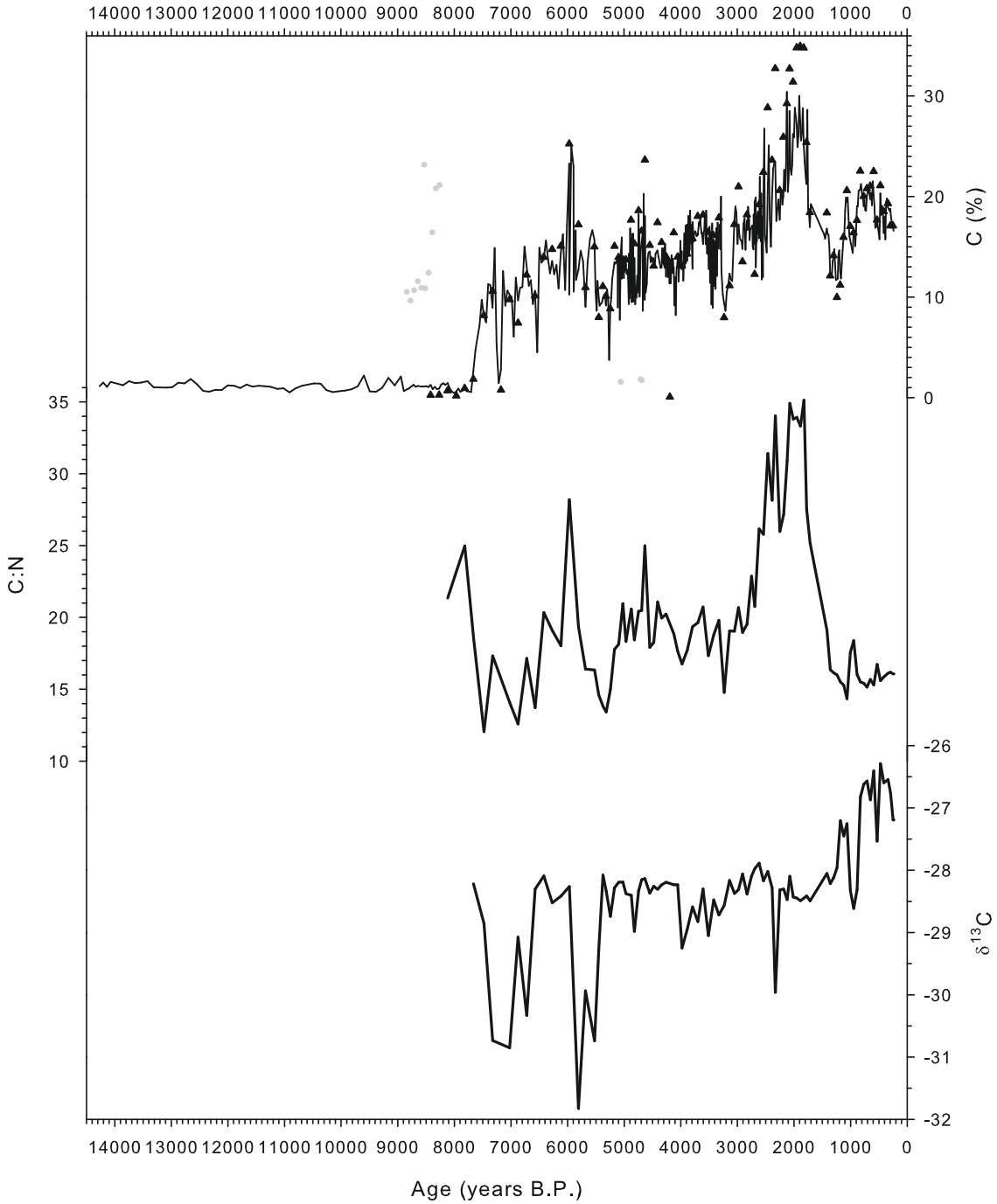

FIGURE 10.3: C/N and δ^{13}C values for Laguna Meche. For the graph showing C(%) the triangles represent results obtained using an elemental analyser, and grey circles represent points excluded.

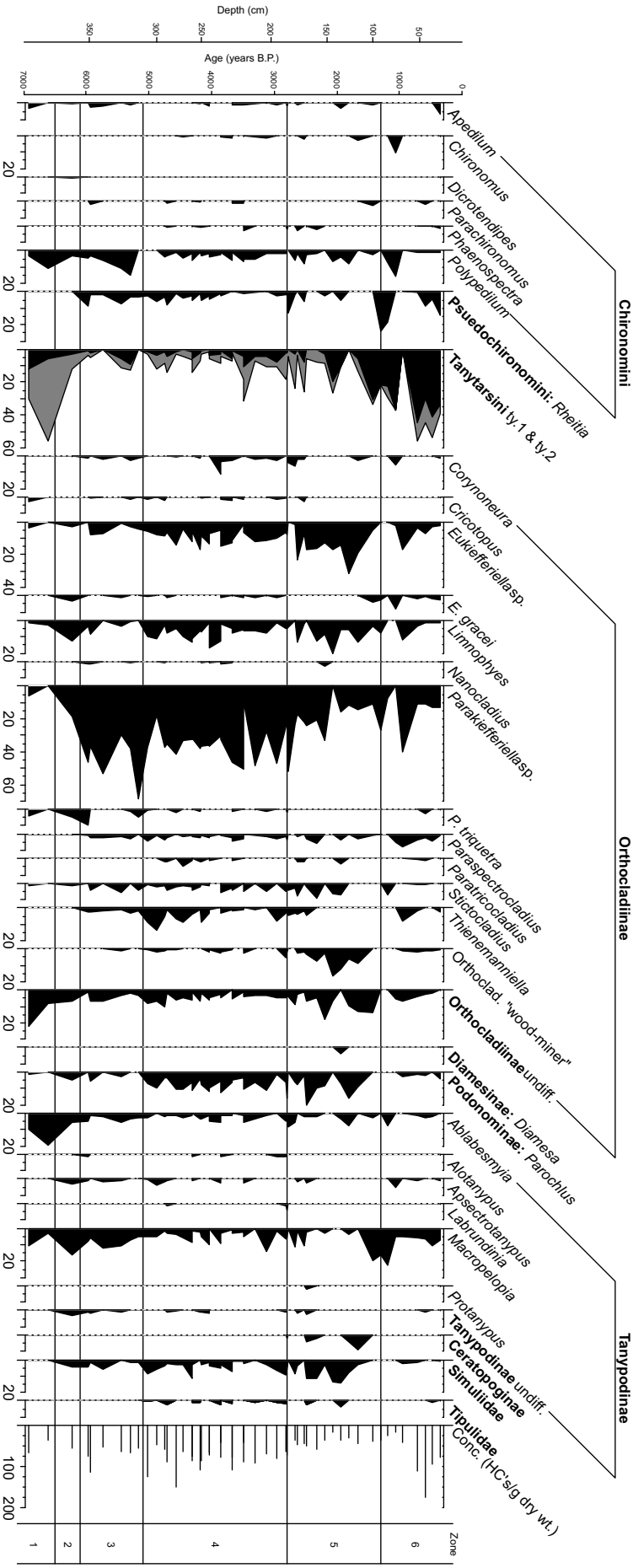

FIGURE 10.4: Chironomid diagram for Laguna Meche, showing the percentage abundance of all taxa. Non-chironomid taxa (Ceratopoginae, Simulidae and Tipulidae) are shown as percentages of the sum of the chironomidae. Zones refer to those described in Section 10.2.4.1.

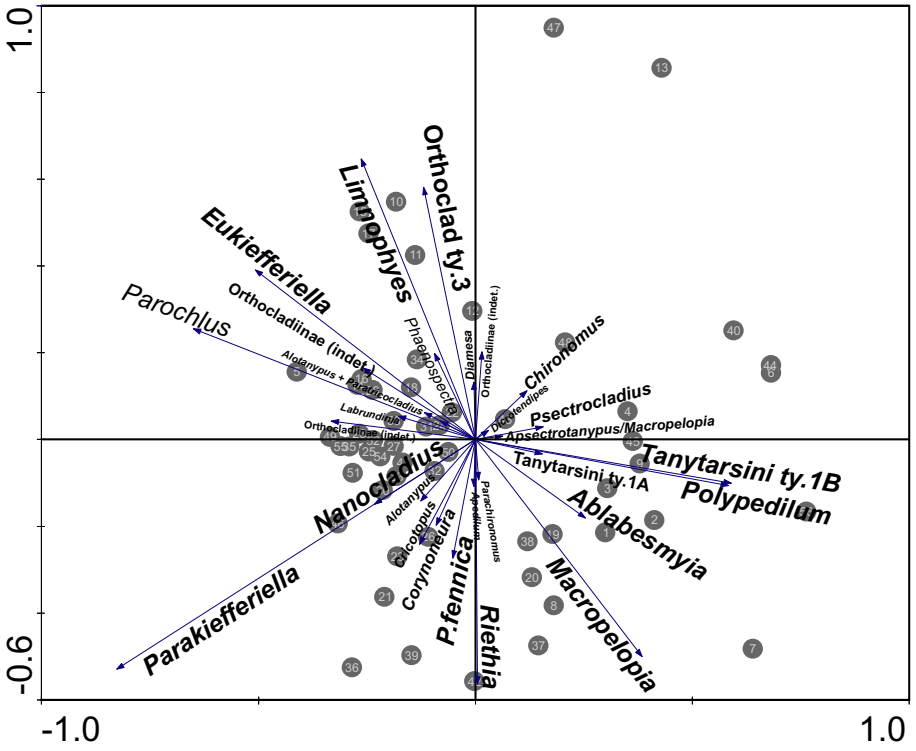

(a) Species and sample scores for axes 1 & 2.

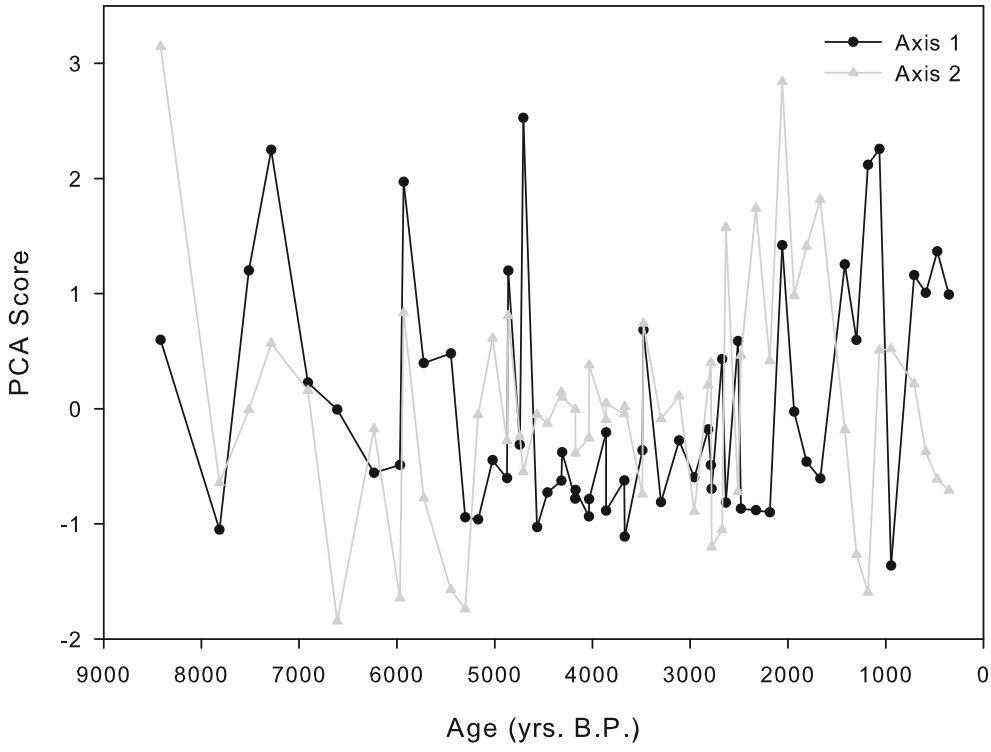

(b) Sample scores for axes 1 & 2 plotted against time.

FIGURE 10.5: Principle co-ordinate analysis scores for Laguna Meche long core. Calculated using Canoco v.4, using scaling focussed on inter-species correlations, species scores are expressed divided by their standard deviation. Species data were square-root transformed and centred by normalization. The eigenvalues for axis 1 and 2 were 0.22 and 0.14 respectively.

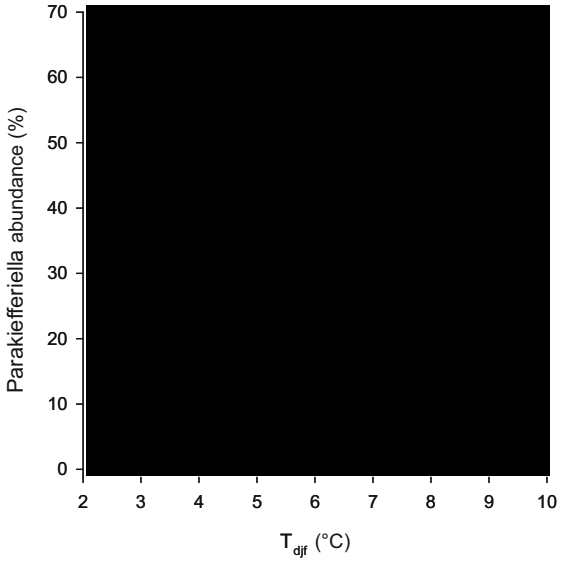

FIGURE 10.6: *Parakiefferiella* temperature distribution from Massaferro and Larocque-Tobler (2013). Apart from one outlier, note the association of the taxon with warmer temperatures.

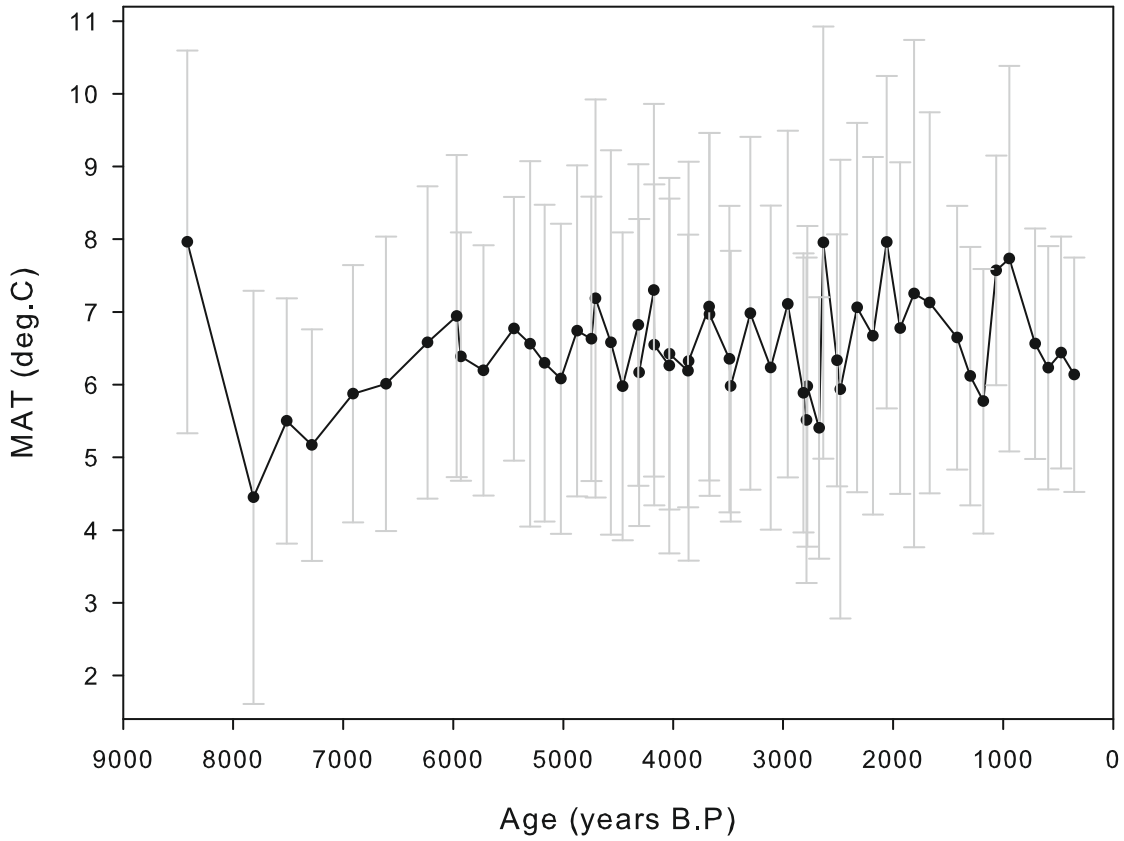

(a) CI-MAT transfer function results, showing bootstrapped estimated standard errors of prediction (SEP's).

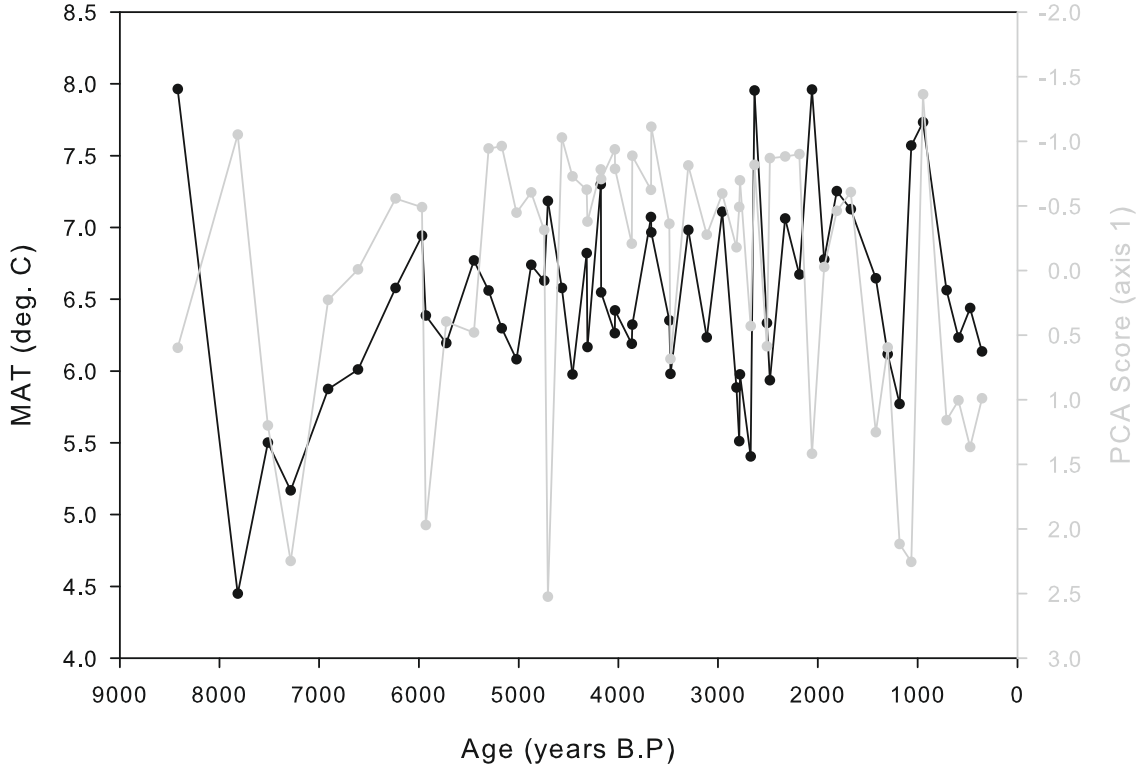

(b) CI-MAT plotted alongside PCA axis 1 scores as shown in Figure 9.6.

FIGURE 10.7: Chironomid inferred mean annual temperature transfer function results for Laguna Meche long core.

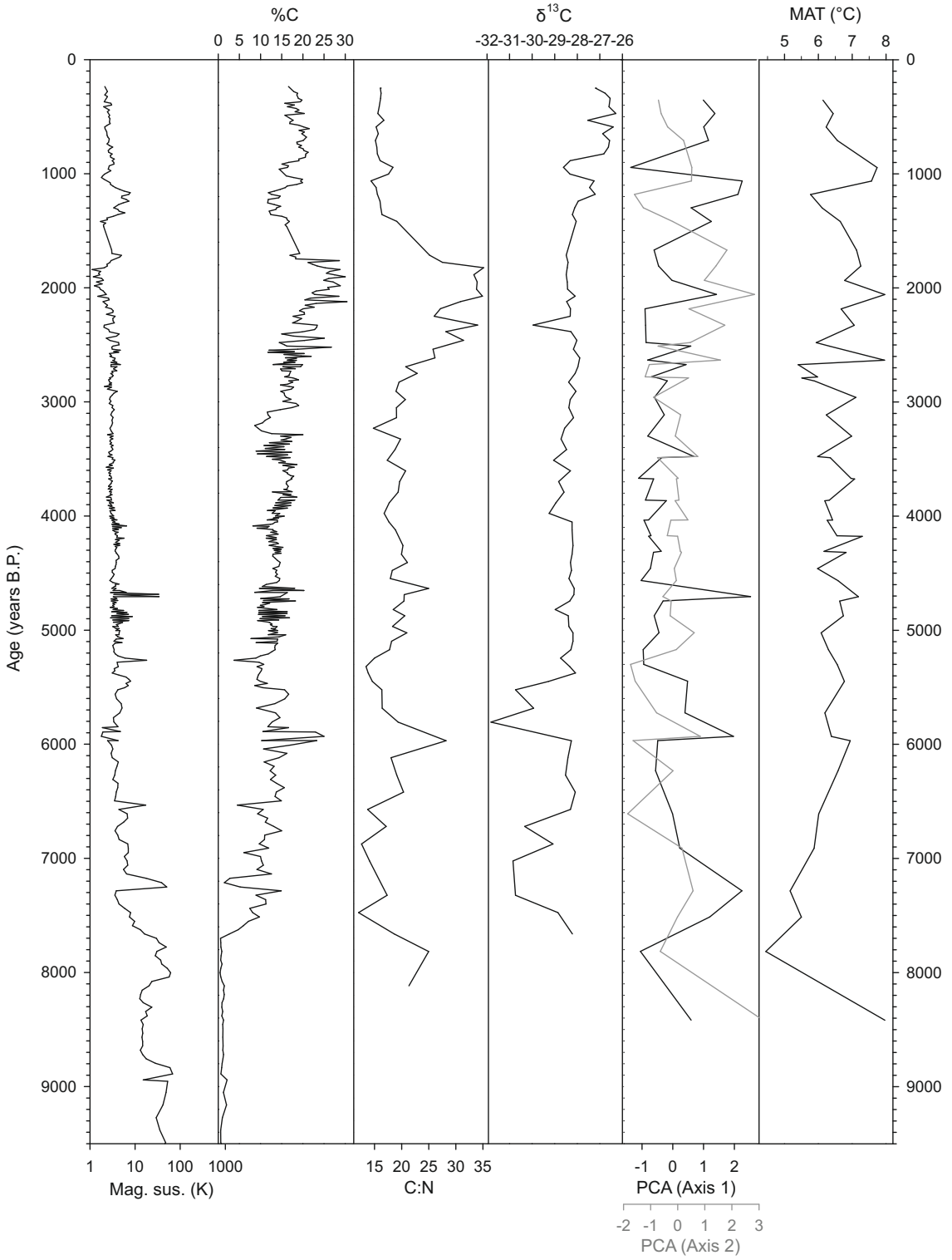

FIGURE 10.8: Summary of available data for Laguna Meche long core, showing magnetic susceptibility, organic carbon content, C/N, δ^{13}C, chironomid PCA scores and chironomid-inferred mean annual temperatures. Note the magnetic susceptibility and organic carbon content data from the bottom of the core have been trunucated.

ambiguous; there is a general absence of cold stenotherms (*e.g.* Podonominae), although the dominant *Parakiefferiella* is considered an indicator of cool conditions in the northern hemisphere. The two dominant taxa are Tanytarsini and *Parakiefferiella*, but there is a diverse range of minor taxa, particularly in the families Orthocladiinae and Tanypodinae. Both of the dominant taxa are generalist. The majority of minor taxa are associated with (but rarely exclusive to) flowing water — for example, *Limnophyes*, *Eukiefferiella*, *Rheitia* and *Parapsectrocladius* are all associated with flowing water. All are indicative of mean temperatures of the warmest month over 12°C (Massaferro and Larocque-Tobler, 2013).

Corynoneura and *Nanocladius* are found only in locations where the average temperature of the warmest month is ≤12°C (Massaferro and Larocque-Tobler, 2013), but *P.triquetra* is often regarded as an indicator of cooler water, although the overall relative abundance is low. This mix of taxa indicative of warmer conditions and the presence of those taxa commonly found in cooler conditions suggests that altitude (temperature) may not be the primary control on the faunal composition. Rather, the common factor in several of the taxa is the association with littoral and/or lotic environments — this is discussed further in the following subsections.

10.3.2 Early Catchment & Lake Development and Tephra Deposition

Initially high magnetic susceptibility and negligible %TOC but the occasional presence of aquatic macrophytes in the basal clays suggest a lacustrine sedimentary environment dominated by the influx of re-worked glacial till from the catchment; this is common for lake sediments in the region (*e.g.* Iglesias *et al.*, 2014; Villa-Martínez *et al.*, 2012).

Unlike Laguna Edita, organic sedimentation (gytjja) does not begin in the sequence until directly after H1, and following H1 there is no grading to gytjja; the sediment is immediately a dark brown (Figure 10.11). This could suggest a discontinuity in the record, as a gradual grading from inorganic to organic-rich sedimentation is expected; alternatively this could be caused by changes induced by tephra deposition, including fertilization by tephra starting organic sedimentation (*e.g.* Urrutia *et al.*, 2007).

Two large tephra events in close sucession, one of which has been identified as the H1 tephra (Section 6.3.3.3) punctuate the lower part of the record at 8,000 years B.P. These layers exhibit very high values of K_{HF} due to both the large magnetically susceptible component of volcanic ash and the density of the material — this is also true of the smaller tephra layer just above this and is in keeping with evidence elsewhere in Patagonia of large eruptions having high K_{HF} (Charlet *et al.*, 2007; Guilizzoni *et al.*, 2009; Arnaud *et al.*, 2006).

This first organic sedimentation begins with initially high C/N, suggesting a dominant terrestrial source of carbon at the very base of the sequence (Meyers and Teranes, 2001; Leng *et al.*, 2006), supporting the possibility that the lake status was permanently

changed by the affects of the H1 tephra on the catchment for reasons similar to those discussed in Section 9.3.3. This is rapidly followed by reduced C/N values between 15–20 that are modal for the remainder of the core. Reduced values of δ^{13}C in Zone 1 suggest either increased macrophyte productivity or a change in inwash of terrestrial material (see Section 8.3.2). The combination of reduced C/N and reduced δ^{13}C is indicative of a change in the catchment soil and vegetation (see Figure 8.2 and Section 8.3.2); the isotopic composition of inflowing waters is dependent on the properties of local soils or the proportion of the contribution of this component of the carbon cycle to the sediment (Leng, 2004; Gibson *et al.*, 2002; Mayr *et al.*, 2008). Depleted δ^{13}C could be due to increased autogenic productivity, or an increase in terrestrially derived material, but there are no indicators of increased lotic input or chironomids associated with woody debris at this time so the productivity change is the more likely of the two.

10.3.3 Bistable Carbon Geochemical Stratigraphy Until 5,100 years B.P.

Between 8,000–5,000 years B.P. carbon isotope values switch between lower C/N and generally more depleted carbon isotope values (Zones 1 and 3) and less depleted isotope values with higher C/N ratios (Zones 2 and 4; see Figure 10.9). In addition, both carbon Zones 1 and 3 start with a brief peak in C/N, followed immediately by a decrease in δ^{13}C. The spikes in C/N at the beginning of these zones, particularly clear in carbon Zone 3, is indicative of a change in the source of carbon, suggesting these may be inwash events rather than changes in the composition of a more constant flux (*e.g.* Langdon *et al.*, 2007). As discussed in the previous section, where C/N ratios indicate a mixed contribution from allochthonous and autochthonous carbon sources, depleted δ^{13}C could be due to a number of factors, but where C/N and δ^{13}C change together it is reasonable to assume a change in carbon source. However, this only occurs at the start of Zones 1 and 3; it appears that a brief increase in terrestrial carbon is the precursor to longer term changes in productivity and/or the properties of catchment soils at this time. Given that the more depleted δ^{13}C values are associated with lower C/N (less allogenic carbon), the episodes of more depleted δ^{13}C could be tentatively attributed to increased autogenic productivity between 6,500–8,400 and 5,100–6,100 years B.P.

The early chironomid zone that covers the period from 8,200–6,100 years B.P. is indicative of a predominately lentic environment with a small lotic input; this further supports the interpretation of depleted δ^{13}C values between 6,500–8,400 years B.P. as indicative of an increase in autogenic productivity rather than allogenic isotopic carbon composition. From 6,100 years B.P. onwards there is an increase in the lotic chironomid component, indicating more depleted δ^{13}C values between 5,100–6,100 years B.P. could be due to allogenic carbon isotope composition or autogenic productivity; further work using δ^{15}N could differentiate between these two possible interpretations. In addition, terrestrial pollen analysis could provide a measure of catchment vegetation, a change in

which could affect the isotopic composition of inflowing catchment-derived carbon.

10.3.4 Increased Lotic Input From 6,100–2,500 years B.P.

As discussed in the previous section, the initial chironomid zone suggests a predominately lentic environment until 6,100 years B.P.; the following zone, from 6,100–2,000 years B.P. is strongly suggestive of a relatively warm, macrophyte rich lake with a significant lotic element. Figure 10.10 summarises taxa by their ecological niche, showing the increase in taxa such as *Thienemanniella*, *Parochlus* and *Eukiefferiella* from 6,100 years B.P. onwards. The presence of large numbers of Simuliidae, which are almost exclusively found in running water, further indicate the presence of a significant stream inflow to the lake during this period (Luoto, 2010; Verschuren and Eggermont, 2006). This is most likely to be from the now vegetated palaeo-channel that enters the lake in the south-west corner. This channel drains part of the forested catchment, and so its presence or absence is likely to be a function of surface moisture and/or forest canopy cover. Changes in the strength of the flow could have modulated delivery of Simuliidae head capsules to the coring site (Currie and Walker, 1992).

The reducing trend in K_{HF} throughout the gytjja is suggestive of gradual stabilisation of the catchment throughout the Holocene, as bedrock surfaces are covered with soils and slope erosional processes slow (*e.g.* Mayr *et al.*, 2005). Overall K_{HF} values are elevated compared to Laguna Edita, unsurprisingly indicating a proportionally higher ratio of minerogenic to organic input in keeping with increased bedrock weathering (Morgan, 1986, ch.4) and lower productivity at a site some 412 meters higher in altitude (Dearing, 1999; Thompson *et al.*, 1975).

Aside from the fluctuations at the early part of this zone (between 6,100–5,100), δ^{13}C and C/N values are relatively stable around -28.5‰ and 22 respectively. Average values are very similar to those from the short core from this lake, although C/N is slightly higher in these cores than in the short cores, suggesting depositional conditions similar to the present day, possibly with terrestrial carbon a more important contributor than in recent times. Carbon Zones 1–4 suggest a system that is bistable in the early Holocene between a mixed, stable (Zones 2 & 4) and an elevated or modified catchment input (Zones 1 & 3).

10.4 Increased Terrestrial Input Between 1,500–2,500 years B.P.

Continuing the trend towards increased lotic inputs to the lake, between 1,500–2,500 years B.P. taxa characteristic of lotic environments that appeared and/or increased from 6,100 years B.P. onwards reach a peak. This is in addition to a reduction in

Parakiefferiella and an increase in Orthoclad "wood-miner", along with an increase in the exclusively lotic Simuliidae head capsules. These changes are partly indicative of a further increase in the lotic input to the lake, and a simultaneous increase in C/N and %TOC values during this zone suggests a significantly increased terrestrial input to the lake at this time. The biostratigraphy does not indicate any (semi)terrestrial accumulation *in-situ* at the coring site, but does suggest increased woody-debris and lotic input at this time. It is perhaps surprising that there are no observed changes in δ^{13}C during a period of change in sediment source, but Figure 8.2 shows there are significant overlaps between δ^{13}C values of organic components of the lake and catchment, so a change in source could occur without a corresponding change in δ^{13}C, particuarly in the balance between allogenic sources. The possible explanations could be summarised as:

- A decrease in autogenic productivity, thus a proportional increase in terrestrial organic matter. Because overall carbon content increases during this phase, this is unlikely (a decrease would be expected if this were the case).
- An increase in the quantity or proximity of terrestrial vegetation. At present the *Nothofagus* tree stand runs right up to the lake (see Figure 4.5). As such, the tree-line could not get any closer to the lake than it is at present unless lake level was lower.
- A change in the transport mechanism of terrestrial organic matter would have the effect of increasing both %TOC and C/N without invoking a change in terrestrial or lake productivity. An increase in the flux of lotic input to the lake, or a destabilisation of catchment soils is possible. The presence of lotic Simuliidae in the midge fauna at relatively high abundances suggest an increase in lotic transport of terrestrially derived material. An increase in precipitation would both increase transport of catchment material and lotic input to the lake. However, magnetic susceptibility shows falling values at this time, indicative of less allogenic mineral inwash.
- Semi-terrestrialisation of parts of the lake due to reduced lake volume. This would have the effect of increasing the semi-terrestrial area of the lake, and so changing the C/N signal, although one might expect some change in δ^{13}C due to the significant effect this would have on carbon cycling within the lake. in addition, this would be reflected in the chironomid stratigraphy.

These data best fit the expectations and predictions of a decrease in lake level causing semi-terrestrialisation of parts of the lake between 2,500–1,500 years B.P. — this would have the effect of bringing terrestrial vegetation and more submerged macrophytes nearer to the coring location, explaining both the increase in terrestrial carbon and chironomids associated with macrophytes. The nearer lake margin also explains the increased lotic and terrestrial chironomid presence.

10.5 Lower Productivity From 1,500 years B.P. Onwards

By 1,500 years B.P. the episode of increased lotic taxa and terrestrial inputs to the lake reverts to a condition similar to those that 6,200 years B.P. at the same lake, where the depositional environment is mainly lentic, with a small influx of lotic derived material; the C/N data also indicate a mixed source of allo- and autochthonous carbon at this time, although compared to previous conditions the C/N is slightly lower and more similar to values observed in the modern core from this lake. From 1,500 years B.P. onwards there is a rise in δ^{13}C without any accompanying changes in %TOC or C/N. This rules out the possibility of a change in carbon source, so a decrease in productivity is the most likely alternative explanation. Due to the mixed C/N ratio it is unclear whether δ^{13}C reflects catchment or lake productivity, but given the reduction in chironomid taxa associated with submerged macrophytes (Orthocladiinae *spp.*) and an increase in nr.*Macropelopia*, associated with cooler conditions, there is some evidence for a reduction in productivity associated with cooler temperatures at this time.

10.5.1 Chironomid Inferred Temperatures

Average inferred temperatures for this sequence are greater than those inferred for Laguna Edita, which is problematic given that Laguna Meche is located 412m above Laguna Edita, and as such a temperature drop of around 2.7°C would be expected, assuming a lapse rate of 6.5°C/1000m. Although there may be some local solar radiation differences, these fail to account for a temperature difference of this magnitude. The same problem was encountered with chironomid-inferred temperatures from short cores from the same lakes (Chapter 8). At best, the inferred temperatures must be treated as indicative only, and given that the faunal composition suggests that temperature may not be the primary control of the fauna in this dataset, the inferred temperatures might be considered unreliable.

The failure of the temperature transfer function could be due to the dominance of *Parakiefferiella* in this dataset and the unreliability of its representation in the training set data. In the training dataset employed (Massaferro and Larocque-Tobler, 2013) *Parakiefferiella* is present in 30/67 lakes and has a maximum abundance of 64%, comparable to the abundances in this record. The taxon has a temperature optimum of [redacted]°C, and the lake at which the highest abundances occur has a summer temperature average of [redacted]C (see Figure 10.6). The training set data indicate the taxon is thermophilic, although a single site shows high abundances where T_a[redacted]°C, suggesting there may be multiple species with at least the possibility of a bimodal distribution within this taxon. In the northern hemisphere, this genus is considered indicative of cooler conditions (Brooks *et al.*, 2007), and bimodal distributions at genus level are encountered elsewhere in the southern hemisphere, for example *Chironomus* (Woodward and Shulmeister, 2006, 2007). Only by expanding the modern training dataset, and/or

further refining the sub-fossil taxonomy, could this be resolved.

10.6 Summary

Figure 10.8 summarises the data presented in this chapter and Figure 10.11 summarises the palaeoenvironmental interpretation of that data. The early development of the lake is complex; the stratigraphy does not present a gradual development of organic sedimentation in the lake and thus the record may be trunucated beneath the H1 tephra layer. Alternatively, tephra deposition may have engendered a rapid set of changes in the catchment leading to the rapid onset of organic sedimentation.

Between the H1 eruption and 5,100 years B.P. several changes can be interpreted in terms of environmental change within the catchment: in the the early Holocene there are two phases of lower δ^{13}C and C/N that indicate a change in lake productivity or carbon source at this time, although the mixed contribution of carbon to the lake makes a more precise interpretation difficult. Chironomid data suggest an increased lotic input between 5,100–1,500 years B.P. In the late Holocene between 2,500 and 2,000 years B.P., carbon geochemistry and chironomid indicators suggest an episode of increased terrestrial carbon deposition and a more important lotic input to the lake. From 1,500 years B.P. onwards an increase in δ^{13}C suggests a less productive lake fauna (with the same caveats as above), associated with an increase in cold-tolerant taxa.

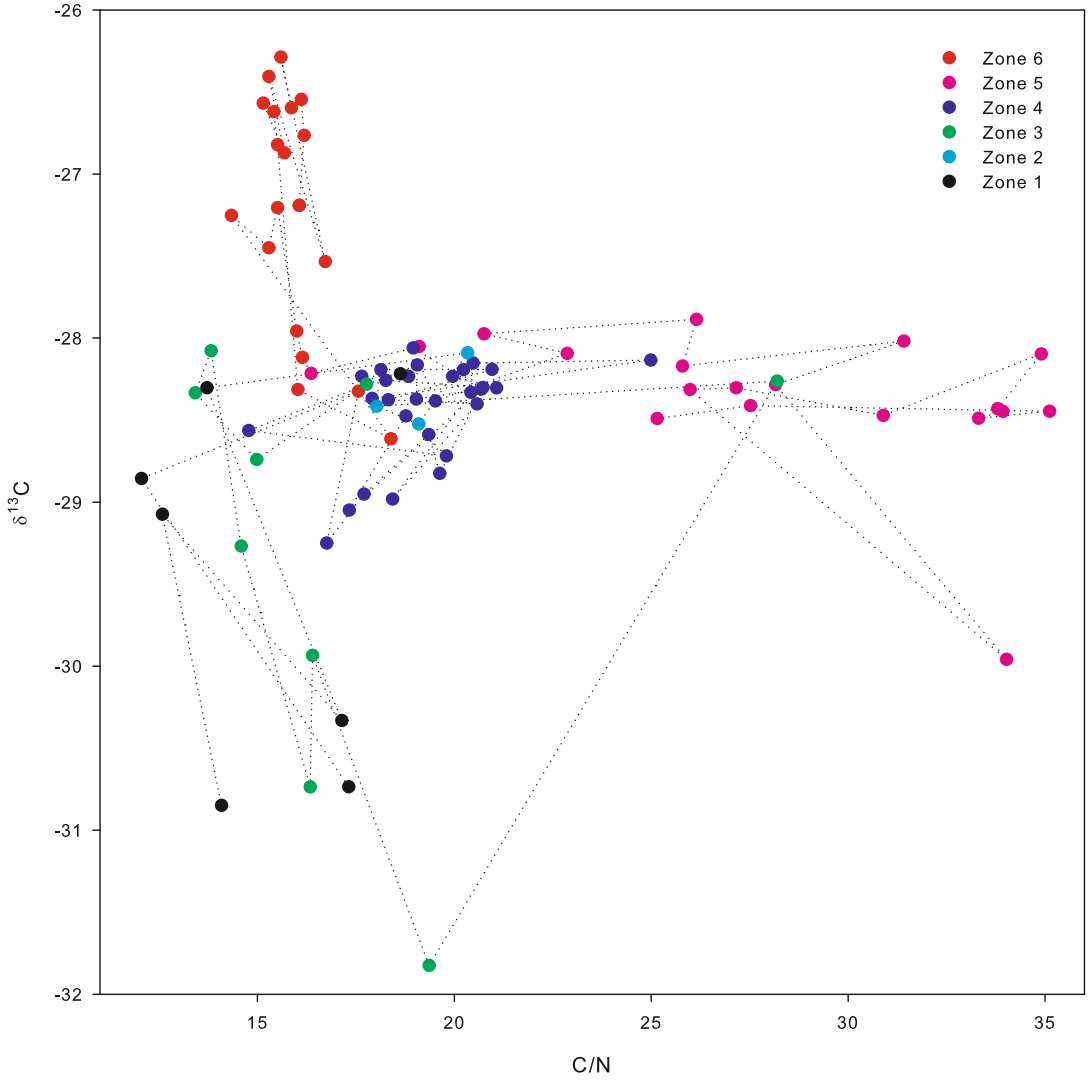

FIGURE 10.9: C/N, and δ^{13}C values for Laguna Meche. Zones are shown in different colours (see legend) and the dotted line joins adjacent samples.

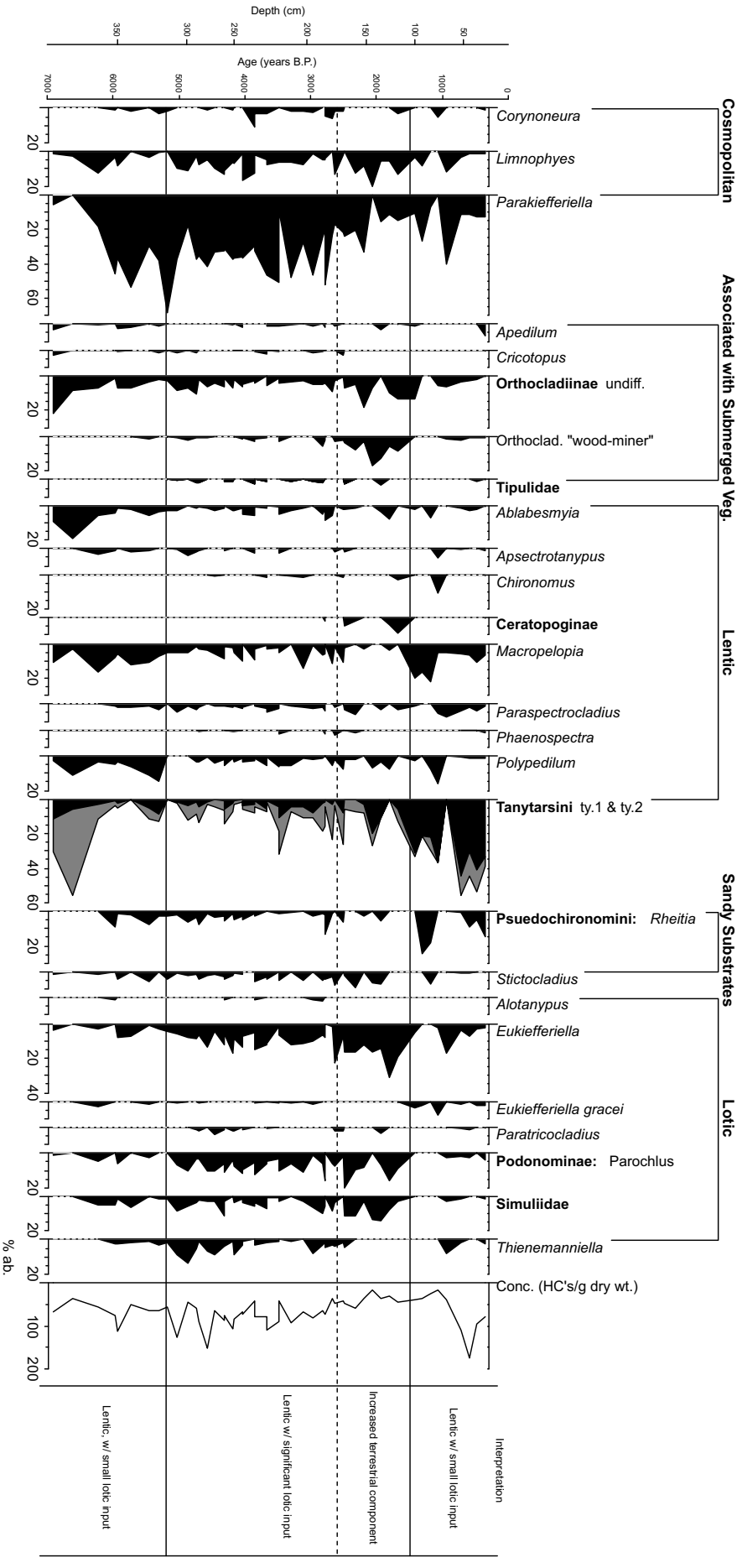

FIGURE 10.10: Simplified & annotated chironomid diagram for Laguna Meche, showing the percentage abundance of all taxa. Non-chironomid taxa (Ceratopoginae, Simuliidae and Tipulidae) are shown as percentages of the sum of the chironomidae. The taxa have been arranged in terms of their habitat preferences and a summary of the palaeoecological interpretation is included. Some rare, cosmopolitan taxa have been removed; the full fauna is shown in Figure 10.4.

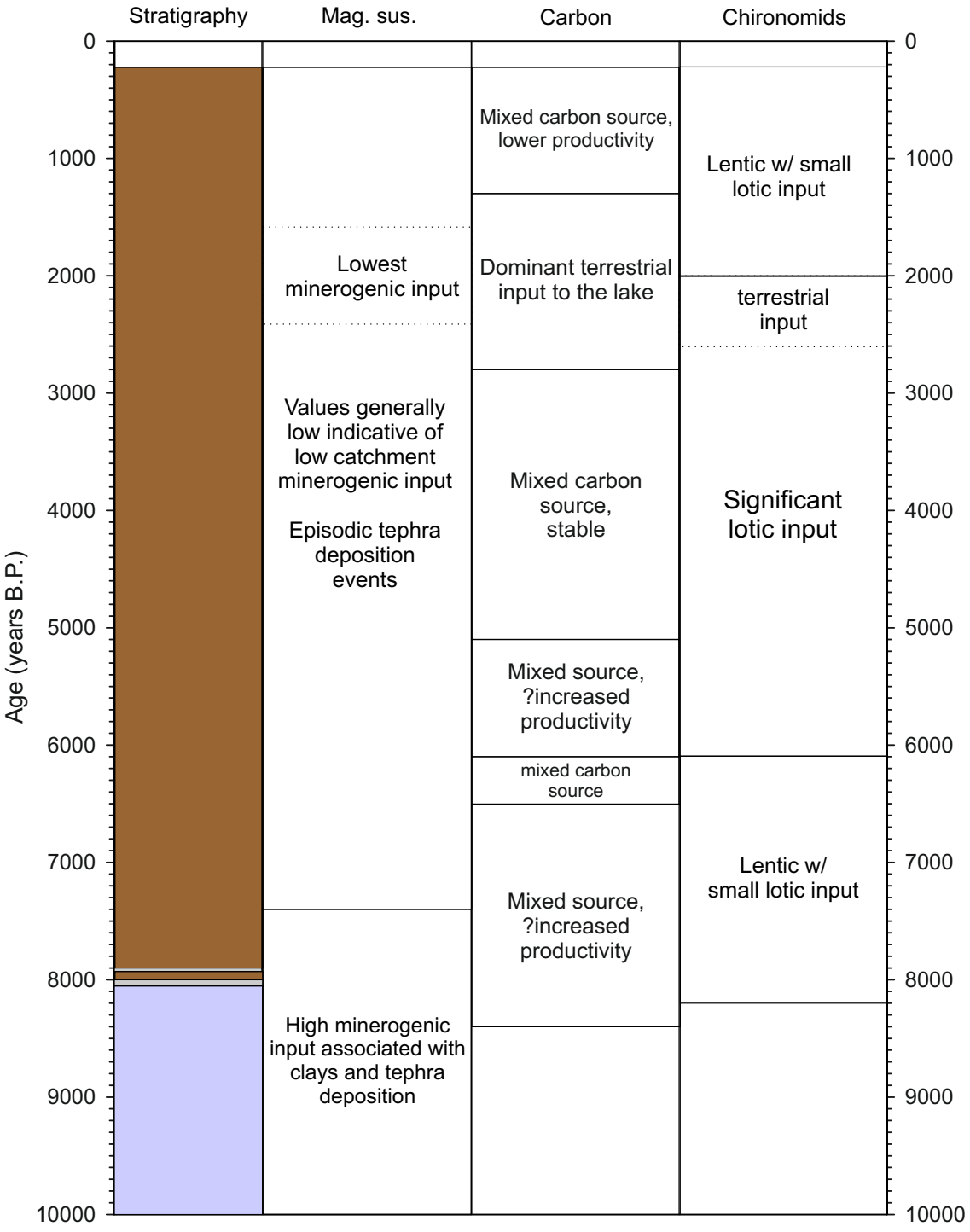

FIGURE 10.11: Summary of interpretation of long core data from Laguna Meche.

Chapter 11

Discussion and Analysis of Long Core Data

11.1 Introduction

Together, the data presented and discussed in Chapter 9 (Laguna Edita) and 10 (Laguna Meche) provide palaeoclimatic records for the Chacabuco Valley. This chapter begins by comparing the data and palaeolimnological interpretations presented in Chapters 9 and 10, followed by a comparison of the palaeoclimatic inferences from Laguna Edita and Laguna Meche, and a discussion of the reasons for differences in the records. This is followed by a summary of the palaeoclimatic record derived from the totality of the data for the Chacabuco Valley. The chapter ends with a comparison and discussion of this record with relevant palaeoclimatic data for Patagonia, and finally, for the Southern Hemisphere.

11.2 Comparisons Between Laguna Edita & Laguna Meche

11.2.1 Comparisons Between Long and Short Core Data

The short cores provide useful comparison data that contextualises the long core data, although it should be noted that the cores were taken in different locations from the long cores (shown in Figures 4.4 and 4.6). The chironomid data likely reflect this difference in coring depth (Kurek and Cwynar, 2008b) as the faunal compositions are slightly different; a full survey of intra-lake habitats and faunas would assist in testing the reason for these slight differences, but such a survey is beyond the scope of this study. However Figure 11.3 shows that there is good overlap in the sample scores from long and short cores in both lakes, suggesting they are not dissimilar in the context of the totality of the data.

The organics data is similarly comparable: for example, in Laguna Edita the top of the long core has C/N ratios of around 10.4 and δ^{13}C values of -30.3‰, and the bottom of the short cores have corresponding values of 11.5 and -29.74‰. In Laguna Meche the top of the long core has C/N ratios of around 16.1 and δ^{13}C values of -27.2‰, and the bottom of the short cores have corresponding values of 14.8 and -29.5‰. The %TOC and magnetic susceptability values are also comparable. As the tops of the long cores do not include the AD1891 Mt. Hudson ash found at the bottom of the short cores, these cores definately do not overlap.

11.2.2 Between-Lake Similarities and Differences

11.2.2.1 Stratigraphic Differences

At the macro/visual level, the stratigraphies presented here are both consistent with each others and with the stratigraphy for Laguna Augusta (Villa-Martínez *et al.*, 2012), although Laguna Augusta is a marl lake and is thus has a higher inorganic component. Specifically, the two basal tephra layers are present in all three lakes (Villa-Martínez *et al.* ascribe the upper unknown eruption to Mentolat or Maca) and the dates for these events are consistent among the three sequences. Villa-Martínez *et al.* also observe uninterrupted organic sedimentation from *c.*8,000 years B.P. onwards, although the lack of radiocarbon dates beyond 7,583 years B.P. for Laguna Augusta limits this interpretation.

The magnetic susceptability results show a number of events common to both lakes (Figure 11.1); some have been positively identified as tephra events, others are likely to be tephra but have not been proven as such. The identical visual stratigraphies in both lakes from the H1 tephra event to the tops of the cores adds confidence in the integrity and equivalence of the cores above this ash, although the differences below this layer deserve further discussion.

The most important difference is that organic sedimentation starts before the H1 eruption at Laguna Edita, gradually grading from a blue-grey clay, whereas Laguna Meche shows the dominance of minerogenic sedimentation right up until H1, where it shifts suddenly to organic sedimentation. This could be in part because development of soils in the higher altitude catchment are delayed compared to Laguna Edita; the increasing productivity in both the catchment and lake that cause organic sedimentation were delayed at Laguna Meche compared to Laguna Edita due to the higher altitude and delayed tree-line migration up-slope. However, the sudden shift is unexpected — a gradual shift from mineral to organic-dominated sedimentation is common in post-glacial lake development sequences. Alternatively, there may be a trunucated record at Laguna Meche. When the dates for the establishment of highly organic deposition from Laguna Augusta (9,900 years B.P.), Laguna Edita (8,500 years B.P.) and Laguna Meche (8,200

years B.P.) are combined, a negative relationship between the establishment of organic sedimentation and altitude is apparent, suggesting the former interpretation is correct.

Both lakes exhibit surprisingly late onset of organic sedimentation. Gyttja accumulation begins shortly before H1, dated at 8,200 years B.P. The current evidence for ice retreat in the valley suggests ice-free conditions at the lakes from 13,500 years B.P. (see Section 4.2.2), and both lakes lie above the maximum inferred height of the Lateglacial proglacial lake that filled the valley, thus the delayed onset appears unusual. It appears there was a period of deposition of blue clays, which are difficult to date due to the lack of organic remains, although a fragment of aquatic plant macrofossil from the clays in Laguna Meche yielded an age of 10,898±154 years B.P. This indicates the depositional environment from as early as 11,052 years B.P. to the H1 eruption was a slowly accumulating, low productivity environment. It is highly likely that there was residual perennial ice in the catchment at this time, but full glacial gemorphological mapping of the locale is required to confirm this.

11.2.2.2 Carbon Geochemistry

The carbon geochemistry differs between two lakes — this is shown in Figure 11.2. Laguna Meche has a considerably higher C/N than Laguna Edita, whereas Laguna Edita has generally lower δ^{13}C values. Following the interpretations for the carbon data detailed in Section 8.3.2, this suggests Laguna Edita has a more autogenic, algal source of carbon and, conversely, Laguna Meche a more important allochthonous source of carbon. This is a function of the lower productivity and higher catchment instability characteristic of the higher altitude of Laguna Meche. Few high-altitude lakes in Patagonia have been studied, but in European lakes nutrients are found to be more dilute in higher-altitude lakes (Müller *et al.*, 1998; Mosello *et al.*, 2002), and mountain environments are well understood to have higher catchment instability and higher weathering rates with altitude (Gerrard, 1990; French, 2007).

11.2.2.3 Chironomids

The differences in the chironomid compositions are clearly represented in a PCA (Figure 11.3). They suggest the primary control on faunal difference between the two lakes is related to lake depth. The dominant axis 1 variation is also present when both lake faunas are plotted passively on a PCA of the training set data (Figure 11.4). Massaferro and Larocque-Tobler (2013) do not rank the importance of the five environmental variables that best explained the variation in the modern calibration set (Secchi depth, conductivity, depth, MAT and water temperature), but other published training sets consistently put water depth and temperature as the most important explanatory variables (Nazarova *et al.*, 2010; Rees *et al.*, 2008; Olander *et al.*, 1999; Luoto, 2009b; Larocque *et al.*, 2001). This is in keeping with Pinder (1995), who asserts the importance

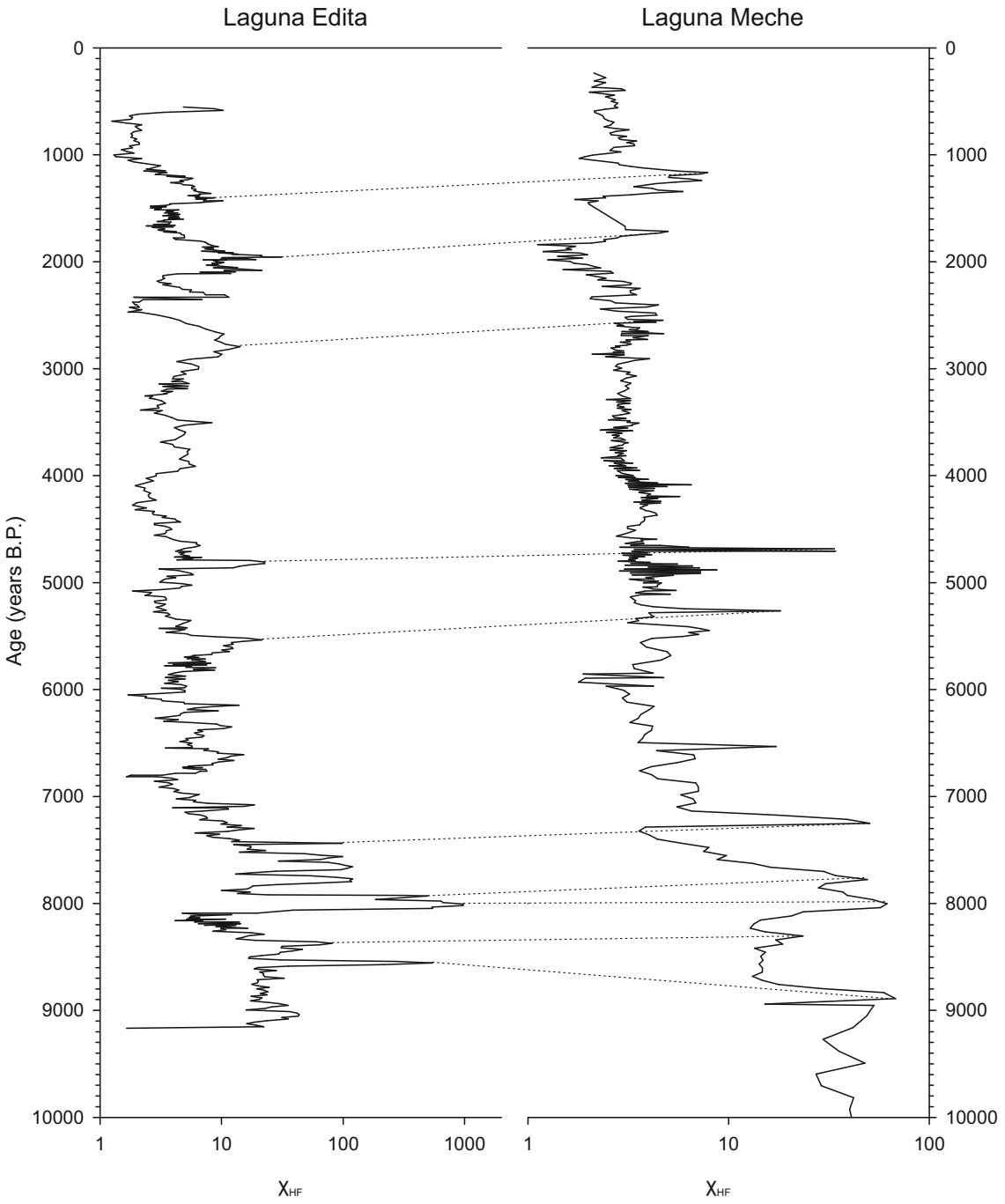

FIGURE 11.1: Magnetic susceptability of Laguna Edita and Laguna Meche long cores, showing possible correlations between events. The errors between these events are within the 1σ errors of the age/depth model, but with further tephrochronological work age-equivalence could be established and age/depth model errors reduced.

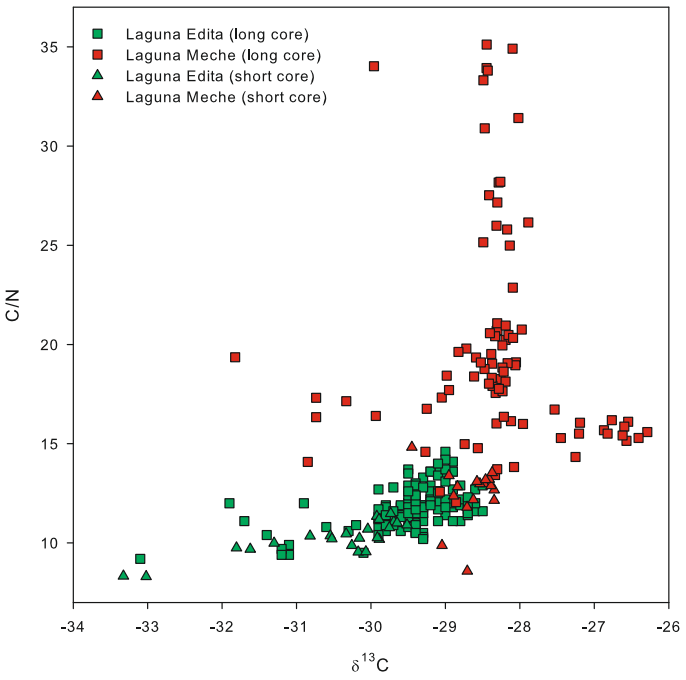

FIGURE 11.2: C/N *vs.* δ^{13}C for Laguna Edita and Laguna Meche long and short cores.

of water depth and lake chemistry conditions in controlling chironomid faunal compositions at the local scale. Given the failure of the training set to reflect the expected temperature difference between the two lakes (Section 8.4.5) it seems likely that water depth is a more important explanatory variable than temperature; the coring depths reflect this to some extent. This study reinforces the points made by Juggins (2013) on the importance of giving due consideration to secondary variables in transfer functions.

11.2.3 Differences in Lake Response to Environmental Change

Differences in the sensitivity of the two study sites to climatic forcing were expected because only Laguna Meche lies above the regional evaporation line. In addition the catchments differ in vegetation and relief, and high-altitude lakes near the tree-line, like Laguna Meche, are generally considered more sensitive to environmental changes. Furthermore, Laguna Edita appears to have a significant groundwater input which buffers changes in lake level (Section 8.2). This is borne out in the data, as Laguna Edita exhibits fewer changes that are of a generally lower magnitude than the record from Laguna Meche. In Laguna Edita, the δ^{13}C and C/N values are remarkably stable from 7,800 years B.P. onwards; this is not the case in Laguna Meche, where large excursions in both punctuate the record. With regard to the chironomid records, the importance of the species composition in determining the utility of chironomid-inferred temperature reconstructions is exemplified by the apparently poor Laguna Meche reconstructions, where the fauna is dominated by taxa that have strong affinities with vegetation and/or flowing water. This is perhaps unsuprising given the strong role of of allochthonous

inputs to Laguna Meche (see Section 10.3.1).

The slightly marginal coring locations chosen for the long cores may have influenced this situation. Slightly marginal positions were selected because the centres of these lakes were impractical to core with the available rod-driven equipment due to their depth. It is evident from the dual short cores from Laguna Edita (see Section 7.3.2.4) that there are important differences in the faunal composition of cores obtained from the centre and more marginal positions in these lakes. This echoes the findings of Kurek and Cwynar (2008a); Velle *et al.* (2012), where a transect of samples showed considerably different faunas in the accumulated sediments. Coring from the centre of the lake, even if it were practical, would not neccesarily provide better temperature reconstructions (*sensu* Heiri *et al.*, 2003; Heiri, 2004); deeper, central parts of the lake are more stable environments and can be insensitive to climatic changes, and the assumption of sediment focussing integrating chironomid remains from the lake does not necessarily hold true (ibid). Rather, a transect of cores would be necessary to elucidate the profundal–littoral gradient and differentiate within-lake faunal gradients from climatically driven changes down-core. The following interpretations are cautious in differentiating lake level and temperature changes from chironomid faunas where other proxy evidence does not agree or offer further insight on the chironomid interpretation.

11.3 Interpretation of Proxies in the Chacabuco Valley

11.3.1 The Link Between Carbon and Climate

The interpretation of C/N ratios as indicative of source carbon is a relatively straitforward and robust model that is supported by the modern catchment survey data. Because bulk material was analysed, a fall in C/N could be due to a fall in autogenic productivity and/or a rise in the flux of catchment derived material, and *vise versa* (Section 8.3.1). These changing sources can be variously attributed to climatic or catchment changes and these are discussed fully in Section 8.3.1.

The interpretation of δ^{13}C is more complex, and discussed more fully in Section 8.3.2, but, noteably, changes in δ^{13}C occur without concurrent changes in C/N. Phases like this occur in Laguna Meche (1,300–200 years B.P.) and Laguna Edita (8,800–8,690 & 8,570–8,290 years B.P.) This could be due to an increase in relative phytoplankton abundance, or a change in oxidation state or lake volume. Given the relationship between chironomid fauna and lake volume (see Section 11.3.2 below), the lack of simultaneous chironomid change during these phases leaves an increase in phytoplankton activity as the most likely explanation for these reduced δ^{13}C phases.

Phytoplankton dependence on light and nutrients means that an increase in phytoplankton activity is associated with low turbidity, allowing good light penetration,

and/or increased nutrient availability. The occurence of periods of increased phytoplankton activity near to the start of organic sedimentation in the lakes can be explained as part of the normal lake development, as there is good micro-nutrient availability from basal clays and supply of macro-nutrients increases; nitrate and phosphate builds as food-chains and nutrient cycles becomes established. The phytoplankton activity is reduced as the turbidity increases and the availability of micro-nutrients decreases relative to previous conditions.

11.3.2 The Link Between Chironomid Fauna and Climate

Massaferro and Larocque-Tobler (2013) demonstrate that the transfer function used in this study suggests that air temperatures and water temperatures are important factors in controlling chironomid fauna in Patagonia, although turbidity, conductivity and depth are also important. This set of secondary variables are representative in many ways of the profundal/littoral spectrum (see also Sections 5.6.2 & 5.6.3). Data presented in Section 8.4.4 demonstrate that the transfer function in its current form fails to adequately represent the temperature differences induced by altitude between the two study sites, although there is limited evidence that reconstructed trends of recent climate presented in Chapter 7 show the expected pattern of 20^{th} century global climate change.

A PCA ordination of all the chironomid data in this study (Figure 11.3) clearly differentiates the lakes on the strong (eigenvalue=0.56) axis 1 gradient. This gradient is characterised by taxa indicative of deep, profundal conditions at one end, and of sub-littoral, macrophyte associated and lotic species at the other. This suggests that axis 1 of this ordination represents the profundal/littoral spectrum, and that factors like water depth and turbidity are the primary controls on chironomid populations in the valley, explaining the failure of the transfer function to pick out the temperature difference between the lakes. Although there may be some utility in the temperature transfer function results, the data show that the chironomid data are more likely to provide a records of lake level and weaker temperature reconstruction data, not least beause the fauna appears to respond to the littoral/profundal gradient and there is a significant lotic input. In this sense, the PCA axis 1 scores are likely to reflect lake level change.

In Figure 11.4 the samples are plotted passively on an ordination of the training set data (Massaferro and Larocque-Tobler, 2013). It shows that the vast majority of the samples sit well within the environmental limits of the training set data, and as such the training set data are a good fit to the fossil data in this study (*c.f.* Bigler *et al.*, 2002). If the temperature reconstructions presented here were to be accepted as an indicator of relative temperature change, it is useful to compare the record presented here to those chironomid-inferred temperature records both quantitative and qualitative already published (Massaferro and Larocque-Tobler, 2013; Massaferro *et al.*, 2005, 2013, 2009; Massaferro and Brooks, 2002). Figure 11.5 summarises the available quantative Holocene

chironomid data for Patagonia, including the data presented here. It is clear that the cooling seen in Laguna Potrok Aike, in the Argentinian steppe *c.*52°S, after 4,000 years B.P. (Massaferro and Larocque-Tobler, 2013) is not reflected in the chironomid-inferred temperatures in the Chacabuco Valley. Rather, in Laguna Edita, inferred temperatures rise slightly after 3,500 years B.P. The evidence presented in Chapters 7 and 8, combined with the argument presented above for water depth being the most most likely the most important environmental variable in these data, along with the lack of consistency of these records with the temperature record of Laguna Potrok Aike strongly suggests that the quantative temperature inferences from these two sites are unreliable.

11.4 Summary of Holocene Palaeoclimatic History of the Chacabuco Valley

One aim of this study (Section 2.4) was to provide a palaeoclimatic history for the Chacabuco Valley. Section 4.2.2 outlined the Late-glacial and early Holocene palaeoclimate of the valley, suggesting deglaciation of the valley floor around 15,000 years B.P. (Turner *et al.*, 2005), and subsequent pro-glacial lake occupation of the valley until 13,500 years B.P. (Hein *et al.*, 2010). Organic sedimentation starts in lakes in the base of the valley around 13,000 years B.P., and some 4,000 years later in the higher catchments of Laguna Edita and Meche, although there is good evidence of inorganic sedimentation from as early as 13,000 years B.P. The totality of this evidence suggests that the period between 13,000–8,500 years B.P. was characterised by a low productivity environment, probably due to low temperature and/or low rainfall, although the *N.dombeyi* forest was gradually developing throughout this period. It is unknown at which altitudes *Nothofagus* was developing at at this time; further pollen work from these sequences would be beneficial but is outside the scope of this study. The possibility of the persistence of ice in the catchment would probably not affect regional forest, but may well have been quite close to the lake, a configuration analogous with Alpine lakes like Meidsee in the Valais Alps (Thevenon *et al.*, 2012). At 8,500 years B.P. *N.dombeyi* forest development achieving roughly pre-European settlement conditions (Villa-Martínez *et al.*, 2012) and organic sedimentation begins in the higher catchments in the Tamango Range of the Chacabuco Valley.

The high frequency, low amplitude variation in a number of palaeoenvironmental indicators from Laguna Edita and Laguna Meche in the Tamango range reduces from around 5,000 years B.P. and lake productivity also increases slightly in the mid-Holocene. A mid-Holocene warm/wet event occurs between 6–5,000 years B.P. There is evidence for a reduction in precipitation between 2,800–1,300 years B.P., and a subsequent reduction in lake volume at this time. There is also evidence of less productive lakes in the late Holocene, from *c.*1,500 years B.P. onwards, possibly as a result of cooler water.

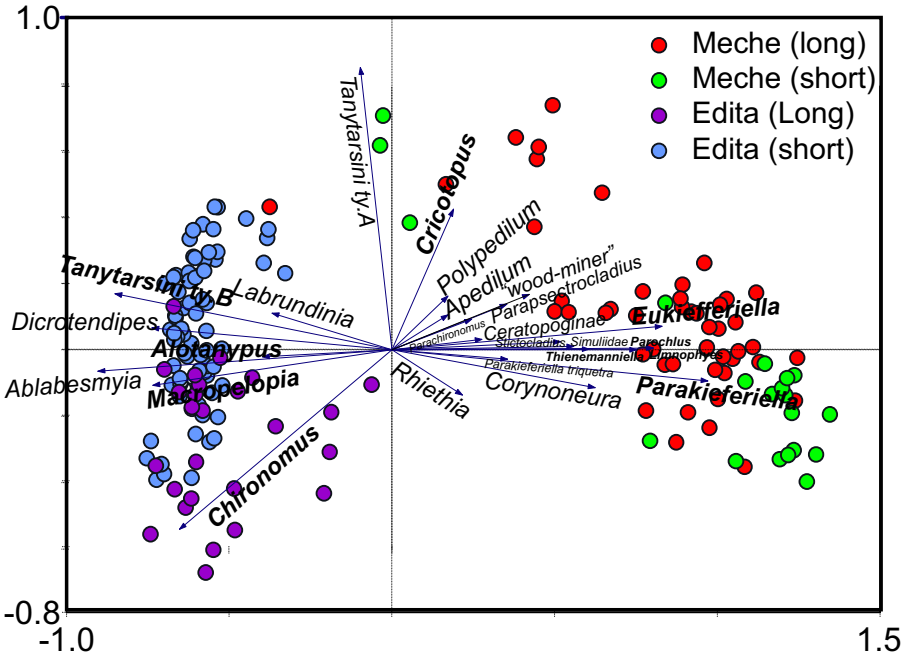

FIGURE 11.3: PCA scores from Laguna Edita and Laguna Meche long and short cores. Calculated using Canoco v.4, using scaling focussed on inter-species correlations, species scores are expressed divided by their standard deviation. Species data were square-root transformed and centred by normalization. Eigenvalues are 0.56 and 0.07 for axes 1 & 2 respectively.

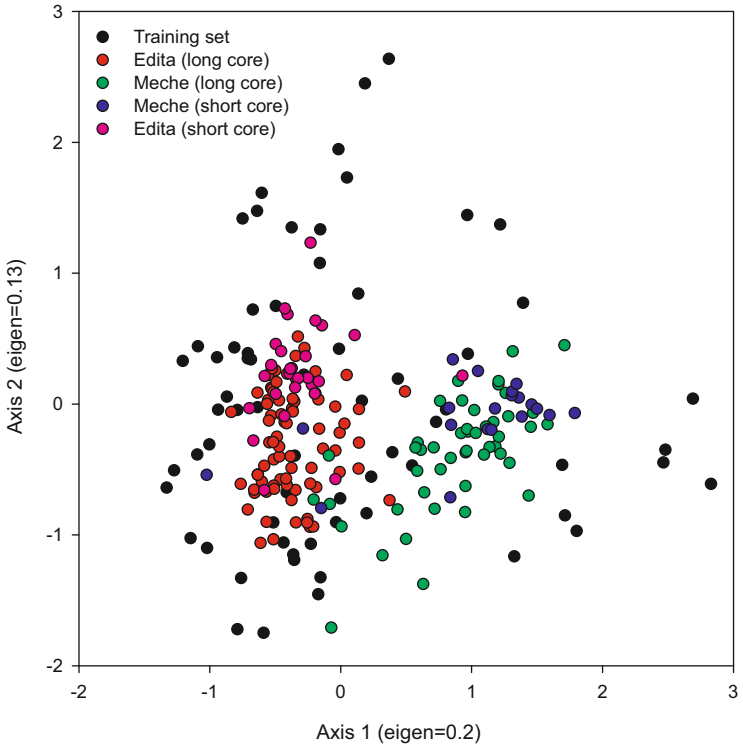

FIGURE 11.4: PCA scores of all Chironomid data in this study plotted passively on a PCA of training set data from Massaferro and Larocque-Tobler (2013). Calculated using Canoco v.4, using scaling focussed on inter-species correlations, with species scores expressed divided by their standard deviation. Species data were square-root transformed and centred by normalization.

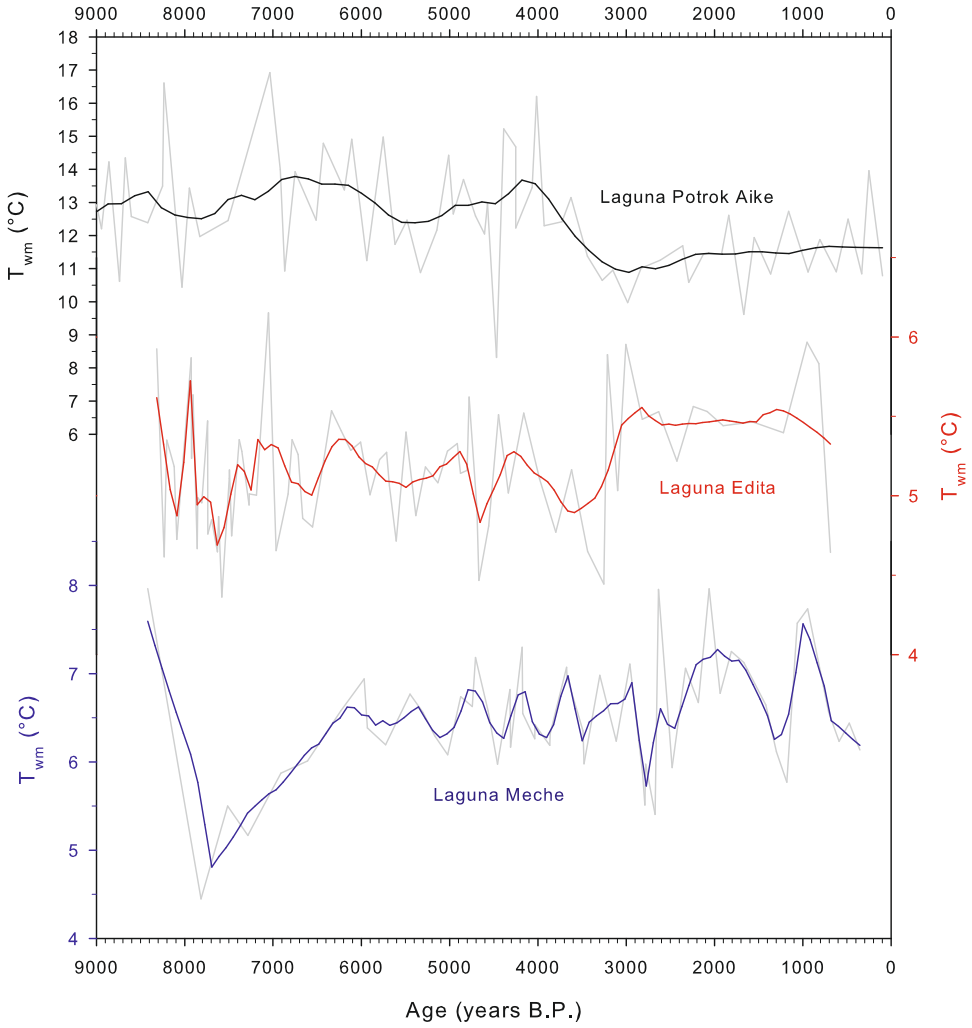

FIGURE 11.5: Chironomid inferred temperatures from Laguna Potrok Aike, Laguna Meche and Laguna Edita. Laguna Potrok Aike data digitised from Massaferro and Larocque-Tobler (2013), all data shown with LOESS smoothing.

11.5 Comparison With Regional and Global Palaeoclimate Records

This section compares the records summarised in the previous section with those previously published, firstly for the Chacabuco Valley and secondly for the wider Patagonian region. The third subsection briefly compares and discusses the palaeoclimatic history of Patagonia, and the main palaeoclimatic events as identified in this study (Section 11.4), to the Holocene palaeoclimatic records for Antarctica, New Zealand and elsewhere.

11.5.1 Comparison With Proximal Records

As discussed in Section 2, there is a paucity of palaeoclimatic histories for the Holocene that are proximal to the site. In the Chacabuco Valley a pollen and charcoal

stratigraphy is presented for Laguna Augusta which infers stable vegetation conditions from 9,800 years onwards in the study area (Villa-Martínez *et al.*, 2012). Villa-Martínez *et al.* explain that the dominant vegetation type (*Nothofagus pumilio* deciduous forest) is unlikely to be sensitive to climate changes as it occupies a transitional ecological niche with wide precipitation tolerance, although *Nothofagus*/Poaceae ratios may provide some additional information (*e.g.* Moy *et al.*, 2008). This is likely why changes in more sensitive proxies (like the data presented in this study) reflect changes where pollen data do not. Pollen stratigraphies alone are probably not useful indicators of palaeoclimatic change for this region; for example, none of the Holocene climatic events identified in Section 11.4 are reflected in the pollen record.

11.5.2 Comparison with Patagonian Climate Records

11.5.2.1 Early Holocene Changes

Fletcher and Moreno (2012a) suggest generally drier conditions due to reduced westerly wind strength between 8–11,000 years B.P. based on pollen stratigraphy; the increase in wetness from *c.*8,000 years B.P. onwards coincides with the start of organic sedimentation in the Chacabuco Valley. It is possible that the drier conditions prior to *c.*8,000 years B.P. led to generally lower catchment biomass and lake productivity, although the presence of organic sedimentation early in the Laguna Augusta record (Villa-Martínez *et al.*, 2012) indicates the late onset of organic sedimentation is more likely due to delayed vegetation and soil development and stabilisation due to the cooler conditions at altitude, steeper catchment slopes, and residual ice within the catchment.

11.5.2.2 Local Wet/Warm Event Between 5–6,000 Years B.P.

Villa-Martínez *et al.* (2012) do not discuss an obvious, sudden and relatively long decline in macroscopic charcoal concentration between 5–6,000 years B.P. that occurs in the stratigraphy they present; this is coincident with a depression in δ^{13}C, increase in C/N & %TOC and some significant changes in the chironomid fauna in Laguna Edita. A switch in the dominant species from Tanytarsini to *Parakiefferiella* suggests a change in source carbon, and a reduction in both δ^{13}C and increase in C/N is very likely to represent an increase in the proportion of allochthonous carbon to the lake (see Section 8.3.2). A reduction in macroscopic charcoal at this time suggests a local reduction in burning frequency and magnitude, possibly as a result of temperature reduction but more likely as a result of an increase in precipitation. Considering a temperature reduction would decrease productivity, but there is increased %TOC and no change in δ^{13}C, this can be discounted, and there are other reasons (like a change in summer ignition conditions) that can cause lower charcoal occurrence. As such, the explanation of a increased

effective precipitation caused by increased rainfall, at least in summer, is the most parsimonious interpretation of these data.

This 1,000 year event coincides with a period of elevated sea surface temperatures (SST's), salinity, opal and iron in waters off the Chilean coast around 41°S (Lamy *et al.*, 2001, 2002, see Figure 11.6); the former is indicative of continental rainfall in southern Chile and the latter indicative of decreased advection of subpolar water to the fjord region. Lamy *et al.* (2001, 2002) demonstrate wetter conditions in areas north of this study site, and infer a southerly shift of the westerlies at this time. This is consistent with Holocene maxima in other regions at this time, including the Ross Sea (Masson, 2000) and the Antarctic interior (Steig, 1998), suggesting a poleward shift of the polar front and enhanced westerly winds at this time. For Laguna Meche δ^{13}C changes independent of C/N changes are indicative of increased or decreased productivity (Section 10.5). Lake productivity is partly a function of temperature (Wetzel, 2001) but may also be affected by lake volume concentrating or diluting dissolved nutrients. It appears that the wet/warm event in Laguna Meche around 5–6,000 years B.P. is also reflected in Peru-Chile current sea surface temperatures, but data from Laguna Edita do not show any excursion during this period. Because Laguna Edita has a significant groundwater input (Section 8.2) it is less sensitive to lake level changes, indicating this event may be a lake level, rather than a temperature change.

11.5.2.3 Evidence of a mid-Holocene Climate Shift in the Chacabuco Valley

Variability in the chironomid fauna and the small-amplitude, high-frequency C/N variations in Laguna Edita become muted from 4,000 years B.P. onwards. In Laguna Meche the last bimodal switch in organic carbon geochemistry occurs at 5,000 years B.P. In addition, the highly variable chironomid stratigraphy for Laguna Edita prior to 5,000 years B.P. suggests unstable lake conditions prior to 5,000 years B.P. However, there is no difference in the mean chironomid populations pre-and post 5,000 years B.P.; it is only the variability that changes.

These records do not show a fundamental change in long-term lake conditions, and as such the data are consistent with the pollen stratigraphy for the valley (but see Section 11.5.1) and sites at similar latitude west of the Andes where no major mid-Holocene climate shift is observed (Massaferro *et al.*, 2005; Massaferro and Brooks, 2002). The climate history for this region differs from more northerly regions, where the majority of the evidence for a mid-Holocene shift in climate originates (see Section 3.3.1), as well as evidence for a similar shift in areas south of these sites (Markgraf *et al.*, 2003). If the site were at the margin of the westerly winds up until 5,000 years B.P., the chironomid population may be unstable because the site would be on a boundary between a maritime and semi-arid climate where polar and easterly airmasses are more influential than the present day.

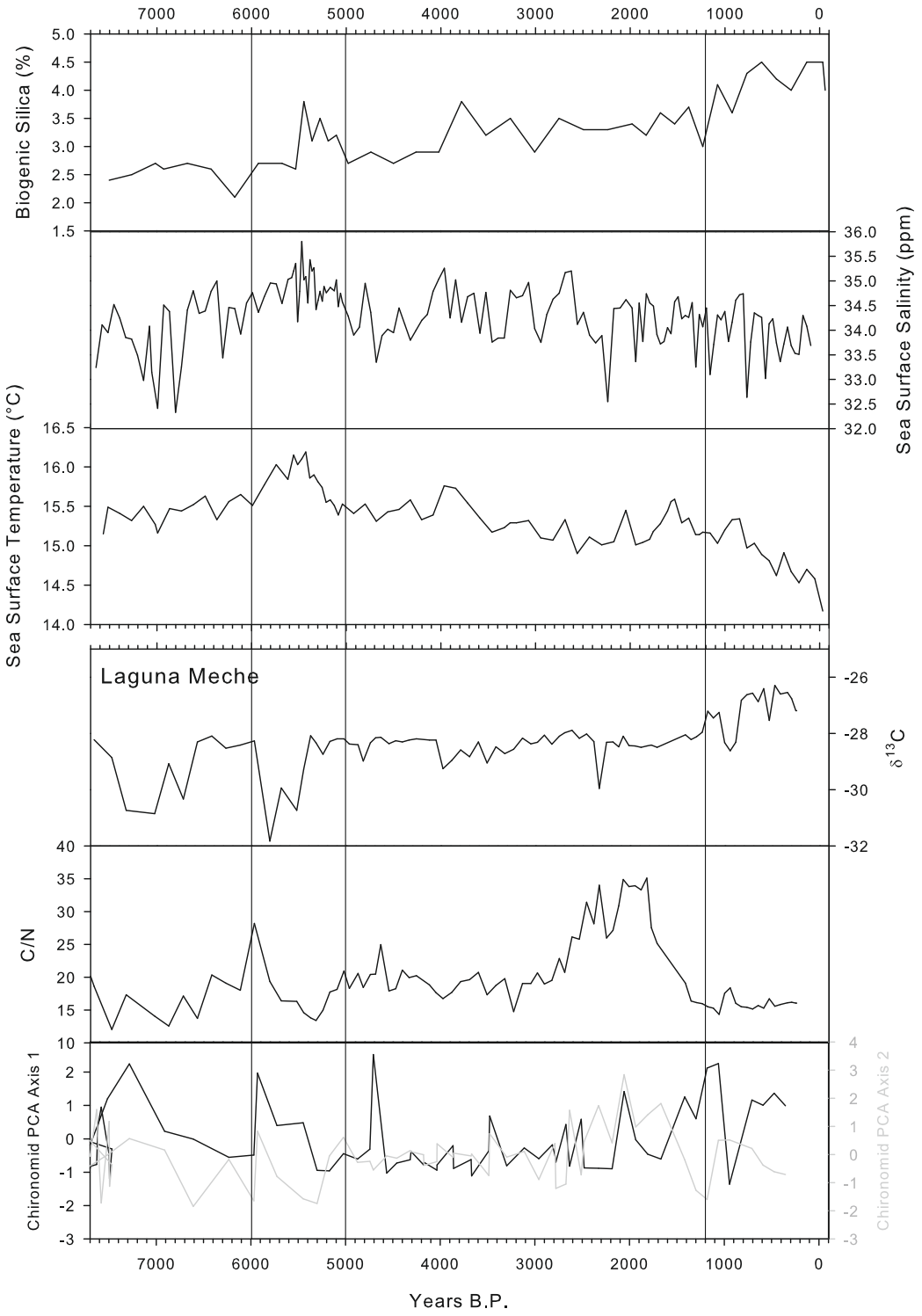

FIGURE 11.6: Palaeoenvironmental data for Lamy *et al.* (2001, 2002) and carbon C/N, δ^{13}C and chironomid PCA data for Laguna Meche. The events between 5–6,000 years B.P. and from 1,200 years B.P. onwards, mentioned in the text, are highlighted.

This reinforces the hypothesis, presented in Chapter 3, that central Patagonia defines a unique climate space between the northern and southern regions. The mid-Holocene shift observed in the northern and southern regions has previously been attributed to zonally weaker westerlies focussed in more northerly latitudes in the early Holocene, shifting south and becoming meridionally stronger and seasonally more variable in the late Holocene (Haberle and Bennett, 2004). Villa-Martínez *et al.* (2012) suggest a slight rise in long-range transport of *P. nubigena* between *c.*2,000–5000 years B.P. represents increased entrainment of pollen from more westerly areas (higher westerly winds) and/or a vegetation response to cooler/wetter conditions in the source areas, but find no evidence for local climate change at this time. Being located in the centre of the westerly wind belt these sites are relatively insensitive to latitudinal shifts in the exent of the westerlies, but are sensitive to the strength of the westerlies (see Chapter 3). As such this study cannot fully support the interpretation of a mid-Holocene strengthening of the westerlies suggested by Villa-Martínez *et al.*, but rather indicates a possible shift in the stability of the westerlies in the region from the mid-Holocene to the present day.

11.5.2.4 Regional Aridity Between 1,300–2,800 years B.P.

The strongest evidence for palaeoclimatic change in these cores comes from Laguna Meche where a rise in %TOC, C/N, and chironomid PCA axis 2 scores (driven by *Limnophyes*, *Eukiefferiella* and Orthoclad. "wood-miner") occurs between 2,800 and 1,300 years B.P.

The increase in C/N without any accompanying change in δ^{13}C does not preclude a change in carbon source because δ^{13}C, stable at *c.*-28.5‰ throughout much of the Holocene, could encompass a range of sources including aquatic plants, terrestrial vegetation, grass or trees (Figure 8.2). However, C/N values >17 are characteristic of a predominately (semi)terrestrial source of carbon. The presence of chironomids with associations with aquatic vegetation, along with higher %TOC support the conclusion that this is indicative of semi-terrestrialisation rather than full terrestrialisation of the lake, at least at the coring location.

This phase is co-incident with a reported drier phase between 2,400–1,450 years B.P. at Laguna Stibnite, in the Taitao Peninsula *c.*46°S (Massaferro and Brooks, 2002). Chironomid data from Laguna Stibnite indicate elevated temperatures during this period, although this contrasts with cooling at this time further afield in southern Patagonia (*e.g.* Massaferro and Larocque-Tobler, 2013). Regional pollen and charcoal diagrams indicate increased fire abundance at this time, suggesting more arid conditions (Haberle and Bennett, 2004, pp.2440 & 2442), although local records do not reflect this (Villa-Martínez *et al.*, 2012) and across Patagonia there are indications of more humid conditions at this time (see Section 3.3.3.1 and references therein). Arid conditions on both the east and west side of the North Patagonian Icecap indicate that there was no increased rain shadow due to expansion of the North Patagonian Icecap. Lake Shamen

(44°S) shows further evidence of increased fire-episode frequency between around 1–2,500 years B.P., indicating drier and/or warmer conditions, although human ignition agents are also considered important at this time (de Porras *et al.*, 2012).

The C/N and chironomid data from this study point to generalised aridity in the central Patagonian region during this time, and although the lack of temperature or lake level reconstructions in northern Patagonia prevents bounding the extent of the warming, an opposite (cooling) trend observed in data from Laguna Potrok Aike (52°S; Massaferro and Larocque-Tobler 2013; Massaferro *et al.* 2013) bounds the southern extent of this aridity.

It is possible that the magnitude of the increase in temperature or reduction in rainfall during this event is great enough to affect lake level in Laguna Meche, but not in Laguna Edita, probably due to one being at higher elevation and the other below the LEL. In addition, modern surface water data suggest Laguna Edita may recharge in part from a groundwater source (Section 8.2). Two hypotheses are proposed to explain the reduced volume of Laguna Meche:

- The westerly winds bring moist air from the Pacific; a reduction in the strength of the westerly winds would have the effect of reducing rainfall over the region, thus reducing precipitation input to lakes. This would reduce lake levels without increasing in temperature, a situation supported by the data presented in this study.
- A change in regional temperatures, a possibility proposed by Massaferro and Brooks (2002) from the Laguna Stibnite record, would have the effect of increased evaporative losses. Changes in temperature can be seasonal or uniform. Warmer summers would explain increased evaporative losses. The AAO may be implicated (Garreaud *et al.*, 2009).

Because of uncertainties with interpreting the chironomid data as representative of temperature it is not possible to confidently discern between these possibilities soley using the proxy data. Because Laguna Meche is above the regional evaporation altitude, the lake is not currently evaporative — it would require a significant increase in temperature to change this situation, but the lake is sensitive to any change in precipitation, a reduction in the strength of the westerly winds and thus precipitation is the most likely explanation. In addition, there may be considerable auto-correlation between precipitation and temperatures, depending on the mechanism implicated in their moderation (see Section 3.2).

This period occurs at a time where neoglacial expansion is observed in some more southerly and northerly regions in South America (Rodbell *et al.*, 2009). Inferred cooling and/or increased precipitation in extreme northerly and southerly areas but not in the core of the westerlies suggests changes in ENSO, PDO or SAM/AO are implicated. In

southern Patagonia El Niño events are associated with warmer, drier conditions whereas in northern Chile ($<c.50°$S) they are associated with drier and cooler conditions. Alternatively, a trend towards positive SAM/AO would cause warmer conditions between 40–50°S, but likely to cause colder, wetter conditions in southern Chile (Section 3.4.2.2), in keeping with records presented by Chambers *et al.* (2007).

11.5.2.5 Lower Lake Level Post-1,300 years B.P.

In Laguna Meche lower δ^{13}C from 1,300 years onwards suggests lower productivity in the lake from this time onwards, and cooler conditions are also inferred from *c.*2,000 years B.P. onwards in Laguna Edita. The latter co-incides with inferred cooler conditions in northerly ocean cores around 41°S (Lamy *et al.* 2001, 2002; see Figure 11.6). Figure 3.13 and Section 3.2 demonstrate that in central and northern Patagonia, the relationship between mean annual temperature and precipitation is weaker. The data from Laguna Meche indicate less a productive lake, possibly as a result of cooler conditions, and reduced effective precipitation at this time (Section 10.6), in keeping with the positive temperature *vs.* precipitation relationship described in Section 3.2. This situation could be caused by fewer storm tracks bring warm, moist air from the Pacific. Laguna Edita does not reflect these changes in the same way, although there are changes in the chironomid fauna (Section 9.2.4.1). Chironomid interpretation from similar latitudes west of the Andes suggest a "[period] of low precipitation ... between 2,400 ^{14}C years [2,460 cal. years B.P.] and the present day" (Massaferro and Brooks, 2002, p.108) — although the onset is earlier, this is consistent with drier conditions from the Late Holocene to the present day.

Moy *et al.* (2002) present a reconstruction of ENSO variability for the Holocene that indicates the occurence of ENSO events becomes more regular from around 1,500 years B.P. onwards, reaching a peak at around 900 years B.P. In central Patagonia, ENSO events are associated with drier, cooler conditions consistent with lower productivity at this time; this is consistent with lower productivity observed in the lake at this time. Drier conditions are also observed in quantitative precipitation reconstructions from Cerro Frias (50°S) but not Laguna Aculeo (34°S) at this time (shown in Figure 11.7).

11.5.2.6 Climate and Causation in Patagonia

Chapter 3 outlined the concept of three main climate sectors in Patagonia (northern, central and southern) and outlined trends and differences between them. The data presented here are consistent with other data from the central region, particularly with respect to early-Holocene stabilisation of climate and the presence of a late-Holocene climate event, but this palaeoclimatic history is also consistent with features of northern climate, for example late-Holocene productivity changes as recorded off the coast of Chile at this time. Southerly climate features like the 8,200 years B.P. event and 2,400

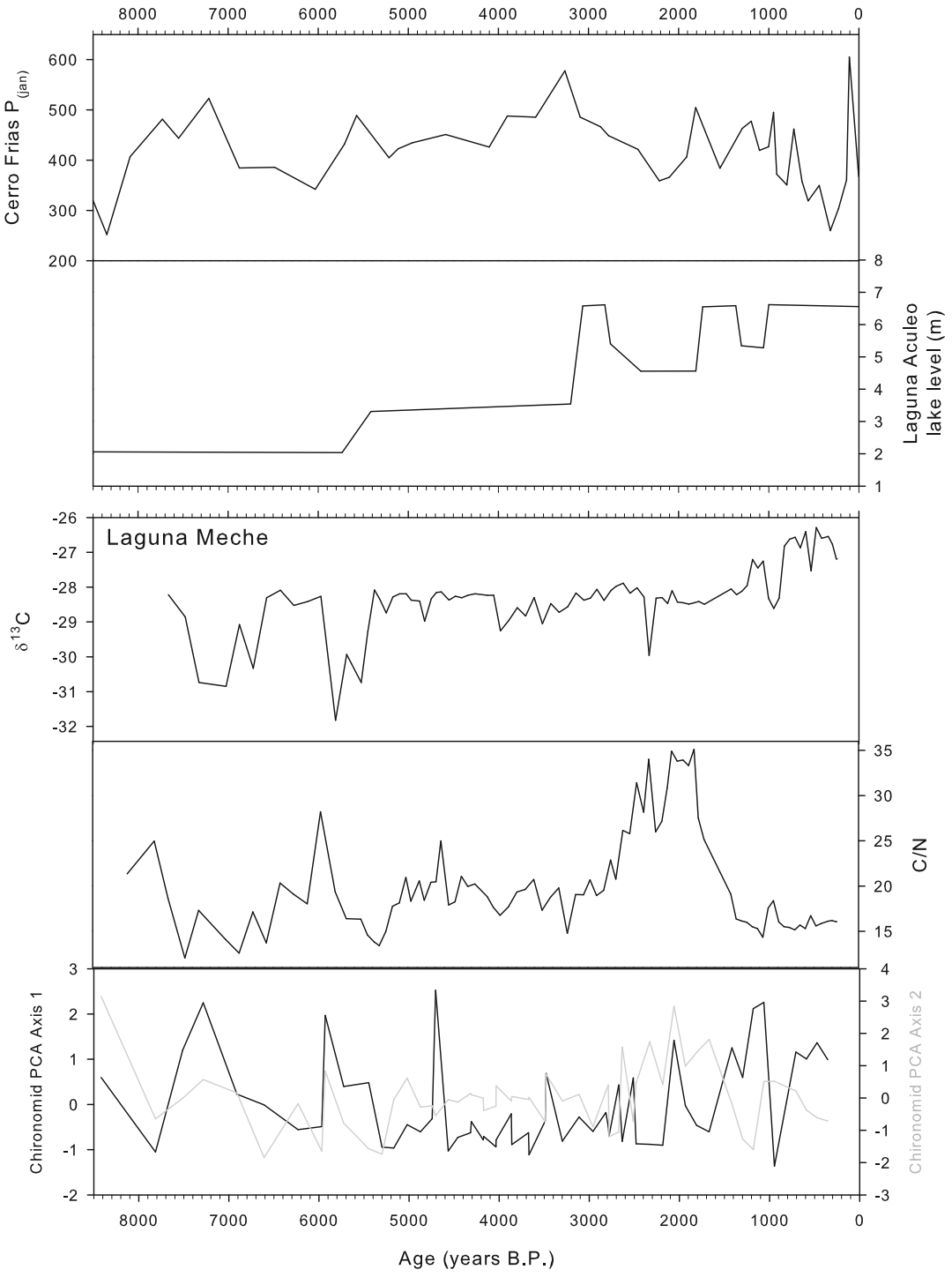

FIGURE 11.7: Cerro Frias (Tonello *et al.*, 2009) & Laguna Aculeo (Jenny, 2002) precipitation reconstructions, redrawn from the aforementioned sources, and Laguna Meche carbon and chironomid data.

years B.P. event are not well defined in central Patagonia. The subtle differences between regions should be considered when designing future studies or comparing palaeoclimatic records for Patagonia.

Section 3.3.4.6 discussed the various mechanisms proposed by which changes in the southern westerly winds have modulated palaeoclimate in Patagonia. By virtue of these sites position firmly within the core of the modern westerly winds, any palaeoclimatic changes linked to the westerly winds will be directly reflecting the strength, not the position of the westerlies — this does not preclude shifts in the westerlies, as a shift in the westerlies may also affect the strength, but it does allow a narrowing of the possible options concerning the nature of changes during the Holocene. For example, since no major reconfigurations are seen at the mid-Holocene, but are present in northern and to some extent southern Patagonia, a mid-Holocene expansion of the westerlies, rather than a strengthening thereof, better explains the absence of a mid-Holocene shift in the central region. As such, assertions of generally "enhanced" windspeeds from 5,000 years B.P. onwards (*e.g.* Iglesias *et al.*, 2011) cannot be supported by this study, although local enhancements in areas peripheral to the core westerlies may still have occured (*e.g.* Heusser, 1982; Ashworth *et al.*, 1991). Another subset of postulated hypotheses/explanations regarding the mid-Holocene climate shift includes the possibility that the westerlies shifted equatorward (Sottile *et al.*, 2011; de Porras *et al.*, 2012; Moreno *et al.*, 1999), and the data presented here do not support nor disagree with this. To fully distinguish between shifts and strengthening of the westerlies, a more complete dataset on palaeoclimatalogical change across both the latitudes and longitudes of southernmost South America is necessary (see Chapter 12).

Late-Holocene events observed predominately in palaeoclimatic reconstructions from the north and central regions are present in this study. This study adds to the mounting body of evidence for regional aridity around 1,300–2,800 years B.P. (see Section 11.5.2.4). Because regional moisture is positively linked to precipitation (Figure 3.2) it may be fair to implicate less strong westerly winds as a causal factor in this observed aridity. ENSO modulation of SST's is known to cause drier and cooler conditions in central Patagonia, which would explain the event observed in these and other records, particularly the similarities between the record presented here and those of SST's from the Peru-Chile Current (Figure 11.6). High resolution peat and lake records for central Patagonia would greatly assist in explaining the climatic causation of this event — numerous suitable archives exist around the Chonos Archipelago and the vicinity of Coyhaique, for example.

11.5.3 Comparison with Global Climate Records

Antarctic temperature proxies suggest an early Holocene optimum (Augustin *et al.*, 2004), as do northern hemisphere records (Mayewski *et al.*, 2004; Wanner *et al.*, 2008). This early Holocene optimum is also observed in southern hemisphere terrestrial records (McGlone *et al.*, 2004). Augustin *et al.* (2004) also identify cooler conditions centered on

8,500 years B.P. and a gradual rise in temperatures until they stabilise at around 5,800 years B.P.; this is reflected in the chironomid-inferred temperatures from Laguna Meche but not in the chironomid-inferred temperatures in Laguna Edita (shown in Figure 11.8). As previously discussed, the chironomid transfer function fails to reproduce the expected modern temperatures and patterns of recent climate change, and this is likely to be as a result of lake level co-variance with temperature as a result of changes in precipitation-evaporation balance.

Peak temperatures around 6–5,000 years B.P. observed in these data are also observed further afield at Campbell Island (New Zealand), as well as cooling in the late Holocene between 3–1,700 years B.P. (McGlone *et al.*, 2010) that could be associated with the arid event observed in these data. Weaker than present westerly winds are identifed as a feature of the southern hemisphere during the early Holocene (Shulmeister, 2004); McGlone *et al.* (2004, 2010) suggest relatively early onset (7,500 years B.P.) of "modern" circulation conditions in New Zealand, inferred from pollen records. This is earlier than that commonly inferred for Patagonia (*c.*5,000 years B.P.). This earlier onset of "modern" conditions in New Zealand is, interestingly, in keeping with the findings from Laguna Meche and Laguna Edita, as well as other non-pollen proxies of climate in Patagonia (see Section 3.3.4.5).

11.6 Summary

Compared to Laguna Meche, Laguna Edita is far less sensitive to climate due to the significant groundwater input to the lake. The chironomid stratigraphy is responsive to lake level but, in combination with an exisiting temperature inference function, fails to provide reasonable estimates of palaeotemperature. A cohesive picture of regional climate for central Patagonia distinct from the northern and southern regions is emerging from these data. Most significantly, a period of low lake level at Laguna Meche between 1,300–2,800 years B.P., due to reduced precipitation from storm tracks caused by reduced westerly meriodonal strength is indicative and characteristic of regional aridity at this time, as observed in other local records. In addition a local wet/warm event between 5–6,000 years B.P. observed in these cores is reflected in ocean cores located north of the site. Changes in lake productivity from 1,300 years B.P. (Laguna Meche) or *c.*2,000 years B.P. (Laguna Edita) are tentatively correlated with cooler conditions in central Patagonia at this time.

Key palaeoclimatic observations from this long core data are: i) the comparability to modern conditions throughout large portions of the lake history, ii) a noteable phase of aridity in the late Holocene, iii) a warm/wet event between 5–6,000 years B.P. is present and iv) that mid-Holocene climate shifts are subtle but probably also present in these data.

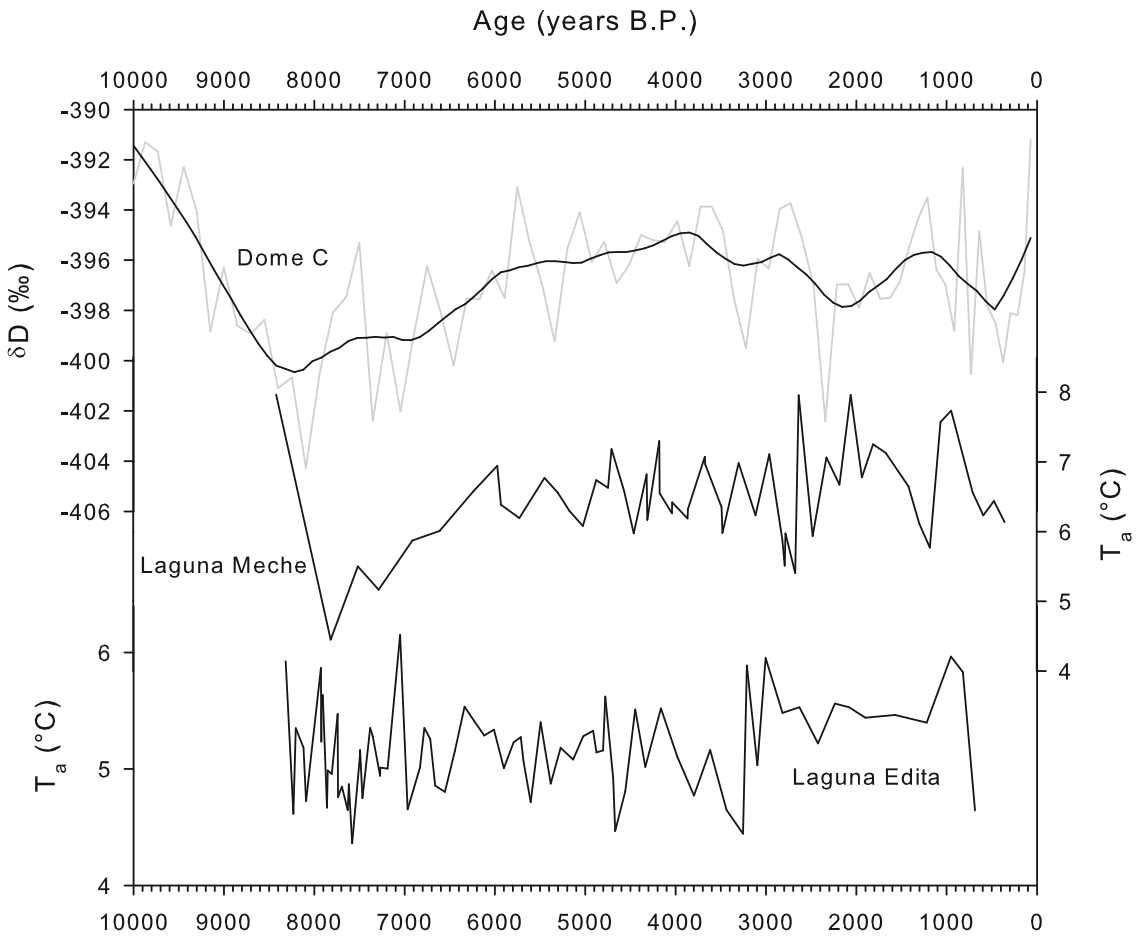

FIGURE 11.8: Dome C δ^2H data from Augustin *et al.* (2004) and CI-T from Laguna Edita and Laguna Meche.

Chapter 12

Conclusions

12.1 Nature of Lake Deposits in the Chacabuco Valley

Given the current lack of basic palaeolimnological data in the region, this thesis includes certain details (basal dates, taxonomic inventories *etc.*) that have proved to be the building blocks on which North American and European palaeoclimatic studies have been built on, and for Patagonia these are noteworthy, as they are the foundation upon which further research will be built. This includes the identification of an unusually late onset of organic sedimentation in the higher lakes of the Chacabuco Valley, and of the identification, geochemical characterisation and dating of a number of regionally important tephra layers. Simply establishing basal dates, the undisturbed nature of the sequence and an age/depth model will be of use to future palaeoclimatic investigations in the valley.

The modern samples and short core data have provided useful information on the hydrology of the valley, not least that Laguna Edita has a significant groundwater input. In addition, this study presents a local evaporation line for surface waters in the valley. The inventory of carbon isotopes and C/N ratio of terrestrial and aquatic vegetation will assist in interpretation of these data downcore in future studies. The short core stratigraphies, whilst at too low a resolution to offer less than centennial-scale data, offer interesting insights into the recent histories of the region.

In addition, this thesis has highlighted the differing manners in which palaeolimnological proxies in the Chacabuco Valley can represent the same climatic forcing — the sensitivity of Laguna Edita to Holocene palaeoclimate appears to be dampened by the groundwater recharge, whereas Laguna Meche appears to be sensitive to changes in precipitation-evaporation balance.

It is unfortunate that it proved impossible to obtain δ^{18}O data from these lakes, due to the underlying geological conditions on the south side of the valley, although useful records have been obtained from Laguna Augusta at the bottom of the valley (Langdon

& Bishop, in prep.). However, the carbon isotope and geochemical data combined with the chironomid stratigraphy have provided a palaeoclimatic record that serves to reinforce and add to the information for this region. In addition the identification of the lack of carbonate geology in these lakes is advantageous to any future radiocarbon dating effort in these lakes.

12.2 Improved Tephrochronology and Validation of Dating Methods in Central Patagonia

In Chapter 3 the need for more robust age models in palaeoecological studies in southernmost South America was described. Chapter 6 presented improved data on the shard chemistry of the previously recorded Mt. Hudson AD1991 tephra, alongside shard chemistry and dating evidence for the AD1891 eruption of Mt. Hudson and a previously unrecorded eruption in central Patagonia. In addition, shard chemistry and new dating evidence has been presented for the Mt. Hudson H2 ash, as well as confirmation of the currently accepted dating and geochemical character of the Mt. Hudson H1 eruption. This will be of considerable utility to future palaeoecological research in the region by improving the resolution and robustness of future age/depth models, although there is considerably more work to be done towards a complete eruptive history for the region, especially considering the additional data required to work around problems caused by re-working and instability of tephra in some records. For recent ashes, the successful results from ^{210}Pb and ^{137}Cs chronologies offer an opportunity to apply robust age estimates for these ashes in other contexts.

The high-resolution, precise magnetic susceptability stratigraphies and exisiting radiocarbon and geochemical data for these two cores should form the basis of future tephra shard counts and a full tephrostratigraphic study for the valley. This would require preparation and counting of tephra, separating size fractions and colours in order to overcome the problems of the high background levels of tephra. SEM/EDX techniques may also assist in distinguishing between background and other tephra.

12.3 Holocene Climate Change in Central Patagonia

A local study of this sort cannot address the complete range of palaeoclimatic enigmas in South America, but by process of addition, cumulative studies will paint a clearer picture of the past. This study adds to the current understanding of the regional climate of central Patagonia by expanding the geographical range of current data, but, perhaps more importantly, tilting the balance of the current conflicting evidence towards an increasingly coherent history of Holocene climate in central Patagonia. The synthesis of

the regional differences between northern, central and southern Patagonian climate records provides a framework for further work of this nature.

The identification of a muted mid-Holocene climate shift, a arid event between 2,800–1,300 years B.P. and possible cooler conditions in the late Holocene from 1,500 years B.P. onwards are in keeping with a number of other palaeoclimatic records from central Patagonia. In particular, the identification of regional aridity between 2,800–1,300 years B.P. builds consensus regarding the nature, position and timing of this event, allowing the research effort to move towards a more thorough theory of the causation, rather than identification, of this event. A warm/wet event identified between 5–6,000 years B.P. is tentatively correlated with increased SST's along the Peru-Chile current at this time, and it is hoped further work of this sort may identify the nature and extent of this event.

12.4 Possibilities from Chironomid Inferred Palaeo-Depth Reconstructions

This study has presented two largely complete Holocene chironomid stratigraphies that add to the exisiting records from Laguna Potrok Aike (Massaferro *et al.*, 2013), Lago Stibnite (Massaferro and Brooks, 2002) and Laguna Facil (Massaferro *et al.*, 2005), as well as two recent stratigraphies to add to the limited exisiting studies of this type in the region (Guilizzoni *et al.*, 2009). Although research is at a relatively early stage, this study demonstrates both the complications and advantages of using chironomids as palaeoclimatic indicators in the region. In particular, further work on the autoecologies of chironomid taxa is necessary to make full use of these data, both as a temperature proxy (*e.g.* Massaferro and Larocque-Tobler, 2013) and as an indicator of lake level (this study).

Chironomids have been used as indicators of lake level elsewhere (*e.g.* Kurek and Cwynar, 2008b; Velle *et al.*, 2012; Engels *et al.*, 2012; Cwynar *et al.*, 2012; Luoto, 2009b), and this study suggests it may be possible to create a similar chironomid-inferred lake level transfer function for Patagonia, which would be of considerable utility in constraining palaeoenvironmental reconstructions, particuarly east of the Andes. The extensive use of lentic/lotic taxa in discerning these changes in this study is of particular note. In the same way workers like Julieta Massaferro have revisited previously published chironomid stratigraphies to see what quantitative reconstructions can add to the data, it is hoped these two chironomid stratigraphies will form the basis of future quantitative lake-level reconstructions for Patagonia. The improved taxonomy of Chironomidae of the Chacabuco Valley (see Appendix A) will assist in developing these training sets.

In the formation of future chironomid training sets, be they for temperature or lake level, modern methods of cross validation, both internal (traditional leave-one-out) and

external (leave-one-site-out, or LOSO) validation, and LOTO (leave-one-transect-out) for water depth reconstructions are necessary (van Bellen *et al.*, 2014). Repeat measurements between years would be advantageous for temperature reconstructions, as would direct determination of temperatures. Direct measurements of suspected co-variables (*e.g.* oxygen availability, various nutrients, food availability by functional feeding type), particularly where lake level studies are attempted, should be included in future training sets.

12.5 The Need for Modern Ecological and Environmental Data in Patagonia

Given the uniformitarian principles that underpin palaeoecology, the quality of palaeoenvironmental reconstructions is directly related to the quality of modern environmental data. By attempting to apply cutting edge palaeoecological methodology to a region where basic ecological, geological, meteorological and environmental data are lacking, the research community run the risk of gathering data without the tools to fully understand or utilise the information those records contain. It is becoming increasing common, particularly in larger research projects, to combine palaeoecological research with modern environmental data collection and observation. The potential for chironomid and geochemical climate proxies has been demonstrated in this thesis and elsewhere, but the continued development of chironomid training sets is limited at present by the lack of basic, recent climatic data and the entomological community's incomplete understanding of the fauna of the Patagonian lakes. Compared to the quality of data available for parts of Europe and North America, the South American research is decades behind.

The geochemical data are more advanced, and our knowledge of carbon cycling is considerably less geographically polarised than for chironomid-inferred palaeoecological records, but the lack of consideration of the catchment, particularly hydrological pathways, in palaeolimnological investigation is again limiting the inferences that can be made from these datasets.

Future chironomid and isotopic palaeolimnological research in Patagonia requires considerably more investigation of contemporary environmental processes and states than is currently commonly practiced. These include the following:

- Survey of catchment topography, channels, drift and structural geology and vegetation.
- Bathymetry and sub-bottom lake sediment profiling. This is particularly important in lakes affected by a particularly strong and dominant wind, *e.g.* the southern westerlies.

- Detailed, long-term in-situ monitoring of physical and chemical properties of the water body, including water/air temperature, lake volume and isotopic composition of surface and atmospheric waters.
- Habitat specific inventories of chironomid faunas.
- Taxon-specific stable isotope inventories of terrestrial, marginal and submerged vegetation.

If the advances outlined above can be considered in future (palaeo)limnological research in Patagonia, lake archives can continue to provide answers to critical questions surrounding Holocene climate in central Patagonia, particularly surrounding the nature of the Lateglacial in the region, the precise timing and nature of the mid-Holocene climate shift and discerning the causes of late-Holocene changes in preciptation-evaporation balance.

12.6 Further Research

12.6.1 Chacabuco Valley

As discussed above, more could be made of the data collected here if a more complete understanding of the catchment and other lakes in the area could be gained. Further (palaeo)limnological research in nearby lakes, particularly larger lakes (*e.g.* Lago Gutiérrez, Laguna Guagua & Laguna Elefantita), as well as in-filled lakes in the valley, are obvious locations for further research in the region.

To expand the records presented here, the interpretation of δ^{13}C could be improved, and the importance of changes in productivity *vs.* (in)organic input balance on δ^{13}C could be elucidated by the addition of δ^{15}N data for these cores (*c.f.* Zhu *et al.*, 2013; Bertrand *et al.*, 2010). In addition, an understanding of catchment vegetation by way of pollen analysis would benefit the palaeoenvironmental interpretation of the stratigraphy; this should be accompanied by a catchment vegetation survey to allow the building of a further pollen-vegetation transects, allowing the possibility of further modelling in this area. Preliminary analysis has produced good yeilds of pollen from the stratigraphies presented in this thesis.

12.6.2 Transect Studies of Patagonia

On a broader note, the core problem in understanding Patagonian palaeoclimate is the density and quality of data, as discussed in Section 12.5. One solution to this problem is a large-scale study involving a transect of palaeoecological studies across both the latitudes and longitudes of Patagonia, where each investigation is conducted in similar

and comparable ways. This would allow for the construction of chironomid, diatom and other training sets, the construction of a detailed tephrochronology, as well as a dense network of palaeoenvironmental records, allowing for an understanding of the spatial characteristics of palaeoclimatic events. This network of sites would also serve to link the current foci of research around the Lake District, the Taitao Peninsula and Tierra del Fuego. The current piecemeal approach will eventually yield the data we require, but is likely to take considerably longer and at greater cost — a co-ordinated approach to research in the region will aid efficient, reliable studies to be produced.

The southern hemisphere has in some ways been neglected in favour of Arctic, North American and European research areas, and although the more recent interest in the Antarctic, South America and New Zealand has helped address this balance, the continued palaeoclimatic research effort in Patagonia will offer considerable insight into hemispheric and global-scale processes. Modern dating and proxy techniques are shown in this thesis to be effective in yielding the palaeoclimatic information we require to understand these processes in the southern latitudes.

Appendix A

Taxonomy of Chironomidae from the Chacabuco Valley

A.1 Overview

The Appendix details the taxonomy used in this study. Photomicrographs, annoted where appropriate, are used to illustrate taxa, and a brief description of the taxonomy of the fossil material examined in this study is given. For most taxa notes on ecology are given based on a number of synopses and summaries — most published ecological work is conducted at species level so good documentary sources on chironomid ecology at genus level are uncommon, but where possible sources are given. This taxonomy is intended to:

- act as a basis for a harmonized taxonomy for the Chacabuco Valley
- allow other workers to easily harmonize taxonomy with the data presented in this study
- be a working document that is updated, modified and extended in light of new material, measurements or insight.

This taxonomy was prepared with reference to a number of unpublished taxonomic guides for Chile (J. Massaferro), New Zealand (A. Dieffenbacher-Krall), Ecuador and Peru (N. Prat & M. Rieradevall), Australia (P. Cranston) and North America (J. Epler). Published guides used included McAlpine, Peterson, Shewell, Teskey, Vockeroth, and Wood (McAlpine *et al.*); Brooks *et al.* (2007); Cranston (1982); Andersen *et al.* (2013). Papers that included small taxonomic sections included Williams *et al.* (2012); Massaferro *et al.* (2009); Massaferro and Brooks (2002). Papers that dealt with specific taxonomic issues included Currie and Walker (1992); Trivinho-Strixino *et al.* (2009); Rieradevall and Brooks (2001); Donato *et al.* (2008), Cranston and Edward (1999) on *Botryocladius*, Cranston and Nolte on *Fissimentum*, and Cranston (2000b,c) describing

Parapsectrocladius. Many, but not all determinations were checked with P. Langdon, S. Brooks and J. Massaferro.

A.2 List of Taxa in This Study

CHIRONOMIDAE

Chironominae: Chironomini

Apedilum
Chironomus
Dicrotendipes
Parachironomus
Stictochironomus
Polypedilum
Zavreliella

Chironominae: Pseudochironomini

Riethia

Chironominae: Tanytarsini

Tanytarsini "sp.A"
Tanytarsini "sp.B"

Tanypodinae

Ablabesmyia "ty.A"
Ablabesmyia "ty.B"
Labrundinia
nr. *Macropelopia*
Alotanypus

Podonominae

Parochlus

Orthocladiinae

Orthoclad. "wood-miner"
Cricotopus "sp.1"
Parapsectrocladius
Pseudosmittia
Parakiefferiella triquetra-type
Parakiefferiella
Limnophyes
Corynoneura
Thienemanniella
Stictocladius
Eukiefferiella
Nanocladius

TIPULIDAE

SIMULIIDAE

CERATOPOGINAE

CHIRONOMINAE: Chironomini: *Apedilum*

FIGURE A.1: *Apedilum* half head capsule.

Description: Head capsule relatively light coloured. **Mentum** with two median teeth and six lateral teeth; median teeth lighter than lateral teeth, first lateral reduced and fused to second lateral. **Ventromental plate** has a right angle on the apical margin.

Similar taxa: None in this study.

Observations/notes: *Apedilum* are associated with submerged vegetation in lentic enviroments and slowly moving water (Andersen *et al.*, 2013). Full description can be found in Epler (1988).

CHIRONOMINAE: Chironomini: *Chironomus*

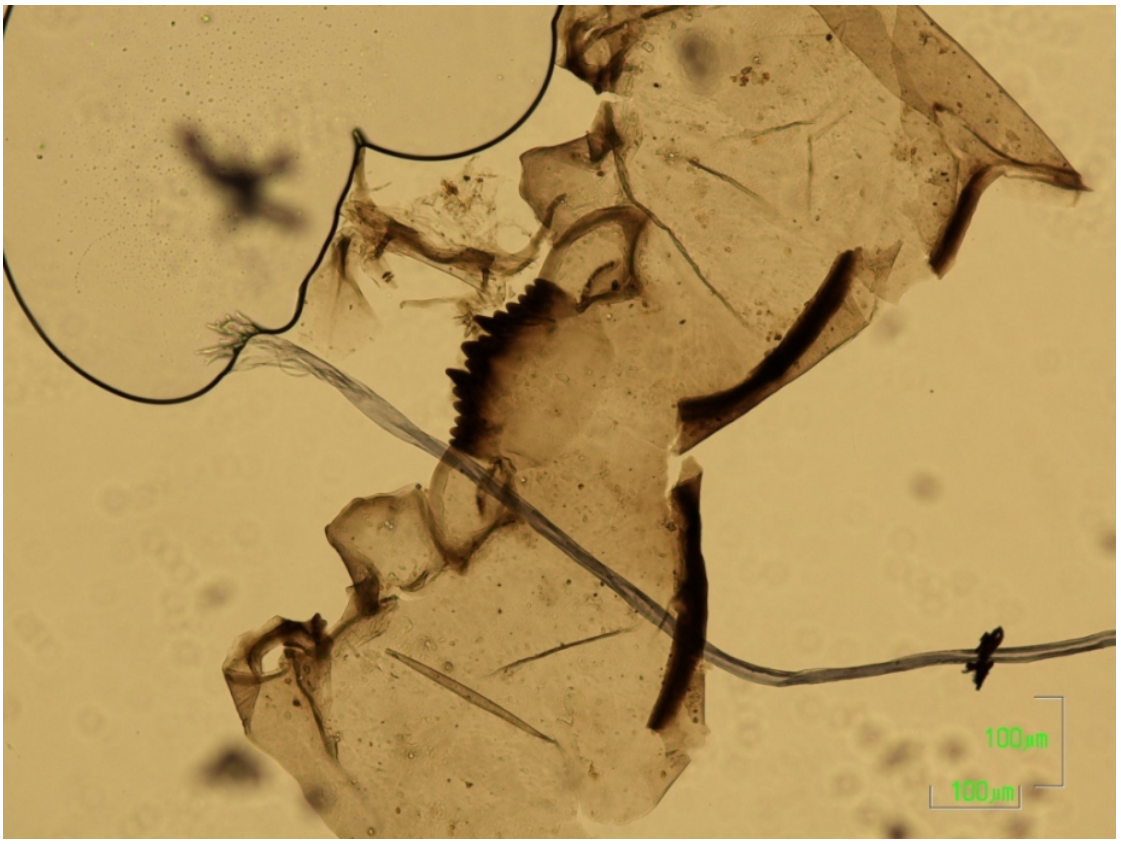

FIGURE A.2: *Chironomus* head capsule.

Description: Head capsule large and often heavily pigmented. **Mentum** with three (trifid) median teeth and six lateral teeth. The second median teeth and subequal to the first median and first lateral teeth. First lateral taller than second lateral and partially fused. Laterals four to six subequal. **Ventromental plate** broad and fan shaped with striations particularly at the base. **Mandible** has 2 or three inner teeth. **Premandible** is bifid apically.

Similar taxa: None in this study.

Observations/notes: Grazers of detritus or filter feeders in soft sediment, normally in standing water. Generally confined to the profundal but can occur in the littoral. Has been identified as an early coloniser after environmental change even in sub-optimal conditions (Andersen *et al.*, 2013). In South America considered a warm indicator, although it has also shown to be abundant at high-elevation sites with low water temperatures. Woodward and Shulmeister (2006) identify the morphotype as taxonomically problematic, as the morphotype encompasses a number of ecologically distinct but morphologically similar taxa.

CHIRONOMINAE: Chironomini: *Dicrotendipes*

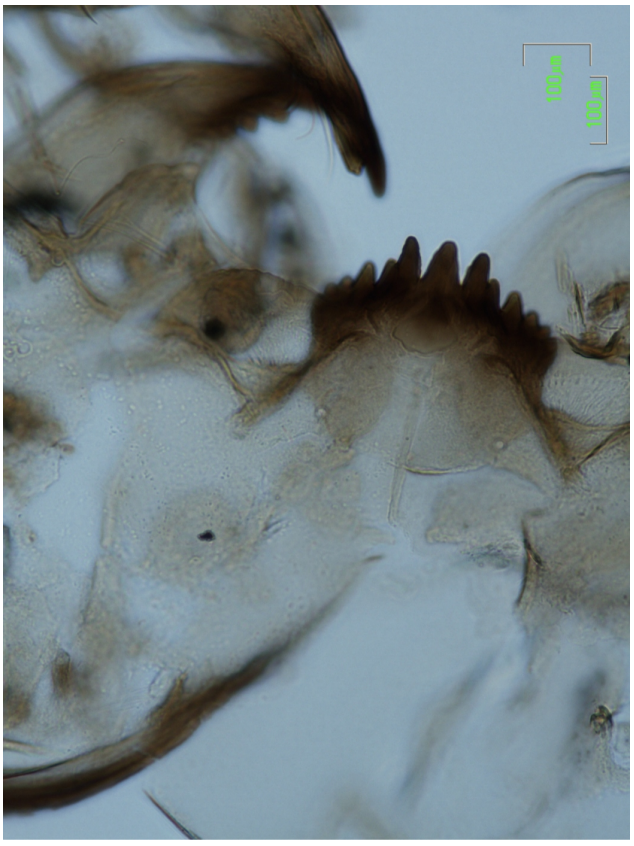

FIGURE A.3: *Dicrotendipes* head capsule.

Description: Head capsule medium to large. **Mentum** has a single median tooth and six lateral teeth. The median tooth is subequal with the first lateral. The first lateral is taller than the other lateral teeth, and splays away slightly from the median tooth. The second lateral is partially fused to the first lateral. The **ventromental plates** are narrow, around half the width of the mentum, triangular and striated with possible crenulations along the anterior margin. The **mandible** has a single long apical tooth with a pale dorsal tooth and three inner teeth.

Similar taxa: None in this study.

Observations/notes: Found in littoral sediments of standing water, may be common in lentic environments (Andersen *et al.*, 2013). More abundant in lakes between 3 and 5°C, but found in lakes up to 7°C. Considered eutrophic by (Araneda *et al.*, 2013).

CHIRONOMINAE: Chironomini: *Parachironomus*

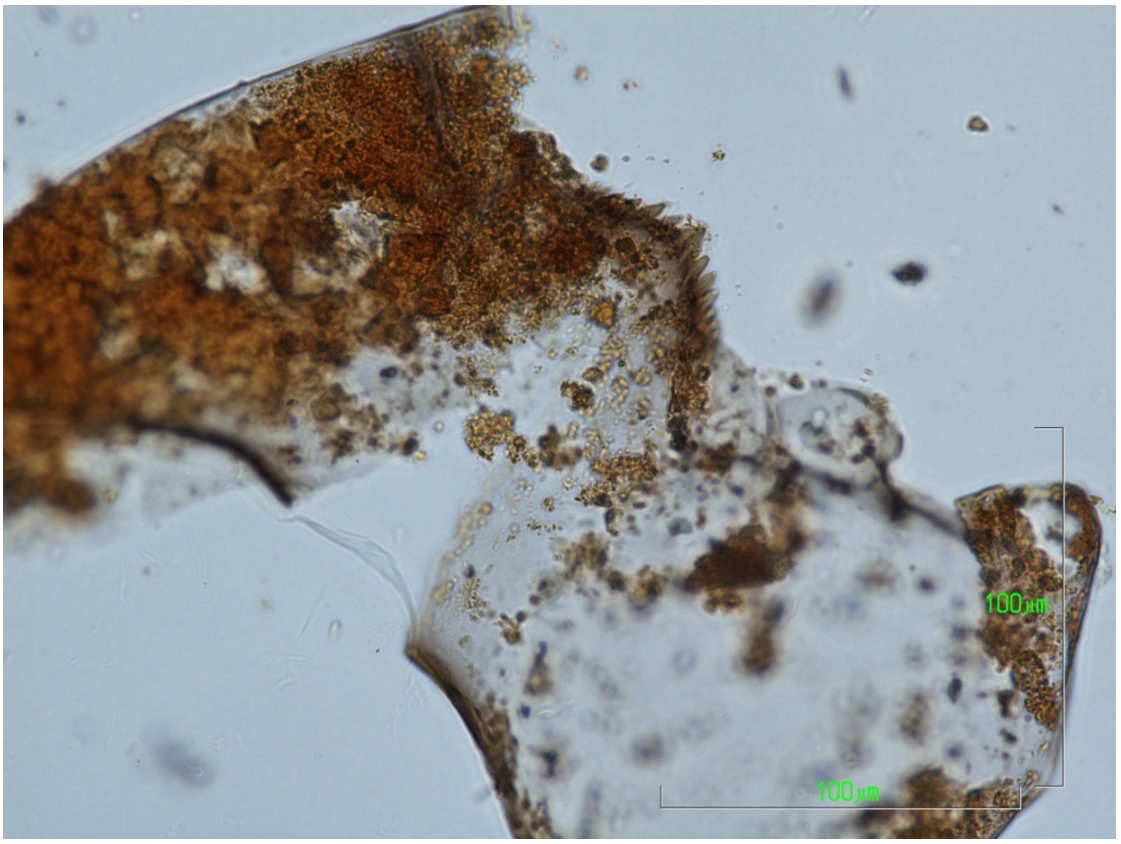

FIGURE A.4: *Parachironomus* head capsule.

Description: Head capsule lightly pigmented, often small. **Mentum** broad with a single median tooth and seven lateral teeth. The median tooth is sometimes notched. The seven lateral teeth are small and often sharply pointed. The **ventromental plates** are about as broad as the width of the mentum and triangular.

Similar taxa: None in this study.

Observations/notes: Littoral of standing waters and flowing waters, sometimes associated with macrophytes (Andersen *et al.*, 2013). Found only in lakes warmer than 12°C (Massaferro and Larocque-Tobler, 2013). Observed to increase in abundance following tephra deposition by Urrutia *et al.* (2007). Dominates during reduced precipitation phase in Laguna Stibnite (Verschuren and Eggermont, 2006; Massaferro and Brooks, 2002). Considered eutrophic by Araneda *et al.* (2013).

CHIRONOMINAE: Chironomini: *Stictochironomus*

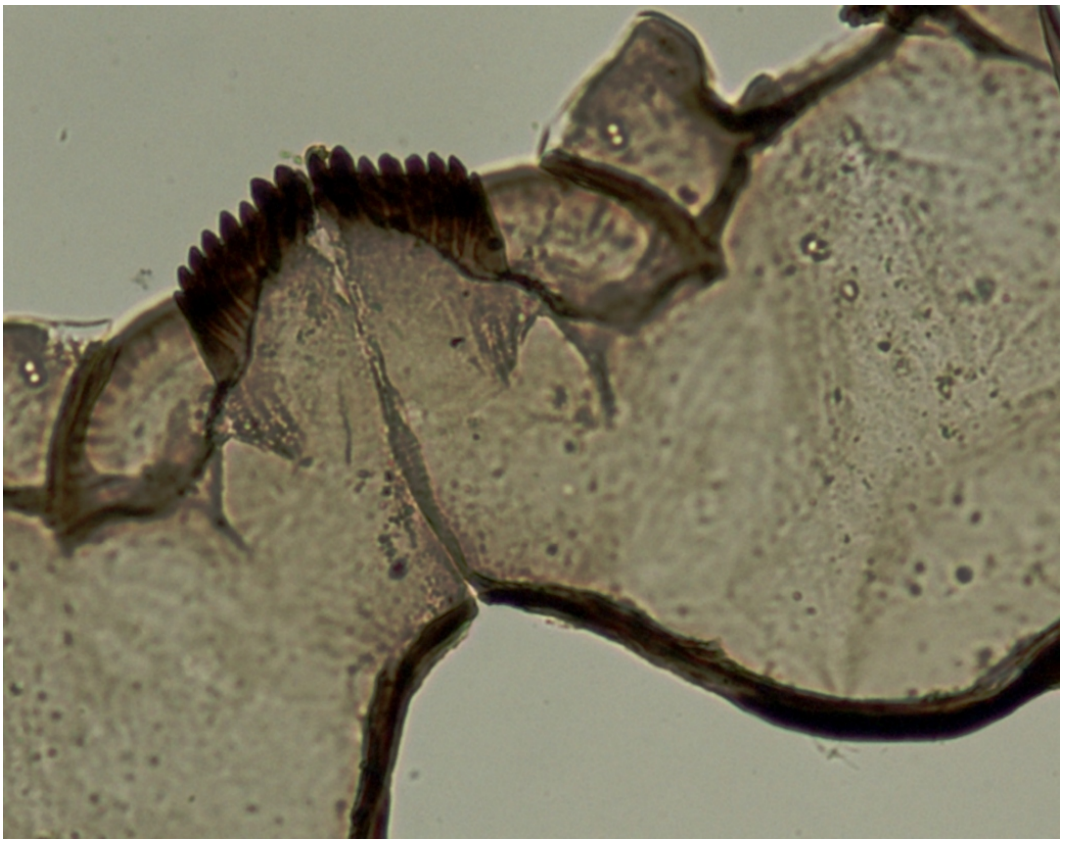

FIGURE A.5: *Stictochironomus* head capsule.

Description: Mentum with four median teeth and seven lateral teeth. First to fifth lateral teeth subequal, seventh lateral reduced. **Ventromental plates** fan shaped and slightly shorter than the mentum with a pointed apex and slightly curved posterior margin.

Similar taxa: None in this study.

Observations/notes: Profundal sediments or littoral sand, also sandy sediments of lakes and streams. Mesotropic or oligotropic (Porinchu and Macdonald, 2003) conditions (Andersen *et al.*, 2013), or transitional between the two (Walker, 1987). Present in low percentages between 10–12°C, highest percentage at c.15°C. Water depths <10m (Kurek and Cwynar, 2008a,b). Possibly associated with sandy substrates and macrophytes (Millet *et al.*, 2009).

CHIRONOMINAE: Chironomini: *Polypedilum*

FIGURE A.6: *Polypedilum* head capsule with enlargement of mentum and mandible inset.

Description: Head capsule small to large. **Mentum** with two median teeth and seventh lateral teeth. The first lateral is reduced in comparison with the median teeth and second lateral. The **ventromental plate** is broad with a strait apical margin. The **mandible** has one apical tooth, two inner teeth and one dorsal tooth. The **premandible** has paired apical teeth and a broad, blunt basal tooth.

Similar taxa: *Zavreliella*, but the shape of the ventromental plate is different.

Observations/notes: *Polypedilum* are known in many kinds of lotic and lentic environments, except in very cold environments (Andersen *et al.*, 2013). In the Holarctic it is an indicator of temperate conditions and occurs in the littoral zone of eutrophic lakes or amongst vegetation (Porinchu and Macdonald, 2003; Ruiz *et al.*, 2006; Langdon *et al.*, 2004), although has also been suggested to be indicative of oligotrophy (Woodward and Shulmeister, 2007). In New Zealand, indicative of warmer conditions $>13°C$ (Woodward and Shulmeister, 2006), as they are in the Holarctic (Brooks *et al.*, 2007), an assertion also possible in South America (Araneda *et al.*, 2013) where it may be associated with mesotrophy (Verschuren and Eggermont, 2006) Possibly more abundant in shallow water $<1m$ (Kurek and Cwynar, 2008a; Engels and Cwynar, 2011). Phylogentically close to *Reithia* (Cranston *et al.*, 2010).

CHIRONOMINAE: Chironomini: *Zavreliella*

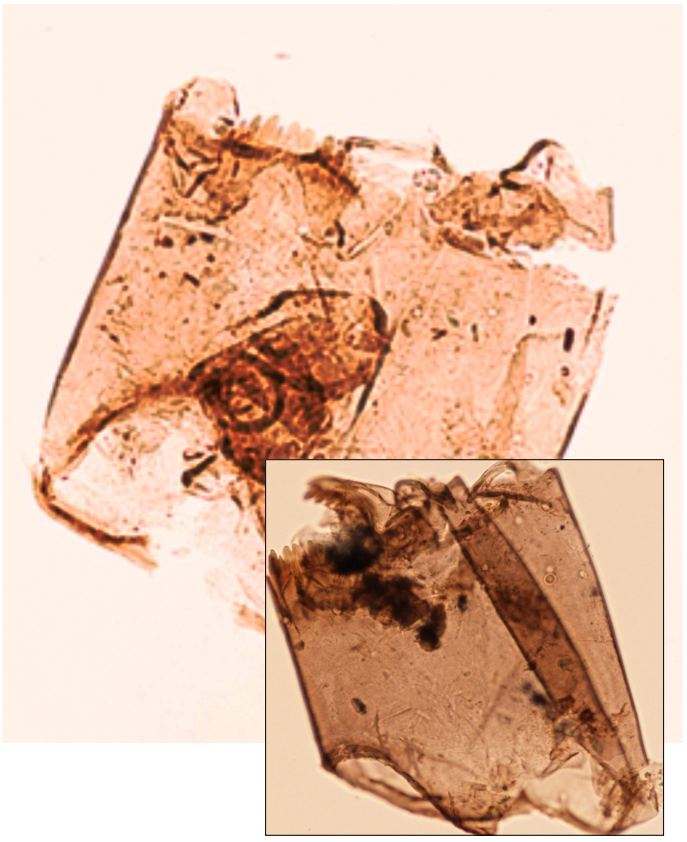

FIGURE A.7: *Zavrelliella* head capsule (head capsule from angle with better definition of lighter median tooth inset).

Description: Head capsule small to large. **Mentum** with two median teeth and seventh lateral teeth. The first lateral is reduced in comparison with the median teeth and second lateral. The **ventromental plate** is approximately as tall it is long, with a particularly acute angle at the base. The **mandible** has one apical tooth, two inner teeth and one dorsal tooth. The **premandible** has paired apical teeth and a broad, blunt basal tooth.

Similar taxa: *Polypedilum*, but the **ventromental plates** differ.

Observations/notes: *Zavreliella* larvae are mobile case-bearers, living in submerged vegetation, at least in the Holarctic (Andersen *et al.*, 2013). Possibly sub-littoral (Engels and Cwynar, 2011).

CHIRONOMINAE: Psuedochironomini: *Riethia*

FIGURE A.8: *Riethia* head capsule.

Description: Head capsule slightly elongate for the subfamily. **Mentum** with distinctive s-shaped margin, one rounded median tooth and six lateral teeth. First lateral tooth subequal to the median tooth. Second lateral reduced compared to the first and third lateral and partially fused to the first lateral. The **ventromental plate** is sausage shaped and the plates almost touch medially. The **mandible** has one apical tooth and ?four inner teeth. Full description in Trivinho-Strixino *et al.* (2009).

Similar taxa: None in this study.

Observations/notes: Associated with the profundal (Guilizzoni *et al.*, 2009). Other members of the putative tribe Pseudochironomini in the northern hemisphere favour sandy or gravelly littoral substrates, in meso- to oligtrophic lakes, but this may not be valid for *Rhiethia* (Andersen *et al.*, 2013). *Riethia* are known only in the southern hemisphere. Indicative of middle to low temperatures in a number of training sets including in Australia (Cranston, 2000a; Verschuren and Eggermont, 2006; Rees *et al.*, 2008) and has highest abundances between 5–5.5°C (Massaferro and Larocque-Tobler, 2013).

CHIRONOMINAE: Tanytarsini: Tanytarsini "sp.A"

FIGURE A.9: Tanytarsini "sp.A" head capsule with enlargement of a specimen with better definition of the antennal pedestals, also exhibiting a worn mentum.

Description: Head capsule medium or large, sometimes heavily pigmented. **Mentum** with one median tooth and five lateral teeth. Median tooth not prominent, sometimes notched. **Mandible** with three inner teeth and one dorsal tooth, premandible with three apical teeth. **Antennal pedestal** with a short, narrow and rounded spur that is sometimes slightly crenulated at the margin. **Post-occipital plate** present and heavily pigmented. **Ventromental plates** elongated, almost touching medially.

Similar taxa: Tanytarsini "sp.B", but note the presence of a post-occipital plate.

Observations/notes: These taxa are named to be in harmony with Massaferro and Larocque-Tobler (2013). Massaferro and Brooks (2002) also knew this taxon as Tanytarsini ty.1B.

CHIRONOMINAE: Tanytarsini: Tanytarsini "sp.B"

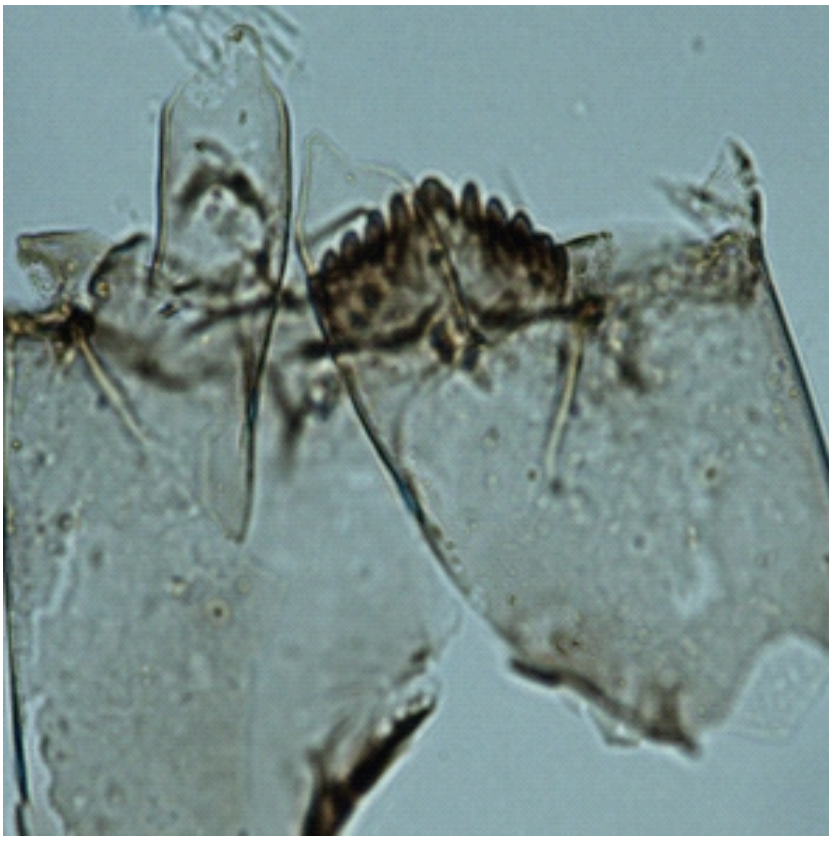

FIGURE A.10: Tanytarsini "sp.B" head capsule.

Description: Head capsule small and occasionally medium, normally lightly pigmented. **Mentum** with one median tooth and five lateral teeth. **Mandible** with three inner and one dorsal tooth. **Premandible** with three apical teeth. **Antennal pedestal** longer than it is broad, with relatively broad rounded spur. **Post-occipital plate** is absent. **Ventronmental plates** elongate, almost touching medially.

Similar taxa: Tanytarsini "sp.A".

Observations/notes: These taxa are named to be in harmony with Massaferro and Larocque-Tobler (2013). Massaferro and Brooks (2002) also knew this taxon as Tanytarsini ty.1B.

TANYPODINAE: *Ablabesmyia* "ty.A"

FIGURE A.11: *Ablabesmyia* "ty.A" head capsule shown with annotations to mark the ventral setation.

Description: Head capsule slight narrow, relatively small. **Ligula** with five teeth where the central tooth is the shortest and the outer tooth the longest. **Paraligular** bifid, **pecten hypopharyngis** with around fifteen teeth. **Dorsomental teeth** absent. **Cephalic setation** as shown.

Similar taxa: *Ablabesmyia* "ty.B", but note the difference in the arrangement of the ventral setation.

Observations/notes: *Ablabesmyia* are eurytopic and cosmopolitan; late-instar larvae are predatory (Andersen *et al.*, 2013).

TANYPODINAE: *Ablabesmyia* "ty.B"

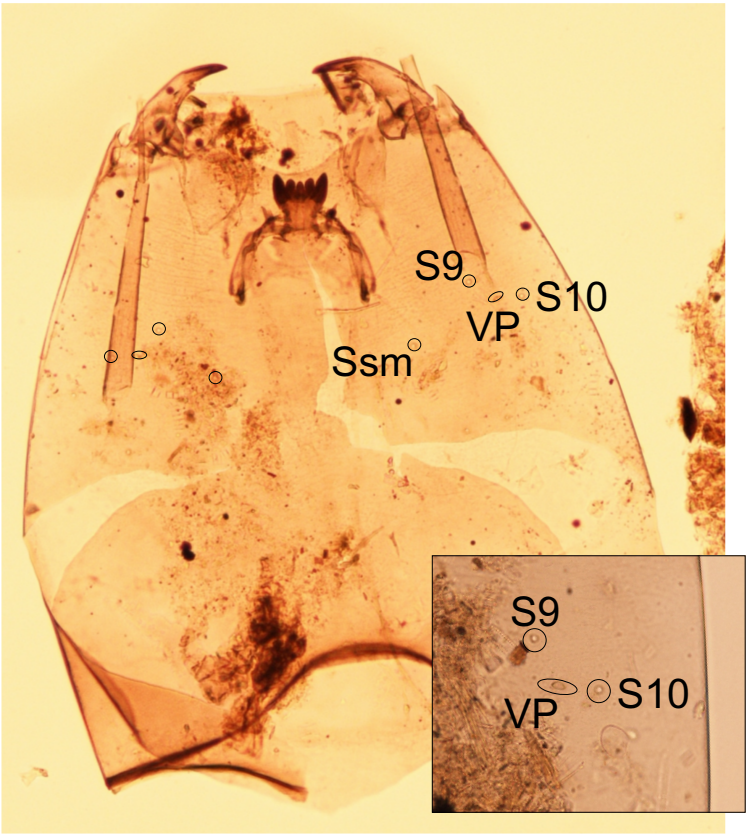

FIGURE A.12: *Ablabesmyia* "ty.B" head capsule, shown with annotations marking the ventral setation, with an enlargement of S9, S10 and the ventral pore inset.

Description: Head capsule slight narrow, large. **Ligula** with five teeth where the central tooth is the shortest and the outer tooth the longest. **Paraligular** bifid, **pecten hypopharyngis** with around fifteen teeth. **Dorsomental teeth** absent. **Cephalic setation** as shown.

Similar taxa: *Ablabesmyia* "ty.A", but note the difference in the arrangement of the ventral setation.

Observations/notes: *Ablabesmyia* are eurytopic and cosmopolitan. Late-instar larvae are predatory (Andersen *et al.*, 2013).

TANYPODINAE: *Labrundinia*

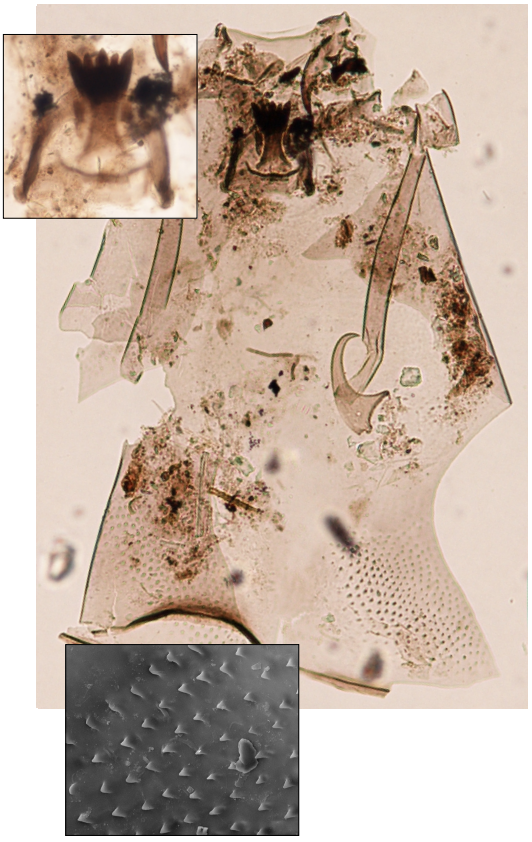

FIGURE A.13: *Labrundinia* head capsule, with an enlargement of the ligula (top) and a scanning electron microscope image of the barbs found on the posterior.

Description: Head capsule narrow with short spines in patches towards the rear of the head. **Ligula** with five teeth where the central tooth and outmost teeth longer than the remaining two. The **paraligula** is bifid and the **pectin hypopharyngis** has aorund seven teeth. **Dorsomental teeth** are absent.

Similar taxa: None in this study.

Observations/notes: Live in small standing water bodies as well as streams. Have particularly high diversity in South America (Andersen *et al.*, 2013). Appears in lakes warmer than 12°. Considered warm stenotherms in the Holarctic (Watson *et al.*, 2010), and is associated with shallow, littoral zones (Millet *et al.*, 2007; Engels *et al.*, 2012) in meso/eutrophic lakes (Verschuren and Eggermont, 2006), which may also be the case in Patagonia (Araneda *et al.*, 2013).

TANYPODINAE: nr.*Macropelopia*

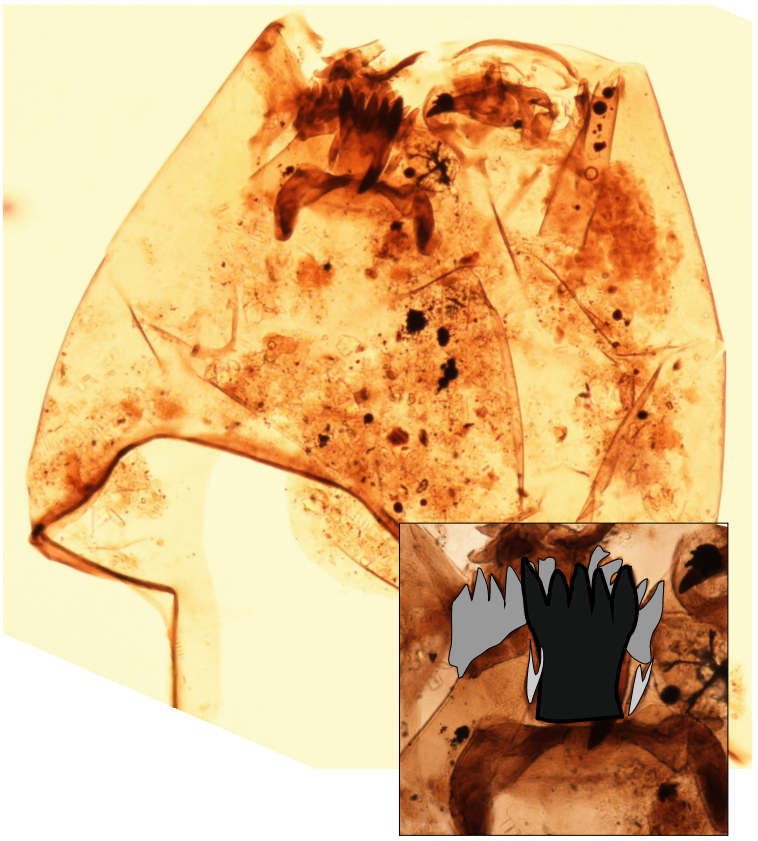

FIGURE A.14: nr. *Macropelopia* head capsule.

Description: Head capsule often large, wide. **Ligula** with five teeth where the inner and outermost teeth are taller than the remaining two. **Paraligula** is bifid and the **pectin hypopharyngis** has about twenty teeth. There are around five **dorsomental teeth** that often appear to curl inwards. The innermost tooth is often notched on the side.

Similar taxa: Similar to *Alotanypus* but the ligula is not concave. Could be a variation of *Apsectrotanypus*.

Observations/notes: This taxon is problematic, because most taxa in the Macropelopiini have a concave shaped ligula, but in this taxa it is complex, suggestive of *Tanypus*, but it is not because of the simple bifid paraligula. If this taxa is *Macropelopia*, which is less common in South America, this is characteristic of fine sediments in cool waters (Andersen *et al.*, 2013), but if *Apsectrotanypus* it is indicative of small, cool flowing waters.

TANYPODINAE: *Alotanypus*

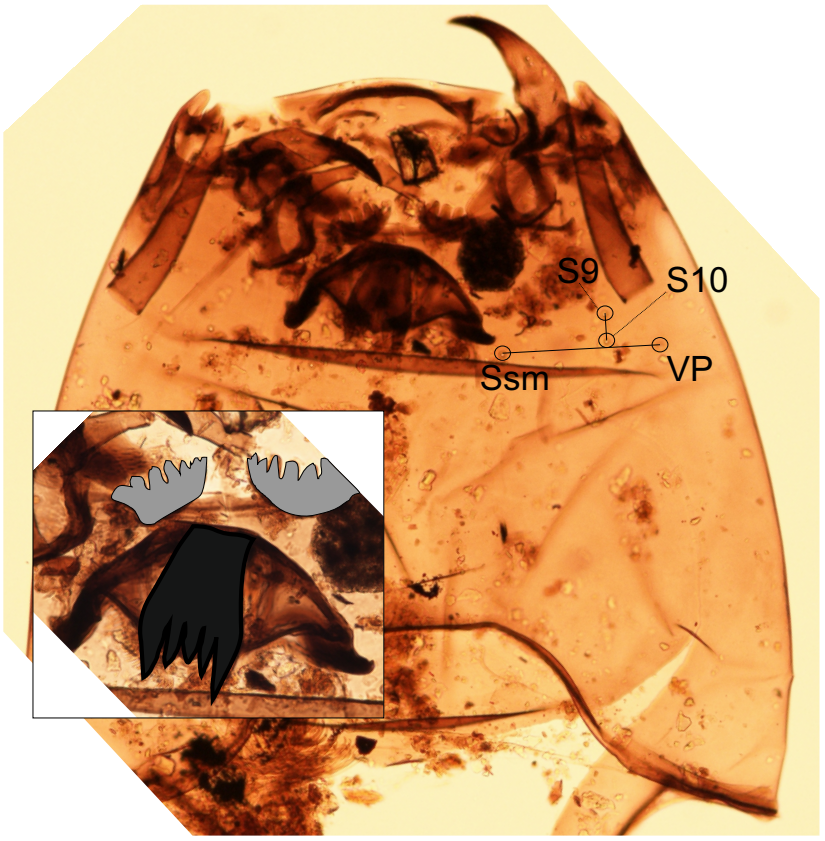

FIGURE A.15: *Alotanypus* head capsule.

Description: Head capsule often large, wide. **Ligula** with five teeth where the innermost is the smallest and the outermost the largest. **Paraligula** is bifid, the **pectin hypopharyngis** has around ten teeth. **Dorsomental teeth** are present with five teeth on each side (occasionally a reduced six teeth may be visible). **Cephalic setation** is shown; the line between the setae submenti to the ventral pore and the line between S9 and S10 should not cross — they should form a right angle.

Similar taxa: Similar to *Macropelopia* but the ligula is concave in *Alotanypus*. It may be the case that the dorsomental teeth tend not to curl inwards in *Alotanypus*.

Observations/notes: Capable of inhabiting a wide range of lentic and slowing flowing waters (Andersen *et al.*, 2013).

PODONOMINAE: *Parochlus*

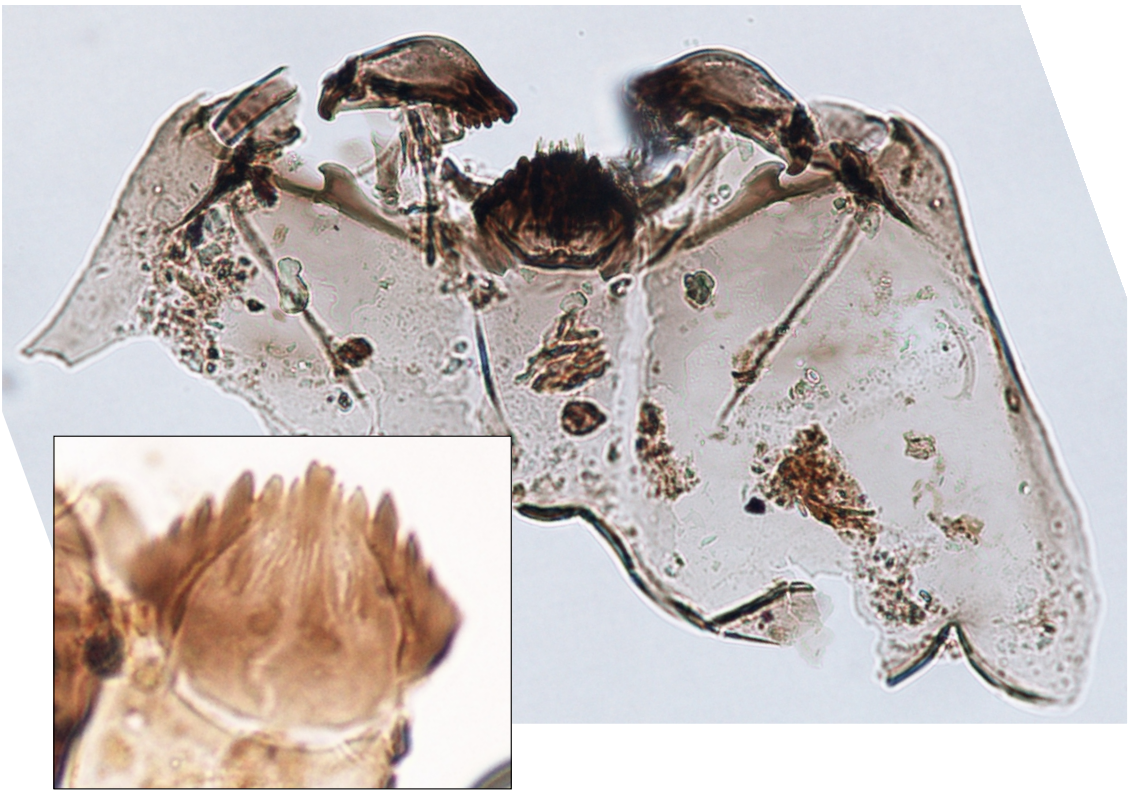

FIGURE A.16: *Parochlus* head capsule, with an enlargement of the mentum inset.

Description: Head capsule small and rounded, sometimes light brown with irregular lines on. **Mentum** has one median and seven lateral teeth. The first and second laterals are short, lighter in colour and the first lateral is partially fused to the median tooth.

Similar taxa: If the mentum is worn this could be mistaken for several types of ORTHOCLADIINAE, but the mandible and the patterned mentum are distinguishing.

Observations/notes: *Parochlus* has high diversity in the austral continents (Cranston *et al.*, 2010). The immature stages are confined to running waters (Garcia and Anonsuarez, 2007), and although there are >30 species known in the South America and the Andes, only habitat preferences for the single European species (*P.kiefferi*) are known: it inhabits cool running water (Andersen *et al.*, 2013) and this is also the case in New Zealand (Woodward and Shulmeister, 2006). It may also have a preference for deeper water (Rees *et al.*, 2008). In the transfer function of Massaferro and Larocque-Tobler (2013) it appears indicative of cooler conditions.

ORTHOCLADIINAE: Orthoclad. "wood-miner"

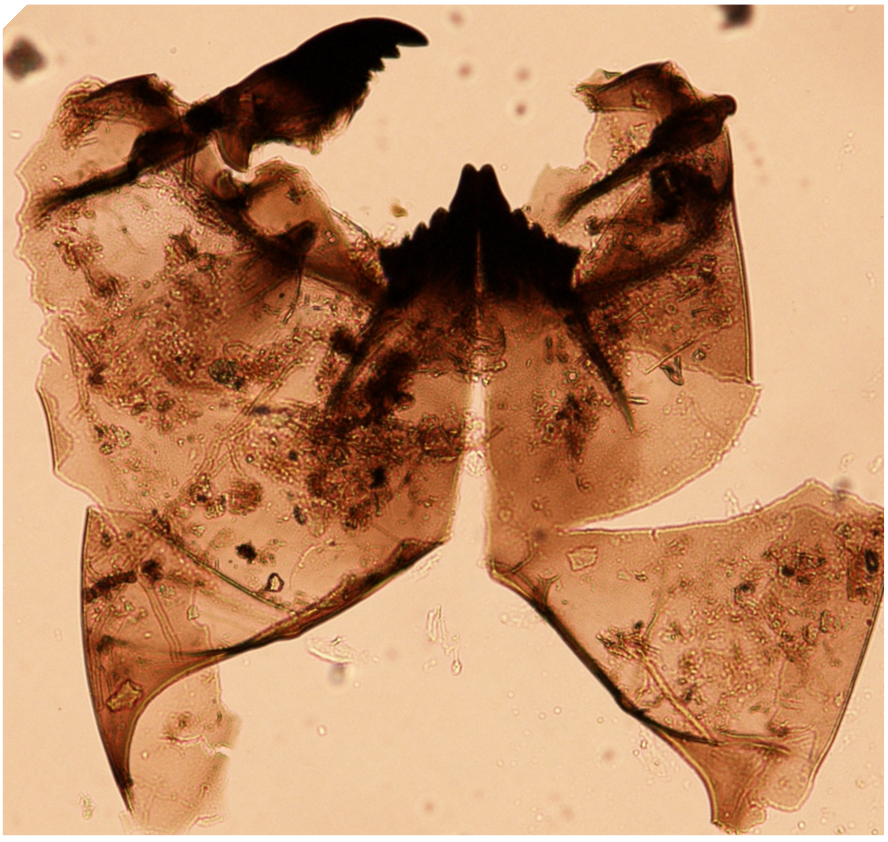

FIGURE A.17: Orthoclad. "wood-miner" head capsule.

Description: Head capsule often heavily pigmented. **Mentum** with a pair of median teeth and five lateral teeth; the median teeth are much taller than the laterals. The first and second laterals are subequal and the third to fifth laterals are smaller, the mentum is flatter and they may appear to be in a distinct group.

Similar taxa: None in this study.

Observations/notes: The name used here is from an identical taxa in an unpublished guide to Patagonian chironomids by J. Massaferro, who tenatively suggest it is associated with submerged woody debris.

ORTHOCLADIINAE: *Cricotopus* "sp.1"

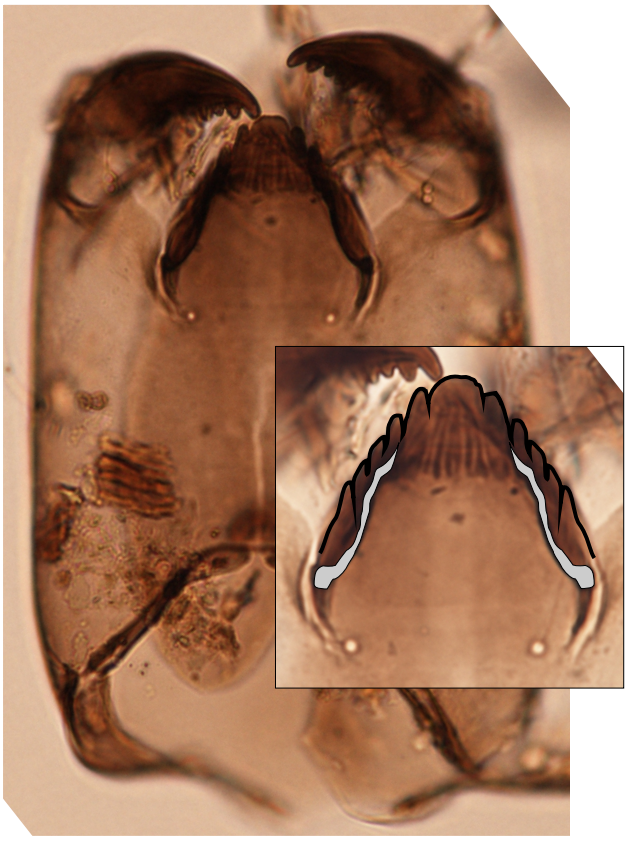

FIGURE A.18: *Cricotopus* "sp.1" head capsule.

Description: Head capsule small, heavily pigmented. **Mentum** with trifid median tooth and four lateral teeth (could be a single median tooth and five lateral teeth but the central three teeth appear to be on a different focal plane). The central tooth is about twice the width of the second median teeth and it is slightly taller. There is patterning underneath the median teeth. The lateral teeth and subequal. **Ventromental plates** are thin, starting from beneath the first lateral and extending to just below the last lateral tooth.

Similar taxa: This is similar to *Paratricocladius* but has one less lateral tooth. It could be part of the *Cricotopus*-group.

Observations/notes: *Cricotopus* inhabit all kinds of water bodies, and are frequently associated with aquatic plants including algae (Andersen *et al.*, 2013).

ORTHOCLADIINAE: *Parapsectrocladius*

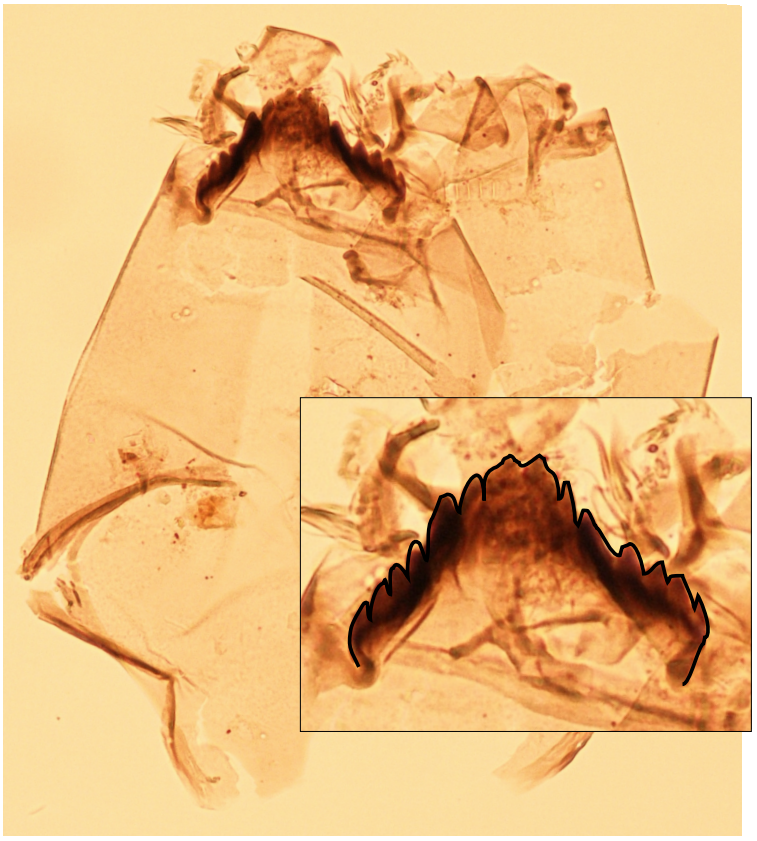

FIGURE A.19: *Parapsectrocladius* head capsule.

Description: Mentum with a double median tooth and five lateral teeth. The median teeth are broad and paler than the rest of the tooth, and are notched (which may give the appearance of an additional median tooth on each side).The first lateral is often slanted towards to median tooth, whereas the remaining four lateral teeth are roughly subequal, although the last lateral may be reduced.

Similar taxa: When the median teeth are worn *Parapsectrocladius* can be mistaken for a number of ORTHOCLADIINAE.

Observations/notes: *Parapsectrocladius* are only known from southern Chile (Cranston, 2000b,c), where they appear to have a wide range. They have often been found in cooler lakes, and one species has been identified in running water. May have a preference for tephra deposits (Guilizzoni *et al.*, 2009; Urrutia *et al.*, 2010).

ORTHOCLADIINAE: *Pseudosmittia*

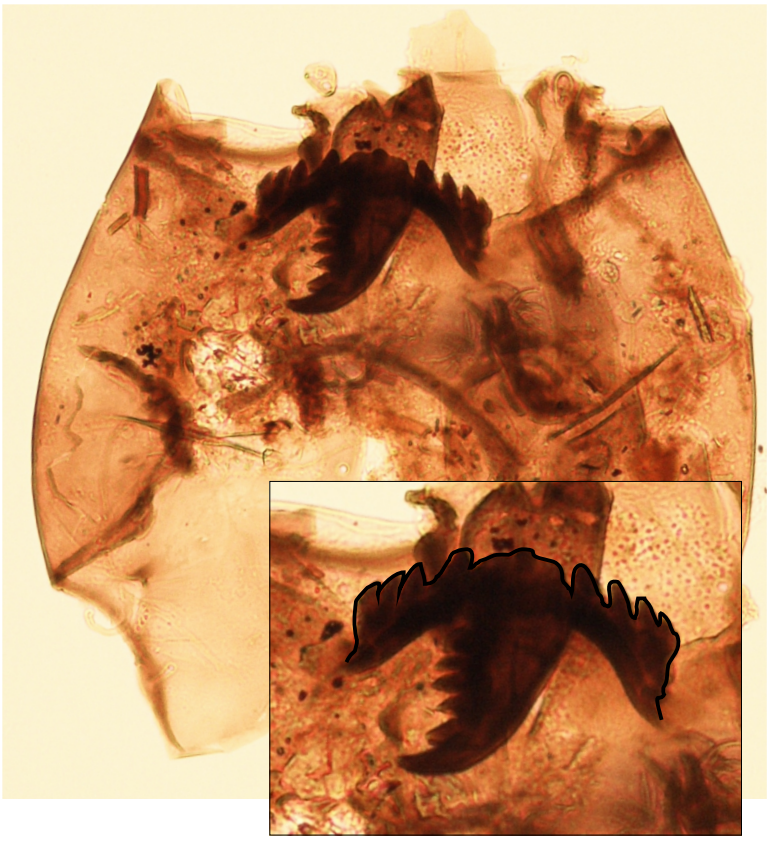

FIGURE A.20: *Pseudosmittia* head capsule, with an annotated enlargement of the mentum inset, showing the outline of the mentum.

Description: Mentum with single median tooth and four lateral teeth. The median tooth is wide and often peaked. The lateral teeth reduce in size progressively outwards, and the fourth lateral is occasionally slighlty bulged on the margin. **Mandible** with 4 or 5 inner teeth.

Similar taxa: None in this study.

Observations/notes: Predominately terrestrial or semi-terrestrial, but some are associated with the splash-zone or littoral, where they are associated with macrophytes (Andersen *et al.*, 2013). Considered a cold indicator by Guevara *et al.* (2010), and may be associated with organic content (Kurek and Cwynar, 2008b), but Massaferro and Larocque-Tobler (2013) find it is associated with warmer lakes.

ORTHOCLADIINAE: *Parakiefferiella triquetra*-type

FIGURE A.21: *Parakiefferiella triquetra*-type mentum, with a flattened mentum inset.

Description: Head capsule is small and light coloured. **Mentum** is prominent with one very large mentian tooth and five small subequal trapeziod lateral teeth. **Ventromental plates** are large, lobate and extend well beyond the mentum.

Similar taxa: None in this study.

Observations/notes: Considered to be a cold-stenotherm that occurs in oligotropic lakes, at least in western Europe, and the training set of Massaferro and Larocque-Tobler (2013) also shows it to be a cold-stenotherm in South America. *Parakiefferiella triquetra*-type is also known as *Parakiefferiella fennica*-type.

ORTHOCLADIINAE: *Parakiefferiella*

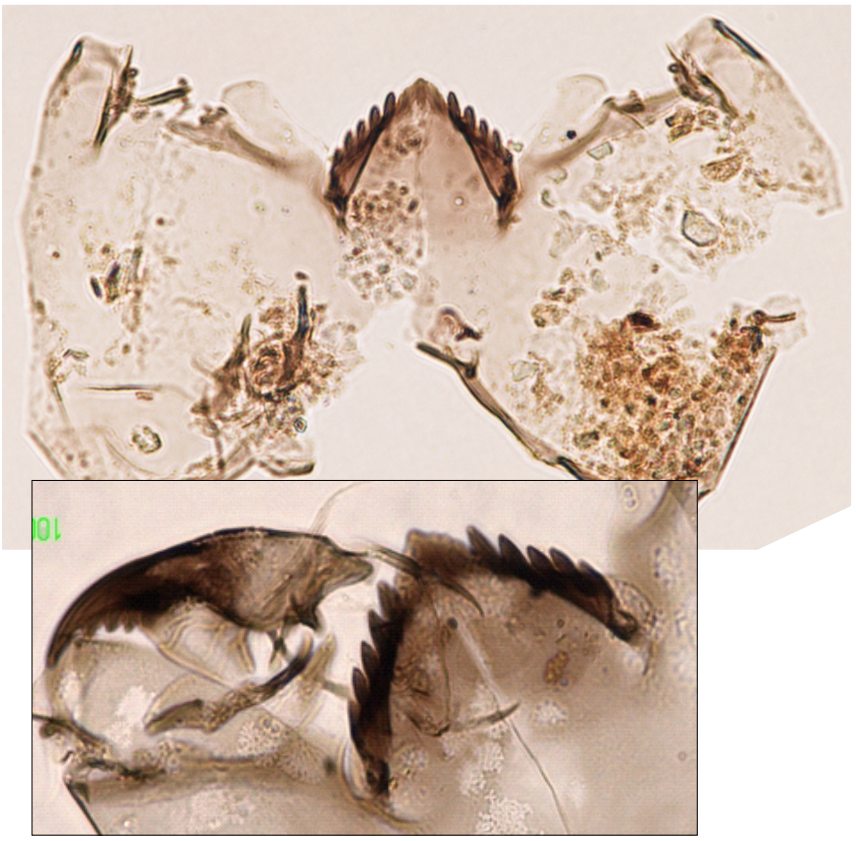

FIGURE A.22: *Parakiefferiella* head capsule, with an enlargement of the mentum and mandible inset.

Description: Mentum with a single median tooth and six lateral teeth. The median tooth is usually broad and slightly taller than the lateral teeth and is often notched. The **ventromental plates** broaden downwards and are round at the apex, generally lobate. The rounded apex protrudes from underneath the last lateral tooth.

Similar taxa: There are superficial similarities to *Cricotopus*.

Observations/notes: A diverse genus that has South American specific species (Wiedenbrug and Andersen, 2002). Often abundant in temperate lakes (Andersen *et al.*, 2013) and associated with well oxygenated conditions (Porinchu and Macdonald, 2003), but in South America associated with cold lakes (Ariztegui *et al.*, 1997; Verschuren and Eggermont, 2006; Urrutia *et al.*, 2010) although Massaferro and Larocque-Tobler (2013) suggest a bimodal distribution. Seen to dominate lakes in Patagonia (*e.g.* Massaferro *et al.*, 2005), and can become dominant following tephra deposition (Urrutia *et al.*, 2007).

ORTHOCLADIINAE: *Limnophyes*

FIGURE A.23: *Limnophyes* head capsule.

Description: Mentum with paired median teeth and five lateral teeth. Median teeth often lighter than the laterals. Laterals one to three reducing in size, laterals four and five much smaller and subequal. **Ventromental plates** are narrow, extending at the base into a "knot" below the outer edge of the mentum.

Similar taxa: None in this study.

Observations/notes: *Limnophyes* are eurytopic, found in aquatic, semi- and terrestrial habitats (Andersen *et al.*, 2013). Usually associated with very shallow water in the littoral zone (Guilizzoni *et al.*, 2009; Araneda *et al.*, 2013; Verschuren and Eggermont, 2006; Urrutia *et al.*, 2010), but also may be associated with streams (Garcia and Anonsuarez, 2007) or semi-terrestrial zones (Massaferro *et al.*, 2005). Usually in temperate waters. Massaferro and Brooks (2002) use *Limnophyes* as a lake level indicator.

ORTHOCLADIINAE: *Corynoneura*

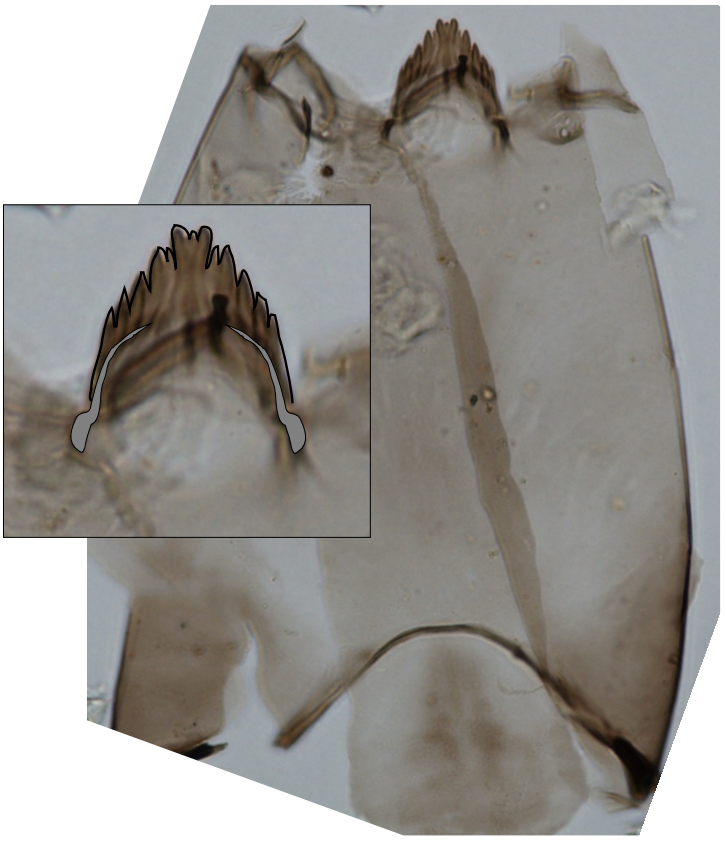

FIGURE A.24: *Corynoneura* head capsule, with an annotated enlargement of the mentum inset showing the outline of the mentum (in black) and the position of the ventromental plates (in grey).

Description: Head capsule small and narrow. **Mentum** narrow and small compared to head capsule, with three median teeth and five lateral teeth. The central median tooth is reduced and sometimes appears to be absent. The first lateral tooth may be reduced compared to the outer four laterals which are subequal. **Ventromental plates** are narrow , at least as long as the mentum and abruptly angled at the bottom.

Similar taxa: *Thienemanniella*, but can be differentiated by subtle features of the ventromental plates and mentum. The size of the mentum relative to the length of the head capsule is also distinctive. The two are often grouped together.

Observations/notes: Found in all types of aquatic habitat (Andersen *et al.*, 2013), but in the northern hemisphere commonly associated with lotic waters (Porinchu and Macdonald, 2003),or the littoral and associated with macrophytes (Ruiz *et al.*, 2006), possibly in more productive lakes in Patagonia (Massaferro *et al.*, 2005). Has a temperature optima $<5°C$ in the Patagonian training set, making it a cold indicator (Massaferro and Larocque-Tobler, 2013).

ORTHOCLADIINAE: *Thienemanniella*

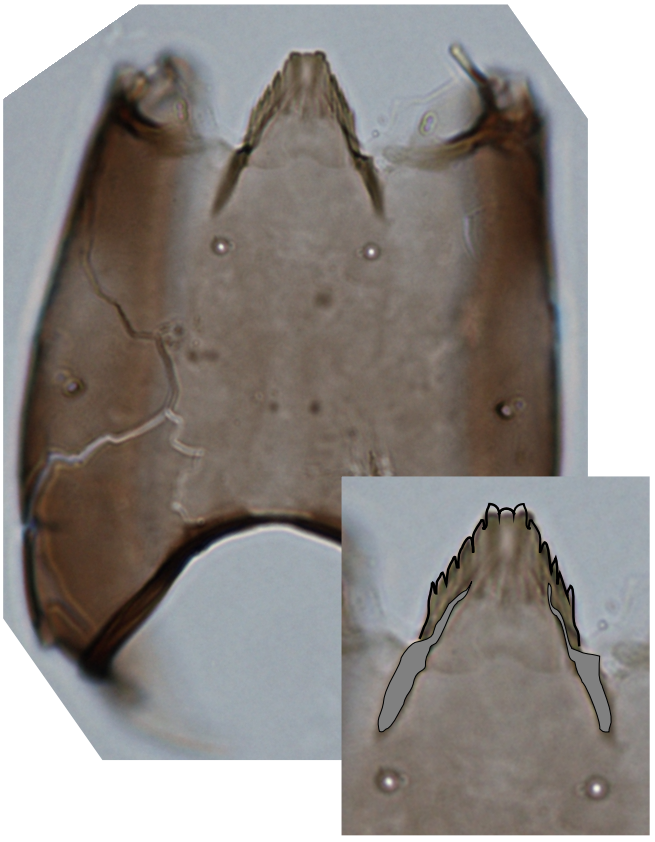

FIGURE A.25: *Thienemanniella* head capsule, with an enlargement of the mentum inset showing the outline of the mentum (in black) and the position of the ventromental plates (in grey). Note the slightly worn median teeth.

Description: Head capsule small and heavily pigmented with a dark brown hue. The **mentum** is narrow and triangular but may be worn flat. Three median teeth that are prominent and five subequal small lateral teeth. The **ventromental plate** is narrow and long extending well below the base of the mentum, with a small notch in at the base of the mentum (about halfway along the plate).

Similar taxa: *Corynoneura* but the condition of the lateral teeth and the ventromental plates differ, and the length of the mentum when compared to the length of the head capsule is longer in *Thienemanniella* compared to that of *Corynoneura*. The two are often grouped together.

Observations/notes: Found in lotic environements of all types (Andersen *et al.*, 2013), although may also be present in cooler lakes. Very similar preferences to *Corynoneura*.

ORTHOCLADIINAE: *Stictocladius* sofour-type

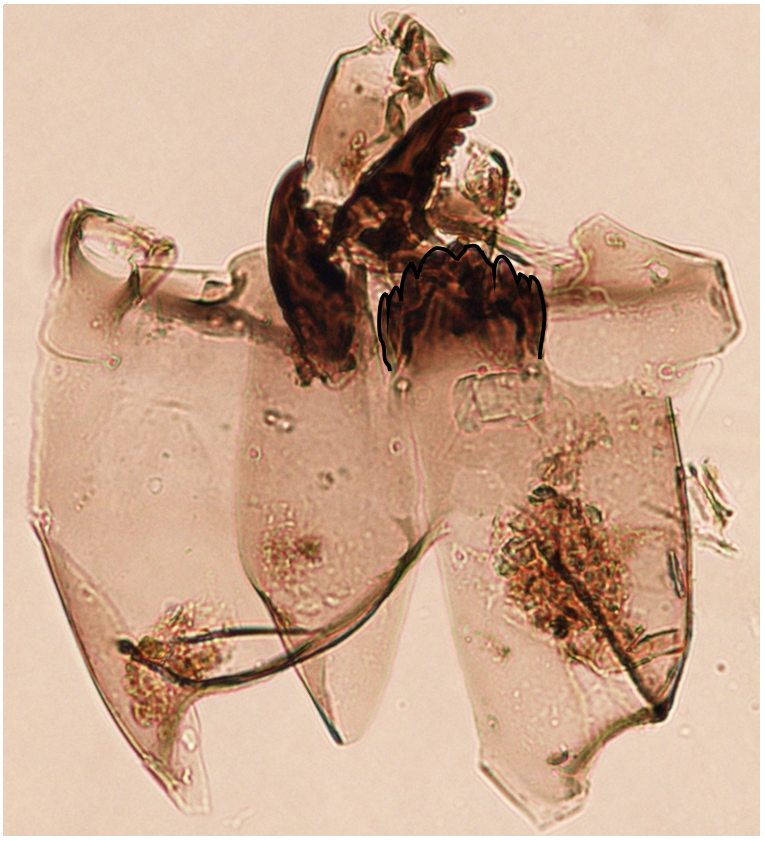

FIGURE A.26: *Stictocladius* sofour-type head capsule annotated to show the outline of the mentum.

Description: Head capsules small, often damaged or missing. **Mentum** with paired median teeth and three lateral teeth, where the second and third laterals are subequal and reduced. Full description in Saether and Cranston (2012).

Similar taxa: None in this study.

Observations/notes: In the southern hemisphere these larvae are adapted to sandy environments, with a morphology similar to the *Harnischia* complex (Andersen *et al.*, 2013). However, Saether and Cranston (2012) suggest in Patagonia the type is associated with clear, fast flowing water. This is a match to a taxon in an unpublished taxonomy of chironomids from sediments in New Zealand by A. Dieffenbacher-Krall ("SO4"). It also appears which this name in an unpublished guide to New South Wales by P. Cranston.

ORTHOCLADIINAE: *Eukiefferiella*

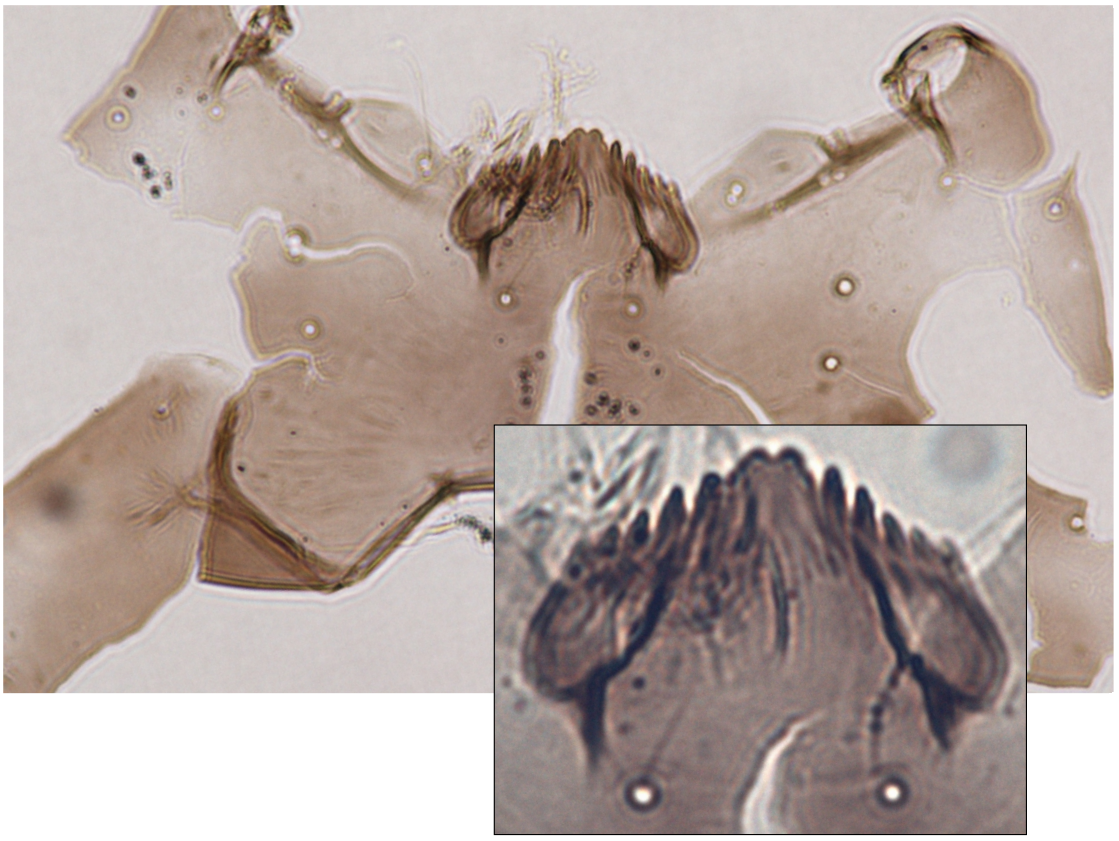

FIGURE A.27: *Eukiefferiella* head capsule with an enlargement of the mentum inset.

Description: Head capsule often dark brown. **Mentum** with paired median teeth and five lateral teeth. The first laterals are almost as tall as the median teeth, with the second and third laterals reducing in size. The fourth and fifth laterals are smaller yet and subequal. The **ventromental plates** are narrow and extend in a strait line from between the first and second lateral teeth. They turn at 45° and end in a small bulge.

Similar taxa: *Limnophyes* but the ventromental plates differ.

Observations/notes: Almost exclusively lotic (Woodward and Shulmeister, 2007; Holmes *et al.*, 2008; Cranston, 2000a), with some species restricted to colder waters, or possibly eurythermic (Andersen *et al.*, 2013). Has been associated with the littoral in Patagonia (Guilizzoni *et al.*, 2009).

ORTHOCLADIINAE: *Nanocladius*

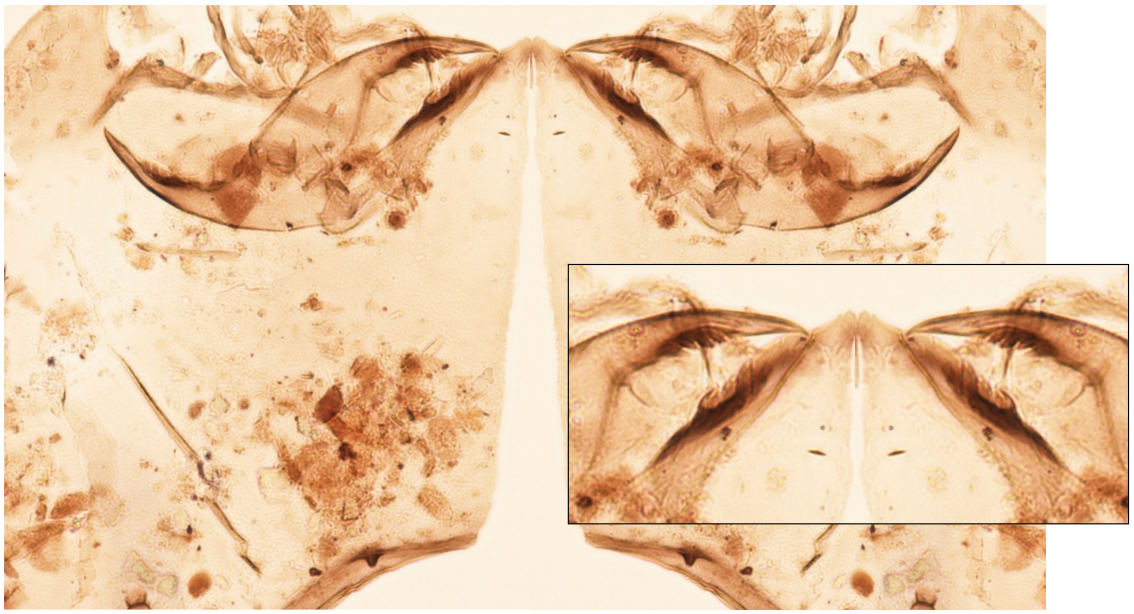

FIGURE A.28: *Nanocladius* head capsule, with an enlargement of the mentum inset. This image has been mirrored from a photomicrograph of a half head capsule torn along the medial suture, which is why the specimen appears to possess four mandibles.

Description: Head capsule often dark brown. Mentum with paired median teeth and five lateral teeth. The first laterals are almost as tall as the median teeth, with the second and third laterals reducing in size. The fourth and fifth laterals are smaller yet and subequal. The ventromental plates are narrow and extend in a strait line from between the first and second lateral teeth. They turn at 45° and end in a small bulge.

Similar taxa: *Limnophyes* but the ventromental plates differ.

Observations/notes: Lentic or lotic, sometimes rheophilic. Found in the littoral to upper profundal in oligotrophic and mesotrophic lakes (Andersen *et al.*, 2013).

TIPULIDAE

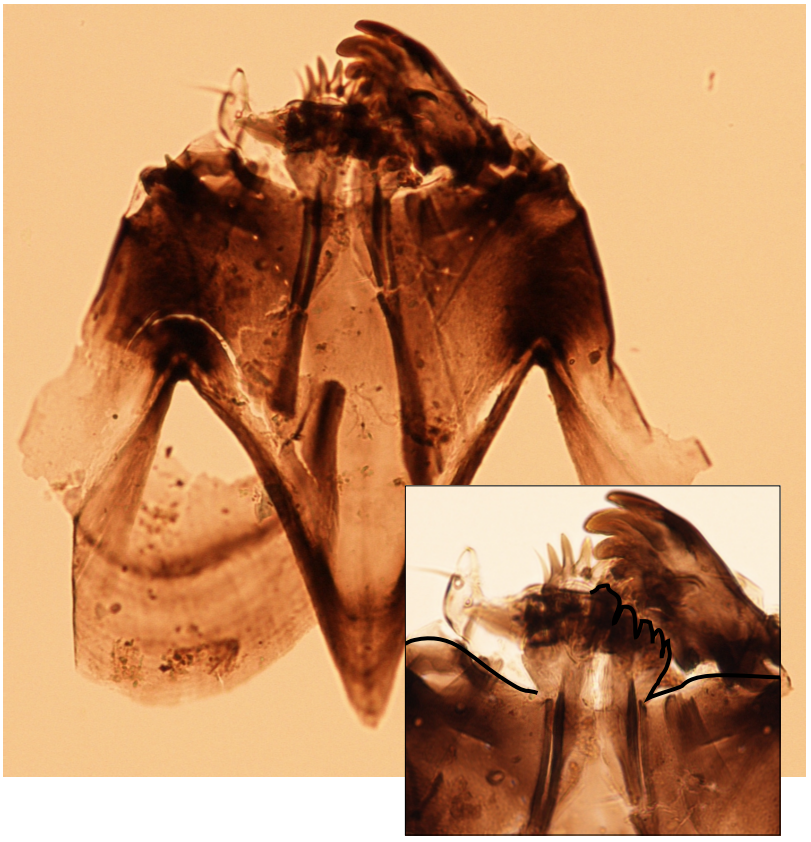

FIGURE A.29: TIPULIDAE head capsule, with annotated enlargement of the hypostomium inset showing the outline of the mentum.

Description: Head capsule deeply pigmented, large, with deep dorsolateral incisions. **Mentum** proud of head capsule, with single complex median tooth and around four lateral teeth. **Mandible** large with around six teeth. Neugart *et al.* (2009) describes the morphology of the head capsule fully.

Similar taxa: None: the deep dorsolateral incisions of the head capsule are distinctive.

Observations/notes: The family TIPULIDAE have aquatic or semi-aquatic larvae, although some species are fully terrestrial (Pritchard, 1983). Adult tipulids are fully terrestrial and are normally found in shaded, humid areas of woodland (Jong *et al.*, 2007).

SIMULIIDAE

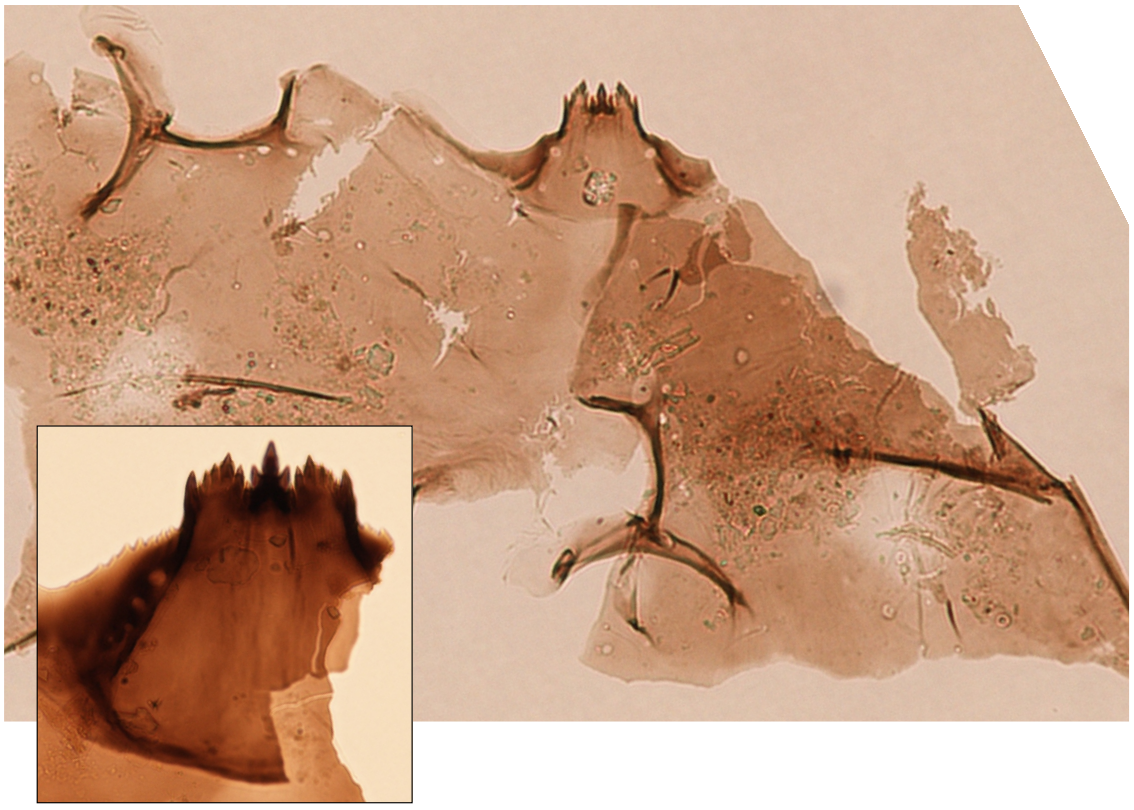

FIGURE A.30: SIMULIIDAE head capsule, with enlargement of the mentum inset.

Description: Head capsule large compared to size of **mentum**, often deeply pigmented. **Mentum** distinctive with a large number of variously sized teeth, generally trifid in appearance.

Similar taxa: None.

Observations/notes: Currie and Walker (1992) explores the importance of the family as indicators of palaeohydrological indicators. The family SIMULIIDAE live exclusively in free-flowing water and as such are largely confined to streams and rivers Currie and Walker (1992). They tend to inhabit the erosional sections of these environments. In lake sediments, found in areas close to lake tributaries (Heiri, 2004) and are indicative of flowing water (Luoto, 2010; Verschuren and Eggermont, 2006) in lakes and their catchments and are often associated with rheophilic chironomidae and chironomids with a preference to sand subrates (Porinchu and Macdonald, 2003).

CERATOPOGONIDAE

FIGURE A.31: CERATOPOGINAE head capsule.

Description: Head capsule with large, distinctive **setae** and no **mentum**.

Similar taxa: None.

Observations/notes: The family CERATOPOGINAE are found in aquatic and semi-aquatic environments (Verschuren and Eggermont, 2006). They can be included in regional training sets as they appear to be sensitive to summer temperatures (Rees *et al.*, 2008; Luoto, 2010) but can also be associated with macrophytes (Luoto, 2010). Can also be adapted to low-oxygen conditions (van Hardenbroek *et al.*, 2010).

Appendix B

List of Sources Used to Construct Figures 3.3 & 3.4

Site Name	Proxies Used	Reference(s)
Bajo de la Quienta	P	Marcos *et al.* (2012)
Canal de la Puntilla	P	Moreno *et al.* (1999); Moreno (1997)
Cerro Frías	P,CH	Sottile *et al.* (2011); Mancini (2002); Tonello *et al.* (2009)
Chandler	P,GS,G	Kilian *et al.* (2006)
Cordillera Pelada	P	Heusser (1982)
Eberhard	P,CH	Moreno *et al.* (2012)
Estancia Esmeralda	P,CH,M,D	McCullock *et al.* (2005)
Fu. Llanquihue	P	Heusser (1981)
GeoB 3313-1	AL,IS,E	Lamy *et al.* (2002)
Gran Campo Nevado	E	Biester *et al.* (2002)
Haberton	P,IS	Pendall *et al.* (2001); Markgraf and Huber (2010)
Hambre	G	Hermanns and Biester (2011)
Hinojales	P	Stutz *et al.* (2012)
Huelmo	P,CH	Hajdas (2003); Massaferro *et al.* (2009)
Isla de los Estados	P,MA,HU,G	Björck *et al.* (2012); Ponce *et al.* (2011)
Isle Sante Inés	P	Fontana and Bennett (2012)
La Cumbre	P	Heusser (1974)
La Tercera	P,CH	Sottile *et al.* (2011)
Lago Argentino	P	Wille and Schäbitz (2008)
Lago Argentino (circa)	P	Mancini (2002)
Lago Augusta	P	Villa-Martínez *et al.* (2012)
Lago Calvario	Basal date	Moreno *et al.* (2009)
Lago Cardiel	MA,P,	Gilli *et al.* (2005); Markgraf *et al.* (2003)

Site Name	Proxies Used	Reference(s)
Lago Condorito	P	Heusser *et al.* (1999); Moreno and Leon (2003)
Lago Fagano	MA,E	Waldmann *et al.* (2009)
Lago Galvarne	E,MS,CA	Unkel *et al.* (2008)
Lago Guanaco	IS,CN,P	Moy *et al.* (2008); Moreno *et al.* (2009)
Lago Huala Hue	P,CH	Iglesias *et al.* (2012)
Lago Lonkoy	P	Stutz *et al.* (2012)
Lago Mascardi	P	Bianchi and Ariztegui (2011); Hajdas (2003)
Lago Mosquito	P,CH	Iglesias *et al.* (2011)
Lago Padre	P,CH	Iglesias *et al.* (2011)
Lago Pantano	P,CH	Moreno *et al.* (2012)
Lago Pichilafquen	P,CH	Jara and Moreno (2012)
Lago Plomo	V	Elbert *et al.* (2011)
Lago Puyehue	D,GS,G,MA,V,S,P	Vargas-Ramirez *et al.* (2007); Batist *et al.* (2007); Sterken *et al.* (2007); Bertrand *et al.* (2007); Boës and Fagel (2007b); Charlet *et al.* (2007)
Lago Six Minutes	P	Bennett *et al.* (2000)
Lago Aculeo	P,D,E,BS	Jenny (2002)
Laguna Azul	P,CH,D,IS,CN	Mayr *et al.* (2005)
Laguna Cari-Laufquén	S	Cartwright *et al.* (2011)
Lago Cascada (circa)	E,MS,CA	Unkel *et al.* (2008)
Laguna de Cóndor	P,CH	Iglesias *et al.* (2011)
Laguna Facil	P,MA,CH,C	Haberle and Bennett (2004); Massaferro *et al.* (2005)
Laguna las Vizcachas	IS,E,D,BS,CN	Fey *et al.* (2009)
Laguna Oprasa	P,MA	Haberle and Bennett (2004)
Laguna Pastahue	P	Heusser *et al.* (1999)
Laguna Potrok Aike	P,D,MA,IS,E,C,S	Recasens *et al.* (2011); Anselmetti *et al.* (2009); Wille *et al.* (2007); Massaferro and Larocque-Tobler (2013); Mayr *et al.* (2008)
Laguna San Pedro	P,CH	Fletcher and Moreno (2012b)
Laguna Stibnite	P,CH	Bennett *et al.* (2000); Massaferro and Brooks (2002)
Lake Laja	GS,G,D,C	Urrutia *et al.* (2010)
Lake Lincoln	P	Bennett *et al.* (2000)
Lake Lofel	P	Bennett *et al.* (2000)
Lake Mallín Pollux	P,CH	Markgraf *et al.* (2007)
Lake Nahuel Rucá	P,M,D	Stutz *et al.* (2010, 2012)
Lake Shamen	P,CH	de Porras *et al.* (2012)
Los Cotorras	P,D	Borromei *et al.* (2010)
Los Mallines	P	Vargas-Ramirez *et al.* (2007)

Site Name	Proxies Used	Reference(s)
Nuevo Branau	P	Moreno *et al.* (1999)
ODP1233	P,RL,AL,IS	Pisias *et al.* (2006); Lamy *et al.* (2004); Kaiser *et al.* (2005); Heusser *et al.* (2006)
Pantano Margarita	P	Moreno *et al.* (2009)
Paso Garibaldi	P,CH,M	Markgraf and Huber (2010); Huber *et al.* (2004)
Puerto del Hambre	P,CH,M,D,E	McCullock *et al.* (2005); Biester *et al.* (2003)
Puerto Eden	P,B	Ashworth *et al.* (1991)
Puerto Octay	P,B	Heusser (1981); Hoganson and Ashworth (1992)
Puerto Varas	B	Hoganson and Ashworth (1992)
Punta Arenas	P	Heusser (1995)
Punta Pelluco	P	Heusser (1981)
Rio Caunahue	B,P	Hoganson and Ashworth (1992); Heusser (1981); Markgraf (1991)
Rio Rubens	P	Markgraf and Huber (2010); Huber *et al.* (2004)
Rucanancu	P	Heusser (1984)
Rupanco	P	Heusser (1974)
Seno Glaciar	E,IS	Schimpf *et al.* (2011)
Seno Skyring	E	Lamy *et al.* (2010)
Skyring	E,IS	Biester *et al.* (2003); Schimpf *et al.* (2011)
Torres del Paine	P	Heusser (1995)
Valle de Andorra	P,HU,M	Chambers *et al.* (2007); Mauquoy *et al.* (2004)
Vega Capón	Basal date	Moreno *et al.* (2009)
Vega Ñandú	P,CH	Villa-Martínez and Moreno (2007); Moreno *et al.* (2009)

TABLE B.1: Sources used in Figures 3.3 & 3.4, arranged alphabetically by site name.P=pollen, D=diatoms, E=elemental profiles, BS=biogenic silica, GS=grain size, G=geochemistry, C=chironomids, M=macrofossils, CH=charcoal, B=beetles, MA=magnetics, V=varves, S=survey, RL=radiolaria, AL=alkenone, IS=stable isotopes, CA=carbon, CN=C:N ratio, HU=peat humification.

Appendix C

Bulk XRF Data

Bulk samples of the light cream tephra layer at the base of the gtyjja sequence in both Laguna Meche and Laguna Edita, subsequently analysed for tephra chemistry by way of electron microprobe, were initially submitted for bulk XRF to test if the chemistries were identical. Samples were prepared and analysed by the GAU at NOC, Southampton. Samples were ground and prepared as both pressed powder pellets and as borate fusion beads. The results are reproduced in Table C.1.

Element		Meche	Edita
SiO_2	wt. %	67.5	64.767
TiO_2	wt. %	0.416	0.436
Al_2O_3	wt. %	14.911	14.890
Fe_2O_3	wt. %	3.542	3.732
MnO	wt. %	0.124	0.112
MgO	wt. %	0.987	1.045
CaO	wt. %	3.457	3.764
K_2O	wt. %	1.206	1.092
Na_2O	wt. %	4.750	4.706
P_2O_5	wt. %	0.183	0.197
S	wt. %	0.030	0.011
Cl	wt. %	0.210	0.203
Total	wt. %	97.32	94.95
LOI_{XRF}	wt. %	2.68	5.05
Co	ppm	9	8
Cr	ppm	<6	<6
V	ppm	37	39
Cu	ppm	13	12
Zn	ppm	60	59
Pb	ppm	14	13
Ba	ppm	400	354
Rb	ppm	28	26
Sr	ppm	304	335
Y	ppm	29	28
Zr	ppm	220	211
Nb	ppm	7	7
Th	ppm	14	13
La	ppm	19	15
Ce	ppm	38	43
Ga	ppm	15	16
As	ppm	4	2

TABLE C.1: Bulk XRF Analysis of MEC-5, 36-37cm (Meche) and EDI-6, 89-90cm (Edita).

Bibliography

Abril, J. (2004). Constraints on the use of 137Cs as a time-marker to support CRS and SIT chronologies. *Environmental Pollution 129*(1), 31–37.

Abril, J., M. García-León, R. García-Tenorio, C. Sánchez, and F. El-Daoushy (1991). Dating of marine sediments by an incomplete mixing model. *Journal of Environmental Radioactivity 15*(2), 135–151.

Alloway, B., G. Larsen, D. Lowe, P. Shane, and J. Westgate (2008). Quaternary Stratigraphy/Tephrochronology. In S. A. Elias (Ed.), *Encyclopedia of Quaternary Science*, pp. 2869–2898. Oxford: Elsevier.

Alloway, B. V., D. J. Lowe, D. J. A. Barrell, R. M. Newnham, P. C. Almond, P. C. Augustinus, N. A. N. Bertler, L. Carter, N. J. Litchfield, M. S. McGlone, J. Shulmeister, M. J. Vandergoes, and P. W. Williams (2007). Towards a climate event stratigraphy for New Zealand over the past 30 000 years (NZ-INTIMATE project). *Journal of Quaternary Science 22*(1), 9–35.

Andersen, T., P. S. Cranston, and J. H. Epler (2013). Chironomidae of the Holarctic Region - Keys and Diagnosis. *Insect Systematics & Evolution 66*(1), 1–571.

Anderson, R. F., S. Ali, L. I. Bradtmiller, S. H. H. Nielsen, M. Q. Fleisher, B. E. Anderson, and L. H. Burckle (2009). Wind-driven upwelling in the Southern Ocean and the deglacial rise in atmospheric CO2. *Science 323*(5920), 1443–8.

Andres, M. S., S. M. Bernasconi, J. A. McKenzie, and U. Röhl (2003). Southern Ocean deglacial record supports global Younger Dryas. *Earth and Planetary Science Letters 216*(4), 515–524.

Anselmetti, F. S., D. Ariztegui, M. De Batist, A. Catalina Gebhardt, T. Haberzettl, F. Niessen, C. Ohlendorf, and B. Zolitschka (2009). Environmental history of southern Patagonia unravelled by the seismic stratigraphy of Laguna Potrok Aike. *Sedimentology 56*(4), 873–892.

Appleby, P. and F. Oldfield (1978). The calculation of lead-210 dates assuming a constant rate of supply of unsupported 210Pb to the sediment. *CATENA 5*(1), 1–8.

Applegate, P. J., T. V. Lowell, and R. B. Alley (2008). Comment on "Absence of cooling in New Zealand and the adjacent ocean during the Younger Dryas chronozone". *Science 320*(5877), 746.

Araneda, A., P. Jana, C. Ortega, F. Torrejón, S. Bertrand, P. Vargas, N. Fagel, D. Alvarez, A. Stehr, and R. Urrutia (2013). Changes in sub-fossil chironomid assemblages in two Northern Patagonian lake systems associated with the occurrence of historical fires. *Journal of Paleolimnology 50*, 41–56.

Araneda, A., F. Torrejon, M. Aguayo, I. Alvial, C. Mendoza, and R. Urrutia (2009). Historical records of Cipreses glacier (34S): combining documentary-inferred 'Little Ice Age' evidence from Southern and Central Chile. *The Holocene 19*(8), 1173–1183.

Araneda, A., F. Torrejon, M. Aguayo, L. Torres, F. Cruces, M. Cisternas, and R. Urrutia (2007). Historical records of San Rafael glacier advances (North Patagonian Icefield): another clue to 'Little Ice Age' timing in southern Chile? *The Holocene 17*(7), 987–998.

Aravena, R., O. Suzuki, H. Peña, A. Pollastri, H. Fuenzalida, and A. Grilli (1999). Isotopic composition and origin of the precipitation in Northern Chile. *Applied Geochemistry 14*(4), 411–422.

Arblaster, J. M. (2006). Contributions of external forcings to southern annular mode trends. *Journal of Climate 19*(12), 2896–2905.

Ariztegui, D., M. M. Bianchi, J. Masaferro, E. Lafargue, and F. Niessen (1997). Interhemispheric synchrony of Lateglacial climatic instability as recorded in proglacial Lake Mascardi, Argentina. *Journal of Quaternary Science 12*(4), 333–338.

Ariztegui, D., A. Gilli, F. S. Anselmetti, R. A. Goñi, J. B. Belardi, and S. Espinosa (2010). Lake-level changes in central Patagonia (Argentina): crossing environmental thresholds for Lateglacial and Holocene human occupation. *Journal of Quaternary Science 25*(7), 1092–1099.

Armitage, P. D., P. S. Cranston, and L. C. V. Pinder (1995). *The Chironomidae: Biology and Ecology of non-biting midges*. London: Chapman & Hall.

Arnaud, F., O. Magand, E. Chapron, S. Bertrand, X. Boës, F. Charlet, and M. A. Mélières (2006). Radionuclide dating (210Pb, 137Cs, 241Am) of recent lake sediments in a highly active geodynamic setting (Lakes Puyehue and Icalma-Chilean Lake District). *Science of The Total Environment 366*(2-3), 837–850.

Ashworth, A. C., V. Markgraf, and C. Villagran (1991). Late Quaternary climatic history of the Chilean Channels based on fossil pollen and beetle analyses, with an analysis of the modern vegetation and pollen rain. *Journal of Quaternary Science 6*(4), 279–291.

Augustin, L., C. Barbante, P. R. F. Barnes, J. M. Barnola, M. Bigler, E. Castellano, O. Cattani, J. Chappellaz, D. Dahl-Jensen, B. Delmonte, G. Dreyfus, G. Durand,

S. Falourd, H. Fischer, J. Flückiger, M. E. Hansson, P. Huybrechts, G. Jugie, S. J. Johnsen, J. Jouzel, P. Kaufmann, J. Kipfstuhl, F. Lambert, V. Y. Lipenkov, G. C. Littot, A. Longinelli, R. Lorrain, V. Maggi, V. Masson-Delmotte, H. Miller, R. Mulvaney, J. Oerlemans, H. Oerter, G. Orombelli, F. Parrenin, D. a. Peel, J.-R. Petit, D. Raynaud, C. Ritz, U. Ruth, J. Schwander, U. Siegenthaler, R. Souchez, B. Stauffer, J. P. Steffensen, B. Stenni, T. F. Stocker, I. E. Tabacco, R. Udisti, R. S. W. Van De Wal, M. Van Den Broeke, J. Weiss, F. Wilhelms, J.-G. Winther, E. W. Wolff, and M. Zucchelli (2004). Eight glacial cycles from an Antarctic ice core. *Nature 429*(6992), 623–8.

Barbante, C., J.-M. Barnola, S. Becagli, J. Beer, M. Bigler, C. Boutron, T. Blunier, E. Castellano, O. Cattani, J. Chappellaz, D. Dahl-Jensen, M. Debret, B. Delmonte, D. Dick, S. Falourd, S. Faria, U. Federer, H. Fischer, J. Freitag, A. Frenzel, D. Fritzsche, F. Fundel, P. Gabrielli, V. Gaspari, R. Gersonde, W. Graf, D. Grigoriev, I. Hamann, M. Hansson, G. Hoffmann, M. a. Hutterli, P. Huybrechts, E. Isaksson, S. Johnsen, J. Jouzel, M. Kaczmarska, T. Karlin, P. Kaufmann, S. Kipfstuhl, M. Kohno, F. Lambert, A. Lambrecht, A. Lambrecht, A. Landais, G. Lawer, M. Leuenberger, G. Littot, L. Loulergue, D. Lüthi, V. Maggi, F. Marino, V. Masson-Delmotte, H. Meyer, H. Miller, R. Mulvaney, B. Narcisi, J. Oerlemans, H. Oerter, F. Parrenin, J.-R. Petit, G. Raisbeck, D. Raynaud, R. Röthlisberger, U. Ruth, O. Rybak, M. Severi, J. Schmitt, J. Schwander, U. Siegenthaler, M.-L. Siggaard-Andersen, R. Spahni, J. P. Steffensen, B. Stenni, T. F. Stocker, J.-L. Tison, R. Traversi, R. Udisti, F. Valero-Delgado, M. R. van den Broeke, R. S. W. van de Wal, D. Wagenbach, A. Wegner, K. Weiler, F. Wilhelms, J.-G. Winther, and E. Wolff (2006). One-to-one coupling of glacial climate variability in Greenland and Antarctica. *Nature 444*(7116), 195–198.

Barichivich, J., D. J. Sauchyn, and A. Lara (2009). Climate signals in high elevation tree-rings from the semiarid Andes of north-central Chile: Responses to regional and large-scale variability. *Palaeogeography, Palaeoclimatology, Palaeoecology 281*(3-4), 320–333.

Barker, S., P. Diz, M. J. Vautravers, J. Pike, G. Knorr, I. R. Hall, and W. S. Broecker (2009). Interhemispheric Atlantic seesaw response during the last deglaciation. *Nature 457*(7233), 1097–102.

Barrows, T. T., S. J. Lehman, L. K. Fifield, and P. De Deckker (2007). Absence of cooling in New Zealand and the adjacent ocean during the Younger Dryas chronozone. *Science 318*(5847), 86–9.

Barry, R. G. and R. J. Chorley (2010). *Atmosphere, Weather and Climate, 9th ed.* (9th ed.). Oxon: Routledge.

Batist, M., N. Fagel, M.-F. Loutre, and E. Chapron (2007). A 17,900-year multi-proxy lacustrine record of Lago Puyehue (Chilean Lake District): Introduction. *Journal of Paleolimnology 39*(2), 151–161.

Battarbee, R. W. (1994). Diatoms, lake acidification and the Surface Water Acidification Programme (SWAP): a review. *Hydrobiologica 274*, 1–7.

Bengtsson, L. and M. Enell (1986). Chemical Analysis. In *Handbook of Holocene palaeoecology and palaeohydrology*. Chichester: Wiley.

Bennett, K. D., S. G. Haberle, and S. H. Lumley (2000). The Last Glacial-Holocene Transition in Southern Chile. *Science 290*(5490), 325–328.

Bentley, M., D. A. Hodgson, J. A. Smith, C. Cofaigh, E. Domack, R. Larter, S. Roberts, S. Brachfeld, A. Leventer, C. Hjort, C. D. Hillenbrand, and J. Evans (2009). Mechanisms of Holocene palaeoenvironmental change in the Antarctic Peninsula region. *The Holocene 19*(1), 51–69.

Bertrand, S., A. Araneda, P. Vargas, P. Jana, N. Fagel, and R. Urrutia (2012). Using the N/C ratio to correct bulk radiocarbon ages from lake sediments: Insights from Chilean Patagonia. *Quaternary Geochronology 12*, 23–29.

Bertrand, S., J. Castiaux, and E. Juvigne (2008). Tephrostratigraphy of the late glacial and Holocene sediments of Puyehue Lake (Southern Volcanic Zone, Chile, 40deg.S). *Quaternary Research 70*(3), 343–357.

Bertrand, S., F. Charlet, B. Charlier, V. Renson, and N. Fagel (2007). Climate variability of southern Chile since the Last Glacial Maximum: a continuous sedimentological record from Lago Puyehue (40deg.S). *Journal of Paleolimnology 39*(2), 179–195.

Bertrand, S., M. Sterken, L. Vargas-Ramirez, M. De Batist, W. Vyverman, G. Lepoint, and N. Fagel (2010, August). Bulk organic geochemistry of sediments from Puyehue Lake and its watershed (Chile, 40ÂřS): Implications for paleoenvironmental reconstructions. *Palaeogeography, Palaeoclimatology, Palaeoecology 294*(1-2), 56–71.

Best, E. P. H., J. H. A. Dassen, J. J. Boon, and G. Wiegers (1990). Studies on decomposition of Ceratophyllum demersum litter under laboratory and field conditions: losses of dry mass and nutrients, qualitative changes in organic compounds and consequences for ambient water and sediments. *Hydrobiologia 194*(2), 91–114.

Bianchi, M. M. and D. Ariztegui (2011). Vegetation history of the Rio Manso Superior catchment area, Northern Patagonia (Argentina), since the last deglaciation. *The Holocene 22*(11), 1283–1295.

Bidegain, J. C. and Y. Rico (2012). Magnetostratigraphy and magnetic parameters of a sedimentary sequence in Punta San Andres, Buenos Aires, Argentina. *Quaternary International 253*, 91–103.

Biester, H., R. Kilian, C. Franzen, C. Woda, A. Mangini, and H. Schöler (2002). Elevated mercury accumulation in a peat bog of the Magellanic Moorlands, Chile (53deg.S) - an anthropogenic signal from the Southern Hemisphere. *Earth and Planetary Science Letters 201*(3-4), 609–620.

Biester, H., A. Martinez-Cortizas, S. Birkenstock, and R. Kilian (2003). Effect of peat decomposition and mass loss on historic mercury records in peat bogs from patagonia. *Environmental Science & Technology 37*(1), 32–9.

Bigler, C., I. Larocque, S. M. Peglar, H. Birks, and R. I. Hall (2002). Quantitative multiproxy assessment of long-term patterns of Holocene environmental change from a small lake near Abisko, northern Sweden. *The Holocene 12*(4), 481–496.

Bitušík, P., V. Kubovčík, E. Štefková, P. G. Appleby, and M. Svitok (2009). Subfossil diatoms and chironomids along an altitudinal gradient in the High Tatra Mountain lakes: a multi-proxy record of past environmental trends. *Hydrobiologia 631*(1), 65–85.

Björck, S., M. Rundgren, K. Ljung, I. Unkel, and A. Wallin (2012). Multi-proxy analyses of a peat bog on Isla de los Estados, easternmost Tierra del Fuego: a unique record of the variable Southern Hemisphere Westerlies since the last deglaciation. *Quaternary Science Reviews 42*, 1–14.

Blaauw, M. (2010). Methods and code for classical age-modelling of radiocarbon sequences. *Quaternary Geochronology 5*(5), 512–518.

Blaauw, M., G. B. M. Heuvelink, D. Mauquoy, J. van der Plicht, and B. van Geel (2003). A numerical approach to 14C wiggle-match dating of organic deposits: best fits and confidence intervals. *Quaternary Science Reviews 22*(14), 1485–1500.

Blaauw, M., J. van der Plicht, and B. van Geel (2004). Radiocarbon dating of bulk peat samples from raised bogs: non-existence of a previously reported reservoir effect? *Quaternary Science Reviews 23*(14-15), 1537–1542.

Blockley, S., S. Pyne-ODonnell, J. Lowe, I. Matthews, A. Stone, A. Pollard, C. Turney, and E. Molyneux (2005). A new and less destructive laboratory procedure for the physical separation of distal glass tephra shards from sediments. *Quaternary Science Reviews 24*(16-17), 1952–1960.

Blunier, T. and E. J. Brook (2001). Timing of millennial-scale climate change in Antarctica and Greenland during the last glacial period. *Science 291*(5501), 109–12.

Boës, X. and N. Fagel (2007a, July). Relationships between southern Chilean varved lake sediments, precipitation and ENSO for the last 600 years. *Journal of Paleolimnology 39*(2), 237–252.

Boës, X. and N. Fagel (2007b). Timing of the late glacial and Younger Dryas cold reversal in southern Chile varved sediments. *Journal of Paleolimnology 39*(2), 267–281.

Boggero, A., L. Füreder, V. Lencioni, T. Simcic, B. Thaler, U. Ferrarese, A. F. Lotter, and R. Ettinger (2006). Littoral Chironomid Communities of Alpine Lakes in Relation to Environmental Factors. *Hydrobiologia 562*(1), 145–165.

Boninsegna, J. A., J. Argollo, J. C. Aravena, J. Barichivich, D. Christie, M. E. Ferrero, A. Lara, C. Le Quesne, B. H. Luckman, and M. Masiokas (2009). Dendroclimatological reconstructions in South America: A review. *Palaeogeography, Palaeoclimatology, Palaeoecology 281*(3-4), 210–228.

Borromei, A. M., A. Coronato, L. G. Franzén, J. F. Ponce, J. A. L. Sáez, N. Maidana, J. Rabassa, and M. S. Candel (2010). Multiproxy record of Holocene paleoenvironmental change, Tierra del Fuego, Argentina. *Palaeogeography, Palaeoclimatology, Palaeoecology 286*(1-2), 1–16.

Bowen, G. J. and J. Revenaugh (2003). Interpolating the isotopic composition of modern meteoric precipitation. *Water Resources Research 39*(10), 9–13.

Braak, C. J. and P. Smilauer (1998). *CANOCO Reference Manual User's Guide to Canoco for Windows*. Number version 4. New York: Microcomputer Power.

Brodersen, K. P. and C. Lindegaard (1999). Classification, assessment and trophic reconstruction of Danish lakes using chironomids. *Freshwater Biology 42*(1), 143–157.

Brodersen, K. P., B. V. Odgaard, O. Vestergaard, and N. J. Anderson (2001). Chironomid stratigraphy in the shallow and eutrophic Lake Søbygaard , Denmark: chironomid-macrophyte co-occurrence. *Freshwater Biology 46*, 253–267.

Brodersen, K. P. and R. Quinlan (2006). Midges as palaeoindicators of lake productivity, eutrophication and hypolimnetic oxygen. *Quaternary Science Reviews 25*(15-16), 1995–2012.

Brodin, Y. W. and M. Gransberg (1993). Responses of insects, especially Chironomidae (Diptera), and mites to 130 years of acidification in a Scottish lake. *Hydrobiologica 250*, 201–212.

Bronk Ramsey, C. (2009). Bayesian Analysis of radiocarbon dates. *Radiocarbon 51*(1), 337.

Bronk-Ramsey, C., J. V. D. Plicht, and B. Weninger (2001). Wiggle matching radiocarbon dates. *Radiocarbon 43*(2), 381–389.

Brooks, S. J., H. Bennion, and H. J. B. Birks (2001). Tracing lake trophic history with a chironomid-total phosphorus inference model. *Freshwater Biology 46*(4), 513–533.

Brooks, S. J. and H. Birks (2001). Chironomid-inferred air temperatures from Lateglacial and Holocene sites in north-west Europe: progress and problems. *Quaternary Science Reviews 20*(16-17), 1723–1741.

Brooks, S. J., P. G. Langdon, and O. Heiri (2007). *The identification and use of palaearctic chironomidae larvae in palaeoecology*. London: QRA.

Caldenius, C. (1932). Las Glaciaciones Cuaternarias en la Patagonia y Tierra del Fuego. *Geografiska Annaler 14*, 133.

Calvo, E., C. Pelejero, P. De Deckker, and G. A. Logan (2007). Antarctic deglacial pattern in a 30 kyr record of sea surface temperature offshore South Australia. *Geophysical Research Letters 34*(13), 1–6.

Carroll, J. and I. Lerche (2003). *Sedimentary Processes: Quatification Using Radionuclides*. London: Elsevier.

Carter, L., B. Manighetti, G. Ganssen, and L. Northcote (2008). Southwest Pacific modulation of abrupt climate change during the Antarctic Cold Reversal-Younger Dryas. *Palaeogeography, Palaeoclimatology, Palaeoecology 260*(1-2), 284–298.

Cartwright, A., J. Quade, S. Stine, K. D. Adams, W. Broecker, and H. Cheng (2011). Chronostratigraphy and lake-level changes of Laguna Cari-Laufquén, Río Negro, Argentina. *Quaternary Research 76*(3), 430–440.

Caseldine, C. J., C. Turney, and A. J. Long (2010). IPCC and palaeoclimate -ÂĂÂŞ an evolving story? *Journal of Quaternary Science 25*(1), 1–4.

Chambers, F., D. Mauquoy, S. Brain, M. Blaauw, and J. Daniell (2007). Globally synchronous climate change 2800 years ago: Proxy data from peat in South America. *Earth and Planetary Science Letters 253*(3-4), 439–444.

Charlet, F., M. Batist, E. Chapron, S. Bertrand, M. Pino, and R. Urrutia (2007). Seismic stratigraphy of Lago Puyehue (Chilean Lake District): new views on its deglacial and Holocene evolution. *Journal of Paleolimnology 39*(2), 163–177.

Christie, D. A., A. Lara, J. Barichivich, R. Villalba, M. S. Morales, and E. Cuq (2009). El Niño-Southern Oscillation signal in the world's highest-elevation tree-ring chronologies from the Altiplano, Central Andes. *Palaeogeography, Palaeoclimatology, Palaeoecology 281*(3-4), 309–319.

Clerk, S., R. Hall, R. Quinlan, and J. P. Smol (2000). Quantitative inferences of past hypolimnetic anoxia and nutrient levels from a Canadian Precambrian Shield lake. *Journal of Paleolimnology 23*, 319–336.

Coleman, D. C. and B. Fry (1991). *Carbon Isotope Techniques*. San Diego, USA: Academic Press Inc.

Cranston, P. (2000a). August ThienemannâĂŹs influence on modern chironomidology-an Australian perspective. *Verh. Internat. Verein. Limnol. 27*, 278–283.

Cranston, P. S. (1982). *A Key to the Larvae of the British Orthocladiinae (Chironomidae)*. Ambleside: Freshwater Biological Associaion.

Cranston, P. S. (2000b). Parapsectrocladius: a new genus of orthocladiine Chironomidae (Diptera) from Patagonia, the southern Andes. *Insect Systematics & Evolution 31*(1), 103–120.

Cranston, P. S. (2000c). Validation of Parapsectrocladius escondido Cranston & Añón Suárez (Diptera: Chironomidae) by declaration of type depository. *Insect Systematics & Evolution 31*(4), 103–103.

Cranston, P. S. and D. H. D. Edward (1999). Botryocladius gen.n.: a new transantarctic genus of orthocladiine midge (Diptera: Chironomidae). *Systematic Entomology 24*(4), 305–333.

Cranston, P. S., N. B. Hardy, G. E. Morse, L. Puslednik, and S. R. McCluen (2010). When molecules and morphology concur: the Gondwanan midges (Diptera: Chironomidae). *Systematic Entomology 35*(4), 636–648.

Cranston, P. S. and U. Nolte. Fissimentum, a new genus of drought-tolerant Chironomini (Diptera: Chironomidae) from the Americas and Australia.

Cronan, D., G. Rothwell, and I. Croudace (2010). An ITRAX Geochemical Study of Ferromanganiferous Sediments from the Penrhyn Basin, South Pacific Ocean. *Marine Georesources & Geotechnology 28*(3), 207–221.

Croudace, I. W., A. Rindby, and R. G. Rothwell (2006). ITRAX: description and evaluation of a new multi-function X-ray core scanner. *Geological Society, London, Special Publications 267*(1), 51–63.

Currie, D. C. and I. R. Walker (1992). Recognition and palaeohydrologic significance of fossil black fly larvae , with a key to the Nearctic genera (Diptera: Simuliidae). *Journal of Paleolimnology 7*, 37–54.

Cuven, S., P. Francus, and S. F. Lamoureux (2010). Estimation of grain size variability with micro X-ray fluorescence in laminated lacustrine sediments, Cape Bounty, Canadian High Arctic. *Journal of Paleolimnology 44*(3), 803–817.

Cwynar, L. C., A. B. H. Rees, C. R. Pedersen, and S. Engels (2012). Depth distribution of chironomids and an evaluation of site-specific and regional lake-depth inference models: a good model gone bad? *Journal of Paleolimnology 48*(3), 517–533.

Dabrio, C. J., J. I. Santisteban, R. Mediavilla, E. Lo, G. Garci, S. Castan, M. B. R. Zapata, M. Jose, and P. E. Marti (2004). Loss on ignition: a qualitative or quantitative method for organic matter and carbonate mineral content in sediments? *Journal of Paleolimnology 32*, 287–299.

Darling, W. G., A. H. Bath, J. J. Gibson, and K. Rozanski (2005). Isotopes in Water. In M. J. Leng (Ed.), *Isotopes in Palaeoenvironmental Research*, Chapter 1, pp. 1–66. Netherlands: Klewer.

de Porras, M. E., A. Maldonado, A. M. Abarzúa, M. L. Cárdenas, J. P. Francois, A. Martel-Cea, C. R. Stern, C. Méndez, and O. Reyes (2012). Postglacial vegetation, fire and climate dynamics at Central Chilean Patagonia (Lake Shaman, 44deg.S). *Quaternary Science Reviews 50*, 71–85.

Dean, W. E. (1974). Determination of Carbonate and Organic Matter in Calcareous Sediments and Sedimentary Rocks by Loss on Ignition: Comparison With Other Methods. *SEPM Journal of Sedimentary Research 44*(1), 242–248.

Dearing, J. (1999). Magnetic Susceptability. In J. Walden (Ed.), *Environmental Magnetism: A Practical Guide*. London: Quaternary Research Association.

Divine, D., N. Koç, E. Isaksson, S. Nielsen, X. Crosta, and F. Godtliebsen (2010). Holocene Antarctic climate variability from ice and marine sediment cores: Insights on ocean-atmosphere interaction. *Quaternary Science Reviews 29*(1-2), 303–312.

Donato, M., J. Massaferro, and S. J. Brooks (2008). Chironomid (Chironomidae : Diptera) checklist from Nahuel Huapi National Park, Patagonia, Argentina. *Rev. Soc. Entomol. Argent. 67*(1-2), 163–170.

Dungait, J. A. J., R. Bol, E. Lopez-Capel, I. D. Bull, D. Chadwick, W. Amelung, S. J. Granger, D. A. C. Manning, and R. P. Evershed (2010). Applications of stable isotope ratio mass spectrometry in cattle dung carbon cycling studies. *Rapid Communications in Mass Spectrometry 24*(5), 495–500.

Dytham, C. (2011). *Choosing and Using Statistics: A Biologists Guide* (3rd ed.). Chichester: Blackwell.

Eastwood, W., J. Tibby, N. Roberts, H. Birks, and H. Lamb (2002). The environmental impact of the Minoan eruption of Santorini (Thera): statistical analysis of palaeoecological data from Gölhisar, southwest Turkey. *The Holocene 12*(4), 431–444.

Elbert, J., M. Grosjean, L. von Gunten, R. Urrutia, D. Fischer, R. Wartenburger, D. Ariztegui, M. Fujak, and Y. Hamann (2011). Quantitative high-resolution winter (JJA) precipitation reconstruction from varved sediments of Lago Plomo 47deg.S, Patagonian Andes, AD 1530-2002. *The Holocene 22*(4), 465–474.

Elbert, J., R. Wartenburger, L. von Gunten, R. Urrutia, D. Fischer, M. Fujak, Y. Hamann, N. D. Greber, and M. Grosjean (2013). Late Holocene air temperature variability reconstructed from the sediments of Laguna Escondida, Patagonia, Chile (45deg.30min.S). *Palaeogeography, Palaeoclimatology, Palaeoecology 369*, 482–492.

Engels, S. and L. C. Cwynar (2011, January). Changes in fossil chironomid remains along a depth gradient: evidence for common faunal thresholds within lakes. *Hydrobiologia*.

Engels, S., L. C. Cwynar, A. B. H. Rees, and B. N. Shuman (2012). Chironomid-based water depth reconstructions: an independent evaluation of site-specific and local inference models. *Journal of Paleolimnology 48*(4), 693–709.

Epler, J. H. (1988). A reconsideration of the genus Apedilum Townes, 1945. *Spixiana Supp. 14*, 105–116.

Esper, J. and D. Frank (2009). Divergence pitfalls in tree-ring research. *Climatic Change 94*(3-4), 261–266.

Espizua, L. E. and P. Pitte (2009). The Little Ice Age glacier advance in the Central Andes (35deg.S), Argentina. *Palaeogeography, Palaeoclimatology, Palaeoecology 281*(3-4), 345–350.

Fairbanks, R. G., R. A. Mortlock, T.-C. Chiu, L. Cao, A. Kaplan, T. P. Guilderson, T. W. Fairbanks, A. L. Bloom, P. M. Grootes, and M. J. Nadeau (2005). Radiocarbon calibration curve spanning 0 to 50,000 years BP based on paired 230Th/234U/238U and 14C dates on pristine corals. *Quaternary Science Reviews 24*(16-17), 1781–1796.

Fallu, M. A., R. Pienitz, I. R. Walker, and J. Overpeck (2004). AMS 14C dating of tundra lake sediments using chironomid head capsules. *Journal of Paleolimnology 31*(1), 11–22.

Fast, A. W. (1970). An Evaluation of the Efficiency of Zoobenthos Separation by Sugar Flotation. *The Progressive Fish-Culturist 32*(4), 212–216.

Fernandez, R., J. Anderson, S. Bertrand, and J. Wellner (2011). Gualas Glacier sedimentary record of climate and environmental change, Golfo Elefantes, Western Patagonia (46.5deg.S). *The Holocene 22*(4), 451–463.

Fey, M., C. Korr, N. I. Maidana, M. L. Carrevedo, H. Corbella, S. Dietrich, T. Haberzettl, G. Kuhn, A. Lücke, and C. Mayr (2009). Palaeoenvironmental changes during the last 1600 years inferred from the sediment record of a cirque lake in southern Patagonia (Laguna Las Vizcachas, Argentina). *Palaeogeography, Palaeoclimatology, Palaeoecology 281*(3-4), 363–375.

Fletcher, M. S. and P. I. Moreno (2012a). Have the Southern Westerlies changed in a zonally symmetric manner over the last 14,000 years? A hemisphere-wide take on a controversial problem. *Quaternary International 253*, 32–46.

Fletcher, M. S. and P. I. Moreno (2012b). Vegetation, climate and fire regime changes in the Andean region of southern Chile (38deg.S) covaried with centennial-scale climate anomalies in the tropical Pacific over the last 1500 years. *Quaternary Science Reviews 46*, 46–56.

Fogwill, C. and P. Kubik (2005). A Glacial Stage Spanning The Antarctic Cold Reversal In Torres Del Paine (51deg.S), Chile, Based On Preliminary Cosmogenic Exposure Ages. *Geografiska Annaler, Series A: Physical Geography 87*(2), 403–408.

Fontana, S. L. and K. Bennett (2012). Postglacial vegetation dynamics of western Tierra del Fuego. *The Holocene 22*(11), 1337–1350.

French, H. M. (2007). *The Periglacial Environment* (3rd ed.). Chicester: Wiley.

Garcia, P. and D. Anonsuarez (2007, February). Community structure and phenology of chironomids (Insecta: Chironomidae) in a Patagonian Andean stream. *Limnologica - Ecology and Management of Inland Waters 37*(1), 109–117.

Garreaud, R. D. and P. Aceituno (2007). Atmospheric Circulation and Climate Variablity. In *The Physical Geography of South America*. Oxford: Oxford University Press.

Garreaud, R. D., M. Vuille, R. Compagnucci, and J. Marengo (2009). Present-day South American climate. *Palaeogeography, Palaeoclimatology, Palaeoecology 281*(3-4), 180–195.

Gerrard, A. J. (1990). *Mountain Environments: An Examination of the Physical Geography of Mountains*. London: Belhaven.

Gibson, J. J., E. E. Prepas, and P. Mceachern (2002). Quantitative comparison of lake through flow, residency, and catchment runoff using stable isotopes: modelling and results from a regional survey of Boreal lakes. *Journal of Hydrology 262*, 128–144.

Gillett, N. P., T. D. Kell, and P. D. Jones (2006). Regional climate impacts of the Southern Annular Mode. *Geophysical Research Letters 33*(23), 1–4.

Gilli, A., D. Ariztegui, F. Anselmetti, J. Mckenzie, V. Markgraf, I. Hajdas, and R. Mcculloch (2005). Mid-Holocene strengthening of the Southern Westerlies in South America-Sedimentological evidences from Lago Cardiel, Argentina (49deg.S). *Global and Planetary Change 49*(1-2), 75–93.

Glasser, N., S. Harrison, V. Winchester, and M. Aniya (2004). Late Pleistocene and Holocene palaeoclimate and glacier fluctuations in Patagonia. *Global and Planetary Change 43*(1-2), 79–101.

Glasser, N. F. and M. C. Ghiglione (2009). Structural, tectonic and glaciological controls on the evolution of fjord landscapes. *Geomorphology 105*(3-4), 291–302.

Glasser, N. F., S. Harrison, K. N. Jansson, K. Anderson, and A. Cowley (2011). Global sea-level contribution from the Patagonian Icefields since the Little Ice Age maximum. *Nature Geoscience 4*(5), 303–307.

Glasser, N. F., S. Harrison, C. Schnabel, D. Fabel, and K. N. Jansson (2012). Younger Dryas and early Holocene age glacier advances in Patagonia. *Quaternary Science Reviews 58*, 7–17.

Glasser, N. F., K. N. Jansson, S. Harrison, and J. Kleman (2008). The glacial geomorphology and Pleistocene history of South America between 38deg.S and 56deg.S. *Quaternary Science Reviews 27*(3-4), 365–390.

Glew, J. R., J. P. Smol, and W. M. Last (2001). Sediment core collection and extrusion. In *Tracking Environmental Change Using Lake Sediments: Vol. 1: Basin Analysis, Coring, and Chronological Techniques*. Dordrecht: Kluwer.

Gnanadesikan, A. and R. W. Hallberg (2000). On the Relationship of the Circumpolar Current to Southern Hemisphere Winds in Coarse-Resolution Ocean Models. *Journal of Physical Oceanography 30*(8), 2013–2034.

Gonzalez-Carranza, Z., H. Hooghiemstra, and M. I. Velez (2012). Major altitudinal shifts in Andean vegetation on the Amazonian flank show temporary loss of biota in the Holocene. *The Holocene 22*(11), 1227–1241.

Grey, J., A. Kelly, and R. I. Jones (2004). High intraspecific variability in carbon and nitrogen stable isotope ratios of lake chironomid larvae. *Limnology and Oceanography 49*(1), 239–244.

Grimm, E. C., L. J. Maher Jr., and D. M. Nelson (2009). The magnitude of error in conventional bulk-sediment radiocarbon dates from central North America. *Quaternary Research 72*(2), 301–308.

Grootes, P. M., E. J. Steig, M. Stuiver, E. D. Waddington, D. L. Morse, and M. J. Nadeau (2001). The Taylor Dome Antarctic 18O Record and Globally Synchronous Changes in Climate. *Quaternary Research 56*(3), 289–298.

Guevara, S. R. and M. Arribére (2002). 137Cs dating of lake cores from the Nahuel Huapi National Park, Patagonia, Argentina: Historical records and profile measurements. *Journal of Radioanalytical and Nuclear Chemistry 252*(1), 37–45.

Guevara, S. R. and M. Arribére (2007). Comment on the article Radionuclide dating (Pb-210, Cs-137, Am-241) of recent lake sediments in a highly active geodynamic setting (Lakes Puyehue and Icalma-Chilean Lake District). *The Science of the Total Environment 385*(1-3), 310–1.

Guevara, S. R., M. Meili, A. Rizzo, R. Daga, and M. Arribere (2010). Sediment records of highly variable mercury inputs to mountain lakes in Patagonia during the past millennium. *Atmospheric Chemistry and Physics 10*(7), 3443–3453.

Guilderson, T. P., P. J. Reimer, and T. A. Brown (2005). The boon and bane of radiocarbon dating. *Science 307*(5708), 362–4.

Guilizzoni, P., J. Massaferro, A. Lami, E. L. Piovano, S. R. Guevara, S. M. Formica, R. Daga, A. Rizzo, and S. Gerli (2009). Palaeolimnology of Lake Hess (Patagonia, Argentina): multi-proxy analyses of short sediment cores. *Hydrobiologia 631*(1), 289–302.

Gut, B. (2008). *Trees In Patagonia*. Switzerland: Springer.

Haberle, S. (1998). Age and origin of tephras recorded in postglacial lake sediments to the west of the southern Andes, 44deg.S to 47deg.S. *Journal of Volcanology and Geothermal Research 84*(3-4), 239–256.

Haberle, S. and K. D. Bennett (2004). Postglacial formation and dynamics of North Patagonian Rainforest in the Chonos Archipelago, Southern Chile. *Quaternary Science Reviews 23*(23-24), 2433–2452.

Hajdas, I. (2003). Precise radiocarbon dating of Late-Glacial cooling in mid-latitude South America. *Quaternary Research 59*(1), 70–78.

Hajdas, I., D. J. Lowe, R. M. Newnham, and G. Bonani (2006). Timing of the late-glacial climate reversal in the Southern Hemisphere using high-resolution radiocarbon chronology for Kaipo bog, New Zealand. *Quaternary Research 65*(2), 340–345.

Hammer, O. (2010). *PAST Reference Manual*. Number 1999. Private Press.

Hann, B. J., B. G. Warner, and W. F. Warwick (1992). Aquatics invertebrates and climatic change: A comment on Walker et al. (1991). *Canadian Journal of Fisheries and Aquatic Science 49*, 1274–1276.

Harrison, S., V. Winchester, and N. Glasser (2007). The timing and nature of recession of outlet glaciers of Hielo Patagónico Norte, Chile, from their Neoglacial IV (Little Ice Age) maximum positions. *Global and Planetary Change 59*(1-4), 67–78.

Hatfield, R. G. and B. A. Maher (2009). Fingerprinting upland sediment sources: particle size-specific magnetic linkages between soils, lake sediments and suspended sediments. *Earth Surface Processes and Landforms 34*(10), 1359–1373.

Hayward, C. (2011). High spatial resolution electron probe microanalysis of tephras and melt inclusions without beam-induced chemical modification. *The Holocene 22*(1), 119–125.

Hein, A. S., N. R. Hulton, T. J. Dunai, D. E. Sugden, M. R. Kaplan, and S. Xu (2010). The chronology of the Last Glacial Maximum and deglacial events in central Argentine Patagonia. *Quaternary Science Reviews 29*(9-10), 1212–1227.

Heiri, O. (2004). Within-lake variability of subfossil chironomid assemblages in shallow Norwegian lakes. *Journal of Paleolimnology 32*(1), 67–84.

Heiri, O. (2007). Chironomid Records: Postglacial Europe. In *Encyclopaedia of Quaternary Science*, pp. 390. Netherlands: Elsevier.

Heiri, O., H. Birks, S. Brooks, G. Velle, and E. Willassen (2003). Effects of within-lake variability of fossil assemblages on quantitative chironomid-inferred temperature reconstruction. *Palaeogeography, Palaeoclimatology, Palaeoecology 199*(1-2), 95–106.

Heiri, O. and A. F. Lotter (2001). Effect of low count sums on quantitative environmental reconstructions: an example using subfossil chironomids. *Journal of Paleolimnology 26*, 343–350.

Heiri, O. and A. F. Lotter (2010). How does taxonomic resolution affect chironomid-based temperature reconstruction? *Journal of Paleolimnology 44*(2), 589–601.

Heiri, O., A. F. Lotter, and G. Lemcke (2001). Loss on ignition as a method for estimating organic and carbonate content in sediments: reproducibility and comparability of results. *Journal of Paleolimnology 25*, 101–110.

Hermanns, Y. M. and H. Biester (2011). A Holocene record of mercury accumulation in a pristine lake in Southernmost South America (53deg.S)-climatic and environmental drivers. *Biogeosciences Discussions 8*(4), 6555–6588.

Heusser, C. (1984). Late-Glacial-Holocene of the Lake District of Chile. *Quaternary Research 22*(1), 77–90.

Heusser, C. (1995). Three Late Quaternary pollen diagrams from Southern Patagonia and their palaeoecological implications. *Palaeogeography, Palaeoclimatology, Palaeoecology 118*(1-2), 1–24.

Heusser, C. J. (1974). Vegetation and Climate of the southern Chilean lake district during and since the last glaciation. *Quaternary Research 4*(3), 290–315.

Heusser, C. J. (1981). Palynology of the Last Interglacial-Glacial in Mid-latitudes of Southern Chile. *Quaternary Research 16*, 293–321.

Heusser, C. J. (1982). Palynology of Cushion Bogs of the Cordillera Valdivia, Chile Pelada, Province of Vaidivia, Chile. *Quaternary Research 17*, 71–92.

Heusser, C. J., L. E. Heusser, and T. V. Lowell (1999). Paleoecology of The Southern Chilean Lake District-Isla Grande de Chiloe During Middle-late Llanquihue Glaciation and Deglaciation. *Geografiska Annaler, Series A: Physical Geography 81*(2), 231–284.

Heusser, C. J. and J. Rabassa (1987). Cold climatic episode of Younger Dryas age in Tierra del Fuego. *Nature 328*(6131), 609–611.

Heusser, L., C. Heusser, and N. Pisias (2006). Vegetation and climate dynamics of southern Chile during the past 50,000 years: results of ODP Site 1233 pollen analysis. *Quaternary Science Reviews 25*(5-6), 474–485.

Hibbert, F. D., W. E. N. Austin, M. J. Leng, and R. W. Gatliff (2009). British Ice Sheet dynamics inferred from North Atlantic ice-rafted debris records spanning the last 175000 years. *Journal of Quaternary Science 25*(4), 461–482.

Hodgson, D. A. and L. C. Sime (2010). Palaeoclimate: Southern westerlies and CO2. *Nature Geoscience 3*(10), 666–667.

Hoefs, J. (2009). *Stable Isotope Geochemistry* (6 ed.), Volume 46. London: Kluwer.

Hoganson, J. W. and A. C. Ashworth (1992). Fossil Beetle Evidence for Climatic Change 18,000-10,000 Years B.P. in South-Central Chile. *Quaternary Research 37*, 101–116.

Hogg, A., C. Bronk-Ramsey, C. Turney, and J. Palmer (2009). Bayesian evaluation of the southern hemisphere radiocarbon offset during the Holocene. *Radiocarbon 51*(4), 1165–1176.

Holmes, N., P. G. Langdon, and C. J. Caseldine (2008). Subfossil chironomid variability in surface sediment samples from Icelandic lakes: implications for the development and use of training sets. *Journal of Paleolimnology 42*(2), 281–295.

Holmlund, P. and H. Fuenzalida (1995). Anomalous glacier responses to 20th century climatic changes in Darwin Cordillera, southern Chile. *Journal of Glaciology 41*, 465–473.

Holz, A. and T. T. Veblen (2011). The amplifying effects of humans on fire regimes in temperate rainforests in western Patagonia. *Palaeogeography, Palaeoclimatology, Palaeoecology 311*(1-2), 82–92.

Hubbard, A., A. S. Hein, M. R. Kaplan, N. R. J. Hulton, and N. Glasser (2005). A Modelling Reconstruction Of The Last Glacial Maximum Ice Sheet And Its Deglaciation In The Vicinity Of The Northern Patagonian Icefield, South America. *Geografiska Annaler A 87A*(2), 375–391.

Huber, U. M., V. Markgraf, and F. Schäbitz (2004). Geographical and temporal trends in Late Quaternary fire histories of Fuego-Patagonia, South America. *Quaternary Science Reviews 23*(9-10), 1079–1097.

Iglesias, V., C. Whitlock, M. M. Bianchi, G. Villarosa, and V. Outes (2011). Holocene climate variability and environmental history at the Patagonian forest/steppe ecotone: Lago Mosquito (42deg.29min.37.89sec.S, 71deg.24min.14.57sec.W) and Laguna del Condor (42deg.20min.47.22sec.S, 71deg.17min.07.62sec.W). *The Holocene 22*(11), 1297–1307.

Iglesias, V., C. Whitlock, M. M. Bianchi, G. Villarosa, and V. Outes (2012). Climate and local controls of long-term vegetation dynamics in northern Patagonia (Lat 41deg.S). *Quaternary Research 78*(3), 502–512.

Iglesias, V., C. Whitlock, V. Markgraf, and M. M. Bianchi (2014). Postglacial history of the Patagonian forest/steppe ecotone (41-43deg.S). *Quaternary Science Reviews 94*, 120–135.

Janbu, A. D., O. Paasche, and M. R. Talbot (2011). Paleoclimate changes inferred from stable isotopes and magnetic properties of organic-rich lake sediments in Arctic Norway. *Journal of Paleolimnology 46*(1), 29–44.

Jara, I. a. and P. I. Moreno (2012). Temperate rainforest response to climate change and disturbance agents in northwestern Patagonia (41deg.S) over the last 2600 years. *Quaternary Research 77*(2), 235–244.

Jenny, B. (2002). Early to Mid-Holocene Aridity in Central Chile and the Southern Westerlies: The Laguna Aculeo Record (34deg.S). *Quaternary Research 58*(2), 160–170.

Johnsen, S. J., H. B. Clausen, W. Dansgaard, K. Fuhrer, N. Gundestrup, C. U. Hammer, P. Iversen, J. Jouzel, B. Stauffer, and J. P. Steffensen (1992). Irregular glacial interstadials recorded in a new Greenland ice core. *Nature 359*(6393), 311–313.

Jones, V., R. Battarbee, and R. Hedges (1993). The use of chironomid remains for AMS 14C dating of lake sediments. *The Holocene 3*(2), 161–163.

Jong, H., P. Oosterbroek, J. Gelhaus, H. Reusch, and C. Young (2007). Global diversity of craneflies (Insecta, Diptera: Tipulidea or Tipulidae sensu lato) in freshwater. *Hydrobiologia 595*(1), 457–467.

Jouzel, J., V. Masson, O. Cattani, S. Falourd, M. Stievenard, B. Stenni, A. Longinelli, S. J. Johnsen, J. P. Steffenssen, J. R. Petit, J. Schwander, R. Souchez, and N. I. Barkov (2001). A new 27 ky high resolution East Antarctic climate record. *Geophysical Research Letters 28*(16), 3199.

Jouzel, J., R. Vaikmae, J. R. Petit, M. Martin, Y. Duclos, M. Stievenard, C. Lorius, M. Toots, M. A. Mélières, L. H. Burckle, N. I. Barkov, and V. M. Kotlyakov (1995). The two-step shape and timing of the last deglaciation in Antarctica. *Climate Dynamics 11*(3), 151–161.

Juggins, S. (2013). Quantitative reconstructions in palaeolimnology: new paradigm or sick science? *Quaternary Science Reviews 64*, 20–32.

Kaiser, J., F. Lamy, and D. Hebbeln (2005). A 70-kyr sea surface temperature record off southern Chile (Ocean Drilling Program Site 1233). *Paleoceanography 20*(4), 1–15.

Kalnay, E., M. Kanamitsu, R. Kistler, W. Collins, D. Deaven, L. Gandin, M. Iredell, S. Saha, G. White, J. Woollen, Y. Zhu, A. Leetmaa, R. Reynolds, M. Chelliah, W. Ebisuzaki, W. Higgins, J. Janowiak, K. Mo, C. Ropelewski, J. Wang, R. Jenne, and D. Joseph (1996). The NCEP/NCAR 40-Year Reanalysis Project. *Bulletin of the American Meteorological Society 77*(3), 437.

Kansanen, P. H. (1985). Assessment of pollution history from recent sediments in Lake Vanajavesi, southern Finland. II. Changes in chironomidae, chaoboridae and cerapogonidae (Diptera) fauna. *Annales Fennici Zoologicii 22*, 57–90.

Kastner, S., C. Ohlendorf, T. Haberzettl, A. Lücke, C. Mayr, N. I. Maidana, F. Schäbitz, and B. Zolitschka (2010). Southern hemispheric westerlies control the spatial

distribution of modern sediments in Laguna Potrok Aike, Argentina. *Journal of Paleolimnology 44*(4), 887–902.

Keeley, J. E. and D. R. Sandquist (1992). Carbon: freshwater plants. *Plant, Cell & Environment 15*, 1021–1035.

Kilian, R., H. Biester, J. Behrmann, O. Baeza, M. Fesq-Martin, M. Hohner, D. Schimpf, A. Friedmann, and A. Mangini (2006). Millennium-scale volcanic impact on a superhumid and pristine ecosystem. *Geology 34*(8), 609.

Kilian, R. and F. Lamy (2012). A review of Glacial and Holocene paleoclimate records from southernmost Patagonia (49-55deg.S). *Quaternary Science Reviews 53*, 1–23.

Kitzberger, T. (1997). Climatic influences on fire regimes along a rain forest-to-xeric woodland gradient in northern Patagonia, Argentina. *Journal of Biogeography 7*(1), 273–47.

Koch, J. and R. Kilian (2005). 'Little Ice Age' glacier fluctuations, Gran Campo Nevado, southernmost Chile. *The Holocene 15*(1), 20–28.

Krabbenhoft, D. P., C. J. Bowser, M. P. Anderson, and J. W. Valley (1990). Estimating Groundwater Exchange With Lakes 1 . The Stable Isotope Mass Balance Method. *Water Resources Research 26*(10), 2445–2453.

Krishnaswamy, S., D. Lal, J. Martin, and M. Meybeck (1971). Geochronology of lake sediments. *Earth and Planetary Science Letters 11*(1-5), 407–414.

Krosch, M. N., A. M. Baker, P. B. Mather, and P. S. Cranston (2011). Systematics and biogeography of the Gondwanan Orthocladiinae (Diptera: Chironomidae). *Molecular phylogenetics and evolution 59*(2), 458–68.

Kuehn, S., D. Froese, and P. Shane (2011). The INTAV intercomparison of electron-beam microanalysis of glass by tephrochronology laboratories: Results and recommendations. *Quaternary International 246*(1-2), 19–47.

Kurek, J. and L. C. Cwynar (2008a). Effects of within-lake gradients on the distribution of fossil chironomids from maar lakes in western Alaska: implications for environmental reconstructions. *Hydrobiologia 623*(1), 37–52.

Kurek, J. and L. C. Cwynar (2008b). The potential of site-specific and local chironomid-based inference models for reconstructing past lake levels. *Journal of Paleolimnology 42*(1), 37–50.

Lamy, F., D. Hebbeln, U. Ro, and G. Wefer (2001). Holocene rainfall variability in southern Chile: a marine record of latitudinal shifts of the Southern Westerlies. *Earth and Planetary Science Letters 185*, 369–382.

Lamy, F., J. Kaiser, U. Ninnemann, D. Hebbeln, H. W. Arz, and J. Stoner (2004). Antarctic timing of surface water changes off Chile and Patagonian ice sheet response. *Science 304*(5679), 1959–62.

Lamy, F., R. Kilian, H. W. Arz, J.-P. Francois, J. Kaiser, M. Prange, and T. Steinke (2010). Holocene changes in the position and intensity of the southern westerly wind belt. *Nature Geoscience 3*(10), 695–699.

Lamy, F., C. Rühlemann, D. Hebbeln, and G. Wefer (2002). High- and low-latitude climate control on the position of the southern Peru-Chile Current during the Holocene. *Paleoceanography 17*(2), 1–16.

Lang, B., A. P. Bedford, N. Richardson, and S. J. Brooks (2003). The use of ultra-sound in the preparation of carbonate and clay sediments for chironomid analysis. *Journal of Paleolimnology 30*, 451–460.

Langdon, P., K. Barber, and S. Lomas-Clarke (previously Morriss) (2004). Reconstructing climate and environmental change in northern England through chironomid and pollen analyses: evidence from Talkin Tarn, Cumbria. *Journal of Paleolimnology 32*(2), 197–213.

Langdon, P., C. Caseldine, I. Croudace, S. Jarvis, S. Wastegard, and T. Crowford (2011). A chironomid-based reconstruction of summer temperatures in NW Iceland since AD 1650. *Quaternary Research 75*(3), 451–460.

Langdon, P. G., N. Holmes, and C. J. Caseldine (2007). Environmental controls on modern chironomid faunas from NW Iceland and implications for reconstructing climate change. *Journal of Paleolimnology 40*(1), 273–293.

Lara, A. and R. Villalba (1993). A 3620-Year Temperature Record from Fitzroya cupressoides Tree Rings in Southern South America. *Science 260*(5111), 1104–6.

Larocque, I., M. Grosjean, O. Heiri, C. Bigler, and A. Blass (2008). Comparison between chironomid-inferred July temperatures and meteorological data AD 1850-2001 from varved Lake Silvaplana, Switzerland. *Journal of Paleolimnology 41*(2), 329–342.

Larocque, I., R. I. Hall, and E. Grahn (2001). Chironomids as indicators of climate change: a 100-lake training set from a subarctic region of northern Sweden (Lapland). *Journal of Paleolimnology 26*, 307–322.

Larocque, I., G. Velle, and N. Rolland (2009). Effect of removing small (<150micrometre) chironomids on inferring temperature in cold lakes. *Journal of Paleolimnology 44*(2), 709–719.

Larocque-Tobler, I. (2009). Reconstructing temperature at Egelsee, Switzerland, using North American and Swedish chironomid transfer functions: potential and pitfalls. *Journal of Paleolimnology 44*(1), 243–251.

Larocque-Tobler, I., M. Grosjean, and C. Kamenik (2011). Calibration-in-time versus calibration-in-space (transfer function) to quantitatively infer July air temperature using biological indicators (chironomids) preserved in lake sediments. *Palaeogeography, Palaeoclimatology, Palaeoecology 299*(1-2), 281–288.

Larocque-Tobler, I. and F. Oberli (2010). The use of cotton blue stain to improve the efficiency of picking and identifying chironomid head capsules. *Journal of Paleolimnology 45*(1), 121–125.

Le Quesne, C., C. Acuña, J. A. Boninsegna, A. Rivera, and J. Barichivich (2009). Long-term glacier variations in the Central Andes of Argentina and Chile, inferred from historical records and tree-ring reconstructed precipitation. *Palaeogeography, Palaeoclimatology, Palaeoecology 281*(3-4), 334–344.

Lehmann, M. F., S. M. Bernasconi, A. Barbieri, and J. A. McKenzie (2002). Preservation of organic matter and alteration of its carbon and nitrogen isotope composition during simulated and in situ early sedimentary diagenesis. *Geochimica et Cosmochimica Acta 66*(20), 3573–3584.

Leng, M. (2004). Palaeoclimate interpretation of stable isotope data from lake sediment archives. *Quaternary Science Reviews 23*(7-8), 811–831.

Leng, M. J., A. L. Lamb, T. J. Heaton, J. D. Marshall, B. B. Wolfe, M. D. Jones, J. A. Holmes, and C. Arrowsmith (2006). Isotopes in lake sediments. In *Isotopes in Palaeoenvironmental Research*. Springer.

Lepš, J. and P. Šmilauer (1999, January). *Multivariate Analysis of Ecological Data using CANOCO*, Volume 86. Private Press.

Lotter, A. F., I. R. Walker, S. J. Brooks, and W. Hofmann (1999). An intercontinental comparison of chironomid palaeotemperature inference models: Europe vs North America. *Quaternary Science Reviews 18*(6), 717–735.

Lotter, F., H. J. B. Birks, W. Hofmann, and A. Marchetto (1997). Modern diatom, cladocera, chironomid, and chrysophyte cyst assemblages as quantitative indicators for the reconstruction of past environmental conditions in the Alps. I: Climate. *Journal of Paleolimnology 18*, 395–420.

Lowe, D. J. (2011). Tephrochronology and its application: A review. *Quaternary Geochronology 6*(2), 107–153.

Löwemark, L., H. F. Chen, T. N. Yang, M. Kylander, E. F. Yu, Y. W. Hsu, T. Q. Lee, S. R. Song, and S. Jarvis (2011). Normalizing XRF-scanner data: A cautionary note on the interpretation of high-resolution records from organic-rich lakes. *Journal of Asian Earth Sciences 40*(6), 1250–1256.

Luoto, T. (2009a). Subfossil Chironomidae (Insecta: Diptera) along a latitudinal gradient in Finland: development of a new temperature inference model. *Journal of Quaternary Science 24*(2), 150–158.

Luoto, T. P. (2009b). A Finnish chironomid- and chaoborid-based inference model for reconstructing past lake levels. *Quaternary Science Reviews 28*(15-16), 1481–1489.

Luoto, T. P. (2010). Hydrological change in lakes inferred from midge assemblages through use of an intralake calibration set. *Ecological Monographs 80*(2), 303–329.

Luoto, T. P., S. Kultti, L. Nevalainen, and K. Sarmaja-Korjonen (2010). Temperature and effective moisture variability in southern Finland during the Holocene quantified with midge-based calibration models. *Journal of Quaternary Science 25*(8), 1317–1326.

Magand, O. and F. Arnaud (2007). Response on the comment from Ribeiro Guevara and Arribere on the article Radionuclide dating (Pb-210, Cs-137, Am-241) of recent lake sediments in a highly geodynamic setting (Lakes Puyehue and Icalma-Chilean Lake District). *Science of The Total Environment 385*(1-3), 312–314.

Mancini, V. (2002). Vegetation and climate during the Holocene in Southwest Patagonia, Argentina. *Review of Palaeobotany and Palynology 122*, 101–115.

Marcos, M. a., M. V. Mancini, and C. M. F. Dubois (2012, March). Middle- to late-Holocene environmental changes in Bajo de la Quinta, NE Patagonia, inferred by palynological records and their relation to human occupation. *The Holocene 22*(11), 1271–1281.

Markgraf, V. (1991). Younger Dryas in southern South America? *Boreas 20*, 63–69.

Markgraf, V., J. P. Bradbury, A. Schwalb, S. J. Burns, C. Stern, D. Ariztegui, A. Gilli, F. S. Anselmetti, S. Stine, and N. Maidana (2003). Holocene palaeoclimates of southern Patagonia: limnological and environmental history of Lago Cardiel, Argentina. *The Holocene 13*(4), 581–591.

Markgraf, V. and U. M. Huber (2010). Late and postglacial vegetation and fire history in Southern Patagonia and Tierra del Fuego. *Palaeogeography, Palaeoclimatology, Palaeoecology 297*(2), 351–366.

Markgraf, V., C. Whitlock, and S. Haberle (2007). Vegetation and fire history during the last 18,000 cal yr B.P. in Southern Patagonia: Mallín Pollux, Coyhaique, Province Aisén (45deg.41min.30sec.S, 71deg.50min.30sec.W, 640m elevation). *Palaeogeography, Palaeoclimatology, Palaeoecology 254*(3-4), 492–507.

Marshall, G. (2003). Trends in the Southern Annular Mode from observations and reanalyses. *Journal of Climate 16*(1999), 4134–4143.

Masiokas, M. H., B. H. Luckman, R. Villalba, S. Delgado, P. Skvarca, and A. Ripalta (2009). Little Ice Age fluctuations of small glaciers in the Monte Fitz Roy and Lago del Desierto areas, south Patagonian Andes, Argentina. *Palaeogeography, Palaeoclimatology, Palaeoecology 281*(3-4), 351–362.

Masiokas, M. H., A. Rivera, L. E. Espizua, R. Villalba, S. Delgado, and J. C. Aravena (2009). Glacier fluctuations in extratropical South America during the past 1000 years. *Palaeogeography, Palaeoclimatology, Palaeoecology 281*(3-4), 242–268.

Massaferro, J. and S. J. Brooks (2002). Response of chironomids to Late Quaternary environmental change in the Taitao Peninsula, southern Chile. *Journal of Quaternary Science 17*(2), 101–111.

Massaferro, J., S. J. Brooks, and S. G. Haberle (2005). The dynamics of chironomid assemblages and vegetation during the Late Quaternary at Laguna Facil, Chonos Archipelago, southern Chile. *Quaternary Science Reviews 24*(23-24), 2510–2522.

Massaferro, J. and I. Larocque-Tobler (2013). Using a newly developed chironomid transfer function for reconstructing mean annual air temperature at Lake Potrok Aike, Patagonia, Argentina. *Ecological Indicators 24*, 201–210.

Massaferro, J., I. Larocque-Tobler, S. J. Brooks, M. Vandergoes, A. Dieffenbacher-Krall, and P. Moreno (2014). Quantifying climate change in Huelmo mire (Chile, Northwestern Patagonia) during the Last Glacial Termination using a newly developed chironomid-based temperature model. *Palaeogeography, Palaeoclimatology, Palaeoecology 399*, 214–224.

Massaferro, J., P. Moreno, G. Denton, M. Vandergoes, and A. Dieffenbacher-Krall (2009). Chironomid and pollen evidence for climate fluctuations during the Last Glacial Termination in NW Patagonia. *Quaternary Science Reviews 28*(5-6), 517–525.

Massaferro, J., C. Recasens, I. Larocque-Tobler, B. Zolitschka, and N. Maidana (2013). Major lake level fluctuations and climate changes for the past 16,000 years as reflected by diatoms and chironomids preserved in the sediment of Laguna Potrok Aike, southern Patagonia. *Quaternary Science Reviews 71*, 167–174.

Masson, V. (2000). Holocene Climate Variability in Antarctica Based on 11 Ice-Core Isotopic Records. *Quaternary Research 54*(3), 348–358.

Mauquoy, D., M. Blaauw, B. van Geel, A. Borromei, M. Quattrocchio, F. M. Chambers, and G. Possnert (2004). Late Holocene climatic changes in Tierra del Fuego based on multiproxy analyses of peat deposits. *Quaternary Research 61*(2), 148–158.

Mayewski, P., E. Rohling, J. Curtstager, W. Karlen, K. Maasch, L. Davidmeeker, E. Meyerson, F. Gasse, S. Vankreveld, and K. Holmgren (2004). Holocene climate variability. *Quaternary Research 62*(3), 243–255.

Mayr, C., M. Fey, T. Haberzettl, S. Janssen, A. Lucke, N. Maidana, C. Ohlendorf, F. Schabitz, G. Schleser, and U. Struck (2005). Palaeoenvironmental changes in southern Patagonia during the last millennium recorded in lake sediments from Laguna Azul (Argentina). *Palaeogeography, Palaeoclimatology, Palaeoecology 228*(3-4), 203–227.

Mayr, C., A. Lücke, N. I. Maidana, M. Wille, T. Haberzettl, H. Corbella, C. Ohlendorf, F. Schäbitz, M. Fey, S. Janssen, and B. Zolitschka (2008). Isotopic fingerprints on lacustrine organic matter from Laguna Potrok Aike (southern Patagonia, Argentina) reflect environmental changes during the last 16,000 years. *Journal of Paleolimnology 42*(1), 81–102.

Mayr, C., A. Lücke, W. Stichler, P. Trimborn, B. Ercolano, G. Oliva, C. Ohlendorf, J. Soto, M. Fey, and T. Haberzettl (2007). Precipitation origin and evaporation of lakes in semi-arid Patagonia (Argentina) inferred from stable isotopes (δ18O, δ2H). *Journal of Hydrology 334*(1-2), 53–63.

McAlpine, J. F., B. V. Peterson, G. E. Shewell, H. J. Teskey, J. R. Vockeroth, and D. M. Wood. *The Manual of Nearctic Diptera*. Quebec: Canadian Government Publishing Centre.

McCormac, F. G., A. G. Hogg, P. G. Blackwel, C. E. Buck, T. F. G. Higham, and P. J. Reimer (2004). ShCal04 Southern Hemisphere Calibration, 0-11.0 cal. Kyr BP. *Radiocarbon 46*(3), 1087–1092.

McCulloch, R. and S. Davies (2001). Late-glacial and Holocene palaeoenvironmental change in the central Strait of Magellan, southern Patagonia. *Palaeogeography,Palaeoclimatology,Palaeoecology 173*(3-4), 143–173.

McCullock, R., C. Fogwill, D. Sugden, M. Bentley, and P. Kubik (2005). Chronology of The Last Glaciation In Central Strait Of Magellan And Bahia Inutil, Southernmost South America. *Geografiska Annaler, Series A: Physical Geography 87*(2), 289–312.

McGill, J. D., R. S. Wilson, and A. M. Brake (1979). The use of chironomid pupal exuviae in the surveillance of sewage pollution within a drainage system. *Water Research 13*, 887–894.

McGlone, M., C. Turney, and J. Wilmshurst (2004). Late-glacial and Holocene vegetation and climatic history of the Cass Basin, central South Island, New Zealand. *Quaternary Research 62*(3), 267–279.

McGlone, M. S., G. M. J. Hall, and J. M. Wilmshurst (2010). Seasonality in the early Holocene: Extending fossil-based estimates with a forest ecosystem process model. *The Holocene 21*(4), 517–526.

McGlone, M. S., C. S. M. Turney, J. M. Wilmshurst, J. Renwick, and K. Pahnke (2010). Divergent trends in land and ocean temperature in the Southern Ocean over the past 18,000 years. *Nature Geoscience 3*(9), 622–626.

Metcalfe, S. E., M. D. Jones, S. J. Davies, A. Noren, and A. MacKenzie (2010). Climate variability over the last two millennia in the North American Monsoon region, recorded in laminated lake sediments from Laguna de Juanacatlan, Mexico. *The Holocene 20*(8), 1195–1206.

Meyer, I. and S. Wagner (2008). The Little Ice Age in southern Patagonia: Comparison between paleoecological reconstructions and downscaled model output of a GCM simulation Three-dimensional radiocarbon modeling: A tool to assess the last glacial ocean circulation and radiocarbon chrono. *PAGES News 16*(2), 12–13.

Meyers, P. A. and J. L. Teranes (2001). Sediment Organic Matter. In W. M. Last and J. P. Smol (Eds.), *Tracking environmental change using lake sediments vol. 2: Physical and geochemical methods*. Netherlands: Klewer.

Millet, L., F. Arnaud, O. Heiri, M. Magny, V. Verneaux, and M. Desmet (2009, March). Late-Holocene summer temperature reconstruction from chironomid assemblages of Lake Anterne, northern French Alps. *The Holocene 19*(2), 317–328.

Millet, L., B. Vannière, V. Verneaux, M. Magny, J. R. Disnar, F. Laggoun-Défarge, A. V. Walter-Simonnet, G. Bossuet, E. Ortu, and J. L. Beaulieu (2007). Response of littoral chironomid communities and organic matter to late glacial lake-level, vegetation and climate changes at Lago dell'Accesa (Tuscany, Italy). *Journal of Paleolimnology 38*(4), 525–539.

Mitchell, T. D. and P. D. Jones (2005). An improved method of constructing a database of monthly climate observations and associated high-resolution grids. *International Journal of Climatology 25*(6), 693–712.

Montecinos, A., A. Diaz, and P. Aceituno (2000). Seasonal Diagnostic and Predictability of Rainfall in Subtropical South America Based on Tropical Pacific SST. *Journal of Climate 13*, 746–758.

Moreno, P., J. Francois, R. Villamartinez, and C. Moy (2009). Millennial-scale variability in Southern Hemisphere westerly wind activity over the last 5000 years in SW Patagonia. *Quaternary Science Reviews 28*(1-2), 25–38.

Moreno, P., M. Kaplan, J. Francois, R. Villa-Martinez, C. Moy, C. Stern, and P. Kubik (2009). Renewed glacial activity during the Antarctic cold reversal and persistence of cold conditions until 11.5ka in southwestern Patagonia. *Geology 37*(4), 375–378.

Moreno, P., T. Lowell, G. Jacobson Jr, and G. Denton (1999). Abrupt Vegetation and Climate Changes During the Last Glacial Maximumand Last Termination in The Chilean Lake District: A Case Study from Canal De La Puntilla (41deg.S). *Geografiska Annaler, Series A: Physical Geography 81*(2), 285–311.

Moreno, P., R. Villa-Martínez, M. Cárdenas, and E. Sagredo (2012). Deglacial changes of the southern margin of the southern westerly winds revealed by terrestrial records from SW Patagonia (52deg.S). *Quaternary Science Reviews 41*, 1–21.

Moreno, P. I. (1997). Vegetation and climate near Lago Llanquihue in the Chilean Lake District between 20200 and 9500 14C yr. BP. *Journal of Quaternary Science 12*(6), 485–500.

Moreno, P. I., G. L. Jacobson, T. V. Lowell, and G. H. Denton (2001). Interhemispheric climate links revealed by late-glacial cooling episode in southern Chile. *Nature 409*(6822), 804–8.

Moreno, P. I. and A. L. Leon (2003). Abrupt vegetation changes during the last glacial to Holocene transition in mid-latitude South America. *Journal of Quaternary Science 18*(8), 787–800.

Morgan, R. P. C. (1986). *Soil Eroision & Conservation*. Essex: Longman.

Morgan, V., M. Delmotte, T. van Ommen, J. Jouzel, J. Chappellaz, S. Woon, V. Masson-Delmotte, and D. Raynaud (2002). Relative timing of deglacial climate events in Antarctica and Greenland. *Science 297*(5588), 1862–4.

Mosello, R., A. Lami, A. Marchetto, M. Rogora, B. Wathne, L. Lien, J. Catalan, L. Camarero, M. Ventura, R. Psenner, K. Koinig, H. Thies, U. Nickus, D. Tait, B. Thaler, A. Barbieri, and R. Harriman (2002). Trends In The Water Chemistry Of High Altitude Lakes In Europe. *Water, Air, and Soil Pollution: Focus 2*, 75–89.

Mousavi, S. K. (2002). Boreal chironomid communities and their relations to environmental factors-the impact of lake depth, size and acidity. *Boreal Environmental Research 7*, 63–75.

Moxey, L. E. (2004). Mount Hudson's 1991 eruption provides Holocene palaeoclimatic insights. *International Journal of Remote Sensing 25*(6), 1053–1062.

Moy, C. M., R. B. Dunbar, P. I. Moreno, J. P. Francois, R. Villa-Martínez, D. M. Mucciarone, T. P. Guilderson, and R. D. Garreaud (2008). Isotopic evidence for hydrologic change related to the westerlies in SW Patagonia, Chile, during the last millennium. *Quaternary Science Reviews 27*(13-14), 1335–1349.

Moy, C. M., P. I. Moreno, R. B. Dunbar, M. R. Kaplan, J. P. Francois, R. Villalba, and T. Haberzettl (2009). Climate Change in Southern South America During the Last Two Millennia. In F. Vimeux, F. Sylvestre, and M. Khodri (Eds.), *Past Climate Variability in South America and Surrounding Regions*, Volume 14 of *Developments in Paleoenvironmental Research*, pp. 353–393. Dordrecht: Springer Netherlands.

Moy, C. M., G. O. Seltzer, D. T. Rodbell, and D. M. Anderson (2002). Variability of El Niño/Southern Oscillation activity at millennial timescales during the Holocene epoch. *Nature 420*(6912), 162–5.

Müller, B., A. F. Lotter, M. Sturm, and A. Ammann (1998). Influence of catchment quality and altitude on the water and sediment composition of 68 small lakes in Central Europe. *Aquatic Sciences 60*(4), 316.

Nan, S. and J. Li (2003). The relationship between the summer precipitation in the Yangtze River valley and the boreal spring Southern Hemisphere annular mode. *Geophysical Research Letters 30*(24), 1–4.

Naranjo, J. A. and C. R. Stern (1998). Holocene explosive activity of Hudson Volcano, southern Andes. *Bulletin of Volcanology 59*, 291–306.

Naranjo, J. A. and C. R. Stern (2004). Holocene tephrochronology of the southernmost part (42deg.30min.-45deg.S) of the Andean Southern Volcanic Zone. *Revista Geológica de Chile 31*(2), 225–240.

Nazarova, L., U. Herzschuh, S. Wetterich, T. Kumke, and L. Pestryakova (2010). Chironomid-based inference models for estimating mean July air temperature and water depth from lakes in Yakutia, northeastern Russia. *Journal of Paleolimnology 45*(1), 57–71.

Nesje, A. and S. V. Dahl (2001). The Greenland 8200 cal. yr BP event detected in loss-on-ignition profiles in Norwegian lacustrine sediment sequences. *Journal of Quaternary Science 16*(2), 155–166.

Neugart, C., K. Schneeberg, and R. Beutel (2009). The morphology of the larval head of Tipulidae (Diptera, Insecta)-The dipteran groundplan and evolutionary trends. *Zoologischer Anzeiger - A Journal of Comparative Zoology 248*(3), 213–235.

New, M., D. Lister, M. Hulme, and I. Makin (2002). A high-resolution data set of surface climate over global land areas. *Climate Research 21*, 1–25.

Newnham, R. M. and D. J. Lowe (2000). Fine-resolution pollen record of late-glacial climate reversal from New Zealand. *Geology 28*(8), 759.

Newnham, R. M., M. J. Vandergoes, M. H. Garnett, D. J. Lowe, C. Prior, and P. C. Almond (2007). Test of AMS14C dating of pollen concentrates using tephrochronology. *Journal of Quaternary Science 22*(1), 37–51.

Newnham, R. M., M. J. Vandergoes, E. Sikes, L. Carter, J. M. Wilmshurst, D. J. Lowe, M. S. McGlone, and A. Sandiford (2012). Does the bipolar seesaw extend to the terrestrial southern mid-latitudes? *Quaternary Science Reviews 36*, 214–222.

Ohlwein, C. and E. R. Wahl (2012). Review of probabilistic pollen-climate transfer methods. *Quaternary Science Reviews 31*, 17–29.

Ojala, A. E. K. (2004). Application of X-ray radiography and densitometry in varve analysis. In P. Francus (Ed.), *Image analysis, sediments and paleoenvironments.* Netherlands: Springer.

Olander, H., A. Korhola, T. Blom, and H. Birks (1999). An expanded calibration model for inferring lakewater and air temperatures from fossil chironomid assemblages in northern Fennoscandia. *The Holocene 9*(3), 279–294.

O'Leary, M. H. (1981). Caarbon Isotope Fractionation in Plants. *Phytochemistry 20*(4), 553–567.

Ortega, C., G. Vargas, J. A. Rutllant, D. Jackson, and C. Méndez (2012). Major hydrological regime change along the semiarid western coast of South America during the early Holocene. *Quaternary Research 78*(3), 513–527.

Pendall, E., V. Markgraf, J. W. C. White, and M. Dreier (2001). Multiproxy Record of Late Pleistocene-Holocene Climate and Vegetation Changes from a Peat Bog in Patagonia. *Quaternary Research 55*(2), 168–178.

Petit, J. R., J. Jouzel, D. Raynaud, N. I. Barkov, J.-M. Barnola, I. Basile, M. Bender, J. Chappellaz, M. Davis, G. Delaygue, M. Delmotte, V. M. Kotlyakov, M. Legrand, V. Y. Lipenkov, C. Lorius, L. Pepin, C. Ritz, E. Saltzman, and M. Stievenard (1999). Climate and atmospheric history of the past 420,000 years from the Vostok ice core, Antarctica. *Nature 399*, 429.

Pilcher, J. R. and V. A. Hall (1992). Towards a tephrochronology for the Holocene of the north of Ireland. *The Holocene 2*(3), 255–259.

Pinder, L. C. V. (1995). The habitats of chironomid larvae. In P. D. Armitage, P. S. Cranston, and L. C. V. Pinder (Eds.), *The Chironomidae: Biology & Ecology of non-biting midges.* London: Chapman & Hall.

Pisias, N., L. Heusser, C. Heusser, S. Hostetler, A. Mix, and M. Weber (2006). Radiolaria and pollen records from 0 to 50ka at ODP Site 1233: continental and marine climate records from the Southeast Pacific. *Quaternary Science Reviews 25*(5-6), 455–473.

Planas, X., A. Ponsa, A. Coronato, and J. Rabassa (2002). Geomorphological evidence of different glacial stages in the Martial cirque, Fuegian Andes, southernmost South America. *Quaternary International 87*(1), 19–27.

Plociennik, M., A. Self, H. J. B. Birks, and S. J. Brooks (2011). Chironomidae (Insecta: Diptera) succession in Åżabieniec bog and its palaeo-lake (central Poland) through the Late Weichselian and Holocene. *Palaeogeography, Palaeoclimatology, Palaeoecology 307*(1-4), 150–167.

Ponce, J. F., J. Rabassa, A. Coronato, and A. M. Borromei (2011). Palaeogeographical evolution of the Atlantic coast of Pampa and Patagonia from the last glacial maximum to the Middle Holocene. *Biological Journal of the Linnean Society 103*, 363–379.

Porinchu, D., N. Rolland, and K. Moser (2008). Development of a chironomid-based air temperature inference model for the central Canadian Arctic. *Journal of Paleolimnology 41*(2), 349–368.

Porinchu, D. F. and G. M. Macdonald (2003). Progress in Physical Geography The use and application of freshwater midges (Chironomidae: Insecta: Diptera) in geographical research. *Progress in Physical Geography 27*, 378.

Prieto, A., C. R. Stern, and J. E. Estévez (2013). The peopling of the Fuego-Patagonian fjords by littoral hunter-gatherers after the mid-Holocene H1 eruption of Hudson Volcano. *Quaternary International 317*, 3–13.

Prieto, M. D. R. and R. García Herrera (2009). Documentary sources from South America: Potential for climate reconstruction. *Palaeogeography, Palaeoclimatology, Palaeoecology 281*(3-4), 196–209.

Principato, S. M. (2004). X-ray radiographs of sediment cores: a guide to analyzing diamicton. In P. Francus (Ed.), *Image anaylsis, sediments and palaeoenvironments*. Dordrecht: Kluwer.

Pritchard, G. (1983). Biology of tipulidae. *Ann. Rev. Entomol. 28*, 1–22.

Putnam, A. E., G. H. Denton, J. M. Schaefer, D. J. A. Barrell, B. r. G. Andersen, R. C. Finkel, R. Schwartz, A. M. Doughty, M. R. Kaplan, and C. Schlüchter (2010). Glacier advance in southern middle-latitudes during the Antarctic Cold Reversal. *Nature Geoscience 3*(10), 700–704.

Quinlan, R. and J. P. Smol (2001). Setting minimum head capsule abundance and taxa deletion criteria in chironomid-based inference models. *Journal of Paleolimnology 26*, 327–342.

Rabassa, J. (2008). Late Cenozoic Glaciations in Patagonia and Tierra del Fuego. *Developments in Quaternary Science 11*, 151–204.

Rabassa, J. (2009). Natural Hazards and Human-Exacerbated Disasters in Latin America. In *Natural Hazards And Human-Exacerbated Disasters In Latin America*, Volume 13 of *Developments in Earth Surface Processes*, pp. 415–438. Netherlands: Elsevier.

Rahmstorf, S. and M. H. England (1997). Influence of Southern Hemisphere Winds on North Atlantic Deep Water Flow. *Journal of Physical Oceanography 27*(9), 2040.

Ramsey, C. B. (2008). Deposition models for chronological records. *Quaternary Science Reviews 27*(1-2), 42–60.

Recasens, C., D. Ariztegui, C. Gebhardt, C. Gogorza, T. Haberzettl, A. Hahn, P. Kliem, A. Lise-Pronovost, A. Lucke, N. Maidana, C. Mayr, C. Ohlendorf, F. Schabitz, G. St-Onge, M. Wille, B. Zolitschka, and S. Team (2011). New insights into paleoenvironmental changes in Laguna Potrok Aike, southern Patagonia, since the Late Pleistocene: The PASADO multiproxy record. *The Holocene 22*(11), 1323–1335.

Rees, A. B. H., L. C. Cwynar, and P. S. Cranston (2008). Midges (Chironomidae, Ceratopogonidae, Chaoboridae) as a temperature proxy: a training set from Tasmania, Australia. *Journal of Paleolimnology 40*, 1159–1178.

Reimer, P., M. Baillie, E. Bard, A. Bayliss, J. Beck, P. Blackwell, C. Bronk Ramsey, C. Buck, G. Burr, R. Edwards, M. Friedrich, P. Grootes, T. Guilderson, I. Hajdas, T. Heaton, A. Hogg, K. Hughen, K. Kaiser, B. Kromer, F. McCormac, S. Manning, R. Reimer, D. Richards, J. Southon, S. Talamo, C. Turney, and C. van der Plicht, J Weyhenmeyer (2009). IntCal09 and Marine09 Radiocarbon Age Calibration Curves, 0-50,000 Years cal BP. *Radiocarbon 51*(4), 1111–1150.

Rieradevall, M. and S. J. Brooks (2001). An identification guide to subfossil Tanypodinae larvae (Insecta: Diptera: Chironomidae) based on cephalic setation. *Journal of Paleolimnology 25*, 81–99.

Riquelme, R., C. Rojas, G. Aguilar, and P. Flores (2011). Late Pleistocene-early Holocene paraglacial and fluvial sediment history in the Turbio valley, semiarid Chilean Andes. *Quaternary Research 75*(1), 166–175.

Rivera, A., T. Benham, G. Casassa, J. Bamber, and J. Dowdeswell (2007). Ice elevation and areal changes of glaciers from the Northern Patagonia Icefield, Chile. *Global and Planetary Change 59*(1-4), 126–137.

Rodbell, D. T., J. A. Smith, and B. G. Mark (2009). Glaciation in the Andes during the Lateglacial and Holocene. *Quaternary Science Reviews 28*(21-22), 2165–2212.

Roig, F. A., R. Siegwolf, and J. A. Boninsegna (2006). Stable oxygen isotopes (delta18(O)) in Austrocedrus chilensis tree rings reflect climate variability in northwestern Patagonia, Argentina. *International Journal of Biometeorology 51*(2), 97–105.

Rojas, M., P. Moreno, M. Kageyama, M. Crucifix, C. Hewitt, A. Abe-Ouchi, R. Ohgaito, E. C. Brady, and P. Hope (2008). The Southern Westerlies during the last glacial maximum in PMIP2 simulations. *Climate Dynamics 32*(4), 525–548.

Rolland, N. and I. Larocque (2006). The efficiency of kerosene flotation for extraction of chironomid head capsules from lake sediments samples. *Journal of Paleolimnology 37*(4), 565–572.

Rolland, N., D. F. Porinchu, and I. Larocque (2008). The use of high-resolution gridded climate data in the development of chironomid-based inference models from remote areas. *Journal of Paleolimnology 41*(2), 343–348.

Ruiz, Z., a.G. Brown, and P. Langdon (2006, January). The potential of chironomid (Insecta: Diptera) larvae in archaeological investigations of floodplain and lake settlements. *Journal of Archaeological Science 33*(1), 14–33.

Saether, O. A. and P. S. Cranston (2012). New World Stictocladius Edwards (Diptera: Chironomidae). *Neotropical Entomology 41*(2), 124–149.

Saether, O. A. and T. Ekrem (2003). Biogeography of afrotropical Chironomidae (Diptera), with special reference to Gondwanaland. *Cimbebasia 19*, 123–139.

Sandgren, P. and I. Snowball (2001). Application of Mineral Magnetic Techniques to Paleolimnology. In *Tracking Environmental Change Using Lake Sediments: Physical and Chemical Techniques, Developments in Paleoenvironmental Research*, pp. 217–237. Netherlands: Klewer.

Santamaria Tovar, D., J. Shulmeister, and T. R. Davies (2008). Evidence for a landslide origin of New Zealand's Waiho Loop moraine. *Nature Geoscience 1*(8), 524–526.

Scasso, R. A., H. Corbella, and P. Tiberi (1994). Sedimentological analysis of the tephra from the 12-15 August 1991 eruption of Hudson volcano. *Bulletin of Volcanology 56*, 121–132.

Schäbitz, F., M. Wille, J. P. Francois, T. Haberzettl, F. Quintana, C. Mayr, A. Lücke, C. Ohlendorf, V. Mancini, M. M. Paez, A. R. Prieto, and B. Zolitschka (2013). Reconstruction of palaeoprecipitation based on pollen transfer functions-the record of the last 16ka from Laguna Potrok Aike, southern Patagonia. *Quaternary Science Reviews 71*, 175–190.

Schimpf, D., R. Kilian, A. Kronz, K. Simon, C. Spötl, G. Wörner, M. Deininger, and A. Mangini (2011). The significance of chemical, isotopic, and detrital components in three coeval stalagmites from the superhumid southernmost Andes (53deg.S) as high-resolution palaeo-climate proxies. *Quaternary Science Reviews 30*(3-4), 443–459.

Schmidt, S., B. Wagner, O. Heiri, M. Klug, O. Bennike, and M. Melles (2011). Chironomids as indicators of the Holocene climatic and environmental history of two lakes in Northeast Greenland. *Boreas 40*(1), 116–130.

Seltzer, G., D. Rodbell, and S. Burns (2000). Isotopic evidence for late Quaternary climatic change in tropical South America. *Geology 28*(1), 35.

Sheridan, B. (1990). *Radiocarbon Dating*. Los Angeles: UCP.

Shotton, F. W. (1972). An Example of Hard-Water Error in Radiocarbon Dating of Vegetable Matter. *Nature 240*(5382), 460–461.

Shulmeister, J. (2004). The Southern Hemisphere westerlies in the Australasian sector over the last glacial cycle: a synthesis. *Quaternary International 118-119*, 23–53.

Siebert, L., T. Simkin, and P. Kimberly (2010). *Volcanoes of the World* (3rd ed.). Berkeley: University of California Press.

Silvestri, G. and C. Vera (2009). Nonstationary Impacts of the Southern Annular Mode on Southern Hemisphere Climate. *Journal of Climate 22*(22), 6142–6148.

Smith, J. N. (2001). Why should we believe 210 Pb sediment geochronologies? *Journal of Environmental Radioactivity 55*, 121–123.

Sottile, G. D., F. P. Bamonte, M. V. Mancini, and M. M. Bianchi (2011). Insights into Holocene vegetation and climate changes at the southeast of the Andes: Nothofagus forest and Patagonian steppe fire records. *The Holocene 22*(11), 1309–1322.

Steig, E. J. (1998). Synchronous Climate Changes in Antarctica and the North Atlantic. *Science 282*(5386), 92–95.

Stenni, B., D. Buiron, M. Frezzotti, S. Albani, C. Barbante, E. Bard, J. M. Barnola, M. Baroni, M. Baumgartner, M. Bonazza, E. Capron, E. Castellano, J. Chappellaz, B. Delmonte, S. Falourd, L. Genoni, P. Iacumin, J. Jouzel, S. Kipfstuhl, A. Landais, B. Lemieux-Dudon, V. Maggi, V. Masson-Delmotte, C. Mazzola, B. Minster, M. Montagnat, R. Mulvaney, B. Narcisi, H. Oerter, F. Parrenin, J. R. Petit, C. Ritz, C. Scarchilli, A. Schilt, S. Schüpbach, J. Schwander, E. Selmo, M. Severi, T. F. Stocker, and R. Udisti (2010). Expression of the bipolar see-saw in Antarctic climate records during the last deglaciation. *Nature Geoscience 4*(1), 46–49.

Stenni, B., V. Masson-Delmotte, S. Johnsen, J. Jouzel, A. Longinelli, E. Monnin, R. Rothlisberger, and E. Selmo (2001). An oceanic cold reversal during the last deglaciation. *Science 293*(5537), 2074–7.

Sterken, M., E. Verleyen, K. Sabbe, G. Terryn, F. Charlet, S. Bertrand, X. Boës, N. Fagel, M. Batist, and W. Vyverman (2007). Late Quaternary climatic changes in southern Chile, as recorded in a diatom sequence of Lago Puyehue (40deg.40min.S). *Journal of Paleolimnology 39*(2), 219–235.

Stern, C. R. (2007). Holocene tephrochronology record of large explosive eruptions in the southernmost Patagonian Andes. *Bulletin of Volcanology 70*(4), 435–454.

Stern, L. A. and P. M. Blisniuk (2002). Stable isotope composition of precipitation across the southern Patagonian Andes. *Journal of Geophysical Research 107*(D23), 4667.

Stutz, S., C. M. Borel, S. L. Fontana, L. Puerto, H. Inda, F. García-Rodriguez, and M. S. Tonello (2010). Late Holocene climate and environment of the SE Pampa grasslands, Argentina, inferred from biological indicators in shallow, freshwater Lake Nahuel Rucá. *Journal of Paleolimnology 44*(3), 761–775.

Stutz, S., C. M. Borel, S. L. Fontana, and M. S. Tonello (2012). Holocene changes in trophic states of shallow lakes from the Pampa plain of Argentina. *The Holocene 22*(11), 1263–1270.

ter Braak, C. J. F. and S. Juggins (1993). Weighted averaging partial least squares regression (WA-PLS): an improved method for reconstructing environmental variables from species assemblages. *Hydrobiologica 269-270*(1), 485–502.

Thevenon, F., T. Adatte, J. E. Spangenberg, and F. S. Anselmetti (2012). Elemental (C/N ratios) and isotopic (15Norg, 13Corg) compositions of sedimentary organic matter from a high-altitude mountain lake (Meidsee, 2661 m a.s.l., Switzerland):

Implications for Lateglacial and Holocene Alpine landscape evolution. *The Holocene 22*(10), 1135–1142.

Thompson, D. W. J. and S. Solomon (2002). Interpretation of recent Southern Hemisphere climate change. *Science 296*(5569), 895–9.

Thompson, R., R. W. Battarbee, P. E. O'Sullivan, and F. Oldfield (1975). Magnetic susceptibility of lake sediments. *Limnology and Oceanography 20*(5), 687–698.

Tingstad, A. H., K. Moser, G. MacDonald, and J. Munroe (2010). A 13,000-year paleolimnological record from the Uinta Mountains, Utah, inferred from diatoms and loss-on-ignition analysis. *Quaternary International 235*(1-2), 48–56.

Tokeshi, M. (1995). Life cycles and population dynamics. In *The Chironomidae: Biology & Ecology of non-biting midges.* Netherlands: Klewer.

Tonello, M. S., M. V. Mancini, and H. Seppä (2009). Quantitative reconstruction of Holocene precipitation changes in southern Patagonia. *Quaternary Research 72*(3), 410–420.

Trivinho-Strixino, S., F. O. Roque, and P. S. Cranston (2009). Redescription of Riethia truncatocaudata (Edwards, 1931) (Diptera: Chironomidae), with description of female, pupa and larva and generic diagnosis for Riethia. *Aquatic Insects 31*(4), 247–259.

Tuiskunen, J. (1986). The fennoscandian species of Parakiefferiella Thienemann (Diptera, Chironomidae, Orthocladiinae). *Annals of the Zoologici Fennici 23*, 175–196.

Turner, K. J., C. J. Fogwill, and D. E. Sugden (2005). Deglaciation of the Eastern Flank Of The North Patagonian Icefield and Associated Continental-Scale Lake Diversions. *Geografiska Annaler A 87A*(2), 363–374.

Unkel, I., S. Björck, and B. Wohlfarth (2008). Deglacial environmental changes on Isla de los Estados (54.4deg.S), southeastern Tierra del Fuego. *Quaternary Science Reviews 27*(15-16), 1541–1554.

Urrego, D. H., B. A. Niccum, C. F. La Drew, M. R. Silman, and M. B. Bush (2011). Fire and drought as drivers of early Holocene tree line changes in the Peruvian Andes. *Journal of Quaternary Science 26*(1), 28–36.

Urrutia, R., A. Araneda, F. Cruces, L. Torres, L. Chirinos, H. Treutler, N. Fagel, S. Bertrand, I. Alvial, and R. Barra (2007). Changes in diatom, pollen, and chironomid assemblages in response to a recent volcanic event in Lake Galletué (Chilean Andes). *Limnologica - Ecology and Management of Inland Waters 37*(1), 49–62.

Urrutia, R., A. Araneda, L. Torres, F. Cruces, C. Vivero, F. Torrejón, R. Barra, N. Fagel, and B. Scharf (2010). Late Holocene environmental changes inferred from diatom, chironomid, and pollen assemblages in an Andean lake in Central Chile, Lake Laja (36deg.S). *Hydrobiologia 648*(1), 207–225.

van Bellen, S., D. Mauquoy, R. J. Payne, T. P. Roland, T. J. Daley, P. D. M. Hughes, N. J. Loader, F. A. Street-Perrott, E. M. Rice, and V. Pancotto (2014). Testate Amoebae as a Proxy For Reconstructing Holocene Water Table Dynamics in Southern Patagonian Peat Bogs. *Journal of Quaternary Science 29*(5), 463–474.

van Hardenbroek, M., O. Heiri, M. F. Wilhelm, and A. F. Lotter (2010). How representative are subfossil assemblages of Chironomidae and common benthic invertebrates for the living fauna of Lake De Waay, the Netherlands? *Aquatic Sciences 73*(2), 247–259.

Vandergoes, M. J., A. C. Dieffenbacher-Krall, R. M. Newnham, G. H. Denton, and M. Blaauw (2008). Cooling and changing seasonality in the Southern Alps, New Zealand during the Antarctic Cold Reversal. *Quaternary Science Reviews 27*(5-6), 589–601.

Vargas-Ramirez, L., E. Roche, P. Gerrienne, and H. Hooghiemstra (2007). A pollen-based record of late glacial-Holocene climatic variability in the southern lake district, Chile. *Journal of Paleolimnology 39*(2), 197–217.

Veblen, T. and D. Lorenz (1988). Recent Vegetation Changes along the Forest/Steppe Ecotone of Northern Patagonia. *Annals of the Association of American Geographers 78*(1), 93–111.

Veblen, T. T., W. L. Baker, G. Montenegro, and T. W. Swetnam (2003). *Ecological Studies, Vol. 160: Fire and Climate Change in Temperate Ecosystems of the Western Americas*, Volume 160. New York: Springer.

Velle, G., K. P. Brodersen, H. J. B. Birks, and E. Willassen (2010). Midges as quantitative temperature indicator species: Lessons for palaeoecology. *The Holocene 20*(6), 989–1002.

Velle, G. and I. Larocque (2007). Assessing chironomid head capsule concentrations in sediment using exotic markers. *Journal of Paleolimnology 40*(1), 165–177.

Velle, G., R. J. Telford, O. Heiri, J. Kurek, and H. J. B. Birks (2012). Testing intra-site transfer functions: an example using chironomids and water depth. *Journal of Paleolimnology 48*(3), 545–558.

Verschuren, D. and H. Eggermont (2006). Quaternary paleoecology of aquatic Diptera in tropical and Southern Hemisphere regions, with special reference to the Chironomidae. *Quaternary Science Reviews 25*(15-16), 1926–1947.

Villa-Martínez, R. and P. I. Moreno (2007). Pollen evidence for variations in the southern margin of the westerly winds in SW Patagonia over the last 12,600 years. *Quaternary Research 68*(3), 400–409.

Villa-Martínez, R., P. I. Moreno, and M. a. Valenzuela (2012). Deglacial and postglacial vegetation changes on the eastern slopes of the central Patagonian Andes (47deg.S). *Quaternary Science Reviews 32*, 86–99.

Villalba, R., A. Lara, J. A. Boninsegna, M. Masiokas, S. Delgado, J. C. Aravena, F. A. Roig, A. Schmelter, A. Wolodarsky, and A. Ripalta (2003). Large-Scale Temperature Changes Across The Southern Andes: 20th-Century Variations In The Context Of The Past 400 Years. *Climate Change 59*, 177–232.

Vimeux, F., M. de Angelis, P. Ginot, O. Magand, G. Casassa, B. Pouyaud, S. Falourd, and S. Johnsen (2008). A promising location in Patagonia for paleoclimate and paleoenvironmental reconstructions revealed by a shallow firn core from Monte San Valentín (Northern Patagonia Icefield, Chile). *Journal of Geophysical Research 113*(D16), 1–20.

Vimeux, F., P. Ginot, M. Schwikowski, M. Vuille, G. Hoffmann, L. G. Thompson, and U. Schotterer (2009). Climate variability during the last 1000 years inferred from Andean ice cores: A review of methodology and recent results. *Palaeogeography, Palaeoclimatology, Palaeoecology 281*(3-4), 229–241.

Vimeux, F., F. Sylvestre, and M. Khodri (2009). *Past Climate Variability in South America and Surrounding Regions*, Volume 14 of *Developments in Paleoenvironmental Research*. Dordrecht: Springer Netherlands.

Virkanen, J., A. Korhola, M. Tikkanen, and T. Blom (1997). Recent environmental changes in a naturally acidic rocky lake in southern Finland, as reflected in its sediment geochemistry and biostratigraphy. *Journal of Paleolimnology 17*(2), 191–213.

von Gunten, L., M. Grosjean, J. Beer, P. Grob, A. Morales, and R. Urrutia (2008). Age modeling of young non-varved lake sediments: methods and limits. Examples from two lakes in Central Chile. *Journal of Paleolimnology 42*(3), 401–412.

von Gunten, L., M. Grosjean, B. Rein, R. Urrutia, and P. Appleby (2009). A quantitative high-resolution summer temperature reconstruction based on sedimentary pigments from Laguna Aculeo, central Chile, back to AD 850. *The Holocene 19*(6), 873–881.

Walden, J. (1999). Sample Collection and Preparation. In J. Walden, F. Oldfield, and J. Smith (Eds.), *Environomental Magnetism: A Practical Guide*, Chapter 3, pp. 12—-26. London: Quaternary Research Association.

Waldmann, N., D. Ariztegui, F. S. Anselmetti, J. A. Austin, C. M. Moy, C. Stern, C. Recasens, and R. B. Dunbar (2009). Holocene climatic fluctuations and positioning of the Southern Hemisphere westerlies in Tierra del Fuego (54deg.S), Patagonia. *Journal of Quaternary Science 25*(7), 1063–1075.

Walker, I. (1987). Chironomidae (Diptera) in paleoecology. *Quaternary Science Reviews 6*(1), 29–40.

Walker, I., E. Reavie, S. Palmer, and R. Nordin (1993). A palaeoenvironmental assessment of human impact on Wood Lake, okanagan valley, British Columbia, Canada. *Quaternary International 20*, 51–70.

Walker, I. R. and C. G. Paterson (1985). Efficient seperation of subfossil Chironomidae from lake sediments. *Hydrobiologica 122*(2), 189–192.

Walker, I. R., J. P. Smol, D. R. Engstrom, and H. J. B. Birks (1991). An assessment of Chironomidae as quantitative indicators of past climate change. *Canadian Journal of Fisheries and Aquatic Science 48*, 975–987.

Walker, I. R., J. P. Smol, D. R. Engstrom, and H. J. B. Birks (1992). Aquatic invertebrates, climate, scale and statistical hypothesis testing: a response to Hann, Warner and Warwick. *Canadian Journal of Fisheries and Aquatic Science 49*, 1276–1280.

Wanner, H., J. Beer, J. Bütikofer, T. J. Crowley, U. Cubasch, J. Flückiger, H. Goosse, M. Grosjean, F. Joos, J. O. Kaplan, M. Küttel, S. A. Müller, I. C. Prentice, O. Solomina, T. F. Stocker, P. Tarasov, M. Wagner, and M. Widmann (2008). Mid- to Late Holocene climate change: an overview. *Quaternary Science Reviews 27*(19-20), 1791–1828.

Wastegard, S., D. Veres, P. Kliem, A. Hahn, C. Ohlendorf, and B. Zolitschka (2013). Towards a late Quaternary tephrochronological framework for the southernmost part of South America-the Laguna Potrok Aike tephra record. *Quaternary Science Reviews 71*, 81–90.

Watson, J. E., S. J. Brooks, N. J. Whitehouse, P. J. Reimer, H. J. B. Birks, and C. Turney (2010). Chironomid-inferred late-glacial summer air temperatures from Lough Nadourcan, Co. Donegal, Ireland. *Journal of Quaternary Science 25*(8), 1200–1210.

Weltje, G. J. and R. Tjallingii (2008). Calibration of XRF core scanners for quantitative geochemical logging of sediment cores: Theory and application. *Earth and Planetary Science Letters 274*(3-4), 423–438.

Wetzel, R. G. (2001). *Limnology: Lake and River Ecosystems* (3rd ed.). San Diego, USA: Academic Press.

Wiedenbrug, S. and T. Andersen (2002). New Species of Parakiefferiella Thienemann, 1936 from South America (Chironomidae, Orthocladiinae). *Studies on Neotropical Fauna and Environment 37*(2), 119–132.

Wiederholm, T. (1979). Chironomid remains in recent sediments of Lake Washington. *Northwest Science 53*, 251.

Wiederholm, T. and L. Eriksson (1978). Subfossil chironomids as evidence of eutrophication in Ekoln Bay, Central Sweden. *Hydrobiologica 62*(3), 195–208.

Wille, M., N. I. Maidana, F. Schäbitz, M. Fey, T. Haberzettl, S. Janssen, A. Lücke, C. Mayr, C. Ohlendorf, and G. H. Schleser (2007). Vegetation and climate dynamics in southern South America: The microfossil record of Laguna Potrok Aike, Santa Cruz, Argentina. *Review of Palaeobotany and Palynology 146*(1-4), 234–246.

Wille, M. and F. Schäbitz (2008). Late-glacial and Holocene climate dynamics at the steppe/forest ecotone in southernmost Patagonia, Argentina: the pollen record from a fen near Brazo Sur, Lago Argentino. *Vegetation History and Archaeobotany 18*(3), 225–234.

Williams, J. J., S. J. Brooks, and W. D. Gosling (2012). Response of chironomids to late Pleistocene and Holocene environmental change in the eastern Bolivian Andes. *Journal of Paleolimnology 48*(3), 485–501.

Williams, P., D. King, J. Zhao, and K. Collerson (2005). Late Pleistocene to Holocene composite speleothem 18O and 13C chronologies from South Island, New Zealand-did a global Younger Dryas really exist? *Earth and Planetary Science Letters 230*(3-4), 301–317.

Wohlfarth, B., M. Blaauw, S. M. Davies, M. Andersson, S. Wastegard, A. Hormes, and G. Possnert (2006). Constraining the age of Lateglacial and early Holocene pollen zones and tephra horizons in southern Sweden with Bayesian probability methods. *Journal of Quaternary Science 21*(4), 321–334.

Wolfe, B. B., T. W. D. Edwards, R. J. Elgood, and K. R. M. Beuning (2001). Carbon and oxygen isotope analysis of lake sediment cellulose: methods and applications. In *Tracking Environmental Change Using Lake Sediments: Physical and Chemical Techniques, Developments in Paleoenvironmental Research*, pp. 373–400. Netherlands: Kluwer.

Wolff, E., J. Chappellaz, T. Blunier, S. Rasmussen, and A. Svensson (2010). Millennial-scale variability during the last glacial: The ice core record. *Quaternary Science Reviews 29*(21-22), 2828–2838.

Woodward, C. and J. Shulmeister (2007). Chironomid-based reconstructions of summer air temperature from lake deposits in Lyndon Stream, New Zealand spanning the MIS 3/2 transition. *Quaternary Science Reviews 26*(1-2), 142–154.

Woodward, C. A. and J. Shulmeister (2006). New Zealand chironomids as proxies for human-induced and natural environmental change: Transfer functions for temperature and lake production (chlorophyll a). *Journal of Paleolimnology 36*(4), 407–429.

Wooller, M., Y. Wang, and Y. Axford (2007). A multiple stable isotope record of Late Quaternary limnological changes and chironomid paleoecology from northeastern Iceland. *Journal of Paleolimnology 40*(1), 63–77.

Wright, H. E., D. H. Mann, and P. H. Glaser (1984). Piston Corers for Peat and Lake Sediments. *Ecology 65*(2), 657–659.

Wyrwoll, K. (2000). On the position of southern hemisphere westerlies at the Last Glacial Maximum: an outline of AGCM simulation results and evaluation of their implications. *Quaternary Science Reviews 19*(9), 881–898.

Zhu, J., A. Lücke, H. Wissel, D. Müller, C. Mayr, C. Ohlendorf, and B. Zolitschka (2013, July). The last GlacialâĂŞInterglacial transition in Patagonia, Argentina: the stable isotope record of bulk sedimentary organic matter from Laguna Potrok Aike. *Quaternary Science Reviews 71*, 205–218.